TECHNISCHE UNIVERSITÄT MÜNCHEN

INGENIEURFAKULTÄT BAU GEO UMWELT

LEHRSTUHL FÜR SIEDLUNGSWASSERWIRTSCHAFT

Influencing Factors on the Treatment of Road Runoff using Decentralized Stormwater Quality Improvement Devices

Steffen Heinz Rommel

Vollständiger Abdruck der von der Ingenieurfakultät Bau Geo Umwelt der Technischen Universität München zur Erlangung des akademischen Grades eines

Doktor-Ingenieurs (Dr.-Ing.)

genehmigten Dissertation.

Vorsitzender:
Prof. Dr.-Ing. Jörg E. Drewes

Prüfer der Dissertation:
1. apl. Prof. Dr. rer. nat. habil. Brigitte Helmreich
2. Prof. Dr.-Ing. Ulrich Dittmer
3. Prof. Dr.-Ing. Markus Disse

Die Dissertation wurde am 18.01.2021 bei der Technischen Universität München eingereicht und durch die Ingenieurfakultät Bau Geo Umwelt am 26.04.2021 angenommen.

Abstract

Road runoff can be contaminated by heavy metals and organic substances mainly due to traffic-related emissions. To enable a sustainable stormwater management, decentralized treatment of stormwater on site is intended to restore the natural water cycle and mitigate detrimental effects on the environment. One promising option for decentralized stormwater treatment in space-constrained urban settings are stormwater quality improvement devices (SQIDs). These commonly consists of two-stage treatment trains using sedimentation to separate particulate-bound contaminants prior to (sorptive) media filtration to retain fine particles and dissolved contaminants. The treatment efficiency of SQIDs is subject to a variety of influencing factors that have not yet been adequately described.

The overarching research goal of this dissertation was to identify, describe and quantify factors influencing treatment efficiency of SQIDs to establish a well-founded background to assess and design SQIDs. Based on the experience and samples of monitoring four full-scale SQIDs that treated road runoff from a heavily trafficked road, four main research topics were studied in this dissertation. Additional lab-scale experiments were conducted to investigate these research topics in order to achieve reproducible conditions.

Firstly, leaching of heavy metals retained in SQIDs by sorptive filter media was studied to provide insights into the long-term treatment efficiency, because retention mechanism for dissolved heavy metals can be reversible. Three commercially available filter media used for stormwater treatment were prestressed with copper and zinc, which are the main heavy metals present in road runoff. Afterwards, these prestressed filter media were exposed to three different synthetic road runoffs in quiescent batch tests to simulate permanently submerged media filters during dry periods. The results demonstrated that even after long contact times, of up to seven days, and the presence of dissolved organic matter or de-icing salt, no leaching of heavy metals was observed. Since the experimental conditions were closer to *in situ* conditions compared to previous studies, the outcome of this study indicate that the risk of heavy metal leaching from sorptive media was potentially overestimated in the past. However, sediments trapped in a SQID exhibited considerable heavy metal leaching in the same experiments, which can reduce the service life of consecutive media filtration stages and/or result in worse effluent quality.

Secondly, the treatment efficiency of SQIDs is commonly examined either at lab scale or in field tests. However, the chemical boundary conditions and composition of stormwater significantly affect the treatment efficiency of sorptive filter media used in SQIDs. These can not be entirely replicated in lab-scale experiments. Thus, sequential extraction was applied for the first time to analyze whether the mobility of heavy metals in sorptive filter media shows a discrepancy after prestressing in lab-scale tests or full-scale application. The analysis revealed that zinc exhibits high mobility in filter media, as well as sediments trapped in SQIDs. The comparison of filter media of different origin, displayed that the currently used lab-scale prestressing results in significantly greater mobility of copper and zinc. Previous lab-scale experiments therefore potentially overestimated heavy metal leaching.

Furthermore, dissolved organic matter (DOM) is well-known to affect mobility of heavy metals in aquatic systems. However, the occurrence and properties of DOM in road runoff have not been comprehensively described yet. In order to enable an assessment of the effect of DOM on stormwater treatment, DOM in road runoff and effluent of SQIDs was analyzed over the course of one year using UV-vis and fluorescence spectroscopy as well as size exclusion chromatography. The results demonstrated that DOM quantity and quality show a strong seasonality. In summer, DOM was present in higher concentrations and showed more humic-like properties. Treatment in SQIDs showed no significant impact on the DOM quantity and properties. Furthermore, it was verified that most of the DOM can be attributed to humic substances. Speciation prediction as well as principal component analysis indicated that the mobility of heavy metals in road runoff and effluent of SQIDs, especially of chromium and copper, is influenced by the presence of DOM due to formation of DOM-metal complexes.

Lastly, further studies investigated the influence of temperature and de-icing salt on the sedimentation of particulate matter in road runoff. These demonstrated that even high de-icing salt concentrations do not significantly affect settling of road-deposited sediment, in contrast to temperature. Furthermore, particle shapes of road-deposited sediments were comprehensively analyzed. Yet, they appeared to be negligible to determine settled fractions.

In summary, this dissertation contributes to the current knowledge about stormwater treatment by describing and evaluating currently insufficiently studied factors influencing treatment efficiency of SQIDs and other stormwater treatment systems. Together with further studies that need to demonstrate the feasibility of the widespread application of SQIDs, this facilitates a well-founded assessment and selection of appropriate stromwater control measures.

Zusammenfassung

Straßenabflüsse können vor allem durch verkehrsbedingte Emissionen mit Schwermetallen und organischen Schadstoffen belastet sein. Um eine nachhaltige Regenwasserbewirtschaftung zu erreichen, soll Niederschlagswasser dezentral vor Ort bewirtschaftet werden, um, ggf. nach einer Behandlung, den natürlichen Wasserkreislauf wiederherzustellen und schädliche Auswirkungen auf die Umwelt abzumildern. Dezentrale Niederschlagswasserbehandlungsanlagen sind eine vielversprechende Möglichkeit insbesondere für den Siedlungsraum mit begrenztem Platzangebot. Diese verfügen in der Regel über zweistufige Behandlungssysteme mit einer Sedimentationsstufe zur Abtrennung von partikulär gebundenen Schadstoffen vor einer Filtrationsstufe mit sorptiven Materialien zum Rückhaltung von Feinpartikeln und gelösten Schadstoffen. Während es zahlreiche Untersuchungen zu dezentralen Behandlungsanlagen im Labormaßstab gibt und diese auch im Labor geprüft werden, ist die Erfahrung mit solchen Anlagen im Praxisbetrieb begrenzt. Die Reinigungsleistung von dezentrale Niederschlagswasserbehandlungsanlagen unterliegt im Praxisbetrieb einer Vielzahl von Einflussfaktoren, die noch nicht hinreichend beschrieben sind.

Das übergeordnete Ziel dieser Dissertation war die Identifizierung, Beschreibung und Quantifizierung von Faktoren, welche die Reinigungsleistung von dezentralen Niederschlagswasserbehandlungsanlagen unter Realbedingungen beeinflussen. Somit kann einen fundierte Grundlage für die Bewertung und Auslegung von dezentrale Niederschlagswasserbehandlungsanlagen geschaffen werden. Basierend auf den Erfahrungen und Proben der Überwachung von vier großtechnischen dezentrale Niederschlagswasserbehandlungsanlagen, die Straßenabflüsse von einer stark befahrenen Straße behandelten, wurden in dieser Dissertation vier Forschungsthemen abgeleitet und untersucht. Hierfür wurden zusätzliche Experimente im Labormaßstab durchgeführt, um reproduzierbare Bedingungen zum Vergleich zu erreichen.

Zunächst wurde die Remobilisierung von Schwermetallen, die von den sorptiven Filtermaterialien zurückgehalten wurden, untersucht, da Wirkmechanismen dieser Materialien reversibel sein können. Hierdurch kann die langfristige Leistungsfähigkeit beurteilt werden. Drei handelsübliche sorptive Filtermaterialien, die in Niederschlagswasserbehandlungsanlagen verwendet werden, wurden mit den relevantesten Schwermetalle in Straßenabflüssen, Kupfer und Zink, vorbelastet.

Anschließend wurden die vorbelasteten Filtermaterialien drei verschiedenen synthetischen Straßenabflüssen in Batch-Tests ohne Schütteln ausgesetzt, um dauerhaft eingestaute Systeme während Trockenperioden zu simulieren. Die Ergebnisse zeigten, dass selbst nach langen Verweilzeiten von bis zu sieben Tagen und dem Vorhandensein von gelösten organischen Substanzen oder Tausalz keine Remobilisierung von Schwermetallen auftrat. Da die Versuchsbedingungen im Vergleich zu früheren Studien näher an realen Bedingungen lagen, deuten die Ergebnisse dieser Studie darauf hin, dass das Risiko der Schwermetallremobilisierung aus sorptiven Filtermaterialien in der Vergangenheit möglicherweise überschätzt wurde. Die in dezentrale Niederschlagswasserbehandlungsanlagen eingeschlossenen Sedimente zeigten jedoch in den selben Experimenten eine deutliche Schwermetallremobilisierung, was die Lebensdauer nachfolgender sorptiver Filtrationsstufen verringern und/oder zu einer schlechteren Ablaufqualität führen kann.

Derzeit wird die Reinigungsleistung von dezentrale Niederschlagswasserbehandlungsanlagen üblicherweise entweder im Labormaßstab oder in Feldversuchen ermittelt. Allerdings beeinflussen die chemischen Randbedingungen und die Zusammensetzung des Straßenabflusses die Reinigungsleistung der sorptiven Filtermaterialien in Niederschlagswasserbehandlungsanlagen erheblich. Diese können jedoch in Experimenten im Labormaßstab nicht vollständig abgebildet werden. Daher wurde erstmals die sequentielle Extraktion angewandt, um zu analysieren, ob die Mobilität von Schwermetallen in sorptiven Filtermaterialien abweicht, wenn die Vorbelastung entweder im Labormaßstab oder im großtechnischen Einsatz erfolgte. Die Analyse ergab, dass vor allem Zink eine hohe Mobilität in Filtermaterialien aufweist, ebenso wie in zurückgehaltenen Sedimenten. Der Vergleich von Filtermaterialien unterschiedlicher Herkunft zeigte, dass die derzeit verwendete Vorbelastung im Labormaßstab zu einer deutlich höheren Mobilität von Kupfer und Zink führt. Frühere Experimente im Labormaßstab überschätzten daher vermutlich die Schwermetallremobilisierung.

Außerdem ist bekannt, dass gelöste organische Substanzen (DOM) die Mobilität von Schwermetallen in aquatischen Systemen beeinflussen. Das Vorkommen und die Eigenschaften von DOM in Straßenabflüssen sind jedoch noch nicht umfassend beschrieben. Um eine Bewertung des Einflusses von DOM auf die Niederschlagswasserbehandlung zu ermöglichen, wurde DOM in Straßenabfluss und Ablauf von dezentralen Niederschlagswasserbehandlungsanlagen über den Verlauf eines Jahres mittels UV-Vis- und Fluoreszenzspektroskopie sowie Größenausschluss-Chromatographie analysiert. Die Ergebnisse zeigten, dass sowohl die Menge als auch die Zusammensetzung des DOM eine starke Saisonalität aufweisen. Im Sommer waren höheren DOM-Konzentrationen vorhanden und die Eigenschaften waren eher Huminstoffen ähnlich. Die Behandlung in Niederschlagswasserbehandlungsanlagen zeigte keinen signifikanten Einfluss auf die Menge und Zusammensetzung des DOM. Außerdem

wurde nachgewiesen, dass der Großteil des DOM auf Huminstoffe zurückzuführen ist. Die Berechnung der Speziierung sowie die Hauptkomponentenanalyse zeigte, dass die Mobilität von Schwermetallen, insbesondere von Chrom und Kupfer, im Straßenabfluss und im Ablauf von Niederschlagswasserbehandlungsanlagen durch die Anwesenheit von DOM durch Bildung von Komplexen beeinflusst wird.

Schließlich wurde in weiteren Studien der Einfluss von Temperatur und Tausalz auf die Sedimentation von Partikeln im Straßenabfluss untersucht. Diese zeigten, dass selbst hohe Tausalzkonzentrationen die Sedimentation von Partikeln nicht signifikant beeinflussen, im Gegensatz zur Temperatur. Außerdem wurde die Form von auf Straßen abgelagerten Partikeln umfassend untersucht. Sie war jedoch vernachlässigbar für die Bestimmung der Absetzbarkeit.

Zusammenfassend trägt diese Dissertation zum aktuellen Wissen über die Niederschlagswasserbehandlung bei, indem sie derzeit unzureichend untersuchte Faktoren, welche die Reinigungsleistung von dezentralen Niederschlagswasserbehandlungsanlagen im Praxisbetrieb beeinflussen, beschreibt und bewertet. Zusammen mit weiteren Machbarkeitsstudien zum flächendeckenden Einsatz von Niederschlagswasserbehandlungsanlagen ist diese Arbeit Grundlage für eine fundierte Beurteilung und Auswahl geeigneter Niederschlagswasserbehandlungssysteme.

Danksagung

Diese Arbeit wäre nicht möglich gewesen ohne die Unterstützung, die ich den letzten Jahren erhalten habe. Insbesondere gilt mein Dank Philipp Stinshoff und Luca Noceti, ohne deren Hilfe das umfangreiche Forschungsvorhaben nicht möglich gewesen wäre. Auch meiner Doktormutter Brigitte Helmreich bin ich sehr dankbar für die angenehme Zusammenarbeit auf Augenhöhe und Unterstützung bei der Umsetzung neuer Forschungsansätze. Ebenfalls wäre der Aufbau und Unterhalt der Versuchsanlagen und Messtechnik nicht möglich gewesen ohne Hubert Mossrainer.

Ich danke allen weiteren Mitautor*innen der Publikationen, die im Zeitraum meiner Dissertation entstanden sind, sowie den vielzähligen Student*innen, die meine Forschungsarbeit unterstützt und bereichert haben.

Des Weiteren danke ich meinem Mentor Harald Hilbig vom Centrum Baustoffe und Materialprüfung der TU München für die Unterstützung bei der Analyse und dem Probentransport. Ich bedanke mich bei Myriam Reif und Wolfgang Schröder für die Analytik und Hilfe im Labor.

Ich danke Maximilian Huber für die Anwerbung der spannenden Forschungsprojekte, die ich im Rahmen meiner Dissertation bearbeitet habe. Zudem danke ich ihm für die Schaffung einer sehr guten Forschungsgrundlage.

Während der Bearbeitung der Forschungsprojekte unterstützte mich insbesondere Susanne Krüger vom Baureferat der Landeshauptstadt München.

Bei der Einrichtung und dem Unterhalt der Versuchsanlagen unterstützen mich die Mitarbeiter der Münchner Stadtentwässerung, unter der Leitung von Konrad Regler, umstandslos. Ebenfalls half mir Rainer Preg, von den Firmen Preg Umwelttechnik und WaterSam, mehrfach die umfangreiche Messtechnik am Laufen zu halten.

Auch danke ich den Herstellern der untersuchten dezentralen Behandlungsanlagen Fränkische Rohrwerke, Hauraton und Mall, vertreten durch Michael Schütz, Claus Huwe und Martin Lienhard, für Ihre Offenheit gegenüber der Forschung und dem Erfahrungsaustausch.

Ebenfalls bedanke ich mich bei allen Kolleg*innen für die schöne Zeit am Lehrstuhl. Ich werde mich gerne an diese Zeit erinnern.

Des Weiteren möchte ich Christoph Schreiber für den nahezu täglichen Austausch zum Forschungsalltag und für die Durchsicht des Manuskripts danken.

Besonders danke ich Pia für ihr Verständnis und die Unterstützung in der herausfordernden Schlussphase dieser Arbeit.

Die Überwachung der dezentralen Niederschlagswasserbehandlungsanlagen wurde im Rahmen des Forschungsprojekts „Praxiserfahrungen zum Umgang mit dezentralen Behandlungsanlagen für Verkehrsflächenabflüsse“ finanziell unterstützt durch das Bayerische Landesamt für Umwelt (AZ: 67-0270-96505/2016 und AZ: 67-0270-25598/2019). Finanzielle Unterstützung erfolgte ebenfalls durch das Baureferat der Landeshauptstadt München im Rahmen des Forschungsprojekts „Wissenschaftliche Untersuchung der Effizienz der Kombination Absetzschacht und Versickerungsschacht zur Reduzierung der stofflichen Belastung von Verkehrsflächenabflüssen“.

Contents

List of Figures

List of Tables

Abbreviations

AADT annual average daily traffic

A:T ratio of the fluorescence peak intensities A:T

BIX biological index

BTEX benzene, toluene, ethylbenzene, and the three xylene isomers

Ca calcium

$CaCl_2$ calcium chloride

Cd cadmium

CEC cationic exchange capacity

CFD computational fluid dynamics

Cl^- chloride

Cr chromium

Cu copper

DIBt Deutsches Institut für Bautechnik

DOC dissolved organic carbon

DOM dissolved organic matter

Em emission wavelength

ETBE ethyl tert-butyl ether

Ex excitation wavelength

Fe iron

GFS Geringfügigkeitsschwellenwerte

Hg mercury

HIX humification index

HM heavy metal

HRT hydraulic retention time

HS humic substances

LANUV Landesamt für Natur, Umwelt und Verbraucherschutz Nordrhein-Westfalen

LOQ limit of quantification

$MgCl_2$ magnesium chloride

Mn manganese

MTBE methyl tert-butyl ether

MTD manufactured treatment device

N nitrogen

Na sodium

NaCl sodium chloride

Ni nickel

NJDEP New Jersey Department of Environmental Protection

P phosphorus

PARAFAC parallel factor analysis

PAHs polycyclic aromatic hydrocarbons

Pb lead

PCA principal component analysis

Pd palladium

PM particulate matter

PP permeable pavement

PSD particle size distribution

Pt platinum

RDS road-deposited sediment

Rh rhodium

Sb antimony

SCM stromwater control measure

SEC size exclusion chromatography

SEP sequential extraction procedure

SO_4^{2-} sulfate

SQID stormwater quality improvement device

SS63 fine suspended solids $<63\,\mu$m

SUDS sustainable urban drainage system

$SUVA_{254}$ specific UV absorbance at 254 nm

TN total nitrogen

TOrCs trace organic contaminants

TSS total suspended solids

TPH total petroleum hydrocarbons

TWP tire wear particle

UVA_{254} UV absorbance at 254 nm

W tungsten

WSUD water sensitive urban design

Zn zinc

1 General introduction

1.1 Problem definition

Increasing impervious cover in urban areas alters hydrology and consequently the transport of sediment, nutrients, and pollutants, originating from traffic areas, building materials and other land uses (Grimm et al., 2008; Sheldon et al., 2019). These contaminants accumulate on impervious surfaces, and are washed off into receiving water bodies during rainfall events. The altering of urban water bodies results in low biodiversity, high concentrations of contaminants and nutrients, and reduced nutrient retention (Grimm et al., 2008; Paul and Meyer, 2001; Walsh et al., 2005). Besides toxic effects to the environment, contaminants in stormwater can as well pose a risk to human health (Bartlett et al., 2012a; Bartlett et al., 2012b; Ma et al., 2016; Jayarathne et al., 2018; Zgheib et al., 2011b).

Increasing vehicle ownership has led globally to a rise in traffic volume and related traffic-generated contaminants (Goonetilleke et al., 2017). As a consequence, vehicular traffic is one of the most important source of contaminants in the environment, especially in urban areas, and can pose a significant threat to the environment and human health (Goonetilleke et al., 2017; Ma et al., 2016). The contaminants accumulate in road-deposited sediments (RDSs) during dry periods on the road surface, and are washed off by road runoff during rainfall events (Goonetilleke and Lampard, 2019; Zafra et al., 2017) into receiving water bodies and the roadside environment. Consequently, road runoff is one significant non-point source of contaminants, which needs to be treated appropriately to mitigate detrimental effects on the environment (Huber et al., 2016c; Kayhanian et al., 2012a; Bannerman et al., 1993).

Within this thesis the term road runoff was used. However, traffic-area runoff exhibits comparable properties. It also considers runoff from parking areas and other impervious surfaces, such as reloading sites with considerable movement of vehicles.

1.1.1 Contaminants in road runoff

The priority contaminants in road runoff are heavy metals and polycyclic aromatic hydrocarbons (PAHs) due to their occurrence, persistence and toxicity (Zgheib et

al., 2011b; Ma et al., 2017; Järup, 2003; Chen and Liao, 2006; Fu and Wang, 2011). Heavy metals describe metals with a density from 3.5 $g\,cm^{-3}$ to 5 $g\,cm^{-3}$. Although 'heavy metals' is the most common term, there is no coherent basis (Duffus, 2002). More specific terms are 'toxic metals' or 'trace metals', which are as well associated with problems (Alloway, 2013). As a consequence, the term 'heavy metals' was used within this thesis due to the common use. Heavy metals can be separated into two groups: trace or micro nutrients, which are essential for the metabolism of animals, microorganisms and plants (e.g. iron (Fe), manganese (Mn), chromium (Cr), copper (Cu), nickel (Ni), and zinc (Zn)), and elements which are not essential for the metabolism, such as lead (Pb), cadmium (Cd), mercury (Hg) (Blume et al., 2016a, p. 496). However, higher concentrations of numerous heavy metals show toxic effects (Gautam et al., 2014; RÖMPP-Redaktion and Blaß, 2016). An overview of the classification is given in Table 1.1.

Most previous studies analyzed the heavy metals Cd, Cr, Cu, Ni, Pb and Zn due to their occurrence in road runoff (Kayhanian et al., 2012a; Huber et al., 2016c; Zgheib et al., 2011a). These metals are among the priority pollutant metals defined by the U.S. Environmental Protection Agency, based on a potential hazard to human health (National Research Council, 2003).

The partition of heavy metals (dissolved or particulate-bound) is element-dependent and affected by various runoff parameters: pH, ionic strength, alkalinity, redox conditions, particulate matter, dissolved organic matter (DOM) (Huber et al., 2016c; Zgheib et al., 2011b; Kayhanian et al., 2012a; Sansalone and Buchberger, 1997; Transportation Research Board, 2014; Revitt and Morrison, 1987). Ni and Cd are predominantly found in the dissolved fraction, Cu and Zn show an intermediate behavior, and Cr and Pb are mostly particulate-bound (Huber et al., 2016c).
Besides heavy metals, other contaminants, such as PAHs, total petroleum hydrocarbons (TPH), pesticides, and other trace organic contaminants (TOrCs) are detected in stormwater and road runoff (Eriksson et al., 2007; Zgheib et al., 2011a; Masoner et al., 2019; Kayhanian et al., 2012a; Spahr et al., 2020; Fairbairn et al., 2018). PAHs are the main organic contaminants (Loganathan et al., 2013), and are predominantly found in the particulate phase (Zgheib et al., 2011b). The distribution of the individual PAHs is depending on their source (Pengchai et al., 2005).

If de-icing salts are applied on roads for snow and ice control, these are another source of contaminants. The most common de-icing salts are the chloride salts calcium chloride ($CaCl_2$), magnesium chloride ($MgCl_2$), and sodium chloride (NaCl) (Fay and Shi, 2012; Huber et al., 2015b). The main contaminant of concern associated with de-icing salts is chloride (Cl^-), which can be present in concentrations causing acute toxicity to aquatic organisms and plants (Huber et al., 2015b; Schuler and Relyea, 2018; Bartlett et al., 2012b). Furthermore, de-icing salts can increase the

Tab. 1.1. Classification of a selection of heavy metals as essential or toxic for animals and plants, adapted from Merian (1984) cited in RÖMPP-Redaktion and Blaß (2016)

Element	Essential for animals	Essential for plants	Toxic for animals	Toxic for plants
Cadmium			•	•
Chromium	•			
Cobalt	•			
Copper	•	•	•	•
Iron	•	•		
Lead			•	•
Manganese	•	•		•
Mercury			•	•
Molybdenum	•	•	•	
Nickel	•			•
Platinum				•
Tin	•			
Vanadium	•	•		
Zinc	•	•		•

mobility and consequently the bioavailability of heavy metals present in road runoff (Schuler and Relyea, 2018; Acosta et al., 2011). In addition, ferric ferrocyanide and sodium ferrocyanide are common anti-caking agents added to de-icing salts, which are water soluble and can be a source of toxic free cyanide after exposure to sunlight (Novotny et al., 1998; Paschka et al., 1999; Field et al., 1973).

Besides the aforementioned contaminants, nutrients (nitrogen, phosphorus), which are present in traffic-area runoff (Kayhanian et al., 2007; Zhang et al., 2019a; Zgheib et al., 2011b; Lucke et al., 2018), can be of concern, if the receiving water bodies are prone to eutrophication (Clark and Pitt, 1999).

In Table 1.2 the concentrations of relevant contaminants found in road runoff are summarized.

The main focus of this thesis are suspended solids, since most relevant contaminants are found predominately in the particulate phase and heavy metals in the dissolved and particulate phase. In addition, nutrients and other contaminants, which have minor relevance and legal requirements, are also covered incidentally.

Tab. 1.2. Concentrations of relevant contaminants in road runoff, reported as median total concentrations unless otherwise stated. Values in parentheses are dissolved concentrations. Definitions of total suspended solids (TSS), TPH, and PAHs used in the studies can vary.

Site	AADT[a]	Source	TSS	Cd	Cr	Cu	Ni	Pb	Zn	Cl^-	TPH	PAHs
			$mg\,L^{-1}$	$\mu g\,L^{-1}$	$\mu g\,L^{-1}$	$\mu g\,L^{-1}$	$\mu g\,L^{-1}$	$\mu g\,L^{-1}$	$\mu g\,L^{-1}$	$mg\,L^{-1}$	$mg\,L^{-1}$	$\mu g\,L^{-1}$
Highway	1,800–328,000	[1]	59.1	0.44 (0.13)	5.8 (2.2)	21.1 (10.2)	7.7 (3.4)	12.7 (1.2)	111 (40.4)	4.3–9,000[b]	1.4	
Road	>15,000	[2]		2 (0.6)	12.9 (3.0)	86.9 (23.0)	9.8 (10.5)	44.5 (4.0)	351 (78.3)			
Highway	45,000–85,600	[3]		0.25[c] (0.14)[c]		120[c] 21[c]		18.2[c] 1.2[c]	355[c] 79.7[c]		1.13[c]	3.46[c] (0.09)[c]
Highway	5,000–200,000	[4]	139	0.29 (0.13)	3.82 (4.08)	43.0 (23.3)	7.10 (2.74)	9.5 (0.55)	140 (58.3)	5.0–9,760[b]	4.82	3.33 (0.25)

[1] Kayhanian et al. (2007), [2] Huber et al. (2016c), [3] Grotehusmann et al. (2014), [4] Crabtree et al. (2008)

[a] annual average daily trafficy

[b] range reported instead of median due to the strong seasonality

[c] mean of flow weighted annual averages of three sites

1.1.2 Contaminant Sources

Most contaminants, present in road runoff, originate from multiple sources (Table 1.3). In addition, most contaminants are particulate bound (Zgheib et al., 2011b). Thus, RDS contribute significantly to the contamination of traffic-area runoff, because RDS is washed off into the surrounding environment and receiving waters during rainfall events (Zafra et al., 2017; Wijesiri et al., 2016). Hong et al. (2020) were able to quantify contributions of different sources to the contamination of RDS. They reported that 33 $\pm$ 26% of RDS mass comprises of tire wear particles (TWPs), which contributes to 28 $\pm$ 25% of the Zn content. Brake linings contribute 59 $\pm$ 30% of the Cu content in RDS, and gasoline engine exhaust is the main source of Cr (29 $\pm$ 28%) and Ni (20 $\pm$ 23%). Since RDS are washed off by road runoff, similar contributions can be expected for traffic-area runoff.

Based on a literature review, Huber and Helmreich (2016) were able to approximate the annual traffic-related heavy metal emission in Germany. According to this study, 0.92 t a^{-1} Cd, 935 t a^{-1} Cu, 84.4 t a^{-1} Pb, and 2094 t a^{-1} Zn are emitted every year in Germany due to traffic. The main sources were brake wear for Cu and Pb, tire wear for Zn, and de-icing salts for Cd.

There are numerous factors affecting road runoff quality: traffic volume, antecedent dry period, rain event characteristics (precipitation height, intensity, and duration), previous rain event characteristics, climatic factors, land-use, road surface, road design, and road sweeping (Opher and Friedler, 2010; Horstmeyer et al., 2016). Analyses of roadside soil (of vegetated infiltration swales) indicate that especially stop-and-go areas, roundabouts, crossings and areas in proximity to road infrastructure like traffic lights, signs and guardrails, show a high contamination level (Horstmeyer et al., 2016; Huber et al., 2016c).

Currently, tire wear has gained attention in the course of the growing awareness of microplastics in the environment (Wagner et al., 2018; Vogelsang et al., 2019; Järlskog et al., 2020; Kim and Lee, 2018; Liu et al., 2019; Lassen et al., 2015; Pant and Harrison, 2013; Kreider et al., 2010; Essel et al., 2015; Wik and Dave, 2009; Wik et al., 2008). TWP and bitumen worn off the surface of asphalt roads are one major source of microplastics in the environment (Järlskog et al., 2020; Vogelsang et al., 2019). Another source are road paint markings (Vogelsang et al., 2019). Wagner et al. (2018) estimated that in Germany 133 000 t a^{-1} TWP are generated due to traffic.

Furthermore, there are various sources of TOrCs for traffic-area runoff, such as corrosion inhibitors, flame retardants, plasticizers, and pesticides (Spahr et al., 2020; Burant et al., 2018; Zgheib et al., 2011a). These can appear distant from their origin due to atmospheric transport and deposition (Burant et al., 2018). However,

Gasperi et al. (2014) conclude that the contribution of atmospheric deposition is low because of high local emission by urban surfaces, buildings and vehicles.

1.1.3 Toxicity

Results of various toxicity tests indicate that road runoff and RDS shows toxic effects (Kayhanian et al., 2008b; Jayarathne et al., 2018; Bartlett et al., 2012a; Bartlett et al., 2012b).

Especially the first flush, which describes elevated contaminant loads discharged in the beginning of a runoff event, exhibits high toxicity, whereas most composite samples of runoff events show no toxicity to freshwater test species (Kayhanian et al., 2008b; Strecker et al., 2005). Kayhanian et al. (2008b) identified Cu and Zn as the main sources of toxicity, however, they were not able to attribute further toxic effects to other contaminants. This finding is supported by Schiff et al. (2002). In contrast, Bartlett et al. (2012a) found no relation between concentrations of heavy metals and PAHs with observed toxicity caused by water and sediment samples of a stormwater management pond, although the concentrations exceeded threshold values and effect levels. Subsequently, they identified Cl^-, which is applied with de-icing salt, as the main cause of toxicity (Bartlett et al., 2012b). Another study also observed no toxic effects by water samples of stormwater ponds and sedimentation tanks (Karlsson et al., 2010). However, they demonstrated that sediments trapped in the treatment facilities exhibit toxic effects. Furthermore, increasing organic contents in the sediments resulted in higher toxicity. In contrast, DOM can decrease bioavailability and consequently toxicity of heavy metals (Koukal et al., 2003; Lorenzo et al., 2002; Luider et al., 2004). Jayarathne et al. (2018) stated that the heavy metals in RDS pose mostly a low ecological risk. Human health risk assessment indicated that heavy metals in RDS pose a low non-cancer health risk. The observed ranking of non-cancer risk associated with the respective heavy metals was Pb > Cu > Cr > Zn > Ni > Cd. Only Cr showed carcinogenic risk. This is supported by the findings of Chen et al. (2019). Gautam et al. (2014) give a comprehensive overview over the adverse health effects caused by heavy metals in water. Ingestion is the most important pathway of heavy metals in RDS for humans, followed by dermal contact and inhalation (Hou et al., 2019). Besides traffic-related emissions, industrial activities in the area can significantly affect pollution and hence the risk associated with it (Hou et al., 2019).

Regardless of the partly contradicting results of toxicity studies, emission of heavy metals into the environment must be limited due to the fact that these contaminants do not decompose in contrast to organic pollutants and consequently accumulate in the environment (Blume et al., 2016a; National Research Council,

Tab. 1.3. Sources of contaminants found in road runoff, adapted from Müller et al. (2020), Huber (2016), Ball et al. (1998), Van Wezel et al. (2009), and Vogelsang et al. (2019)

Source	Contaminants
Vehicle operation and wear	
Anti-freeze and hydraulic fluids	Total petroleum hydrocarbons (TPH)
Batteries	Cadmium (Cd), nickel (Ni), zinc (Zn)
Body paint	Lead (Pb)
Brakes	Total suspended solids (TSS), Cd, Cu, manganese (Mn), Ni, Pb, antimony (Sb), Zn, polycyclic aromatic hydrocarbons (PAHs)
Catalytic converters	Palladium (Pd), platinum (Pt), rhodium (Rh)
Electronic equipment	Cu, Ni
Engine and vehicle body	Cu, chromium (Cr), iron (Fe), Mn, Ni, Zn
Exhaust gases and particles	TPH, polycyclic aromatic hydrocarbons (PAHs), nitrogen oxides, Mn, Ni, Pb [a], benzene, toluene, ethylbenzene, and the three xylene isomers (BTEX)
Fuel	TPH, ethyl tert-butyl ether (ETBE), methyl tert-butyl ether (MTBE), Cd, Mn, Ni, Pb [a]
Oil and grease	TPH, Ni, Pb, Zn
Tires	TSS, Cd, Cu, Mn, Sb, Zn, PAHs, microplastics
Tire studs	Tungsten (W)
Wheel balance weights	Fe, Pb, Zn
Vehicle washing	
Commercial car washing facilities	Cd, Cr, Pb, Zn, phthalates, nonylphenols, nonylphenol ethoxylates
Road abrasion	
Abrasion by tires (non-studded and studded)	TSS, PAHs, microplastics
Asphalt surfaces	PAHs, nickel (Ni), microplastics
Concrete surfaces	Calcium (Ca)
Road paint markings	Microplastics
Road infrastructure (e.g. guard rails, road signs)	Fe, Zn
De-icing salts	Sodium (Na), Ca, chloride (Cl^-), sulfate (SO_4^{2-}), cyanides, Cd
Atmopsheric deposition	TSS, nitrogen (N), phosphorus (P)
Roadside Fertilizer	N, P
Pesticides	Cu, Cd, trace organic contaminants (TOrCs)

[a] Leaded gasoline was phased out during the last decades (Huber et al., 2016c)

2003; Gautam et al., 2014). Furthermore, the bioavailable fraction of heavy metals can increase, if conditions (e.g., redox conditions and pH) in the stormwater quality improvement devices (SQIDs) or environment change (Karlsson et al., 2010).

Besides heavy metals, PAHs pose as well as significant threat to the environment and human health, because these substances increase the carcinogenic risk (Burkart et al., 2013; Chen and Liao, 2006). The assessment of risk associated with PAHs is challenging, since PAHs describe a group of substances with varying toxicity. Liu et al. (2016) highlighted that PAHs with high molecular weight (4–6 rings) are associated with a higher risk. Thus, it is suggested to report not only the sum of PAH concentrations.

The assessment of toxicity caused by TOrCs in stormwater is still a challenge due to the complex chemical mixtures. Yet, previous studies indicate a significant contribution to toxicity of contaminated runoff in addition to conventional contaminants, e.g. heavy metals, PAHs (Spahr et al., 2020).

Another aspect, which have not sufficiently investigated yet, is the impact of contaminants present in road runoff on microbial communities. Recent studies indicate that aquatic microbial communities are affected by heavy metal contamination (Liu et al., 2020; Wang et al., 2020), which can foster the selection of antibiotic resistant bacteria (Baker-Austin et al., 2006; Almakki et al., 2019).

1.1.4 Legal requirements in Germany

In Germany, there are currently no consistent national legal requirements for the management of stormwater pollution (Helmreich and Rommel, 2020). Road runoff is not specified as a waste water category in the ordinance for discharge of waste water (*Abwasserverordnung*, AbwV (2020)). Consequently, there are no national legal requirements for treatment of it. However, the Water Resources Law (*Wasserhaushaltsgesetz*, WHG (2020)) defines road runoff as waste water, which must be treated according to the state of the art to avoid deterioration of the water quality. The state of the art is mainly specified in technical guidelines, which differentiate between urban and non-urban areas. In urban areas, the technical guidelines *DWA-M 153* (2007), *DWA-A 138-1 (Entwurf)* (2020) and DWA-A/M 102 (*e. g. DWA-A 102-1/BWK-A 3-1* (2020)) describe appropriate measures. Decentralized stormwater treatment will be further described in DWA-M 179. In non-urban areas, the technical guideline *RAS-Ew* (2005) is applied and in water protection areas the guideline *RiStWag* (2016).

Depending on the water body, threshold values for the pollution of water bodies are defined in the Surface Water Ordinance (*Oberflächengewässerverordnung*, OGewV (2016)) or Groundwater Ordinance (*Grundwasserverordnung*, GrwV (2017)).

If infiltration of treated road runoff poses a threat to the groundwater quality can be evaluated based on the Federal Soil Protection and Contaminated Sites Ordinance (*Bundes-Bodenschutz- und Altlastenverordnung*, BBodSchV (2020)) according to Ettinger et al. (2018). It must be emphasized that the BBodSchV limits contamination of groundwater *e. g.* by infiltration of treated road runoff, whereas the GrwV assesses the condition of the groundwater volume.

Further legal requirements at the level of the federal states exist, but are not presented in the scope of this thesis.

An overview of the threshold values for heavy metal contamination in water bodies can be found in Table 1.5. The Geringfügigkeitsschwellenwerte (GFS), insignificance threshold values, are not a legal requirement, though they can be used as criteria to assess, if adverse effects can occur due to the impact on the groundwater. The GFS are based on the Predicted No Effect Concentration (PNEC), and thereby the ecotoxic and humanotoxic effects of road runoff can be assessed (Moll and Quadflieg, 2014; LAWA, 2016). The effects of dilution and potential percolation pathways need to be considered, since they can reduce contaminant concentrations (Ettinger et al., 2018). Further information about the GFS and their application can be found in Rösel et al. (2020).

Tab. 1.5. German threshold values for heavy metal contamination in receiving waters, concentrations in $\mu g\,L^{-1}$

	Cd	Cr	Cu	Ni	Pb	Zn	Water body
BBodSchV (2020), exposure pathway soil-groundwater	5	50	50	50	25	500	Groundwater
GrwV (2017)	0.5	-[a]	-[a]	-[a]	10	-[a]	Groundwater
LAWA (2016)[*], GFS	0.3	3.4	5.4	7	1.2	60	Groundwater
OGewV (2016), annual average	0.08–0.25[b, c]	-[d]	-[d]	4[c,e]	1.2[c,e]	-[d]	Surface water[f]
OGewV (2016), permitted maximum concentration	0.45–1.5[b, c]	-	-	34[c]	14[c]	-	Surface water[f]

[*] This document is not a legal requirement

[a] No value specified, however reference to other sources like LAWA (2016) is possible; [b] depending on water hardness; [c] dissolved concentration; [d] only value for suspended solids and sediment are specified; [e] bioavailable fraction determined with appropriate models; [f] excluding saline surface waters

1.2 State of the art

To mitigate the detrimental effects of urban development on natural waters, urban planning have been increasingly considered aspects of water sensitive urban design (WSUD) since the 1980s (Radcliffe, 2019). The main aims of WSUD can be summarized by the following bullet points (Radcliffe, 2019; Sheldon et al., 2019; Boller, 2004; Dierkes et al., 2015):

- Management of stormwater quality
- Reduce the risk of flooding
- Restore the natural water cycle by decentralized infiltration
- Reuse of stormwater for potable and nonpotable use
- Reduce the heat island effect by plantation and enhanced evaporation
- Improve aesthetics of the urban environment

To manage stormwater quality, source control measures are applied to avoid diffuse spreading of contaminants (Boller, 2004), which comprise a variety of measures: e.g. street sweeping and litter control, permeable pavements, catch basin inserts, gross pollutant traps, detention ponds or tanks, hydrodynamic separators, oil-water separators, biofilters, constructed wetlands, and stormwater quality improvement devices (SQIDs) or manufactured treatment devices (MTDs) (Hoban, 2019; Strecker et al., 2005; Transportation Research Board and National Academies of Sciences, Engineering, and Medicine, 2012). SQIDs are one promising decentralized treatment option in space-constrained urban settings due to their small footprint and mostly multi-process treatment, which can retain a variety of contaminants (Huber et al., 2015a; Transportation Research Board and National Academies of Sciences, Engineering, and Medicine, 2012).

Because the terminology in the field of stormwater management is diverse, Fletcher et al. (2015) summarized the currently used terms. This thesis focuses on SQIDs or MTDs due to their increasing relevance. While most SQIDs are MTDs, the term MTD only includes manufactured systems. For example, systems which share a comparable functionality and footprint to MTDs, but are constructed from commonly available pre-cast parts, are only included by the term SQID. Consequently, this term was used, since it closely describes the studied treatment systems and their functionality. Other decentralized treatment systems like bioretention systems and permeable pavements (PPs) are not considered. However, most of the knowledge can also be applied to other systems.

1.2.1 Stormwater quality improvement devices

Common SQIDs can be categorized into three types: catch basin inserts, filter substratum channels and shaft systems (Huber et al., 2015a). The SQIDs are designed in dependence on the receiving water and local legal requirements (*cf.* Section 1.1.4 and 1.2.4). Discharge of treated runoff into surface waters generally sets lower requirements than infiltration into the groundwater.

Most catch basin inserts solely separate particulate matter, though some designs also utilize media filtration for further particle separation and retention of dissolved contaminants (Figure 1.1, B). Filter substratum channels (Figure 1.1, C) use direct media filtration with various media to retain particulate-bound and dissolved contaminants. The most common SQIDs are shaft systems (Figure 1.1, A), which can be either one-stage devices enabling solely particle separation or two-stage devices with subsequent media filtration after primary treatment. Filter substratum channels have typically the largest ratio of filter surface to drainage area, resulting in a larger footprint. Currently, only one catch basin insert is approved by the Deutsches Institut für Bautechnik (DIBt) to treat road runoff for infiltration into the groundwater.

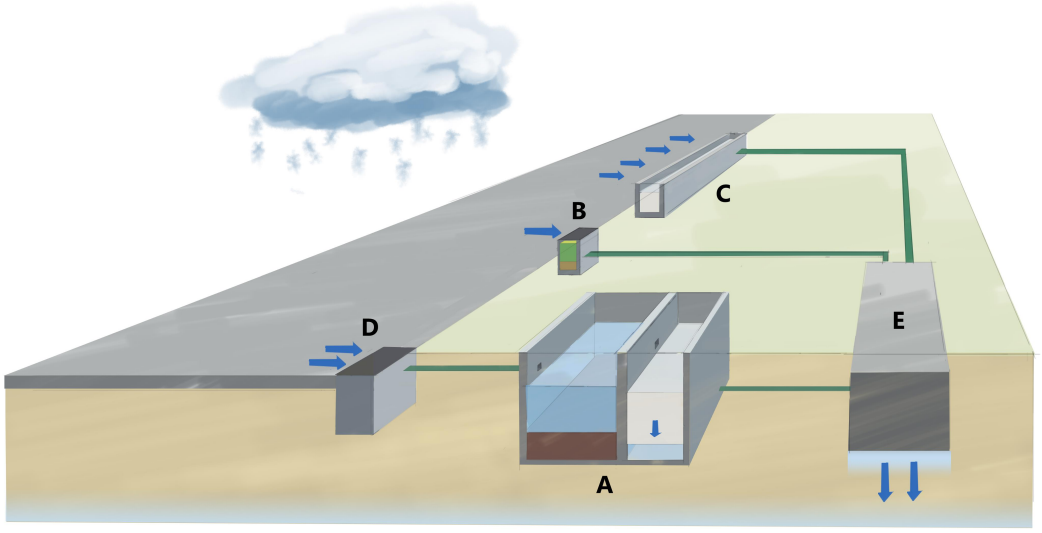

Fig. 1.1. Sketch of different types of SQIDs treating road runoff, A is a two-stage SQID with a primary sedimentation stage and subsequent media filtration stage, B is a catch basin with treatment insert, C is a filter substratum channel, D is a simple catch basin without treatment except for coarse screening, in this example all SQIDs discharge into an infiltration unit (E) to infiltrate the treated runoff into the groundwater. Besides infiltration into the groundwater, discharge into surface waters is another possibility.

Besides the aforementioned types, there exists as well oil separators. However, they are usually not regarded as SQIDs, since they are solely designed to retain oil, gross solids and coarse sediment (Transportation Research Board and National Academies

of Sciences, Engineering, and Medicine, 2012). Consequently, they offer a very limited treatment efficiency for other relevant contaminants (*cf.* Figure 1.7).

The treatment trains of the aforementioned SQID categories can be summarized by three designs (Huber et al., 2015a): basic treatment, two-stage treatment and direct media filtration (Figure 1.2). The utilized processes and related treatment components of SQIDs, as well as their treatment targets, are described in the following Section 1.2.2.

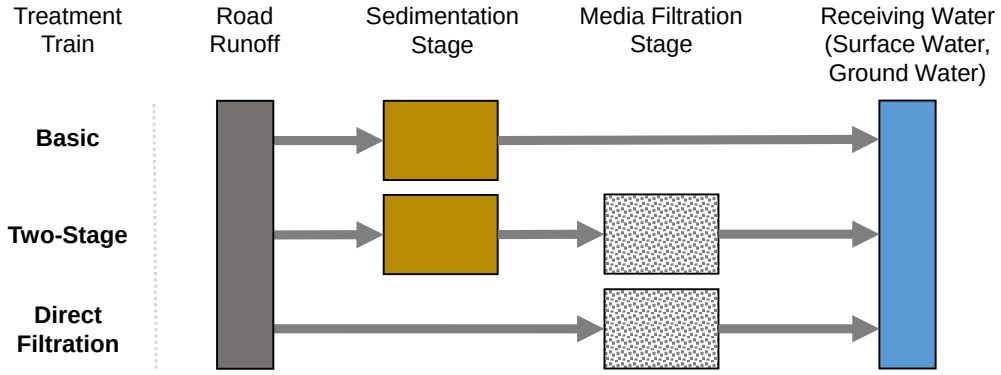

Fig. 1.2. Common treatment trains used in SQIDs

1.2.2 Treatment processes

Most SQIDs use a combination of multiple treatment processes. The most important processes belong to physical and chemical unit operations. In this section, the individual processes are described in detail. Table 1.6 summarizes treatment processes used in stormwater treatment, their targets and allocation to treatment stages or designs.

Screening Screening is a primary treatment process based on size exclusion. Screens separate solids (trash, debris) larger than the screen openings (Strecker et al., 2005). This process mainly aims to protect subsequent treatment stages (Strecker et al., 2005; Tchobanoglous et al., 2014). Screening devices can be nets or screens (Transportation Research Board and National Academies of Sciences, Engineering, and Medicine, 2012), which are able to separate solids up to one third of the size of the screen openings (Strecker et al., 2005). To avoid clogging and minimize headloss caused by a screen, it must be cleaned frequently (Strecker et al., 2005).

Filtration Filtration is another process based on size exclusion (Strecker et al., 2005). In storm water treatment, filtration is utilized to retain fine particles, which are difficult to remove by sedimentation (Transportation Research Board and National Academies of Sciences, Engineering, and Medicine, 2012). Filters remove particles either on their surface by straining (surface filtration) or with depth (depth filtration) in the filter media (Strecker et al., 2005). The depth-filtration involves multiple processes: straining, sedimentation within the filter, impaction, interception by the filter medium, adhesion to filter medium, flocculation within the filter medium and removal by the aforementioned processes (Tchobanoglous et al., 2014). Because the particles are trapped in the pore space of the media, the head loss of the filter increases over time and can clog (Transportation Research Board and National Academies of Sciences, Engineering, and Medicine, 2012). Consequently, filters need to be washed or replaced after a certain time.

If surface filtration or depth-filtration is the predominant mechanism can be evaluated based on the particle diameter of the filter medium (d_m, mass-based median) and the particle diameter in the runoff (d_p, mass-based median). If $d_m/d_p < 10$, the major mechanism is surface filtration. And if $20 > d_m/d_p > 10$, the mechanism is depth-filtration (Teng and Sansalone, 2004; Strecker et al., 2005).

Depending on the used filter medium, filtration stages utilize also other processes, such as sorption, precipitation, microbially-mediated transformation (Strecker et al., 2005), which are explained in the following paragraphs and the paragraph about media filtration. Sorption is the predominant process, if $d_m/d_p > 20$ (Teng and Sansalone, 2004).

Sedimentation Sedimentation is the most common unit operation in storm water treatment. It separates suspended particles from water by gravity separation, which is driven by gravity and the difference of density of the particles and water (Strecker et al., 2005). The terms sedimentation and settling are synonyms (Tchobanoglous et al., 2014). Under quiescent conditions, the terminal settling velocity of spherical particles in the laminar region can be determined by Stoke's law, following Eqauation 1.1 (Sansalone et al., 2009):

$$v_t = \frac{g\,(\rho_s - \rho_f)\,d^2}{18\eta_f} \tag{1.1}$$

where g = gravitational acceleration (9.81 m s^{-2}), η_f = dynamic viscosity of the fluid (kg m^{-1} s^{-1}), ρ_f = density of the fluid (kg m^{-3}), ρ_s = density of the particle (kg m^{-3}), and d = particle diameter (m). Equation 1.2 is only applicable for laminar

flow, indicated by a Reynold's number (Re) < 1 (Tchobanoglous et al., 2014), thus Re needs to be calculated afterwards following Equation 1.2,

$$\mathrm{Re} = \frac{\mathrm{v_t d}}{\nu_\mathrm{f}} \tag{1.2}$$

where ν_f = kinematic viscosity of the fluid ($\mathrm{m^2\ s^{-1}}$).

From Equation 1.1 the main influencing factors for sedimentation can be derived: particle density, particle size, fluid density and fluid viscosity. The particle density and size distribution is site-specific, particle density can vary with respect to particle size (Kayhanian et al., 2012b). Density and viscosity of the fluid, in this context water, are mainly functions of temperature (Kell, 1975; Laliberté and Cooper, 2004; Laliberté, 2007). Furthermore, particle shape affects settling (Tchobanoglous et al., 2014).

There exists as well explicit formulas, which are sufficient to determine settling velocity in the entire subcritical region ($Re < 2 \times 10^5$), e.g. as proposed by Cheng (2009). This enables a more straightforward implementation of terminal settling velocity calculation.

The simplest form to quantify particulate retention is the surface overflow theory, which determines the terminal settling velocity of the critical design particle for a settling unit design v_c, following Equation 1.3 (Strecker et al., 2005),

$$\mathrm{v_c} = \frac{\mathrm{Q}}{\mathrm{A}} \tag{1.3}$$

where Q ($\mathrm{m^3\ s^{-1}}$) = flow rate and A ($\mathrm{m^2}$) = surface of the sedimentation unit. All particles which have a $v_t > v_c$ are retained in the sedimentation unit. However, this a very simplified approach. In practice, non-ideal conditions occur due to turbulence, short circuiting, and sediment storage, which can reduce particle separation (Tchobanoglous et al., 2014). In order to evaluate these non-ideal conditions and complex shapes of the settling units, more complex computational fluid dynamics (CFD) models need to be applied (e.g. Spelman and Sansalone (2018)).

The aforementioned sedimentation process describes discrete settling (type I settling). Yet, other types of settling exist. Above TSS concentrations of $200\,\mathrm{mg\,L^{-1}}$, particle interactions resulting in so called flocculent settling (type II) (Strecker et al., 2005; Sansalone et al., 2009). Under conditions where flocculent settling occurs, discrete particles form larger flocs with differing settling properties. The floc size depends on TSS, which determines collision frequency, hydrodynamic shear forces, and the strength of cohesive forces on the particle surfaces, which depened on multiple properties, such as mineralogy of the particles, surface properties, and the

ionic strength of the water (Sansalone et al., 2009). Flocculent settling depends on the depth of the settling unit (Ying and Sansalone, 2011; Strecker et al., 2005).

If the TSS concentration increases to $>500\,\mathrm{mg\,L^{-1}}$ to $1000\,\mathrm{mg\,L^{-1}}$, hindered settling (type III) arises. Particle interactions hinder settling of surrounding particles, thus particles remain in proximity to each other and settle as a unit (Strecker et al., 2005; Tchobanoglous et al., 2014). Compressed settling occurs, if the particles already formed a structure due to the high TSS concentration. Type III and IV appears at the bottom of settling units, and type IV is important for the resistance of retained sediments against scouring, because it increases shear strength of the sediment (Strecker et al., 2005).

Besides conventional sedimentation units, hydrodynamic separators exist, which are designed to generate a vortex, which separates trash, debris and sediment in the center of the vortex (Strecker et al., 2005).

Because particle retention by sedimentation units is a function of hydraulic properties, they need to be designed with caution, especially with respect to maximum flow capacity. Otherwise scouring can occur. Hence, manufacturers limit the flow by orifices or bypasses (Strecker et al., 2005). However, without further treatment discharge of untreated runoff via a bypass is not allowed in Germany, depending on the receiving water and water authority (Dierkes et al., 2015).

Flotation and skimming Like sedimentation, flotation is a process of density separation. It utilizes the fact that solids and liquids of a lower density than water float on the surface (Strecker et al., 2005). The floating solids and liquids, especially petroleum hydrocarbons and grease, are then separated by baffles (Transportation Research Board and National Academies of Sciences, Engineering, and Medicine, 2012). Commonly this process is used in oil-water separators, but it can be implemented in sedimentation stages.

Sorption The term sorption includes multiple processes occurring at interfaces between solid, and solution phases. It describes an enrichment of dissolved ions or molecules at the surface of solids, which are called sorbents (Blume et al., 2016b, p. 136). In the context of stormwater treatment sorption is used to retain dissolved heavy metals, nutrients and organic contaminants (Strecker et al., 2005). The adsorbed substance is denominated as sorbate. The inverse processes is named desorption. Sorption can be further specified by the interaction forces between the sorbate and surface of the sorbent. Ion exchange describes the adsorption process based on electrostatic forces. It interaction is relatively weak, but the process is fast. In addition it is easily reversible. Stronger bonds occur, if the sorbate and the surface of the sorbent form a coordinative bond, this is called specific adsorption or

chemisorption. This bond is strong, but often much slower, especially desorption. Some adsorbed metal ions can precipitate on mineral surfaces, and thereby form a solid phase. This process is called surface precipitation. Organic molecules can be adsorbed as well by formation of hydrogen bonds or hydrophobic interactions (Blume et al., 2016b, p. 136). The previously described processes are difficult to differentiate (Brezonik and Arnold, 2011, p. 526), thus the more general term sorption is used within this thesis. It includes as well absorption, the transfer of a substance into the solid phase of the sorbent, which can be hard to distinguish from surface processes in the context of natural systems (Worch, 2012b; Brezonik and Arnold, 2011).

Desorption occurs if the properties of the solution change, for example concentration, temperature or pH (Worch, 2012b). Desorption is generally much slower than sorption, therefore sorption is described as partly irreversible (Zhou and Haynes, 2010). Potential explanations of this phenomena are a shift of the sorbate to stronger complexation sites and/or diffusion into the sorbent (Blume et al., 2016b; Zhou and Haynes, 2010; McBride, 2000).

The sorption capacity is determined by the surface characteristics (charge density, reactivity, hydrophobicity), and by the surface area and roughness (Blume et al., 2016b, p. 137). Surfaces charges of solids are caused mainly by two effects. First, isomorphic substitution, which describes the substitution of metal centers in hydrous oxides by a different metal with lower charge, resulting in a net negative charge of the surface. Secondly, ionizable function groups present on the surface, such as hydroxy ($-$OH), carboxylic($-$COOH), amino ($-NH_2$), phosphate ($-OPO(OH)_2$), thiol ($-$SH) groups (Brezonik and Arnold, 2011, p. 520f).

The isomorphic substitution causes a permanent charge (Blume et al., 2016b, p. 139f). In contrast, the charge caused by ionizable functional groups are pH depended. At low pH, the surface charge is more positively charged and more negatively at high pH. The pH, at which the sum of negative equals the positive charges is named point of zero charge and is one important sorbent property (Worch, 2012a). This protonation/deprotonation process on the sorbent surface can be exemplary described by the following equations 1.4 and 1.5, where $\equiv$S is the surface of a sorbent featuring a hydroxy group (Worch, 2012a). As a consequence of the variable, pH-depended surface charge, the sorption affinity is also variable.

$$\equiv S-OH + H^+ \rightleftharpoons \equiv S-OH_2{}^+ \tag{1.4}$$

$$\equiv S-OH \rightleftharpoons \equiv S-O^- + H^+ \tag{1.5}$$

In order to design processes using sorption, knowledge about the capacity and kinetics of the filter media is viable. This knowledge is primarily gained by batch experiments or column experiments. Sorption capacity is determined by sorption isotherms, which describe the relation between content of the adsorbed sorbent and the concentration in the liquid phase at specified experimental conditions. The most common isotherms in the context of stormwater treatment are the linear, Langmuir and Freundlich isotherm (Tedoldi et al., 2019). The isotherms are described according to Equation 1.6 to 1.8:

$$q_{eq} = K_d c_{eq} \tag{1.6}$$

$$q_{eq} = K_f c_{eq}^{n} \tag{1.7}$$

$$q_{eq} = \frac{q_m K_L c_{eq}}{1 + K_L c_{eq}} \tag{1.8}$$

where q_{eq} is the adsorbed concentration of the sorbate in equilibrium in $\mathrm{mg\,kg^{-1}}$, c_{eq} is the equilibrium concentration of the sorbate in solution in $\mathrm{mg\,L^{-1}}$, K_d is the constant distribution coefficient in $\mathrm{L\,kg^{-1}}$, K_f is the Freundlich coefficient in $\mathrm{mg^{1-n}kg^{-1}L^{n}}$, n is the unit-less shape parameter, which is commonly <1, q_m is the maximum sorption capacity $\mathrm{mg\,kg^{-1}}$, and K_L is the Langmuir coefficient in $\mathrm{L\,kg^{-1}}$ (Blume et al., 2016b; Tedoldi et al., 2019). The coefficients K_d, K_f and K_L reflect the affinity of a sorbate to a sorbent.

The Freundlich and Langmuir isotherm are both able to describe a decreasing sorption affinity with increasing sorbate concentration (Blume et al., 2016b, p. 149f). However, only the Langmuir isotherm can reflect a sorption maximum (Figure 1.3). The simple linear isotherm is often only applicable for low concentration ranges and certain contaminants (Tedoldi et al., 2019).

Because these experimental conditions can differ from the conditions present in the full-scale SQIDs, the retention efficiency between lab-scale and full-scale can differ. Potential deviations can derive from following parameters: contact time, liquid to solid ratio, which is the ratio between mass of the solution and the sorbent, agitation, and water quality. Factors affecting water quality are the pH, ionic strength, alkalinity, concentration of contaminants and their partition, other competitive constituents, such as de-icing salts and DOM (Tedoldi et al., 2019; Huber et al., 2016a; Genç-Fuhrman et al., 2016; Barrett et al., 2014; Huber et al., 2016b). As a consequence of the limited capacity of the sorptive media, it must be replaced before the capacity is exhausted to ensure sufficient treatment (Strecker et al., 2005).

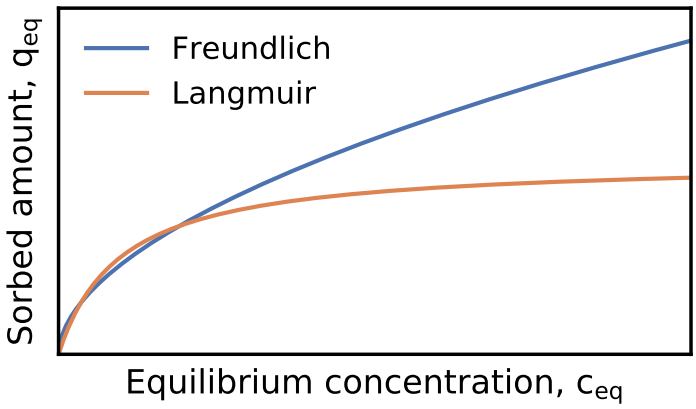

Fig. 1.3. Comparison of the Freundlich and Langmuir isotherms

If the utilized medium uses ion exchange, it must be emphasized that different ions are released, when ions are removed. Most of them are uncritical, but Clark and Pitt (1999) noted that for example sulfate, potassium or sodium are released, which increase water hardness (Strecker et al., 2005). However, this is only problematic, if the ecosystem of the receiving water is sensitive to increasing water hardness. Furthermore, this effect can potentially be used to regenerate the sorptive filter medium (Wang and Peng, 2010).

Precipitation Precipitation describes the process of a dissolved constituent forming a solid (Brezonik and Arnold, 2011). The speciation of metal ions in solution is significantly determined by precipitation processes (Transportation Research Board, 2014). The degree of precipitation is depending on the concentration of the involved species and other water constituents, which determine the ionic strength and pH of the solution (Brezonik and Arnold, 2011; Transportation Research Board, 2014). pH is the main influencing factor, because it determines the OH^- concentration and affects the concentration of other ligands by acid/base reactions (Transportation Research Board, 2014). The fate and transport of heavy metals can be controlled by precipitation of metal hydroxides, oxides, carbonates, and sulfates. Equation 1.9 and 1.10 show exemplary two solubility reactions of copper (Transportation Research Board, 2014).

$$CuCO_3(s) \rightleftharpoons Cu^{2+} + {CO_3}^{2-} \tag{1.9}$$

$$Cu(OH)_2(s) \rightleftharpoons Cu^{2+} + 2\,OH^- \tag{1.10}$$

If precipitation of a substance occurs, can be evaluated based on the ion activity product (IAP) and the solubility product constant K_{sp} or the saturation index (SI), which is derived from the aforementioned values (Brezonik and Arnold, 2011; Blume et al., 2016b).

The precipitates can be subsequently retained by sedimentation or filtration in the storm water treatment train.

Genç-Fuhrman et al. (2007) showed that precipitation can dominate sorption in batch experiments assessing filter media for SQIDs and therefore needs to be considered in the experiment design and interpretation of the results. Furthermore, they presented plots illustrating the speciation of the relevant heavy metals with respect to pH. These can be utilized to estimate heavy metal speciation, however speciation is highly depending on the solution constituents and therefore can vary significantly. Thus, speciation of each solution needs to be calculated. Two common geochemical modeling softwares are PHREEQC (Parkhurst and Appelo, 2013) and VisualMINTEQ (Gustafsson, 2014a), which can further model sorption, amongst other processes.

Microbially-mediated transformation Besides the previously described physical and chemical processes involved in storm water treatment, microbially-mediated transformation can remove or convert dissolved nutrients, metals and organic compounds (Strecker et al., 2005). However, the transformation is relatively slow and consequently demands long residence times, which are mostly not feasible in SQIDs. Thus, biological processes are commonly of minor importance, except for green sustainable urban drainage system (SUDS) like biofilters and constructed wetlands (Transportation Research Board and National Academies of Sciences, Engineering, and Medicine, 2012), which also facilitate plant growth. Furthermore, uptake of organic and inorganic constituents by microbes is possible (Strecker et al., 2005). A selection of potential microbe functions are: oxidation of simple organic compounds, degradation of xenobiotic compounds, nitrification, denitrification, nitrogen fixation, and iron oxidation/reduction (Strecker et al., 2005).

Media filtration In stormwater treatment, fixed bed media filters are utilized to remove contaminants by multiple processes: retention of particles by entrapment and straining; depending on the media properties, dissolved contaminants are retained by surface complexation, sorption, precipitation and/or ion exchange. Furthermore, organic pollutants can be microbially degraded (Strecker et al., 2005; Dierkes et al., 2015; Transportation Research Board, 2014; Huber et al., 2015a). If additional storage volume exists above the filter media, surficial sedimentation can occur (Strecker et al., 2005). Depending on the design, the filter media can be

permanently submerged or dry-running in between the runoff events (Huber et al., 2015a).

The filter media need to fulfill multiple requirements (Transportation Research Board, 2014):

- Structural stability against degradation under varying condition (wetting/drying and oxic/anoxic)
- Sufficient hydraulic conductivity
- Effective filtration (particulate matter (PM) separation and slow clogging)
- Sorptive performance (capacity, kinetics, resistivity against remobilization/leaching)
- Operational (maintenance intervals, regeneration, disposal, cost)

Proposed filter media for SQIDs are limestone, carbonate-rich sand, manganese or iron oxide/hydroxide coated substrates, granular activated carbon, cementious media, perlite, zeolithe and organic/biogenic media like peat, lignite, and chitin/chitosan (Okaikue-Woodi et al., 2020; Transportation Research Board, 2014; Clark and Pitt, 1999; Liu et al., 2005). However, since biogenic-based material are degraded under in situ conditions, the use of such materials should be avoided, because metals and nurtients can be leached (Transportation Research Board, 2014). A comprehensive review of conventional and emerging media for storm water treatment can be found in Okaikue-Woodi et al. (2020).

Pretreatment before media filtration is strongly recommended to avoid premature clogging and consequently increase the service life (Clark and Pitt, 1999). Clark and Pitt (1999) stated that aged media filters perform better because of a potential build up of a biofilm, which enhance permanent retention of contaminants. In addition, no wash-out of small particles occurs during filtration by an aged filter (Clark and Pitt, 1999). Positive redox conditions should be maintained to assure stability of the media and sorbed heavy metals (Liu et al., 2005).

Tab. 1.6. Processes and treatment components involved in stormwater treatment trains of SQIDs, • indicates that the design includes the unit operation or process, (•) indicates a marginal influence of the unit operation or process, adapted from Strecker et al. (2005) and Transportation Research Board and National Academies of Sciences, Engineering, and Medicine (2012)

			Hydrodynamic separators	Settling Tanks	Fine Mesh Screens	Filter Fabric	Media Filters
		Typical location in treatment train [a]	P	P	P	P	P/S
Process category	**Unit operations or processes**	**Targets**					
Hydrological / Hydraulic	Flow attenuation	Peak reduction		(•)			
Physical	Screening	Trash, debris, coarse sediment	•		•		•*
	Flotation and Skimming	Trash, debris, oil & grease	•	•			
	Sedimentation	Sediment, debris, particulate bound conaminants and nutrients	•	•			
	Filtration	Sediment, debris, particulate bound conaminants and nutrients			•	•	•
	Sorption	Dissolved heavy metals, nutrients and organics				(•)	•
Chemical	Sorption	Dissolved heavy metals, nutrients, organics					•
	Ion exchange	Dissolved heavy metals and nutrients					•
	Precipitation	Dissolved heavy metals					•*
Biological	Microbially-mediated transformation	Dissolved nutrients, organics, heavy metals					(•)

[a] P, primary treatment; S, secondary treatment

* depends on filter medium

1.2.3 Factors influencing treatment efficiency

All treatment processes used in SQIDs (Section 1.2.2) underlie various influencing factors, which are described in the following. Figure 1.4 illustrates the relations and effects of the influencing factors.

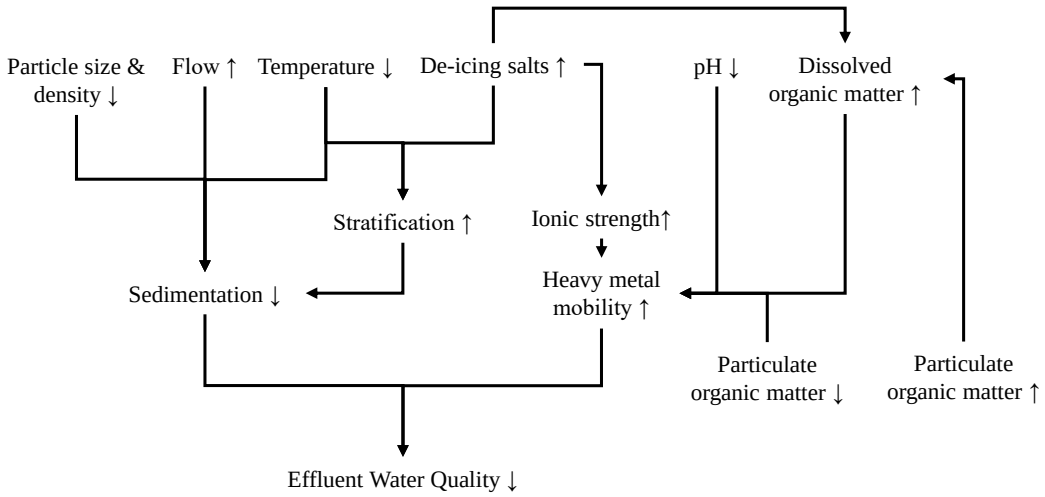

Fig. 1.4. Factors influencing the treatment efficiency of SQIDs, arrows next to the labels indicate an increasing (upwards arrow) or decreasing (downwards arrow) effect, concentration or value; the larger arrows show the relations of the factors

Temperature Water temperature determines water density and viscosity (Semadeni-Davies, 2006). Hence, low temperatures lead to reduced settling velocity and cause stratification in sedimentation stages. Consequently, lower treatment efficiency are achieved (Spelman and Sansalone, 2018; Roseen et al., 2009).

In addition, increasing temperature can increase sorption of dissolved heavy metals (Joseph et al., 2019). However, this phenomena is probably negligible in stormwater treatment, because only ambient temperatures occur in stormwater treatment in contrast to other applications.

pH Speciation, mobility and retention of heavy metals are severely affected by the pH value of water. While at neutral to low pH, heavy metals generally occur in their cationic state, at which they are soluble, and consequently mobile and bio-available (Joseph et al., 2019; Zhou and Haynes, 2010; Paulson and Amy, 1993). With increasing pH value, heavy metals form complexes with hydroxides and other anions, and finally tend to precipitate. At low pH, competitive sorption and repulsive charges of solid surfaces reduce heavy metal retention (Dijkstra et al., 2004). Sorption increases with increasing pH, because of deprotonation of surface

sites and more beneficial surface charges of (hydr)oxide minerals and organic matter (Dijkstra et al., 2004). One exception is the decreasing sorption of Cr, due to its occurrence as anionic species (e.g. $HCrO_4^{2-}$, CrO_4^{2-}), if pH increases (Joseph et al., 2019). At alkaline pH, inorganic and organic complexation of heavy metal cations in solution reduces sorption (Dijkstra et al., 2004). The common behavior of heavy metal solubility as a function of pH is illustrated in Figure 1.5.

The carbonate system mainly determines the pH value in natural waters by dissolution/precipitation of calcium carbonate (Brezonik and Arnold, 2011). Furthermore, it is closely related to the acid neutralizing capacity or alkalinity of water. Phosphate, silicate and humic substances also increase alkalinity (Brezonik and Arnold, 2011).

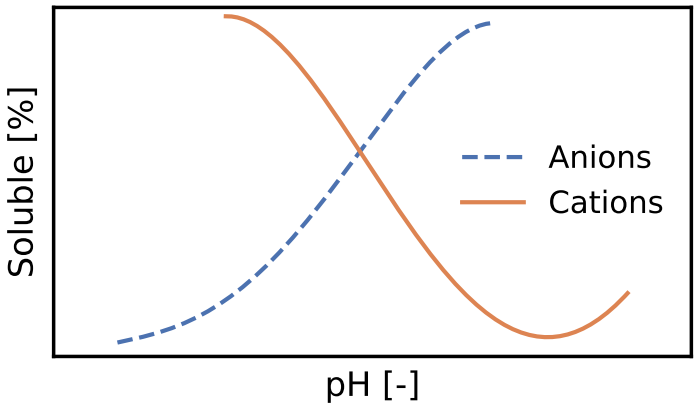

Fig. 1.5. Common adsorptive and precipitative behavior of heavy metal cations and anions as a function of pH, adapted from Bourg and Loch (1995)

Ionic strength, de-icing salts Ionic strength can have various effects affecting sorption as well as desorption of heavy metals: change of solution pH with increasing ionic strength, competitive sorption between heavy metal cations and major cations in solution, changes of the activity of free heavy metals due to ion pair formation with anions (e.g. Cl^-, SO_4^{2-}), and changes of surface charge of the sorbent (Zhou and Haynes, 2010). In NaCl solutions a strong decreasing adsorption of heavy metals on oxide and hydroxide surfaces has been observed with increasing ionic strength (Criscenti and Sverjensky, 1999). Whereas no effect of the ionic strength of $NaNO_3$ solutions on adsorption of heavy metals was observed. In areas with the risk of snowfall and ice, de-icing salts ($CaCl_2$, $MgCl_2$, NaCl) are applied to assure safe traffic (Fay and Shi, 2012; Huber et al., 2015b). The effects of de-icing salts on dissolved heavy metals are closely related to ionic strength, since de-icing salts significantly increase ionic strength of road runoff (Huber et al., 2016a). Competitive

sorption of heavy metals and major cations Na^+, Mg^{2+}, and Ca^{2+}, as well as formation of chloride complexes can lead to reduced sorption and even remoblization of particulate-bound heavy metals (Bäckström et al., 2004b; Huber et al., 2016b; Acosta et al., 2011; Schuler and Relyea, 2018; Kumar et al., 2013a). In addition, de-icing salts promote release of DOM, which increases mobility of heavy metals, as described below (Nelson et al., 2009).

Another effect caused by de-icing salts is an increase of density and viscosity of water in sedimentation stages, resulting in reduced settling velocity and stratification, which consequently reduce treatment efficiency (Semadeni-Davies, 2006; Roseen et al., 2009).

Particle properties Particle size distribution (PSD) and particle density are the main factors influencing settling of particles (Ying and Sansalone, 2011; Tchobanoglous et al., 2014). Decreasing particle size and density reduce settling velocity, which results in lower treatment efficiency. In addition, particles in RDS show irregular shapes, which reduce settling velocity (Kayhanian et al., 2012b; Tchobanoglous et al., 2014). Smaller particles commonly show higher heavy metal concentrations (Kayhanian et al., 2012b; McKenzie et al., 2008), thus sedimentation stages of SQIDs need to enable high hydraulic residence times to consider the low settling velocity of RDS.

Furthermore, particles present in road runoff (RDS) can affect the partition of heavy metals, because they exhibit a high sorption capacity (Zhang et al., 2019b). As a result, mobility and retention of heavy metals are affected. Sorption capacity of RDS is related to the specific surface area of the particles, their content of organic matter, oxides of Mn, Fe, and aluminum, and clay forming minerals (Gunawardana et al., 2014; Gunawardana et al., 2015; Taylor and Robertson, 2009).

Organic matter DOM is well-known to influence mobility and bioavailability of heavy metals by formation of complexes (Brezonik and Arnold, 2011; Blume et al., 2016b). The treatment efficiency of SQIDs can be potentially affected by multiple processes: competitive sorption of DOM and dissolved heavy metals, reduced sorption of DOM-heavy metal complexes on sorptive filter media, DOM-heavy metal complexes adsorb strongly to sorptive media, dissolved heavy metals adsorb on previously adsorbed DOM on filter media (Haynes, 2015). These effects have not been comprehensively studied yet in SQIDs. However, results of lab-scale experiments showed reduced heavy metal retention in the prescence of DOM (Genç-Fuhrman et al., 2016; Charbonnet et al., 2019; Barrett et al., 2014).

As indicated in the paragraph about particle properties, particulate organic matter can increase sorption of dissolved heavy metals on RDS (Gunawardana

et al., 2014; Gunawardana et al., 2015), which potentially increases retention of heavy metals in SQIDs. Furthermore, it must be considered that DOM leaches from particulate organic matter (Kumar et al., 2013a).

Organic matter (particulate and dissolved) is prone to microbial degradation, which can alter binding sites availability and consequently heavy metal mobility (Kumar, 2016; Kumar et al., 2013a). This phenomena is closely related to the redox condition which affects oxidation of organic matter (Blume et al., 2016b; Kumar et al., 2013b).

Hydraulic properties Hydraulic properties (flow and runoff volume) primarily affect sedimentation, since hydraulic retention time determines the treatment efficiency of sedimentation stages (Strecker et al., 2005; Tchobanoglous et al., 2014). Hence, flow needs to be limited to avoid scouring of captured sediments, which can lower the overall treatment efficiency of SQIDs (Strecker et al., 2005). This can be achieved by the installation of flow-splitters, which bypass runoff, if the design flow is exceeded.

Furthermore, increasing flow reduces the retention of dissolved heavy metals by media filtration due to shorter contact times in the sorptive media filter (Huber et al., 2016d).

Dry-wet cycles, redox conditions The impact of dry-wet cycles and redox conditions on the treatment efficiency of SQIDs has not been investigated yet. However, previous studies in related fields indicate a significant effect.

The heavy metal retention efficiency of biofilters decreases with increasing antecedent dry period (Blecken et al., 2009). The authors of this study attributed the reduced efficiency after drying of the filter media to worse treatment efficiency during the first rain event, leaching of heavy metals accumulated in the filter media and mobilization of (contaminated) fine sediment. However, the efficiency recovered fast after re-wetting of the filter media. Worse treatment efficiency after drying can be explained by shorter retention time due to preferential flow paths in the filter media after formation of small fissures (Hatt et al., 2007). Nevertheless, the increasing infiltration capacity after drying can be beneficial to assure long-lasting hydraulic performance of the system. In constrast to the results of Blecken et al. (2009), Hatt et al. (2007) observed no effect of dry-wet cycles on heavy metal retention by biofilters.

In SQIDs, redox conditions are dominated by inorganic species (*e. g.*, Fe, sulfur) and biological processes (*e. g.*, respiration, denitrification), which can establish anoxic conditions, especially in subsurface treatment systems (Okaikue-Woodi et al., 2020). This is relevant for the treatment efficiency, since heavy metal mobility is

affected by the redox conditions (Young, 2013; Blume et al., 2016a). For example, Fe and Mn oxides, which are used as filter media in SQIDs, can dissolve under reducing conditions, which results in a release of sorbed heavy metals (Young, 2013). Hence, Liu et al. (2005) stated that positive redox conditions (oxidizing) need to be maintained to assure stability of filter media. Consequently, permanently submerged anoxic zones in SQIDs, like suggested by Blecken et al. (2009), should be critically evaluated, especially if filter media contain Fe and Mn oxides. However, if nitrogen removal is the treatment goal of the SQID, anoxic conditions are promising, since they enhance denitrification (Blecken et al., 2009). Besides Fe and Mn, Cr is known to be affected by redox conditions present in natural waters (Bourg and Loch, 1995). However, it shows an opposing behavior with decreasing solubility at reducing conditions. The mobility of other heavy metals is mainly indirectly affected by redox conditions in dependence of the availability of complexing agents (Fe and Mn (hydr)oxides) and redox-sensitive anions (e.g., reduced sulfur forms), which can cause precipitation (Bourg and Loch, 1995). Furthermore, microbial degradation and oxidation of organic matter is affected by redox conditions (Blume et al., 2016b; Kumar et al., 2013b).

1.2.4 Treatment efficiency and evaluation

The required treatment efficiency of SQIDs is generally derived from local regulations. For instance, SQIDs with approval of the DIBt are currently designed to achieve effluent quality in accordance with the trigger values of the German Federal Soil Protection and Contaminated Sites Ordinance, BBodSchV (2020) (Ettinger et al., 2018). These devices are designed to treat the runoff prior to infiltration into the groundwater (DIBt, 2017), hence the requirements are stricter in contrast to the LANUV protocol, which sets the requirements for discharge into surface waters in the state North Rhine-Westphalia (LANUV, 2012). The German technical guidelines for drainage of urban areas into surface waters (*DWA-A 102-2/BWK-A 3-2* 2020) and infiltration into the groundwater (*DWA-A 138-1 (Entwurf)* 2020) consider the treatment efficiency of fine suspended solids $<63\,\mu$m (SS63) by DIBt approved SQIDs with 80%. Furthermore, the *DWA-A 138-1 (Entwurf)* (2020) considers the treatment efficiency of dissolved heavy metals (Cu and Zn) with 65 to 75% in dependence of the catchment category. Longer distances of percolation can reduce the requirements.

In the US exist multiple state and multi-state approaches to evaluate SQIDs (Water Environment Federation, 2014). To overcome this barrier, the National Stormwater Testing and Evaluation for Products and Practices (STEPP) Initiative formed, which develops currently a national testing and evaluation program for

stromwater control measures (SCMs) and SQIDs. To given an overview of treatment goals for SQIDs, Table 1.7 summarizes various international evaluation protocols. The protocols of British Water (n.d.) and Stormwater Australia (2018) were added for completeness, even though they do not state required removal efficiencies.

As illustrated in Figure 1.6, the number of SQID approvals per year based on field or lab tests is increasing, which reflects the increasing interest in SQIDs and the awareness that treatment efficiency needs to be evaluated using comparable evaluation protocols.

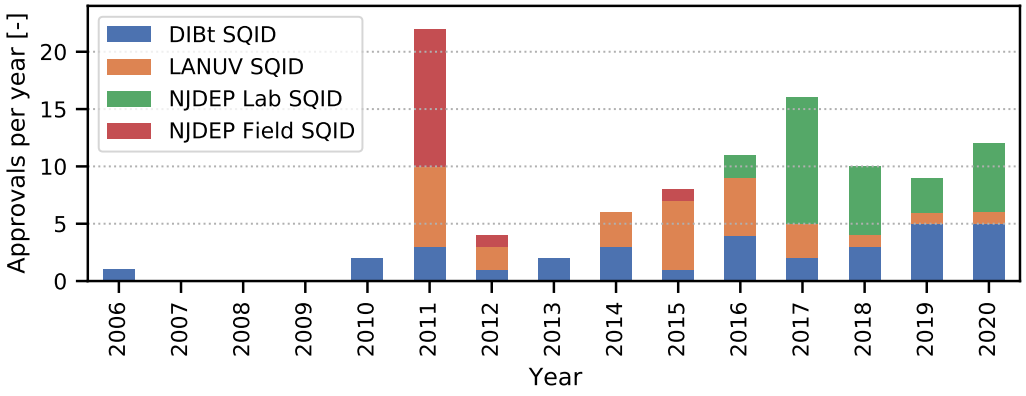

Fig. 1.6. Approvals of SQIDs per year, adapted from Huber (2016). Devices can appear multiple times, if they were approved again. The approvals were differentiated by the institutions, which approved or certified the SQIDs: Deutsches Institut für Bautechnik (DIBt), Landesamt für Natur, Umwelt und Verbraucherschutz Nordrhein-Westfalen (LANUV), New Jersey Department of Environmental Protection (NJDEP); data: Huber (2016), DIBt (2020), LANUV (2020), NJDEP (2020a), and NJDEP (2020b).

Tab. 1.7. Required removal efficiency of TSS, TPH, Cu and Zn for SQIDs according to various international evaluation protocols, removal efficiency in percent removal unless other unit is stated, the determination of percent removal differ, adapted from Huber (2016) and Haile and Fürhacker (2017)

				Removal efficiency [%]					
Protocol	**Country**	**Test procedure***	**Test substances****	**TSS**	**TPH**	**Cu**	**Zn**	**Receiving water**	**Source**
ASTRA									
Class 1	CH	Field	TSS, Cu, Zn, DOC, PAH	<60 [a]		<60 [a]	<60 [a]	Groundwater, surface water	Steiner et al. (2010) and ASTRA (2013)
Class 2				60 [a]		60 [a]	60 [a]		
Class 3				70 [a]		70 [a]	70 [a]		
Class 4				80 [a]		80 [a]	80 [a]		
Class 5				>90 [a]		>90 [a]	>90 [a]		
DIBt	DE	Lab	TSS, TPH, Cu, Zn, NaCl	≥92 [a]	≥80 [a]	≥80 [a]	≥70 [a]	Groundwater	DIBt (2017)
BW	UK	Lab	TSS, Cu, Zn, NaCl					Groundwater, surface water	British Water (n.d.)
LANUV	DE	Lab	TSS	≥50				Surface water	LANUV (2012)

Continued on next page

Tab. 1.7 *Continued from previous page*

NJCAT									
Hydrodynamic sedimentation	US	Lab	TSS	≥50				Not specified	NJCAT (2013)
Filtration				≥80					
ÖNORM B 2506-3[b]	AT	Lab	TSS, TPH, Cu, Zn, Pb, NaCl	≥80	>95	>80[a]	>50[a]	Groundwater	*ÖNORM B 2506-3* (2018)
SQIDEP	AU	Field	Not specified					Not specified	Stormwater Australia (2018)
TAPE									
Pretreatment			TSS	>50[a]					
Basic	US	Field	TSS	≥80[a]				Groundwater, surface water	*WDOE* (2011)
Dissolved metals			Cu, Zn			>30	>60		
Oil treatment			TPH		<10 mg L^{-1} [a]				
VSA									
Standard	CH	Field	TSS, Cu, Zn, pesticides, NaCl	≥80		≥70	≥70	Not specified	*VSA* (2019)
Enhanced				≥90		≥90	≥90		

* additional field or lab tests can be required or optional, but the removal efficiency is assessed under the stated condition

** the methods for the determination of the substances can differ

[a] further treatment goals are specified, e.g. maximum concentrations of subsamples and/or limit for remobilization

[b] there are three different catchment categories defined in the protocol, only imprevious surfaces (e.g. road runoff) was considered

All aforementioned protocols state required removal efficiencies as percent removal. However, there exist various definitions to determine removal efficiency (Guo, 2017), which limits comparability of different performance evaluations. Frequently used definitions of removal efficiency are:

- Event mean concentration reduction for a single test of storm event
- Pollutant load reduction for a single test of storm event
- Pollutant load reduction for multiple tests or storm events
- Mean pollutant concentration removal efficiency
- Linear regression of line between inflow and outflow loads, the slope reflects the treatment efficiency
- Relative achievable removal efficiency
- Effluent water quality relative to water quality standard
- Effluent probability method

Especially if the evaluation is based on field monitoring data, there are numerous reasons against this criteria (International Stormwater BMP Database, 2007):

Percent removal is a function of the influent concentration, thus SQIDs with higher influent concentrations can achieve higher percent removals. Percent removal can vary significantly, although effluent quality is constantly good. There are numerous influencing factors on the removal efficiency, which can not be reflected by one value. Many contaminants show a non removable concentration, which can not be described by percent removal. Depending on the determination method, percent removal can be significantly biased by outliers. Depending on the number of samples, the effluent quality can not significantly differ from the influent quality; this can not be reflected by percent removal. SQIDs with low percent removal can still be sufficient for certain applications. Maximum concentrations can cause acute toxicity, this is not addressed by percent removal.

As a consequence in-situ treatment efficiency of SQIDs should not be evaluated based on percent removal. One promising alternative, which avoids most of the aforementioned issues, is the effluent probability method.

Based on an analysis of data retrieved from the International Stormwater BMP Database (Wright Water Engineers et al., 2020), all categories of treatment devices shown in Figure 1.7 achieve a significant TSS retention. Yet, media filters show a superior TSS retention to all other treatment systems (Figure 1.7a). Furthermore, all devices, which mainly use sedimentation as unit operation, show a minor retention

efficiency. In order to be able to compare the achieved removal efficiency of the analyzed devices to the requirements of the evaluation protocols (Table 1.7), the mean pollutant concentration removal efficiency was determined. Catch basin inserts achieved 40% TSS removal, hydrodynamic separators 53%, media filters 78% and oil/grit separatos and baffle boxes 42%. This emphasizes that there is a discrepancy between treatment goals and achieved treatment efficiency on site. Because TSS is a good indicator for particulate bound contaminants (Kayhanian et al., 2012a; Shinya et al., 2000), this tendency can be transferred to most heavy metals and PAHs. No device category showed a significant retention of dissolved Cu (Figure 1.7b), indicating that the retention of dissolved heavy metals is still a challenge, even for media filters. Even though, the media filters almost exhibited a significant retention of dissolved Cu. Because treatment efficiency of different filter media can differ greatly (Okaikue-Woodi et al., 2020), varying results can be expected, if media filters are grouped by their filter media. The considered categories belong to technical treatment systems, non-technical SUDSs were excluded.

Lastly, it must be highlighted that treatment efficiency of SQIDs is closely related to their maintenance. As summarized by Blecken et al. (2017), appropriate maintenance over the entire service life of SCMs is necessary to achieve good treatment performance. For SQIDs, the most important maintenance is withdrawal of sediments, since most contaminants are particulate-bound (*cf.* Section 1.1.1). The sediments can be scoured off, resulting in significant pollution of receiving waters. Furthermore, downstream media filtration stages can clog, which leads to a hydraulic overload of the SQID. Consequently, backwater can flood the catchment area or, if the design features an overflow, untreated road runoff is discharged. In addition, filter media needs to be replaced to ensure sufficient sorption capacity and hydraulic permeability.

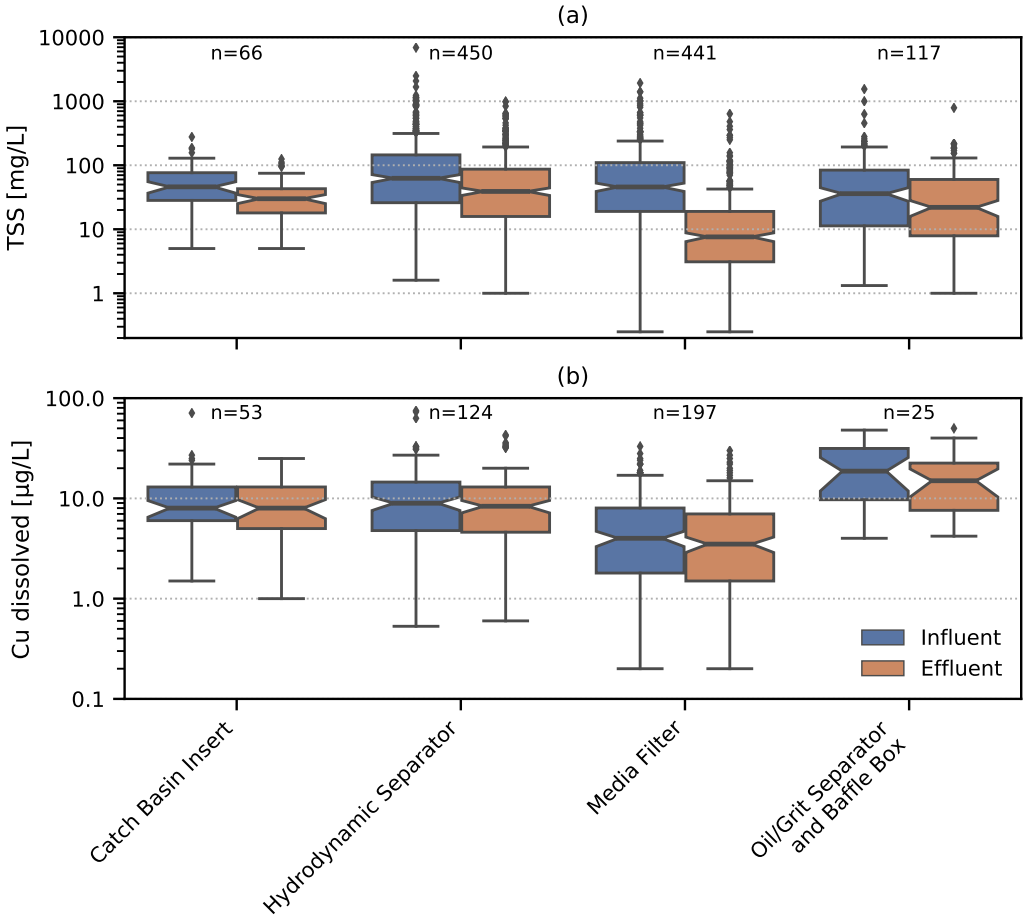

Fig. 1.7. (a) TSS and (b) dissolved Cu concentration in the influent and effluent of various technical storm water treatment systems, notches represent the 95% confidence interval around the median, only paired (influent and effluent sampled) data are shown, source: International Stormwater BMP Database, accessed at `www.bmpdatabase.org` on 2020-10-23

2 Research objectives and hypotheses

The increasing use and development of SQIDs require knowledge about factors influencing the retention of traffic-related contaminants. The scope of this dissertation was to describe and quantify factors, which affect treatment of road runoff in SQIDs. The key research topics were: (i) heavy metal leaching from RDS and filter media of SQIDs, (ii) investigate the effects of varying physico-chemical boundary conditions on the heavy metal fractionation and mobility in filter media, (iii) describe the occurrence, properties, and effects on heavy metal speciation of DOM in road runoff, and (iv) assess the impact of de-icing salt and low temperatures on sedimentation of particulate matter. The gained knowledge will enable a comprehensive evaluation of the contaminant retention performance of SQIDs and improves the basis for future performance tests and developments.

Figure 2.1 illustrates the positions of the respective research objectives in a SQID.

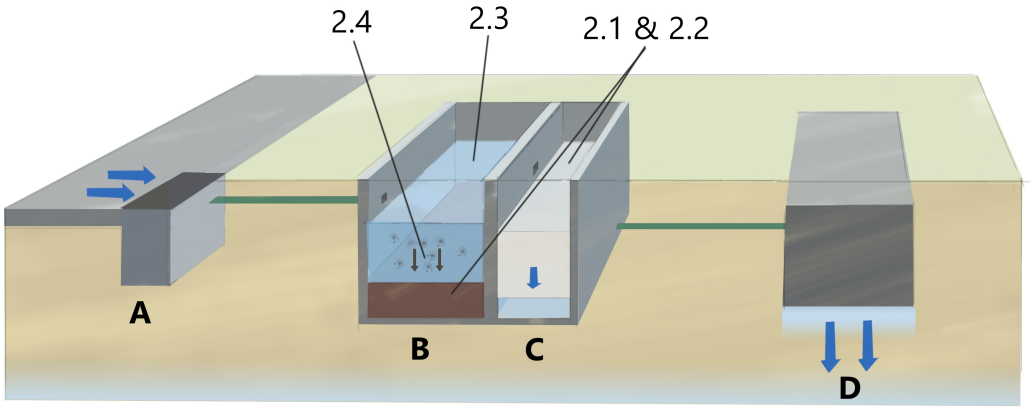

Fig. 2.1. Positions of the research objectives in a SQID, indicated by the section numbers (Section 2.1 to Section 2.4). A is a simple catch basin without treatment except for coarse screening, B is the sedimentation stage of a two-stage SQID, C is the media filtration stage and D is an infiltration unit to infiltrate the treated runoff into the groundwater. Besides infiltration into the groundwater, discharge into surface waters is another possibility.

2.1 Quantification of heavy metal leaching from road-deposited sediment and prestressed sorptive filter media during dry periods

Okaikue-Woodi et al. (2020) highlighted the need for characterization of leaching and desorption in stormwater treatment. Previous lab-scale experiments showed that heavy metals leach from sorptive filter media under the influence of de-icing salts (Huber et al., 2016b). Comparable findings have been reported for a constructed wetland as well (Tromp et al., 2012). Furthermore, previous studies showed the influence of DOM on heavy metal mobility (Kumar et al., 2013a; Transportation Research Board, 2014; Genç-Fuhrman et al., 2016; Zhang et al., 2016). Because contact times during dry periods are considerably longer, if filter media are permanently submerged, more intense leaching was expected during dry periods. Previous studies assessed leaching of heavy metals from RDS in rain water, which features a significantly different composition than road runoff in SQIDs (e.g. pH, ionic strength, alkalinity). Furthermore, the experiments of Huber et al. (2016b) assessed leaching from filter media, which reached their sorption capacity. If leaching occurs, it is not likely that filter media reach their capacity limit.

Given the limitations of previous studies, the first research objective was to quantify leaching of heavy metals from RDS and prestressed sorptive filter media during dry periods in SQIDs. The assumed leaching was studied based on the following hypothesis:

Research hypothesis 1 Remobilization of copper and zinc retained on commercially available filter media for stormwater quality improvement devices occurs (>5% within 7 d) during dry periods, if the filter media are permanently submerged.

To test this hypothesis, three filter media currently utilized in SQIDs were prestressed under lab-scale conditions to achieve realistic Cu and Zn contents in the filter media. Subsequently, dry periods were simulated by quiescent batch leaching experiment. In these experiments, the prestressed filter media were exposed to three different synthetic road runoffs, which reflect the composition of road runoff with and without DOM or de-icing salt (NaCl). After (4), 24, 48, and 168 h the leachates were sampled and analyzed to quantify the extent of leaching. The corresponding study is presented in Chapter 4.

2.2 Sequential extraction of heavy metals from road-deposited sediment and sorptive filter media prestressed in lab-scale experiments and full-scale operation

Currently, media filters utilized in SQIDs to retain heavy metals are increasingly tested in lab-scale experiments to assure comparability (Lucke et al., 2017; Haile and Fürhacker, 2017). However, most of the applied test protocols are not able to replicate all boundary conditions present in full-scale operation, e.g. runoff composition, dry-wet cycles, permanently submerged filter media (Huber et al., 2016d; Barrett et al., 2014; Monrabal-Martinez et al., 2017; Genç-Fuhrman et al., 2016; Haile and Fürhacker, 2017). Okaikue-Woodi et al. (2020) and Huber (2016) concluded that the chemical boundary conditions (e.g. pH, redox potential) and composition of stormwater (suspended solids, ionic strength, competing cations, dissolved organic carbon (DOC), microbes) significantly affect the performance of filter media. Furthermore, Okaikue-Woodi et al. (2020) concluded that there is a lack of research, which demonstrates that media filtration is feasible under real-world application.

Hence, it is unknown, if the involved treatment processes and their contribution to heavy metal retention are the comparable in lab-scale experiments and full-scale operation. Consequently, it is viable to determine the geochemical fractionation patterns of heavy metals in pre-stressed filter media of SQID to analyze the mobility and thereby to assess the risk of remobilization (Sutherland, 2010). To investigate the geochemical fractionation of heavy metals in filter media of SQIDs, the following hypothesis was formulated:

Research hypothesis 2 The geochemical fractionation of heavy metals retained on (sorptive) filter media of stormwater quality improvement devices is significantly different if the filter media are prestressed in lab-scale experiments or full-scale operation.

In order to test this hypothesis, three filter media used in SQIDs were prestressed in lab-scale experiments according to the current German technical approval protocol and in full-scale operation for 2.75 years at a highly trafficked road. These filter media were analyzed using sequential extraction to assess the geochemical fractionation and mobility of the heavy metals. Consequently, the impact of different boundary conditions can be assessed. This study is presented in Chapter 5.

2.3 Dissolved organic matter in road runoff - Occurrence, seasonal fluctuations and its impact on speciation of heavy metals

DOM is widely known to influence transport, fate and bioavailability of contaminants, like heavy metals and organic microcontaminants (Brezonik and Arnold, 2011; Artifon et al., 2019; Adusei-Gyamfi et al., 2019; Zhou and Haynes, 2010; Zhang et al., 2020). While DOM in natural water bodies and effluent of waste water treatment plants has been described comprehensively (Carstea et al., 2016; Ishii and Boyer, 2012; Fellman et al., 2010), DOM in road runoff has not been extensively described in the past. In order to estimate the effect of DOM on the retention of heavy metals in SQIDs, knowledge about occurrence, chemical properties and seasonal fluctuations are necessary. Recent studies showed that DOM decreases heavy metal retention by filter media in lab-scale experiments (Genç-Fuhrman et al., 2016; Charbonnet et al., 2019; Barrett et al., 2014). However, contradicting results have been reported as well (Ray et al., 2019).

To investigate DOM in road runoff with respect to occurrence, seasonality, degradation in SQIDs and its effect on heavy metal speciation, the following research hypothesis was developed:

Research hypothesis 3 (a) Occurrence of dissolved organic matter in road runoff shows strong seasonality and (b) affects the speciation of dissolved heavy metals.

To describe DOM, samples of untreated and treated road runoff were withdrawn in the course of approximately one year (Chapter 3). DOM occurence, properties and fluctuations were analyzed using UV-vis and fluorescence spectroscopy and size exclusion chromatography (SEC). The chemical equilibrium model Visual MINTEQ was used for the calculation of metal speciation and principal component analysis (PCA) was used to analyze the mutlivartiate data of the monitoring. The corresponding study is presented in Chapter 6.

2.4 Influence of temperature and de-icing salt on the sedimentation of particulate matter in traffic area runoff

Sedimentation is the primary process utilized in SQIDs and other SCMs to retain particulate-bound contaminants (Strecker et al., 2005; Huber et al., 2015a). How-

ever, studies have shown that in winter and spring the retention efficiency is reduced under the influence of de-icing salt (Roseen et al., 2009; Semadeni-Davies, 2006). Low temperatures, as well as de-icing salt, can reduce sedimentation efficiency by stratification leading to disadvantageous flow paths, reducing retention time, and increasing density and viscosity of the water in the sedimentation stage (Hendi et al., 2018; Adamsson and Bergdahl, 2006; Marsalek et al., 2003; Tchobanoglous et al., 2014). However, the influence of temperature and de-icing salt have not been quantified yet. To close this research gap, the influence of de-icing salt and temperature was evaluated based on following research hypothesis:

Research hypothesis 4 De-icing salt is the main influencing factor reducing sedimentation of particulate matter in stormwater quality improvement devices under winter conditions.

The analysis of monitoring data of a SQID showed that there are too many influencing factors affecting retention of particulate matter in full-scale application. Hence, a simplified physical settling model was developed to approximate and rank the effects caused by temperature and de-icing salts (Chapter 7). In a second study, lab-scale settling experiments were conducted, the previously model further developed and validated based on the experimental results (8). In addition, particle shape of RDS, which also affects sedimentation (Breakey et al., 2018; Tchobanoglous et al., 2014), was comprehensively analyzed and considered in the settling model. The studies addressing this topic can be found in the Chapters 7 and 8, which build on each other.

2.5 Dissertation structure

This dissertation is based on a cumulative collection of five research articles with major contribution as stated in A.1. Three of them are already peer-reviewed and published, two are submitted to the journals. The monitoring of full-scale SQIDs (Chapter 3) was the basis for deriving research hypotheses and withdrawing samples for the research objectives of this dissertation. However, the results of the monitoring have not been published yet due to confidentiality agreements.

In addition, three research articles were written with major or minor contribution within the time frame of this dissertation (A.1). These were not implemented, because they investigated other research topics.

The structure of the dissertation with the corresponding chapters, utilized methods, hypotheses and publications is shown in Figure 2.2.

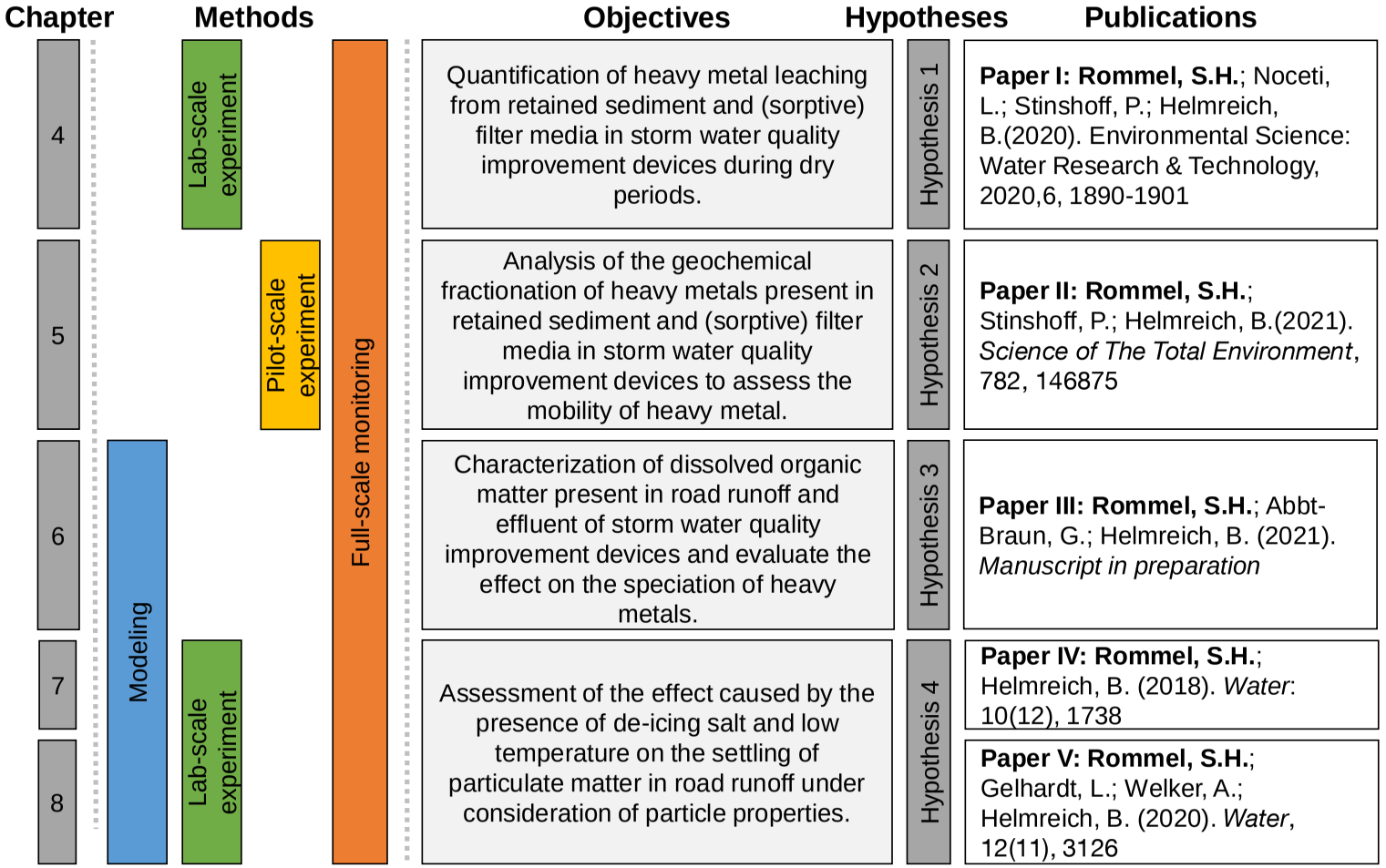

Fig. 2.2. Structure of the cumulative dissertation

3 Monitoring of full-scale stormwater quality improvement devices at a heavily trafficked road

3.1 Introduction

Stormwater quality improvement devices (SQIDs) approved by the DIBt have been installed for several years to treat road runoff (Rommel et al., 2020b). However, only a few scientific studies of field monitorings exist, especially concerning the service life, risk of clogging, as well as maintenance and operation of the devices (Barjenbruch et al., 2016; Pick and Fettig, 2009; Sonnenberg et al., 2019; Vesting, 2018; Werker et al., 2011). Furthermore, theses studies monitored SQIDs without DIBt approval. Besides the aforementioned studies, previous studies mainly focused on lab-scale tests, which are not able to reflect all boundaries conditions present in full-scale application, such as extreme rainfall, coarse particulate matter, street sweeping, organic matter. In addition, there is little knowledge about logistic and financial aspects of frequent use of SQIDs. Since treatment efficiency of SQIDs is influenced by sufficient maintenance (Blecken et al., 2017), these aspects are fundamental to assess the suitability of SQIDs. Furthermore, there is a knowledge gap about the presence of antiknock agents (ETBE, MTBE), cyanides contained in de-icing salts and fine suspended solids (SS63) in road runoff and effluent of SQIDs.

To close the aforementioned knowledge gaps, multiple SQIDs were monitored at a heavily trafficked road as suggested by Huber (2016). The results of the monitoring have not been published yet due to confidentiality agreements, hence this chapter describes the monitoring site as basis for the Chapters 4 to 7.

3.2 Materials and methods

To investigate the contamination of road runoff and the treatment efficiency of SQIDs under equal conditions, we installed four different SQIDs at a heavily trafficked

road in Munich, Germany (48.17940 latitude, 11.54018 longitude, WGS 84). The layout of the monitoring site is illustrated in Figure 3.1. The colorized areas (except green) indicate the different catchment areas of the SQIDs. Two traffic lanes, one accelerating lane and one emergency lane formed the cross-sections of all catchment areas. The material of the road surface was Stone Mastic Asphalt (SMA) and the annual average daily traffic (AADT) was approximately 24,000 vehicles per day. On the road in the opposing direction, an AADT of 22,000 vehicles per day was determined. However, the lanes of the opposing direction were separated from the catchment area by a greened median strip. Although an additional load on the catchment area was expected due to dry and wet deposition. Next to the road was a park located with lawns and trees. Especially in autumn, this increased the organic load due to fall of leaves.

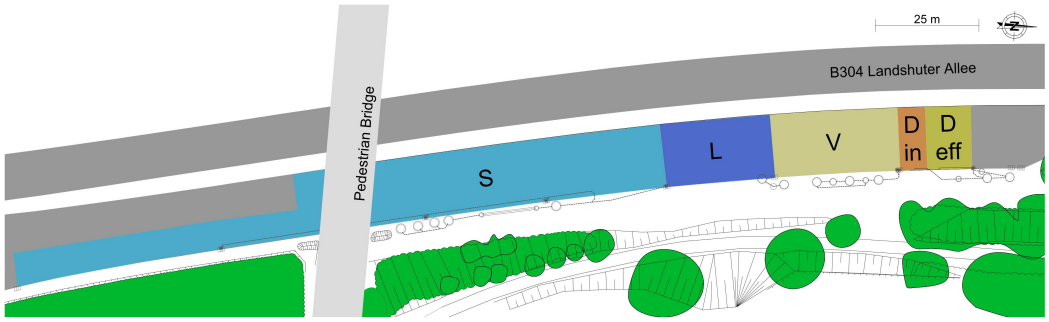

Fig. 3.1. Layout of the monitoring site in Munich, Germany. The different colors (except for green) indicate the catchments of the individual SQIDs. S was the SediSubstrator XL 600/12, Fränkische Rohrwerke; L was the individually designed SQID for the City of Munich; V was the ViaPlus 500 with upstream sedimentation shaft, Mall; D was the Drainfix Clean 300, Hauraton; *D in* indicates the catchment were influent samples of D were withdrawn and *D eff* the catchment of SQID D. Source of the layout: City of Munich.

On the monitoring site four different SQIDs were monitored. Three of the four devices (L, S, and V) were shaft systems and one was a filter substratum channel (H). All SQIDs except for L were DIBt approved systems. The SQIDs L, S and V achieved road runoff treatment by two-stage treatment trains with sedimentation stages and downstream media filtration. SQID D utilized direct media filtration. The used media and other characteristics of the SQIDs are summarized in Table 3.1. In contrast to the other SQIDs, only the filter media of SQID S was permanently submerged. Only D was installed on the surface, the other SQIDs were underground. All SQIDs discharged the treated road runoff into infiltration shafts, which facilitated percolation into the groundwater. Detailed flow schemes of the SQIDs can be found in A.4.

The samples of runoff events were withdrawn volume proportionally during rain events with automatic samplers (WaterSam WS 316, Edmund Bühler PP 84). The

Tab. 3.1. Characteristics of the monitored stormwater quality improvement devices (SQIDs)

SQID	D	L	S	V
Product name	Drainfix Clean 300	- [a]	SediSubstrator XL 600/12	ViaPlus 500
Manufacturer	Hauraton, Rastatt, Germany	- [a]	Fränkische Rohrwerke, Königsberg (Bayern), Germany	Mall, Donaueschingen, Germany
Catchment area	165 m^2 [b]	400 m^2	1660 m^2	473 m^2
Sedimentation stage	-	7.5 m^3	5.1 m^3	7.2 m^3 (additional upstream sedimentation shaft), hydrodynamic separator in SQID
Filter medium	Carbotec60, carbonate rich medium	Carbonate rich sand, after April 2019 Carbotec60 like SQID D	SediSorp plus, iron-based medium with lignite amendment	ViaSorp, zeolite

[a] Constructed from commonly available pre-cast concrete parts; [b] influent samples were withdrawn from a drainage channel without filter medium draining a 100 m^2 large catchment area next to the SQID

monitoring of the SQIDs D, S, and V started in November 2017 and ended at the end of October 2019. Sampling of SQID L was carried out from April 2016 to May 2020 with two interruptions. Influent and effluent samples were withdrawn. Monitoring of L was conducted The sampling was triggered by electro-magnetic flow meters (Optiflux 2300 C or 1300 C, IFC 300 C, Krohne Messtechnik, Duisburg, Germany, DN250 for S, DN40 for L and V, DN25 for D). The flow data were recorded with a frequency of 30 s. The sampling started, if the inflow exceeded the threshold value longer than 1 min. If the inflow was 15 min below the threshold value, sampling stopped. The threshold value was set to $0.4\,\mathrm{L\,s^{-1}\,ha^{-1}}$ discharge, based on the determined catchment areas. The samples were kept in coolers at $4 \pm 1\,^{\circ}\mathrm{C}$ prior to transportation to the lab and analysis. Composite samples per discharge event and sampling position were prepared using the discrete samples of each automatic sampler. The analytic methods are described in the respective chapters and their supplementary information.

3.3 Results

The results of the monitoring have not been published yet due to confidentiality agreements. However, the following research topics are based on the knowledge gained during the monitoring and several research questions were investigated using the data and samples of the full-scale monitoring.

4

Leaching potential of heavy metals from road-deposited sediment and sorptive media during dry periods in storm water quality improvement devices

This chapter has been previously published as follows:
Rommel, S. H., L. Noceti, P. Stinshoff, and B. Helmreich (2020d). "Leaching Potential of Heavy Metals from Road-Deposited Sediment and Sorptive Media during Dry Periods in Storm Water Quality Improvement Devices". *Environmental Science: Water Research & Technology* 6.7, pp. 1890–1901. DOI: 10.1039/D0EW00351D - Reproduced by permission of The Royal Society of Chemistry

Author contributions: Rommel, S. H.: conceptualization, methodology, validation, data curation, writing - original draft, writing - review & editing, visualization, supervision; Noceti, L.: investigation, data curation, visualization; Stinshoff, P.: methodology, investigation; Helmreich, B.: resources, writing - review & editing, supervision, project administration, funding acquisition.

† Supplementary information are available in A.2. Research data is available on Mendeley Data (Rommel et al., 2020c).

Abstract

Storm water quality improvement devices (SQIDs) mitigate the deteriorating effects of traffic-related contaminants, especially heavy metals. Many SQIDs consist of a settling tank to remove road-deposited sediments in the first treatment stage and dissolved heavy metals are removed by sorptive filtration in the second treatment stage. SQIDs are commonly operated under permanent impounding, resulting in

high hydraulic retention times. In this study, we evaluate the leaching potential during dry periods from road-deposited sediment trapped in the settling stage and from three different sorptive media of SQIDs. For this purpose, a new experimental procedure was developed using quiescent batch leaching tests. The sorptive media were pre-stressed with realistic Cu and Zn loads. Three different synthetic road runoffs were used to evaluate the influence of de-icing salts and dissolved organic matter. Strong leaching of heavy metals from road-deposited sediment was observed. In contrast to previous studies on the leaching of Zn from tire wear particles, the process showed limitation by saturation or precipitation after 24 h. Furthermore, no leaching from pre-stressed sorptive media was observed. This highlights that under in situ conditions, leaching from sorptive media is rather unlikely. However, design and operation of SQIDs should consider the leaching potential of road-deposited sediments.

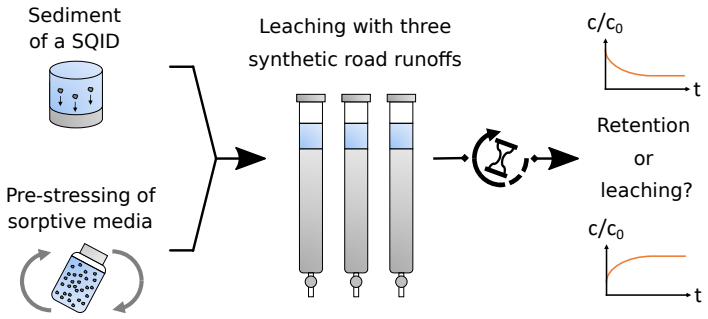

Fig. 4.1. Graphical Abstract of the experiments conducted to evaluate the leaching potential of heavy metals from road-deposited sediment and sorptive media during dry periods in SQIDs.

4.1 Introduction

Storm water quality improvement devices (SQIDs) are utilized to mitigate the deteriorating effects of traffic-related contaminants, especially heavy metals (i.e., Cd, Cu, Ni, Pb, and Zn) (Dierkes et al., 2015). Since most of the heavy metals are found in the particulate fraction (Kayhanian et al., 2012a), SQIDs use sedimentation as the primary treatment stage. In this stage, road-deposited sediment (RDS) is trapped and stored over a long period — mostly in permanently impounded compartments — until withdrawal and disposal during maintenance of the systems. RDS is a complex mixture of various sources, such as soils, atmospheric deposition, abrasion products of road surfaces and vehicles (tire wear particles (TWP), brake linings, etc.) and biogenic material (Loganathan et al., 2013; Sutherland and Tolosa, 2000).

The duration until removal of RDS from SQIDs can vary between months and years, depending on the maintenance schedule. Due to the high contact times, it was hypothesized that heavy-metal leaching would occur, especially since leaching of heavy metals was reported under percolation of roadside soils and RDS with considerably shorter contact times (Bäckström et al., 2004b; Kumar et al., 2013a; Nelson et al., 2009; Zafra et al., 2017).

In addition to the sedimentation stage, many SQIDs use a variety of sorptive filter media as a second treatment stage to retain dissolved heavy metals (Dierkes et al., 2015; Transportation Research Board, 2014; Haynes, 2015). The involved processes are precipitation followed by filtration of the precipitant, as well as sorption — including ion exchange, specific adsorption and surface precipitation (Transportation Research Board, 2014; Huber et al., 2016b; Huber et al., 2015a). Since sorption processes are often reversible (Blume et al., 2016b), desorption of heavy metals from the utilized media can occur under certain conditions (Transportation Research Board, 2014; Zhou and Haynes, 2010). However, desorption was observed to be slower than adsorption and in general sorption can be partly reversible (Zhou and Haynes, 2010). This sorption hysteresis is likely to be related to a shift from weaker to stronger complexation sites and/or diffusion of the adsorbed metals into the adsorbent (Blume et al., 2016b; Zhou and Haynes, 2010; McBride, 2000). Huber et al. (2016b) showed that leaching of heavy metals from sorptive media occurs in SQIDs during rain events under the influence of de-icing salts. Similar findings have been reported for a constructed wetland (Tromp et al., 2012). Additionally, dissolved organic matter (DOM) showed significant influence on the mobility of heavy metals (Kumar et al., 2013a; Transportation Research Board, 2014; Genç-Fuhrman et al., 2016; Zhang et al., 2016).

However, during a rain event, the contact time of the de-icing salt or DOM rich solution with the sorptive media is limited. It is evident that during dry periods, the contact time between the water matrix and the sorptive media is in orders of magnitude higher than during rain events. Thus, leaching should be more intense. However, no studies have yet covered leaching of heavy metals within SQIDs during dry periods with or without de-icing salt influence or under the influence of DOM. Previous studies focused on the leaching from RDS in rain water, which exhibits significantly different water characteristics such as acidic pH and low ionic strength or alkalinity in comparison to road runoff (Zafra et al., 2017). Thus, different results can be expected. Furthermore, the contact of storm water to building materials, such as concrete, will immediately increase pH and alkalinity, which is reproduced in our experiments.

The hypothesis of this paper is that heavy metals leach from sediment as well as from sorptive media in SQIDs during dry periods, if the systems operate with permanent impoundment.

To test that hypothesis, desorption needs to be quantified (Sun and Selim, 2019). While stirred-flow experiments are preferred to observe fast adsorption/desorption reactions (Sun and Selim, 2019), they may overestimate adsorption and desorption due to the reduced limitation by diffusion rates and do not reflect the realistic conditions in SQIDs during dry periods. Furthermore, re-adsorption of leached heavy metals and limitation of the leaching caused by an equilibrium state between the liquid and solid phase cannot be covered by stirred-flow experiments. Thus, quiescent batch leaching tests (without agitation) were conducted in this study to evaluate the leaching potential from RDS trapped in SQIDs and from three pre-stressed commercially available sorptive media during dry periods.

Throughout this paper, the term leaching is used, since it incorporates multiple processes such as desorption and dissolution, which can be hardly differentiable.

4.2 Materials and methods

4.2.1 Materials and chemicals

The examined sportive filter media were granular activated lignite (GAL, HOK© Activated Lignite, Rheinbraun Brennstoff GmbH, Germany), granular ferric hydroxide (GFH, FerroSorp©, HeGo Biotec GmbH, Germany), and zeolite (ZEO, ViaSorp©, Mall GmbH, Germany). The media were sieved to the fraction $>63\,\mu$m and GAL was additionally sieved to ≤ 2 mm, taking the heterogeneity of grain sizes into account.

Furthermore, sediment of a settling tank (SED) treating road runoff from a highly trafficked road with an annual average daily traffic (AADT) of approximately 24 000 vehicles per day for approximately two years was studied (Rommel and Helmreich, 2019b). The SED was sieved wet to ≤ 1 mm to remove unrepresentative trash and leaf debris. All materials were dried at 105 °C and stored in desiccators prior to the analyses. SED needed to be crushed to single grains with pestle and mortar. The physical and chemical characteristics of the materials before pre-stressing are summarized in Tables 4.1 and S1 in the ESI.†

Synthetic road runoff (SRR) was prepared based on the solution of the Transportation Research Board (2014) with $MgSO_4 \cdot 7\,H_2O$, KCl, KNO_3, $NaNO_3$, $CaCl_2$, $CuSO_4 \cdot 5\,H_2O$, $ZnSO_4 \cdot 7\,H_2O$ with the concentrations listed in Table 4.2. The alkalinity was adjusted by adding 97.3 mg L^{-1} $NaHCO_3$ based on own currently unpublished data, since the alkalinity suggested by the Transportation Research Board (2014) seemed to be considerably high. To simulate application of de-icing salt,

NaCl was added to the synthetic runoff (SRR + NaCl) for further experiments.11 Furthermore, experiments with synthetic runoff and DOM (SRR + DOM) were conducted by adding humic acid sodium salt 40–70% (CAS-No. 68131-04-4; Carl Roth, Germany). Preliminary dilution experiments determined a DOC concentration of 12.6 mg L^{-1} of the SRR +DOM (Fig. S1†). This concentration is in accordance with the median DOC in the highway runoff database (Granato and Cazenas, 2009). All constituents were mixed in deionized water (DI water) with an electrical conductivity (EC) $\leq 0.5\,\mu S\,cm^{-1}$ with a magnetic stirrer. The initial pH of the three SRRs was 8.0 $\pm$ 0.1. Analytical grade chemicals were applied (Merck KGaA, Germany), except for the humic acid sodium salt.

4.2.2 Experimental setup

Pre-stressing the sorptive media To simulate a pre-stressed state of the sorptive media, the media was exposed in a liquid/solid (L/S) ratio of 5 to a solution containing $CuSO_4 \cdot 5\,H_2O$ and $ZnSO_4 \cdot 7\,H_2O$ in a rotary shaker for 24 h at 5 rpm and 20 °C. The sum of the dissolved Cu and Zn cation concentration was adjusted to 10% of the cationic exchange capacity (CEC) of the individual sorptive medium (GAL, GFH and ZEO) under the assumption of equal sorption kinetics for Cu and Zn. In order to assess the influence of the pre-stressing extent, experiments with a load of 40, 60 and 80% of the CEC were carried out for ZEO. For the experiments with variable load, the L/S was raised to 10 to reduce the risk of precipitation of Cu and Zn. The chosen molar ratio of Cu/Zn was 0.118, following the German approval standard for SQIDs (DIBt, 2017; Huber et al., 2016d). The pre-stressing loads and equations are summarized in eqn (S1) and (S2) as well as in Table S2.† In order to avoid precipitation of Cu and Zn, the pH of the pre-stressing solution was adjusted to 5.0 by adding 0.1 mol L^{-1} HNO_3 . Pre-stressing was assumed to be successful if the Cu and Zn concentration in the solution was <10% of the initial concentration after the pre-stressing duration. Following the pre-stressing, the sorptive media was washed twice with DI water (L/S of 5) and dried at 105 °C. Prior to the leaching experiments, the pre-stressed media were stored in desiccators. Samples of the pre-stressed media were withdrawn for subsequent analysis of the total Cu and Zn content.

SED was not pre-stressed, since it had a Cu content of 434 mg kg^{-1} and a Zn content of 1367 mg kg^{-1} (Table 4.1).

Tab. 4.1. Chemical characteristics of all materials before pre-stressing based on dry matter, SED was not pre-stressed

Main elements										
	Al	TC	Ca	Fe	K	Mg	Mn	Na	TS	Si
Unit	wt%	wt%	wt%	wt%	wt%	wt%	wt%	wt%	wt%	wt%
GAL	0.08	93.1	2.05	0.70	0.06	0.85	0.01	0.53	0.40	0.35
GFH	0.10	2.31	6.67	39.6	0.03	0.54	1.16	0.04	0.04	5.12
SED	2.54	15.6	12.0	2.52	0.85	2.98	0.04	0.42	0.39	13.0
ZEO	5.89	0.14	2.17	0.56	2.66	0.44	0.05	0.53	0.00	30.0
Heavy metals										
	Cd	Cu	Cr	Ni	Pb	Zn				
Unit	$mg\,kg^{-1}$	$mg\,kg^{-1}$	$mg\,kg^{-1}$	$mg\,kg^{-1}$	$mg\,kg^{-1}$	$mg\,kg^{-1}$				
GAL	<0.1	<0.5	14.7	1.17	0.41	28.2				
GFH	0.35	4.14	<0.5	48.8	0.70	35.4				
SED	0.64	434	129	28.6	42.7	1367				
ZEO	0.10	0.74	2.01	2.87	29.3	34.4				

Tab. 4.2. Composition of synthetic runoffs

Leachate solution	Chemical	Molecular weight $[g\,mol^{-1}]$	Concentration $[mg\,L^{-1}]$	Source
SRR	$MgSO_4 \cdot 7\,H_2O$	246.5	55.0	Transportation Research Board (2014)
	KCl	74.6	25.0	
	KNO_3	101.1	90.0	
	$NaNO_3$	85.0	90.0	
	$CaCl_2$	111.0	200.0	
	$CuSO_4 \cdot 5\,H_2O$	249.7	0.196 (0.050 Cu)	
	$ZnSO_4 \cdot 7\,H_2O$	287.5	0.44 (0.100 Zn)	
	$NaHCO_3$	84.0	97.3	Own data
SRR+DOM	Same as SRR			
	Humic acid Sodium salt (CAS 68131-04-4)		44.5 (12.6 DOC)	FHWA database (Granato and Cazenas, 2009)
SRR+NaCl	Same as SRR			
	NaCl	58.4	10,000	Huber et al. (2016b)

Leaching experiments The leaching experiments were carried out in glass columns that had a diameter of 20 mm and height of 400 mm and were filled with 50 g of pre-stressed media (GAL, GFH and ZEO) per column. The filter media was supported by a fritted glass support and 1 cm of glass beads (2.0 mm to 2.4 mm diameter). In order to avoid clogging of the fritted glass support, the experiments with SED were conducted in 250 mL glass bottles with the same mass of material (50 g). Once the containers were filled with pre-stressed media or SED, 100 mL of the three SRRs (SRR, SRR+ DOM, SRR + NaCl) was added (L/S of 2). The containers filled with SRR + DOM were wrapped in aluminium foil to avoid any photo-degradation. After a contact time of 4, 24, 48 and 168 h, the leachates of the 10% pre-stressed sorptive media was withdrawn respectively. During the other leaching experiments with variably pre-stressed ZEO and SED, samples were withdrawn after 24, 48 and 168 h. All experiments were performed as duplicates at ambient temperature 20.8 ± 2.0 °C. Additionally, the oxidation – reduction potential (ORP) was measured online, with a time resolution of 10 min, in a column or container filled with pre-stressed media or SED and SRR + DOM leachate. Blank experiments without filter media were conducted. Between each experiment, all glassware was thoroughly cleaned with DI water, acetone and 0.1 M HNO_3. The full cleaning procedure is described in the ESI.†

4.2.3 Analyses

Analyses of sediment and sorptive media The bulk density, loss on ignition at 550 °C, particle size distribution (d_{10}, d_{30}, d_{60}) and specific surface areas of SED and the blank sorptive media were determined according to the standards DIN EN 1097-3:1998-06, DIN EN 15935:2012-11, DIN EN 933-1 and DIN ISO 9277:2014-01, respectively. Particle size distribution of SED needed to be analysed using laser diffraction (Mastersizer, Malvern Panalytical Ltd., Netherlands) according to BS ISO 13320:2009 due to the small particle size (mean $<$0.063 mm). The total pore volumes of the materials were determined by Hg intrusion in a pressure range from 0.004 MPa to 400 MPa (AutoPore III, Micromeritics GmbH, Germany).

The CECs of the media were determined in duplicates following DIN EN ISO 11260:2011-09 by saturation of the media with Ba and consequent exposure to a defined $MgSO_4$ solution, which results in precipitation of $BaSO_4$. Total carbon (TC) and total sulphur (TS) were determined using a multi EA 4000 element analyser at 1350 °C (Analytik Jena AG, Germany). The metal(loid) contents of the blank sorptive media and SED were determined using ICP-OES (Avio500, Perkin-Elmer, USA) and ICP-MS (Nexion D, Perkin-Elmer, USA) for Cd and Pb after microwave-assisted hydrofluoric acid digestion at 200 °C. The digestion method is comprehensively

described in the ESI.† The LOQs of the major metal(loid)s Al, Ca, Fe, K, Mg, Mn, Na, Si were 100, 50, 50, 500, 2, 500 and 100 mg kg^{-1}, respectively. The LOQs of Cd, Cu, Cr, Ni, Pb and Zn were 0.5, 1.0, 2.0, 2.0, 2.0 and 2.0 mg kg^{-1}, respectively.

The Cu and Zn content of the pre-stressed sorptive media were analysed using flame atomic absorption spectrometry (AAS, Varian Spectrometer AA-240FS, USA) according to Standard Method 3111 after *aqua regia* digestion (American Public Health Association et al., 2017).

Analyses of leachates The pH and EC were measured immediately after withdrawal of the leachates according to the Standard Methods 4500-H+ and 2520 B (American Public Health Association et al., 2017), respectively (SenTix 41 and TetraCon 325, WTW GmbH, Germany). The ORP was measured following Standard Method 2580 B (American Public Health Association et al., 2017) with a platinum electrode (WTW Multi 3410 and SenTix ORP-T 900, WTW GmbH, Germany).

The leachates before and after the experiments were filtered with syringe filters (0.45 μm, PES, VWR International GmbH, Germany; BGB Analytik Vertrieb GmbH, Germany) to quantify the dissolved fractions of the metals and the DOC. The leachates of the experiments with the SED needed to be centrifuged prior to the filtration (3000 $\times$ g, 20 min). The liquid samples were preserved with HNO_3 (pH $<$ 2) for the metal analysis and 1% V of 32% HCl for the DOC analysis.

The concentration of Cu and Zn were analysed after the pre-stressing procedure by photometric analyses using cuvette tests (LCK360 and LCK329, Hach Lange GmbH, Germany) to ensure a sufficient sorption of the Cu and Zn.

All other Cu and Zn analyses were conducted using flame-atomic absorption spectrometry (AAS, Varian Spectrometer AA-240FS, Palo Alto, USA) in accordance with Standard Method 3111 (American Public Health Association et al., 2017) with limit of quantifications (LOQs) of 50 $\mu g\,L^{-1}$ Cu and 20 $\mu g\,L^{-1}$ Zn. Samples with Cu concentrations below the LOQ were analysed by graphite furnace AAS (Varian Spectrometer AA-240Z with GTA 120, Palo Alto, CA, USA), following the Standard Method 3113 (American Public Health Association et al., 2017), with a LOQ of 5 $\mu g\,L^{-1}$. Considering the additionally found heavy metals in SED, the leachates of it were analysed using ICP-OES (Avio500, Perkin-Elmer, USA) and ICP-MS (Nexion D, Perkin-Elmer, USA) to determine dissolved Cd, Cr, Cu, Ni, Pb and Zn with LOQs of 1, 10, 10, 10, 1 and 10 $\mu g\,L^{-1}$, respectively. Furthermore, the dissolved concentrations of the major metals Ca, Fe, Mg and Na were analysed with LOQs of 500, 100, 100 and 1000 $\mu g\,L^{-1}$. Measured concentrations below the LOQ were substituted by one half of the LOQ value.

Additionally, the DOC concentrations of the SRR + DOM leachates and all leachates of SED were determined after filtration using a varioTOC Cube analyzer

(Elementar, Langenselbold, Germany) according to DIN EN 1484 with a LOQ of 0.25 mg L^{-1}. The UV absorbance of the filtered samples were determined at 254 nm (UVA_{254}) using a 10 mm quartz glass cuvette by a spectrophotometer (DR6000, Hach Lange GmbH, Germany). Leachates of SED were analysed with an Aqualog fluorescence spectrometer (Horiba Scientific, USA). Prior to the UVA_{254} measurements, the samples were adjusted to 20 ± 1 °C, pH was not adjusted. Specific UV absorbance ($SUVA_{254}$) was determined by dividing the UVA_{254} by the DOC concentration of the sample (Weishaar et al., 2003).

The Cl^- concentrations of SRR + NaCl leachates were analysed using cuvette tests with a LOQ of 1 mg L^{-1} (LCK 311, Hach Lange GmbH, Germany).

4.2.4 Hydraulic retention times in SQIDs

To estimate hydraulic retention times (HRTs) present in SQIDs, a SWMM model was utilized. Precipitation data of the years 2010 to 2018 with 10 min frequency of the weather station 3379 (Munich City, Germany) of the Deutscher Wetterdienst was used. The total precipitation was assumed as rain. The model consists of a 400 m2 impervious catchment area with 3% slope connected to a storage unit with 2.00 m water depth and 3.14 m2 surface area. The represented system is described in Rommel and Helmreich (2018c). The SQID was assumed to be empty at the beginning. To export the HRT a proxy pollutant was defined with a constant event mean concentration (EMC) wash-off and the treatment formula $C = HRT$. The simulation was executed using the steady flow routing model with 1 s routing steps.

4.2.5 Speciation with Visual MINTEQ

Visual MINTEQ (version 3.1, Gustafsson (2014a)) was used to examine the speciation of Cu and Zn in the SRRs, as well as their saturation indices (SI). Therefore, the three synthetic runoffs were entered in Visual MINTEQ with the elements present in the composition of the SRRs. DOM was modelled by the NICA-Donnan model, which is recognized as one of the most promising models for speciation of DOM (Transportation Research Board, 2014; Blume et al., 2016b). The ratio of DOM to DOC was assumed to be 1.65 (default setting, Gustafsson (2014a) and Sjöstedt et al. (2010)). In this study, 100% of the DOM was assumed to be humic acids, since the $SUVA_{254}$ of the SRR + DOM (7.7 L mg^{-1} m^{-1}) reflected properties of pedogenic humic acids (Huber et al., 2011). The pH of the solutions were fixed at the measured mean pH of the initial SRRs. Speciation was calculated at 25 °C. In the first calculation, the precipitation was prohibited (default setting). If any

oversaturated compound was found, then precipitation for the compound with the highest value was allowed by specifying it as a possible solid. This step was repeated until all oversaturated compounds were defined as possible solids. Finally, the amounts of the precipitated compounds were determined.

4.3 Results and discussion

The data of the leaching experiments is available on Mendeley Data (`http://dx.doi.org/10.17632/vzn73d448s.2`, Rommel et al. (2020c)).

4.3.1 Hydraulic retention times in SQIDs

By means of using the SWMM model, it was possible to estimate HRTs present in a SQID for a long time series (2010–2018) based on real precipitation data. The results show that HRTs need to be considered to understand processes involved in SQIDs.

The estimated median HRT was 206 h and the HRT varied by a factor of 2.2 between the 25th and 75th percentile (Fig. 4.2a). Thus, the selected contact times of the leaching experiments are supported by these findings. A strong seasonality of the HRT was observed (Fig. 4.2b), with increasing HRTs at the beginning of the spring and a sharp decrease hereafter. The course of the HRTs followed inversely the observed monthly precipitation heights (Fig. S2†). To develop a full picture of the HRT distributions in SQIDs, additional designs, concerning different hydraulic loading rates, were evaluated. The studied settling tank of the SQID was designed for a maximal surface loading q_A, max of 0.7 $\mathrm{m\,h^{-1}}$ according to the German technical standard (*DWA-A 102 (Entwurf)* 2016). Since the technical guideline suggests a $q_{A,max}$ of 4 $\mathrm{m\,h^{-1}}$ to 6 $\mathrm{m\,h^{-1}}$, this is a very low surface loading. With increasing $q_{A,max}$, the determined HRTs decreased to a median HRT of 75 h for $q_{A,max} = 2\,\mathrm{m/h})$ and 36 h for $q_{A,max} = 4\,\mathrm{m\,h^{-1}}$. The results of the model indicate that in winter and especially spring leaching of heavy metals is potentially enhanced by the high HRTs.

These results are only applicable for a temperate climate, such as the climate we experience here in southern Germany. In arid regions, the HRT could be significantly higher. Another source of uncertainty is the simplification that SWMM assumes behaviour of a continuous stirred-tank reactor (CSTR) to determine HRTs of storage nodes (Rossman and Huber, 2016). Especially to model effluent quality, a cascade of CSTRs could reflect the behaviour of SQIDs more realistically (Zahraeifard and Deng, 2011; Zawilski and Sakson, 2008). To determine the appropriate number of CSTRs in a cascade, tracer experiments would be necessary. It must be emphasized

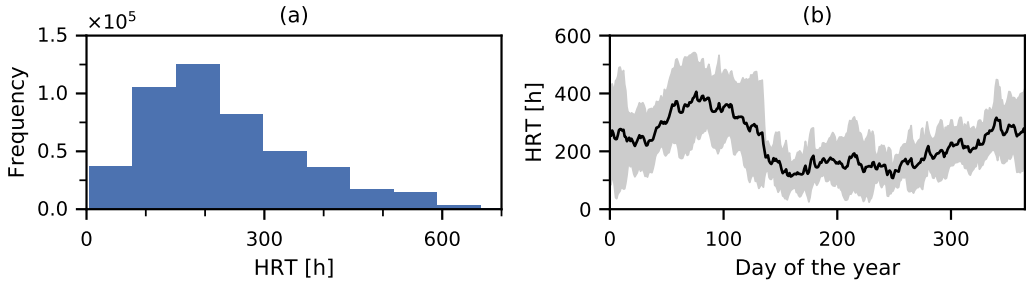

Fig. 4.2. (a) Histogram of the modelled HRT for the years 2010–2018, (b) time series of the modelled HRT, black line shows the mean HRT for the years 2010–2018, grey shaded area indicates the SD.

that the HRT prediction was utilized to gain indicative values of HRTs present in SQIDs. Future experiments are necessary to validate the predicted HRTs.

4.3.2 Leaching from road-deposited sediment

The analysis of the SED from the settling tank after two years of operation showed high traffic-related contents of heavy metals. The high Zn content of 1367 mg kg^{-1} can be attributed to TWP from the road runoff (Councell et al., 2004). Cu was the second heavy metal in the order of their contents with 434 mg kg^{-1}, followed by Cr, Pb, Ni and Cd with contents of 129, 42.7, 28.6, and 0.64 mg kg^{-1}, respectively. According to the German Federal Soil Protection and Contaminated Sites Ordinance, the contents of Zn and Cu exceed precautionary values severely (Blume et al., 2016a). Furthermore, Cr, Pb, Ni and Cd surpassed the precautionary values, depending on the referenced soil. Thus, SED can be considered contaminated material. Main fractions of SED were quartz (SiO_2) and organic carbon (Tables 1 and S1†). The high Fe content of SED (2.5%) needs to be considered, since metal oxides and hydrous oxides are key scavengers of heavy metals in the environment (Brezonik and Arnold, 2011). Cu, Pb and Zn were mostly found in RDS in the reducible fraction, associated with Fe and Mn oxides (Sutherland et al., 2012).

The leaching experiments revealed that severe leaching of the heavy metals Zn, Cu, Ni and Cd from SED occurred (Fig. 4.3). After 24 h equilibrium conditions can be assumed for Zn, Ni and Cd. Only Cu showed a divergent behaviour with decreasing dissolved concentrations after 48 h. Since Cu exhibits a high affinity to organic matter (McBride, 2000; Hamilton et al., 1984; Stone and Marsalek, 1996), this effect may be attributed to degradation of the DOM and particulate organic matter (POM), resulting in a change of the complexation affinity. The effect of the different SRRs on the leaching was not pronounced, except for SRR + NaCl on Zn and Cd, which means that the risk of Zn and Cd leaching from settled particles is

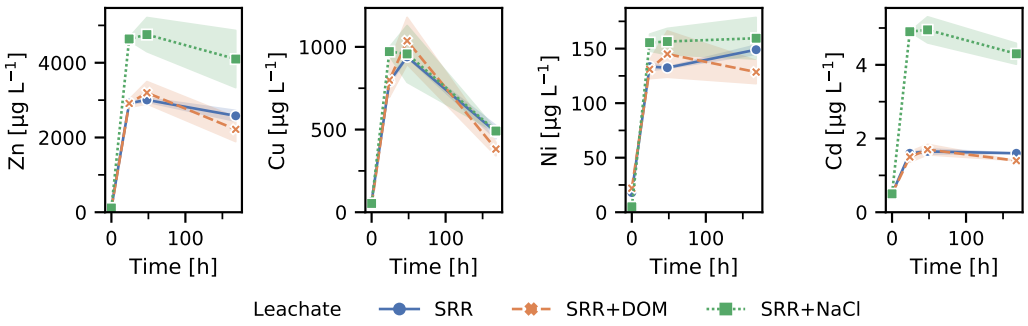

Fig. 4.3. Time-series of dissolved Zn, Cu, Ni and Cd in the leachates of SED from SRR, SRR + DOM and SRR + NaCl, respectively. Shown is the mean of two replicates. The shaded area denotes the SD.

higher under the influence of de-icing salt in winter and spring. Comparable results have been reported by Norrström (2005), who attributed this effect to the formation of Cl^- complexes with Zn and Cd. The highest mobility of Zn and Cd from RDS was reported by multiple studies (Loganathan et al., 2013). Robertson et al. (2003) found Zn associated with the exchangeable fraction, which reflects the present results. Furthermore, this follows the stability of the metal-hydroxo complexes, which affects adsorption on pedogenic oxides (Blume et al., 2016a). However, Ni should exhibit a leaching behaviour between Cd and Zn following this theory. In contrast to the aforementioned metals, Cr and Pb showed no significant leaching (Fig. S3†). The initial concentration of Cr indicates an unknown contamination. Pb was below the LOQ in all samples except for the initial sample of SRR + DOM, which was slightly above the LOQ.

Within 48 h of contact time, up to 1.5% of the total mass of each heavy metal was leached under exposure to the three SRRs, respectively. Previous studies reported significantly higher leaching percentages: 27%, 9%, 8%, 13%, 6%, and 25% for Cd, Cr, Cu, Ni, Pb, and Zn, respectively (Zafra et al., 2017). However, the studies used either permanent agitation, leaching solutions with acidic pH and/or low ionic strength (Zafra et al., 2017), which all enhance leaching potential. Furthermore, these conditions do not occur in SQIDs.

Assuming equilibrium conditions after 48 h, the partition coefficients (K_d) were 388, 6139, 462, 216, 85 356 and 455 L kg^{-1} for Cd, Cr, Cu, Ni, Pb and Zn, respectively. Thus the order of mobility or leaching potential of the heavy metals was Ni > Cd > Zn > Cu $\gg$ Cr $\gg$ Pb. The reported values were determined for SRR. Zafra et al. (2017) determined a similar order of leaching, Cd > Zn > Cu > Pb > Ni > Cr, using 24 h leaching experiments under constant agitation. Degaffe and Turner (2011) determined a comparable K_d of 550 L kg^{-1} for Zn leached from TWP. In contrast to the present results, they observed lower Zn leaching with increasing salinity. The

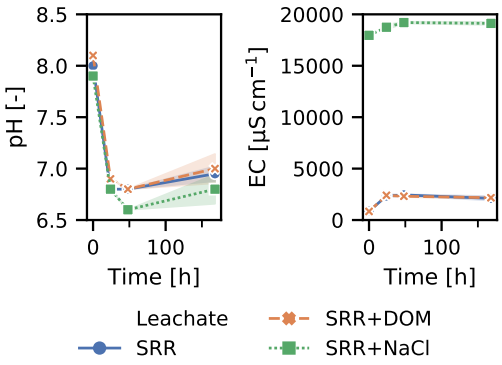

Fig. 4.4. Time-series of pH and EC in the leachates of SED. Shown is the mean of two replicates. The shaded area denotes the SD.

observed leaching kinetic of Zn cannot be described with a linear model such as the one proposed by Rhodes et al. (2012). This discrepancy could be attributed to the ten-fold lower L/S ratio used in our study, which is closer to the conditions present in the sediment trapped in SQIDs. Furthermore, the diffusion-controlled model used by Degaffe and Turner (2011) failed to reproduce the observed concentrations after 48 h (Fig. S4†). This shows that after 48 h, saturation of dissolved species was reached, and not only diffusion-controlled mechanisms were involved. The decrease of Zn, Cu and Cd could partly reflect precipitation of dissolved species. Considering only the data up to 48 h, the rate constant of Zn was 488 $\mu g\,L^{-1}\,h^{-1/2}$. This is approximately two times higher than reported by Degaffe and Turner (2011). However, they used an incredibly high L/S ratio of 1000, which would only be found under turbulent conditions in the water column and not in sediments of artificial or natural water systems.

Besides the aforementioned heavy metals, considerable amounts of the major cations Ca, Mg, Na and Fe leached from the SED (Fig. S5†). The water matrix of the samples was dominated by Ca. The major cations influenced leaching of the heavy metals due to competitive sorption. Interestingly, the leaching of carbonate, indicated by the increase of Ca, was not sufficient to avoid a considerable decrease of pH of approximately one unit (Fig. 4.4). A significant effect to this can be attributed to the considerable amounts of leached DOM. The lower pH values of SRR + NaCl can be explained by the increased release of H^+ from SED surfaces caused by the high Na^+ concentrations (Bäckström et al., 2004b).

The leachates of SED exhibited sever e leaching of DOM (Fig. 4.5). The DOC reached after 24 h a mean of 906 $mg\,L^{-1}$. Hence, significant influence of the DOM on the speciation of the dissolved metals can be expected. After 24 h the DOC showed an equilibrium state. Only slight variations between the different SRRs were observed.

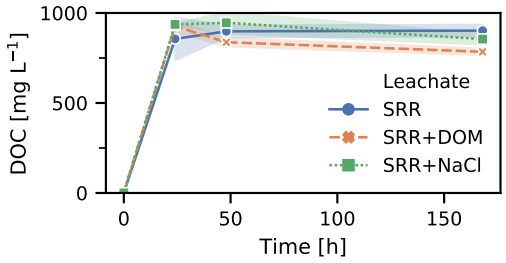

Fig. 4.5. Time-series of DOC in the leachates of SED. Shown is the mean of two replicates. The shaded area denotes the SD.

This is likely, since OM, present in the SED, dominated the leachate composition. After 24 h, no significant deviations of the $SUVA_{254}$ between the different SRRs were observed (Fig. S6†). Furthermore, the $SUVA_{254}$ remained constant. Thus, the aromaticity of the DOM remained constant (Weishaar et al., 2003; Abbt-Braun et al., 2004). The prior-to-hypothesized degradation of DOM was hereby not supported. Fe concentrations in the leachates were expected to have a negligible influence on the UV absorbance (Weishaar et al., 2003). Kumar et al. (2013a) attributed an increase of isotopic exchangeability of heavy metals by a RDS to the alteration of binding sites caused by degradation of OM. Furthermore, they observed that degradation of DOM leads to a reduced heavy metal retention. The initial aromaticity of SRR + DOM was considerably higher with an $SUVA_{254}$ of 7.7 L mg^{-1} m^{-1} in comparison to the average of all leachates after 24 h of 1.2 L mg^{-1} m^{-1}. This describes the differences between the DOM found *in situ* to the SRR + DOM. However, for this certain experiment, no effect can be assumed, since the by far largest fraction of the DOM leached from the SED.

Bordas and Bourg (2001) showed that with an increasing L/S-ratio, the remobilization of heavy metals from polluted river sediment is increasing. Thus, the results of this experiment may show a reduced leaching effect. Furthermore, the repeated exchange of the water in the systems could additionally provoke leaching of the heavy metals from SED. However, contradicting results have been reported for soils as well (Yin et al., 2002).

The temperature during the experiments may increase the leaching potential slightly, since Zhang et al. (2018) showed an increase of Cu leaching at higher temperatures. Changes between oxidizing-reducing conditions are likely to increase heavy metal leaching additionally (Kumar et al., 2013a; Folkeson et al., 2009). These changes can occur due to wet and dry cycles (Kumar et al., 2013a). In our experiments, suboxic to oxic conditions were present (Fig. S7†). With increasing duration, the conditions became more suboxic due to oxygen depletion.

These findings suggest that high retention times in SQIDs lead to leaching of particulate-bound heavy metals. Within 48 h, up to 1.5% mass of the individual heavy metals leached from the SED. Considerably high concentrations of heavy metals were observed, which additionally load sorptive media in the consecutive second treatment stage. Thus, higher loads of the sorptive media can be expected and/or worse effluent quality of the SQIDs. However, previous studies on leaching of heavy metals from RDS potentially overestimated the leaching potential due to permanent agitation, acidic pH and low ionic strength or alkalinity (Zafra et al., 2017).

4.3.3 Leaching from sorptive media

Constant pre-stressing of sorptive media After the pre-stressing step (approximately 10% of CEC), the mean Cu content of the sorptive medium was 20.7 mg kg^{-1} for GAL, 78.8 mg kg^{-1} for GFH and 7.68 mg kg^{-1} for ZEO, respectively. The mean Zn content was 164, 1073 and 345 mg kg^{-1} for GAL, GFH and ZEO, respectively. None of the media reached the designated pre-stressing level of 10% CEC. The reached pre-stressing loads were 7% CEC for GAL, 8% for GFH and 5% for ZEO.

A significant pH increase of the pre-stressing solution was observable. After the 24 h-long contact time, the pH increased from 5.0 to 8.4 for GFH, to 9.0 for ZEO and even to 12.2 for GAL, respectively. Furthermore, dissolution of the solid phase was recognized by the distinctive increase of the EC to 5940 $\mu S\,cm^{-1}$ for GAL, in comparison to 861 $\mu S\,cm^{-1}$ for ZEO and 1130 $\mu S\,cm^{-1}$ for GFH, respectively. Since adsorption and precipitation is mainly controlled by pH and ionic strength, dissolution of the solid phase should be limited. Therefore, the pre-stressing with higher loads was performed with an increased L/S ratio of 10. However, the present results of GAL showed that even with significant dissolution of the solid material, a pre-stressing level of 7% of the CEC was achieved.

Contrary to expectation, all leachates showed a decrease of the dissolved Cu and Zn concentrations (Fig. 4.7). There are two possible explanations for this effect. First, due to the low yet realistic pre-stressing of the media, the adsorption capacity was still high enough to prohibit desorption. Secondly, leaching of the metal occurred, however, the increase in the pH of the leachates (Fig. 4.6) resulted in precipitation of Cu and Zn.

Since the pH of the GAL leachates showed the highest pH, the lowest Cu concentrations have been observed for all GAL leachates, indicating precipitation of Cu and Zn (Genç-Fuhrman et al., 2007).

Generally, the highest concentrations were measured in the SRR + NaCl leachates. This highlights the impact of de- icing salts on the treatment of road

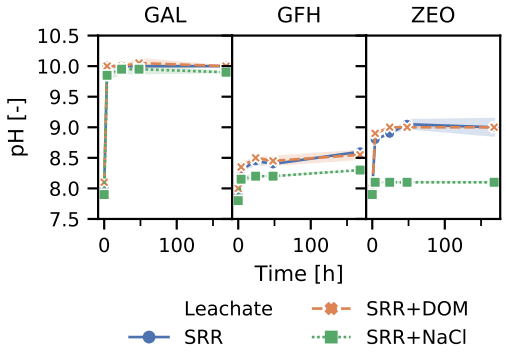

Fig. 4.6. Time-series of pH in the leachates of the different media and SRRs. Shown is the mean of two replicates. The shaded area denotes the SD.

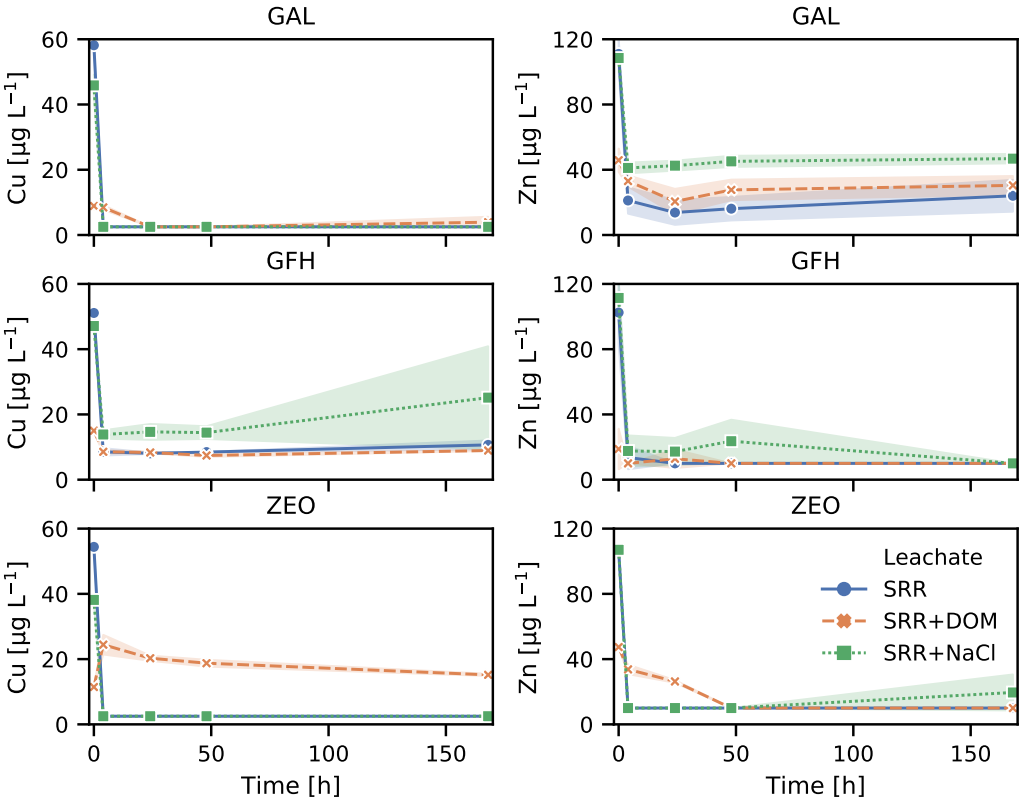

Fig. 4.7. Time-series of dissolved Cu and Zn in the leachates of the different media and SRRs. Shown is the mean of two replicates. The shaded area denotes the SD.

runoff. The main involved processes are ion-exchange, decrease of the pH and formation of chloride complexes (Bäckström et al., 2004b). Ionic strength typically affects the outer-sphere surface complexes. In contrast, chemisorption binds ions stronger (Blume et al., 2016b). Thus, relatively weakly adsorbed metals can desorb in SRR + NaCl. After 48 h minor increases of Cu and/or Zn in the leachates were observed. This phenomenon may be attributed to an increasing metal exchangeability with increasing contact time, as observed by Kumar et al.6 Furthermore, the recorded ORP of the SRR + DOM leachates, except for ZEO, decreased after 50 h (Fig. S7†), which suggests an influence of the oxidizing–reducing conditions (Kumar et al., 2013a).

Huber et al. (2016b) stated a high remobilization risk associated with de-icing salts even at short contact times (flow conditions). Compared to this study, the Cu and Zn content of the pre-stressed GFH was considerably higher (up to a factor of 6 for Zn and 48 for Cu). Consequently, more sorption sites were occupied. Thus, leaching occurred under exposure to de-icing salt rich solution, even during short contact times. Additionally, the experiments were performed without adjustment of the alkalinity and ionic strength of the synthetic runoff. Thus, a worst-case scenario was illustrated by Huber et al. (2016b), which is not comparable to this study.

The Cu concentration of GFH with SRR + NaCl increased slightly at the end of the experiment, however, it remained below the initial concentration. If only 1% of the mass had been leached, Cu and Zn concentrations $>162\,\mu g\,L^{-1}$ and $>931\,\mu g\,L^{-1}$, respectively, depending on the media and its pre-stressing, should have been observed. It must be emphasized that the results of the ZEO leachates need to be interpreted with caution, since the pre-stressing level of the medium was lower than that of the other two media.

One unanticipated finding was that no leaching from ZEO occurred with SRR + NaCl, since it is known that regeneration of zeolites is possible using NaCl (Kesraoui-Ouki et al., 1994).

The pH of the GAL leachate was significantly higher than of the GFH and ZEO leachates. These differences can be attributed to the high TC of GAL (*cf.* Table 4.1). Since GAL is a lignite-based product, most of the TC content was expected to be present in form of coal. However, Huber et al. (2016b) found $CaCO_3$ on the surface of the media, therefore, dissolution of $CaCO_3$ is a likely explanation for the steep pH increase. The leachates with NaCl (SRR + NaCl) showed lower pH values for GFH and ZEO, likely caused by release of H^+ from the sorption sites of the media due to competitive sorption with Na^+ (Bäckström et al., 2004b). The EC of the leachates of GFH and ZEO remained constant over time (Fig. S8†), whereas the GAL leachates increased at the beginning of the experiments, additionally indicating dissolution mineral phases, *e.g.*, calcite.

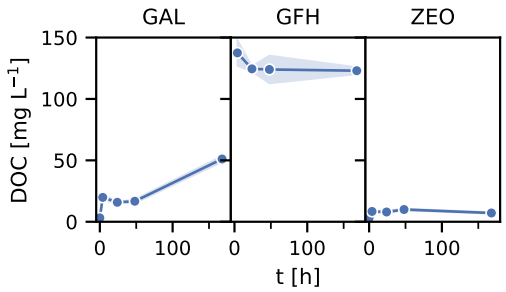

Fig. 4.8. Time-series of DOC in the leachates of the different media and SRR + DOM. Shown is the mean of two replicates. The shaded area denotes the SD.

In contrast to the preliminary experiments (Fig. S1†), the added amount of humic acid sodium salt was not sufficient to establish a DOC of 12.6 mg L^{-1} in the initial leachate SRR + DOM (Fig. 4.8). Only a DOC of 3.2 ± 0.1 mg L^{-1} was measured in the initial solutions. Since the SRR held a considerably higher ionic strength than DI water used for the preliminary tests, it can be expected that complexes formed that were larger than the pore size of the membrane filter (0.45 μm). Due to the alkaline pH of the leachates, the solubility of the humic substances should have been increased, because the functional groups of OM will be ionized with increasing pH (Tuhkanen and Ignatev, 2018). In the course of the experiment, the DOC remained almost constant, except for the leachates of GAL, which exhibited an increase after 48 h. This effect can be attributed to a dissolution and or degradation of the OM originating from the lignite. Hence, the stability of the GAL media may be limited. The mean DOC at the end of experiment was 51.1 mg L^{-1}. One unanticipated finding was that the leachates of GFH showed remarkably high DOC concentrations (116–145 mg L^{-1}). Since the tested GFH was produced from by-products of a drinking water treatment plant, the media contained residuals of adsorbed humic substances (DOM) and polymeric flocculants. These residuals are expected to leach rapidly during operation.

Variable pre-stressing of sorptive media Huber et al. (2016b) showed that as pre-stressing increases, leaching from GFH increases under the influence of de-icing salts. To examine the influence of the pre-stressing load on the leaching of Cu and Zn, additional experiments were performed with 40%, 60% and 80% CEC pre-stressing, respectively. The experiments were performed with ZEO and SRR + NaCl, because strong leaching was expected for this combination, since zeolites are regenerated using NaCl (Kesraoui-Ouki et al., 1994).

The metal contents of ZEO increased linearly with increasing pre-stressing intensity (10, 40, 60 and 80% of CEC). The corresponding mean Cu contents were

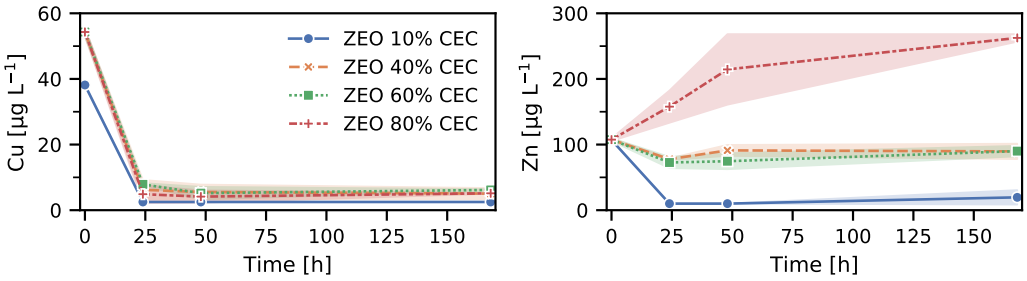

Fig. 4.9. Time-series of dissolved Cu and Zn in the leachates of ZEO with 10%, 40%, 60% and 80% CEC pre-stressing, respectively, exposed to SRR + NaCl. Shown is the mean of two replicates. The shaded area denotes the SD.

7.7, 65.5, 127 and 200 mg kg^{-1}, respectively. Zn contents were 345, 1663, 2593 and 3734 mg kg^{-1}, respectively. The increase of the L/S ratio for the pre-stressing of $\geq$40% CEC was successful and the pH after pre-stressing was more than one pH unit lower. Interestingly, the pH decreased with increasing pre-stressing level from 8.1 to 7.4. This is an indicator of the release of two H^+ in exchange with Cu^{2+} and/or Zn^{2+}. Furthermore, the EC increased significantly with increasing pre-stressing, from 1435 to 2310 μS cm^{-1}. Thus, more solid phase of ZEO dissolved during the pre-stressing procedure.

The leaching experiments of the variably pre-stressed ZEO showed that even with increasing pre-stressing the Cu concentrations in the leachates were similar (Fig. 4.9). In contrast, Zn varied significantly. With increasing pre-stressing, the Zn concentration increased. However, only at the highest pre-stressing (80% CEC) leaching was observed, resulting in higher Zn concentrations in comparison to the SRR + NaCl. However, a pre-stressing of 80% of the CEC is rather unrealistically high, due to the heavy metal concentrations present in road runoff (Kayhanian et al., 2012a; Huber et al., 2016c) and the design of replacement intervals of sorptive media in SQIDs. Thus, no leaching of heavy metals from sorptive filter media can be expected under realistic conditions.

4.3.4 Speciation with Visual MINTEQ

The speciation and saturation indices of the present species of the three SRRs were predicted using Visual MINTEQ. The results revealed that precipitation of tenorite (CuO) and calcite ($CaCO_3$) occurred in the SRR, thereby 15.2%, 23.7% and 83.9% of the added Ca, CO_3^{2-} and Cu precipitated, respectively. This large percentage of precipitated Cu was not supported by the analysis of the initial SRR, with a mean loss of <2%. However, since tenorite is oversaturated in the solution, it will readily precipitate, especially if pH increases during the experiments. The speciation of

SRR + DOM suggested that no Cu (tenorite) precipitated. Yet calcite precipitated, thereby Ca and CO_3^{2-} were reduced by 16.9% and 26.2%. The DOM in the SRR + DOM bound 100% of the dissolved Cu and 69% of the dissolved Zn. In SRR + NaCl tenorite precipitated as well, resulting in 77% precipitated Cu. Again, this does not reflect the lab analysis, where an average loss of 13% Cu was determined. This loss indicates the limitation of species prediction; hence, these results should be interpreted with caution and can just be used for further understanding of the evolved processes.

In all SRRs, the most frequent inorganic Cu species were $CuCO_3(aq)$, Cu^{2+} and $CuOH^+$. Zn occurred mostly in SRR and SRR + NaCl as Zn^{2+}, $ZnCO_3(aq)$, $Zn(OH)_2(aq)$ and $ZnCl^+$ in SRR + NaCl. In SRR + DOM, the DOM complexes involve 100% Cu and 69% Zn. Thus, negatively charged surfaces of the sorptive media are preferred to retain Cu and Zn due to the cationic species. A full overview of the predicted species is given in Table S3.†

The indicated precipitation of Cu is relevant for studies without pre-stressed media or contaminated material, since Cu in solid form cannot be adsorbed. In our experiments, the Cu was just used to establish a background concentration in the SRRs, which affects leaching of particulate-bound Cu. Due to the comparably low Cu concentration in the SRRs, even adsorption of the total Cu would have affected the Cu content of the media by $<1.5\%$.

4.4 Conclusion

The new experimental procedure was capable of describing the fate of heavy metals during dry periods in SQIDs, which consist of a settling tank as first treatment stage and a sorptive filter as second stage. Although SQIDs are gaining in acceptance, this process has not been quantified in the past. Furthermore, most realistic conditions were simulated, considering road runoff composition, L/S ratio and the pre-stressing level of the sorptive media.

RDS, which accumulate in settling tanks, exhibited a high leaching potential of heavy metals. Even if low-mass fractions leached within the duration of the experiment, high heavy metal concentrations were measured in the liquid phase. Thus, subsequent rain events can discharge heavy metals into receiving waters. Furthermore, optional consecutive sorptive filter media will be additionally stressed, reducing their service life. In contrast to previous studies investigating leaching of Zn from TWP, equilibrium between the liquid and solid phase was reached after 24–48 h. Thus, previous results overestimated the leaching due to high L/S ratios, which are not representative for conditions present in sediments. Without turbulent

conditions, TWP would mainly be found in sediments. Furthermore, synthetic runoffs for leaching experiments should consider the ionic strength, alkalinity and neutral to alkaline pH of road runoff to avoid overestimation of the involved leaching processes. Yet, the current results highlight the importance of regular removal of sediments trapped in SQIDs to reduce the risk of heavy metal leaching.

Contrary to the hypothesis, no leaching of Cu and Zn from the three sorptive media was observed. This indicates that under realistic pre-stressing levels, even with long contact times, no significant leaching occurs. However, additional experiments that exerted higher pre-stressing on one sorptive medium supported previous findings that leaching can occur. Nevertheless, this high pre-stressing level of sorptive media will not be reached under *in situ* conditions due to maintenance and low dissolved heavy metal concentrations. Furthermore, if leaching occurs, this high pre-stressing level is unlikely.

Based on the present results, all tested sorptive media are capable of preventing leaching of heavy metals during dry periods under permanent impounding. However, GFH offered the by far highest CEC, which results in a reduced volume of the sorptive filter bed of the SQID at comparable treatment efficiency. GAL exhibited the lowest CEC, thus SQIDs with GAL would require larger sorptive filter bed volumes. Leachates of ZEO showed, in contrast to the other media, a significant pH drop in the presence of de-icing salt, which potentially favours leaching of heavy metals. Furthermore, the Cu retention of ZEO was lower in the presence of DOM, which occurs in full-scale application.

Consequently, the main outcome of this study is that regular removal of sediments trapped in SQIDs can increase heavy metal retention and may increase the service life of utilized sorptive media.

Acknowledgments

This research was supported by the Bavarian Environment Agency (AZ: 67-0270-96505/2016 and AZ: 67-0270-25598/2019). Furthermore, we thank Harald Hilbig of the Centre for Building Materials, Technical University of Munich, for the analysis.

5

Sequential extraction of heavy metals from sorptive filter media and sediments trapped in stormwater quality improvement devices for road runoff

This chapter has been previously published as follows:
Rommel, S. H., P. Stinshoff, and B. Helmreich (2021b). "Sequential Extraction of Heavy Metals from Sorptive Filter Media and Sediments Trapped in Stormwater Quality Improvement Devices for Road Runoff". *Science of The Total Environment* 782, p. 146875. DOI: 10.1016/j.scitotenv.2021.146875

Author contributions: Rommel‡, S. H.: conceptualization, methodology, validation, data curation, writing - original draft, writing - review & editing, visualization, supervision; Stinshoff,‡ P.: investigation, methodology, data curation, writing - original draft, writing - review & editing; Helmreich, B.: resources, writing - review & editing, supervision, project administration, funding acquisition; ‡ these authors contributed equally.

† Supplementary information are available in A.3.

Abstract

The performance of stormwater quality improvement devices (SQIDs), commonly based on sedimentation and media filtration, is generally examined either at lab scale or in field tests. However, there has so far been only little investigation into the remobilization of heavy metals retained in sediments and sorptive filter media. It is, moreover, unknown whether current lab-scale experiments are able to replicate the conditions of full-scale operation. To assess the potential impact of differences in

conditions between lab-scale and field tests on the strength of association of heavy metals, filter media taken from three SQIDs were subjected to analysis by sequential extraction after prestressing both on a lab scale and in field tests. Sediments and filter cake trapped in the SQIDs were additionally analyzed. These displayed significantly higher heavy metal content than filter media that had been prestressed in the field. The zinc in the sediments and filter media displayed particularly high mobility. This study reveals a discrepancy between field and lab-scale conditions that creates differences in the content and strength of association of heavy metals. It is hence possible to show that previous lab-scale experiments potentially overestimated the risk of heavy-metal leaching, due to their predominant occurrence in more mobile fractions.

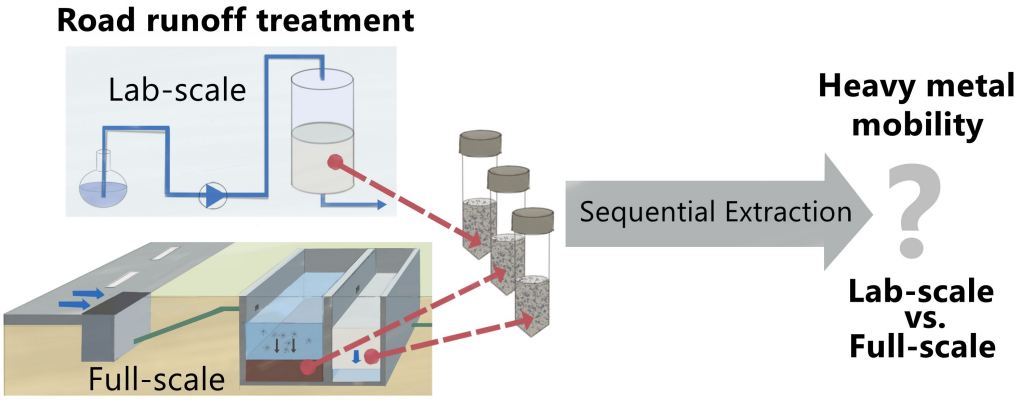

Fig. 5.1. Graphical Abstract of the study "Sequential extraction of heavy metals from sorptive filter media and sediments trapped in stormwater quality improvement devices for road runoff".

5.1 Introduction

Road runoff transports a wide variety of dissolved or particulate- bound contaminants (Huber et al., 2016c; Kayhanian et al., 2012a; Zgheib et al., 2011b; Spahr et al., 2020; Opher and Friedler, 2010). These include heavy metals, particularly cadmium (Cd), chromium (Cr), copper (Cu), nickel (Ni), lead (Pb), and zinc (Zn), all of which are of special concern by virtue of their prevalence, persistence and toxicity (Bartlett et al., 2012a; Huber et al., 2016c; Kayhanian et al., 2012a; Zgheib et al., 2011b). The mobility and resulting bioavailability of these substances is strongly determined by their partitioning (dissolved or particulate-bound) and geochemical distribution (Jayarathne et al., 2018; Bartlett et al., 2012a; Padoan et al., 2017; Stone and Marsalek, 1996; Gunawardana et al., 2015). Most contaminants accumulate as road-deposited sediments (RDS) during dry periods and are washed away in road

runoff during subsequent rainfall events (Zafra et al., 2017; Padoan et al., 2017; Hong et al., 2017). Such contaminants pose a threat to the aquatic ecosystems of the receiving water bodies (Bartlett et al., 2012a; Bartlett et al., 2012b; Kayhanian et al., 2008b). As they have a smaller footprint than other sustainable urban drainage systems, stormwater quality improvement devices (SQIDs) or manufactured treatment devices (MTDs) are examples of stormwater control measures employed for retaining contaminants, especially in dense urban areas (Dierkes et al., 2015; Sample et al., 2012; Fletcher et al., 2015). Commonly used multi-process SQIDs consist of a sedimentation stage to remove particulate matter, and a downstream (sorptive) media filtration stage (Leisenring et al., 2012; Dierkes et al., 2015; Strecker et al., 2005). The filter media can be either organic, such as biochar or activated carbon, or inorganic, such as carbonate-containing sand, zeolite, iron oxides/hydroxides, or manganese oxide-coated sand (Okaikue-Woodi et al., 2020; Reddy et al., 2014). There are various processes involved in media filtration, and their relevance varies according to the filter medium and contaminant in question: on the one hand, sorption (including adsorption, absorption, ion exchange, hydrophobic interactions, and electrostatic attraction) and chemical precipitation of dissolved substances, and, on the other, straining, physical filtration, and sedimentation of particulate-bound contaminants (Okaikue-Woodi et al., 2020; Blume et al., 2016b; Strecker et al., 2005). Even though multiple processes are involved in contaminant retention, we use the term 'filter medium' in this publication on the basis of common practice. Sorption is partly reversible, which means that desorption or leaching of heavy metals previously retained by filter media can occur (Blume et al., 2016b; Zhou and Haynes, 2010; Tedoldi et al., 2016). To ensure comparable assessments, the performance and service life of filter media is frequently assessed in lab-scale tests (Lucke et al., 2017). A number of protocols currently exist (Haile and Fürhacker, 2017; Washington State Department of Ecology, 2011; *VSA* 2019; Huber et al., 2016d; Monrabal-Martinez et al., 2017; Barrett et al., 2014; Genç-Fuhrman et al., 2016). However, none of them are able to replicate all boundary conditions that apply under full-scale use in the field, i.e. pH, ionic strength, alkalinity, particulate matter, concentrations of contaminants and other runoff constituents, dry/wet cycles, permanent impounding of the media (if incorporated in the design), and dissolved organic matter (DOM). This indicates a need to compare filter media that are prestressed in the laboratory with those in the field, to evaluate whether lab-scale tests are sufficiently able to replicate field conditions. According to the International BMP Database, media filters achieve a significant reduction in particulate matter and total Cu and Zn concentrations, but not in dissolved Cu and Zn (Leisenring et al., 2012). Nevertheless, the dataset is limited and does not distinguish between media, which poses the question of whether media filtration achieves the level of

performance indicated by lab-scale tests in full-scale use. One way of evaluating whether the treatment processes are comparable on a lab scale and in full scale is to analyze the strength of association between heavy metals and filter media. The strength of association of heavy metals is linked to their geochemical distribution or fractionation. Sequential extraction procedures (SEPs) are used to characterize the mobility of heavy metals bound to the filter media after prestressing at lab-scale or in a full-scale application (Martin et al., 1987; Pueyo et al., 2008). SEPs have been used for decades to investigate the potential risks of toxic trace elements and are considered a suitable way of performing fractionation of heavy metals (Bacon and Davidson, 2008). Unlike total or pseudo-total analyses, SEPs are capable of revealing the mobility of heavy metals under a variety of ambient conditions present in the environment (Sutherland, 2010; Zhao and Hazelton, 2016).

To ensure comparability to previous and future studies, this study uses the widely adopted optimized BCR SEP method established by the Standards, Measurements and Testing Program (formerly BCR) of the European Commission (Sutherland, 2010; Ure et al., 1993; Rauret et al., 2001). In the optimized BCR SEP method, heavy metals undergo three extraction steps and are separated into three fractions, these being the acid-extractable (F1), reducible (F2), and oxidizable (F3) fractions. A fourth step (F4) is often added to conduct pseudo-total digestion of the residual. These fractions are attributed to the soluble, exchangeable, and acid-extractable species (F1), manganese and iron oxyhydroxides (F2), organic matter and sulfides (F3), and strongly bound species like alumosilicates (F4) (Bacon and Davidson, 2008; Hass and Fine, 2010). The majority of previous studies consider heavy metals in F1 as bioavailable (Bacon and Davidson, 2008). However, the fundamental limitation of SEPs is that all fractions extracted are operationally defined as species. They neither have geochemical significance, nor is there any consistency, for example, when changing the reagent (Bacon and Davidson, 2008; Bäckström et al., 2004a; D'Amore et al., 2005). Nevertheless, SEPs provide useful information about the mobility of heavy metals and have been widely applied to manifold sample media (Sutherland, 2010). In the context of traffic-related contaminants, SEPs have been used primarily in the analysis of RDS (Sutherland et al., 2000; Sutherland, 2002; Sutherland et al., 2012; Zhang et al., 2019b; Kumar et al., 2013b), soakaway sediment (Kumar et al., 2013b; Kumar et al., 2013a) and roadside soils (Bäckström et al., 2004a; Kumar et al., 2013b; Kumar et al., 2013a; Sutherland and Tack, 2000). Only Li and Davis (2008) and Wang et al. (2017) have used SEPs to analyze the filter media employed in bioretention systems. To the best of our knowledge, SEPs have not been used to analyze sorptive filter media of SQIDs.

The aims of this study were (i) to determine the fractionation patterns of heavy metals present in the filter media of SQIDs after prestressing in field tests or on a

lab-scale, (ii) to assess the comparability of prestressed filter media originating from field tests and lab-scale experiments, and (iii) to evaluate the role of road-deposited sediment in the heavy metal content of prestressed filter media.

5.2 Materials and methods

5.2.1 Study site, storm water quality improvement devices, and sampling

The study site was located at a highly trafficked road in Munich (48°10'47" N, 11°32'24" E), Germany, with an annual average daily traffic of approximately 24,000 vehicles per day (Rommel and Helmreich, 2018c). The mean annual precipitation depth in 2018 and 2019 was 955 mm (data source: Deutscher Wetterdienst, station 3379). The catchment area comprised two traffic lanes, consisting of one accelerating and one emergency lane, both with an asphalt surface. In 2017 three SQIDs – Drainfix Clean 300 (D, Hauraton, Rastatt, Germany), SediSubstrator XL 600/12 (S, Fränkische Rohrwerke, Königsberg (Bayern), Germany), and ViaPlus 500 (V, Mall, Donaueschingen, Germany) – were installed in close proximity to each other to test their treatment efficiency under equal on-site conditions and to monitor the contamination of traffic area runoff over a period of 2.75 years (Figure 5.2). SQIDs S and V consisted of underground chambers with sedimentation stages and downstream media filtration, of which the filter media of S was permanently submerged, and that of V was not. A sedimentation shaft with a volume of 7.2 m^3 and a diameter of 2 m was installed upstream of V to enable particle separation in addition to that of the hydrodynamic separator in SQID V. The third SQID (D) was a filter substratum channel. The three SQIDs were connected to different catchment areas in accordance with their technical approval and the on-site boundary conditions, these being 1660 m^2 for S, 473 m^2 for V, and 165 m^2 for D. The filter materials used were carbonate sand in D (Drainfix®Carbotec 60, Hauraton, Rastatt, Germany), an iron-based medium with added lignite in S (SediSorp®plus, Fränkische Rohrwerke, Königsberg (Bayern), Germany), and clinoptilolite, a zeolite mineral, in V (ViaSorp®, Mall, Donaueschingen, Germany). The properties of the blank filter media are set out in Table S1†. The influent of the SQIDs (road runoff) was sampled and analyzed during 30 runoff events, as described in the Supporting Information (Appendices A and B†).

The filter media were withdrawn after approximately 2.75 years in operation. To reduce the amount of samples and because previous studies of bioretention systems reported only relevant heavy metal contamination in the first 5 cm to 10 cm

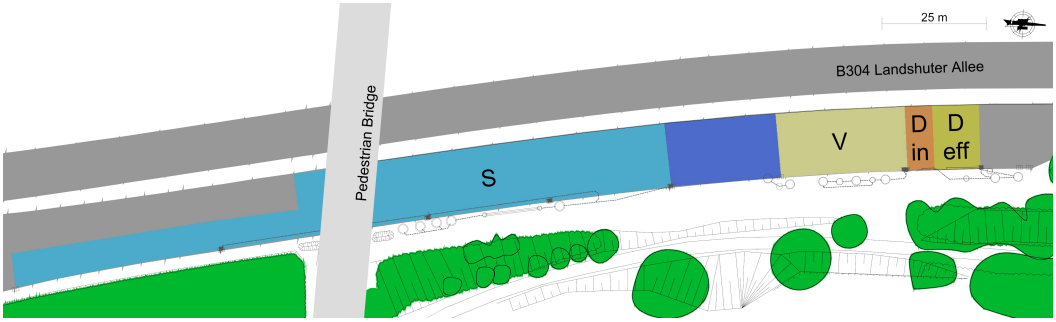

Fig. 5.2. Layout of the monitoring site, the different colors (except green) indicate the catchment areas of the stormwater quality improvement devices S (SediSubstrator XL 600/12), V (ViaPlus 500) and D (Drainfix Clean 300). D in indicates the catchment of the influent sampling for SQID D and D eff indicates the actual catchment of SQID D. (For interpretation of the references to colour in this figure legend, the reader is referred to the web version of this article.)

(Al-Ameri et al., 2018; Hatt et al., 2008; Muthanna et al., 2007), only the first 5 cm in the flow direction of each filter media were withdrawn, using a plastic spatula or stainless-steel soil sampler (approx. 30 punctures); the samples were then homogenized in a bucket and air-dried. The filter media samples withdrawn after the field tests were subsequently denoted D Field, S Field, and V Field, according to the respective SQID. Bacon and Davidson (2008) noted that sample pre-treatment such as drying and grinding could result in more extractable forms of heavy metals. Therefore, no further preparation of the samples was undertaken prior to the extraction procedure. It should be emphasized that the filter media can therefore contain a significant amount of particulate matter that was retained by straining and physical filtration. Consequently, additional samples of trapped sediments were withdrawn from the sedimentation stages of S and V and the filter cake from D to evaluate the proportion of particulate matter among the heavy-metal contaminants. These samples were subsequently labeled S Sediment, V Sediment and D Filter Cake. The samples were sieved to $\leq$1 mm to remove unrepresentative trash and leaf debris. To reduce microbial degradation, all samples were stored in a refrigerator at 4 ± 1 °C prior to analysis.

5.2.2 Prestressing of filter media at lab scale

Blank filter media (the same as were used in the field tests) were prestressed in lab-scale column tests using synthetic runoff, for comparison with the prestressed filter media after the field tests. The method was adapted from Huber et al. (2016d). This protocol is comparable to the evaluation of the service life of SQIDs employed for testing the retention of Cu and Zn for German technical approval (DIBt, 2017). Accordingly, the lab-scale tests were only concerned with Cu and Zn. The Cu and

Tab. 5.1. Conditions and prestressing of the filter media on a lab scale

SQID	Catchment area	Full-scale filter surface	Scale	Zn load	Zn retention	Cu load	Cu retention
Unit	m²	m²	-	mg	%	mg	%
S	830[a]	0.41	1:82	3758	95.8	431	>97.3
D	165	1.55	1:197	1120	>99.3	129	>97.3
V	473	0.63	1:80	2194	99.0	252	>97.3

[a] This represents half of the connected catchment area, as only one of the two installed filter cartridges was analyzed and the loads of the two filter cartridges were assumed to be equal

Zn load applied in the column tests corresponded with 2.75 years of operation in field testing. The samples were withdrawn and preprocessed as described above for the field samples. In the following, they are referred to as D Lab, S Lab and V Lab, according to the respective SQIDs. The applied loads of dissolved Cu and Zn were determined from the respective annual loads of 15.5 mg m^{-2} a^{-1} Cu and 135 mg m^{-2} a^{-1} Zn, multiplied by the number of years in operation, the size of the catchment area of the full-scale SQID, and the model scale. The model scales were determined by dividing the full-scale filter surface by the lab-scale filter surface (Table 5.1). The filter media height was selected in accordance with the full-scale design, and, in the case of circular filter cartridges, on the basis of the mean filter surface and filter height. The sizes and designs of the columns were individually chosen for each filter medium to reflect the flow conditions present in the full-scale SQIDs (permanently submerged filter medium in S and percolation through the filter media in D and V) and to produce a sufficient sample mass.

Copper(II) sulfate pentahydrate ($CuSO_4 \cdot 5\,H_2O$, Merck, Darmstadt, Germany) and zinc sulfate heptahydrate ($ZnSO_4 \cdot 7\,H_2O$, Merck, Darmstadt Germany) were dissolved in 35 to 117.4 L deionized water without buffer to achieve the aforementioned Cu and Zn loads. The pH of the solution was adjusted to 5.0 ± 0.1 to ensure dissolution of the Cu and Zn salts. The electrical conductivity (EC) of the feed solution was $116.0 \pm 0.4\,\mu S\,cm^{-1}$. The feed water volume was chosen to achieve similar concentrations in all experiments: 32.0 mg L^{-1} Zn and 3.67 mg L^{-1} Cu. The feed water was applied at a flow rate that reflected a rain intensity of 10 L s^{-1} ha^{-1} Huber et al. (2016d). The SQID S column was operated in upflow, in accordance with the approval protocol for the device. The other columns were operated in downflow and the water applied through spray nozzles. The total effluent from each filter column was collected and the Cu and Zn concentrations analyzed using photometric cuvette tests (LCK360 and LCK329, Hach Lange, Düsseldorf, Germany) to ensure sufficient sorption. The limits of quantification (LOQs) were 0.1 mg L^{-1} for Cu and 0.2 mg L^{-1} for Zn. The pH and EC were measured immediately after the prestressing experiments in accordance with the Standard Methods 4500-H+ and

2520 B (SenTix 41 and TetraCon 925, WTW, Weilheim, Germany) (American Public Health Association et al., 2017). If the Cu and Zn concentrations in the effluents were found to be >10% of the initial concentrations, then the amount of prestressing was insufficient. In this case, the pH of the collected effluent was then readjusted to 5.0 ± 0.1 and the solution recirculated through the column. Only filter media S required two recirculations to achieve sufficient prestressing. In these recirculations, the EC of the feed was 207 and 248 $\mu S\,cm^{-1}$. The pH values of the effluents from the D, S, and V columns were 8.3, 7.4–7.6, and 9.2, respectively. The EC was 248, 168–265, and 285 $\mu S\,cm^{-1}$, respectively. The analysis of the synthetic runoff can be found in Table S2†.

5.2.3 Analysis of filter media, sediments and filter cake

The samples of the filter media, sediments and filter cake were analyzed using the three-step optimized BCR SEP in accordance with Rauret et al. (1999), which is the commonly adopted SEP method at the present time. The resulting fractions obtained from the SEP were labeled as follows:

- F1: Acid-extractable fraction, extracted with 0.11 $mol\,L^{-1}$ acetic acid
- F2: Reducible fraction, extracted with 0.5 $mol\,L^{-1}$ hydroxylamine hydrochloride
- F3: Oxidizable fraction, extracted with 8.8 $mol\,L^{-1}$ hydrogen peroxide and 1.0 $mol\,L^{-1}$ ammonium acetate
- F4: Residual fraction, additional pseudo-total digestion (inverse *aqua regia*) of the residual

It should be emphasized that the aforementioned fractions are commonly attributable to certain geochemical fractions (e.g. acid-extractable, reducible, etc.). However the SEPs cannot quantitatively determine heavy metals in relation to mineral phases due to (i) the re-distribution of analytes among phases during the SEPs, (ii) the non-selectivity of reagents, (iii) the insufficient extraction, and (iv) the undesirable precipitation of other minerals during the SEPs (Bacon and Davidson, 2008). Nevertheless, SEPs provide a useful indication of the mobility of certain heavy metal fractions (Sutherland, 2010). The sum of the fractions F1–F3 was defined as a potentially mobile fraction, and F1 as a highly mobile fraction (Bacon and Davidson, 2008).

The optimized BCR SEP was conducted in 80 mL PP centrifuge tubes (Herolab, Wiesloch, Germany), and all laboratory ware was made of borosilicate glass,

polypropylene (PP), or polytetrafluoroethylene (PTFE), as required. The centrifuge tubes and PP vessels containing the reagent were cleaned using 4 mol L^{-1} HNO_3 and agitated for a minimum of 16 h in an end-over-end shaker at a speed of 15 ± 5 rpm. The reagents were mixed in ultrapure water with a magnetic stirrer as specified by Rauret et al. (1999). At the beginning of the BCR SEP, the centrifuge tubes were filled with 1.0 ± 0.3 g of sample. 40 mL of reagent solution was added in the extraction step for F1 and F2, and 50 mL in the extraction step for F3. The tubes were then sealed with PTFE tape. The 16 h extraction steps for F1–F3 were subsequently performed in a mechanical end-over-end shaker at a speed of 30 ± 5 rpm and a room temperature of 22 ± 3 °C. The extraction step for F3 differed from the other two by way of its hydrogen peroxide digestion, which involved adding 10 mL H_2O_2 (8.8 mol L^{-1}) twice in sequence and heating in a water bath at 85 ± 2 °C before adding the reagent and shaking. This step is described in more detail in Rauret et al. (1999). After the shaking procedure, the solid residue was separated from the supernatant by centrifugation for 20 min at 3000 g and cooled to 20 °C. After the first and second extraction steps, the interim residues were washed with 20 mL ultrapure water, shaken for 15 min at a speed of 15 ± 5 rpm, and the supernatant discarded after separation by centrifugation, as described above. All samples taken during the BCR SEP were stored in a refrigerator at 4 ± 1 °C prior to analysis. Not only were triplicates of each media analyzed but the certified reference material BCR-701 was analyzed three times in different sample batches together with the other samples, for quality control reasons (Rauret et al., 2001). The evaluation revealed a good agreement with the certified values (Supporting Information, Appendix E†). Only the F4 fraction displayed lower pseudo-accuracy due to the increased bias after the extraction steps. Mean recoveries of 98–108% were achieved for Cr, Cu, Ni, Pb, and Zn after pseudo-total digestion of the reference material. To correct the moisture content of the samples, the dry mass was determined by drying a 1 g sample at 105 ± 2 °C for at least 16 h until constant weight was attained (DIN EN 15934:2012). All analytical results in this study are reported in respect of the dry mass of the samples. The dried samples were further annealed for 2.5 h at 550 °C to determine the loss on ignition (LOI) in accordance with DIN EN 15935:2012.

Cd and Pb concentrations were analyzed using an inductively coupled plasma mass spectrometer (ICP-MS, NexION 300D, Perkin Elmer, Waltham, USA) and those of Cr, Cu, Ni, and Zn with an inductively coupled plasma optical emission spectrometer (ICP-OES, Ultima II, Horiba Jobin Yvon, Kyoto, Japan). The LOQs of Cd, Cr, Cu, Ni, Pb, Zn for the solution samples were 0.001, 0.02, 0.02, 0.02, 0.001, and 0.02 mg L^{-1}, respectively. The residuals after the SEP and the filter media samples for the pseudo-total analysis were digested prior to the HM analysis using inverse *aqua regia* digestion (iAR, *aqua regia* digestion: DIN EN 13346:2001).

Because of the high organic content of the samples, iAR digestion was employed with an inverse HNO_3:HCl ratio (3:1). The filter media were dried at 105 °C and ground prior to iAR digestion to gain representative subsamples for the pseudo-total analysis. The LOQs of Cd, Cr, Cu, Ni, Pb, Zn for the solid samples were 1.0, 5.0, 5.0, 2.0, 10.0, and 1.0 $mg\,kg^{-1}$, respectively. The LOQs for the SEP fractions can vary due to correction of the moisture content in the analyzed samples.

The pH values of the filter media and filter cake were determined in accordance with DIN EN 15933:2012 by adding 0.01 $mol\,L^{-1}$ $CaCl_2$ solution to 5 mL of sample volume. The suspension was agitated using an end-over-end shaker set to 20 ± 2 rpm for 1 h prior to measuring the pH. Frozen retained samples of the sediments were defrosted at ambient temperature, homogenized by manual shaking, and left to stand for 30 min. The pH of the bulk sediment samples was then measured without adding any $CaCl_2$ solution due to the high water content, in accordance with DIN EN 15933:2012. The pH values were determined according to the Standard Method 4500-H+ (SenTix 41, WTW, Weilheim, Germany) (American Public Health Association et al., 2017).

5.2.4 Data analysis

All concentrations determined below the LOQs were substituted by 0.5 times the LOQ values. Depending on the hypothesis, either one- or two-sided t-tests were applied using statsmodel (Seabold and Perktold, 2010). Road runoff data were analyzed using either the Mann-Whitney rank sum test or the Kruskal-Wallis H-test for more than two groups in Scipy (Virtanen et al., 2020), due to the non-normal distribution of the data. All hypothesis tests applied had a significance level of 0.05.

Hierarchical cluster analysis (HCA) was used to evaluate the similarity (or dissimilarity) between the measured parameters and the samples (Giacomino et al., 2011). To map all the variables (measured parameters) to the same range from 0 to 1, the data was minimum-maximum transformed prior to the HCA (Xue et al., 2011; Moreda-Piñeiro et al., 2001). Euclidean distance was used as measure for distance and Ward's method for agglomeration (Giacomino et al., 2011). The HCA was visualized in a dendrogram, and HCA was applied using Scipy (Virtanen et al., 2020).

5.3 Results and discussion

5.3.1 Analysis of road runoff

The observed total concentrations of Cr, Cu, Ni, and Zn in the road runoff (influent of the SQIDs in the field test, see Table 5.2) over the 2 years of field monitoring were comparable to the concentrations found in the runoff from roads with a high annual average daily traffic (>15,000 vehicles per day) (Huber et al., 2016c). In contrast to the review, considerably lower total concentrations of Cd and Pb were quantified in the field monitoring, only 2.5% of Cd and 13.0% of Pb. As expected, no significant differences ($p > 0.05$) were observed between the influent concentrations of the three SQIDs. The concentrations used as the influent load for the prestressing procedure in the lab tests were considerably higher than those in the field test – 44 times higher for Cu and as much as 123 times higher for Zn (Table 5.2, Table S2†). This is because the prestressing procedure in the laboratory is much shorter but still has to reflect a similar period of operation (2.75 years) to achieve the same prestressing of the filter media. It should be noted that the observed concentrations of dissolved heavy metals in the field test were significantly lower (Table 5.2), because the majority of heavy metals in the road runoff were particulate-bound, due to the significantly higher pH than in the lab-scale tests. The median pH was 7.8 in the field, compared with 5.0 in the lab-scale tests. Consequently, 98% of the Cu and 100% of the Zn were found to be dissolved in the lab-scale test. Because the lab-scale test only assesses the retention of dissolved heavy metals (Huber et al., 2016d), it is more appropriate to compare the dissolved Cu and Zn loads. Assuming a discharge coefficient of 0.9 (*DWA-M 153* 2007), the dissolved loads of Cu and Zn were 1.5 and 4.1 times higher, respectively, in the lab tests. Since the dissolved concentrations of Cd were all below LOQ, this element was not considered further in the study. The partition of the heavy metals (dissolved or particulate-bound) is crucial to their retention on sorptive filter media, as only dissolved heavy metals can be retained there by sorption processes. Particulate-bound heavy metals are retained in the filter media solely by filtration (or, in the previous sedimentation stage, by sedimentation). The particulate-bound heavy metals are present in the total suspended solids (TSS). The median TSS concentration in the influent of the SQIDs was 85.1 $mg\,L^{-1}$. As a consequence, sediments accumulated in S and V, and a filter cake formed in D. The non-settled particles from the sedimentation stages accumulated in the filter media by physical straining and filtration.

In addition to pH, both alkalinity and DOM can also have an impact on heavy metal retention in SQIDs (Barrett et al., 2014; Genç-Fuhrman et al., 2016). Increasing alkalinity can increase heavy metal retention by precipitation of dissolved heavy

Tab. 5.2. pH values, electric conductivity (EC), total suspended solids (TSS), total and dissolved concentrations of Cd, Cr, Cu, Ni, Pb, and Zn in the influent of SQIDs in field tests, reported as median (25–75th percentiles).

	pH	EC	TSS	Cd	Cr	Cu	Ni	Pb	Zn
Unit	-	µS cm^{-1}	mg L^{-1}	µg L^{-1}	µg L^{-1}	µg L^{-1}	µg L^{-1}	µg L^{-1}	µg L^{-1}
				Total					
n	90	90	89	90	78	90	90	90	90
	7.8 (7.6–8.1)	132 (75.0–317)	85.1 (36.0–135)	<0.10 (<0.10–0.12)	13.3 (5.3–24.2)	82.8 (51.0–119)	6.4 (3.0–9.5)	5.8 (2.9–9.3)	261 (139–438)
				Dissolved					
n				25	25	25	25	25	25
				<0.50 (<0.50–<0.50)	9.4 (2.0–15.7)	12.2 (6.4–20.8)	1.3 (<1.0–2.0)	<1.0 (<1.0–1.0)	38.2 (25.4–79.8)

metals and increasing adsorption (Barrett et al., 2014). The presence of DOM can also result in reduced heavy metal retention by formation of complexes with heavy metals and competitive sorption (Barrett et al., 2014; Genç-Fuhrman et al., 2016; Haynes, 2015). However, the conducted lab-scale test neither considers alkalinity nor DOM. To gain knowledge about the alkalinity of the influent, this parameter was additionally analyzed, commencing in November 2018. The median alkalinity was 68.9 mg L^{-1}, reported as bicarbonate (HCO_3^-). The 25th and 75th percentiles were 59.6 and 80.5 mg L^{-1}, respectively (n=25). Dissolved organic carbon (DOC) concentrations of 7.0 mg L^{-1} (5.4 mg L^{-1} to 11.4 mg L^{-1}, n=38) were determined as representative parameter for DOM.

5.3.2 Analysis of sediment and filter cake

To evaluate the particulate-bound contamination of road runoff, the sediments trapped in the sedimentation stages of SQIDs S and V were sampled, as was the filter cake formed on the filter surface of SQID D. The sediments and filter cake displayed the highest Cr, Cu, Ni, and Zn total content, expressed as sum of F1 to F4 (Table 5.3, Fig. S2†), which underlines the need for particle separation to retain the heavy metals present in road runoff. The order of occurrence, based on total content, was Zn $\gg$ Cu $\gg$ Cr > Ni $\approx$ Pb, which corresponds with the contamination of the road runoff (*cf.* 5.3.1). The mean total contents (sum of F1–F4) of Cr, Cu, Ni, Pb, and Zn in the analyzed sediments (from SQID S and V) were 171, 479, 51.6, 47.7, and 1546 mg kg^{-1}, respectively. The SQID V sediment was already sampled after

approximately 2 years of operation and displayed a comparable content (Rommel et al., 2020d). This indicates that the content is potentially constant over time, even though the mass of sediment or filter cake will increase over time. To investigate this further, sampling over a longer period of time is necessary. The levels of Cr, Cu, Ni, and Zn detected in the sediment and filter cake samples exceeded those found in the sediments of two sedimentation tanks and two detention ponds in Sweden, which had already displayed effects of toxicity on bioassays using the luminescent bacteria *Vibrio fischeri* (Karlsson et al., 2010). The observed contamination level was comparable to previously reported heavy metal levels in RDSs (Sutherland et al., 2012; Li et al., 2013; Pérez et al., 2008). Consequently, the levels of contamination in RDSs and in sediments trapped in SQIDs are comparable, which makes sense, since RDSs are the source of the sediments. The heavy metal content of the filter cake in SQID D was comparable to that of the sediments, except that only approximately half of the Cu content was present.

Sequential extraction indicates that the Cr in the sediments and filter cake is predominantly associated with the residual fraction (61–97%, Figure 5.3, Fig. S2†) and thus showed a high strength of association and a very low tendency to remobilization. The Cu in the filter cake was mostly found in the oxidizable (45%) and residual fractions (43%). In contrast, the Cu in the sediments was associated with the reducible (52–55%) and oxidizable fractions (29–30%). The fractionation of Ni and Pb also varied between the sediments and the filter cake. In the filter cake, 88% of Ni was detected in the residual fraction, while 57–63% was found in the residual fraction of the sediments. Furthermore, the sediments showed a greater acid-extractable Ni fraction (17–22%) com- pared to the filter cake (3%). Pb was mainly associated with the oxidizable fraction (59%) in the filter cake and with the reducible fraction (66–67%) in the sediments. Zn was predominantly found in the acid-extractable (54–59%) and reducible fractions (21–28%) in both the sediments and the filter cake. Surprisingly, larger Cu and Pb fractions were found in the oxidizable fraction, which can be attributed to the presence of organic matter (Davidson et al., 1998), even though the filter cake had approximately half of the organic matter content (10% LOI) compared to that of the sediments (mean LOI of S sediment: 19%; mean LOI of V sediment: 21%). This may be due to the aging effects of the organic matter under varying conditions (e.g. oxidizing-reducing) (Kumar et al., 2013a; Kumar, 2016). The sediments are permanently submerged, whereas the filter cake is able to dry between runoff events. Kumar et al. (2013b) found that Cu was predominantly detectable in the oxidizable, Pb in the reducible, and Zn in the acid extractable fractions of soakaway sediment in a parking area. In contrast to our results, Camponelli et al. (2010) detected Cu predominantly in the residual fraction and Zn in the residual and reducible fractions. However, these

Tab. 5.3. Cr, Cu, Ni, Pb, and Zn content found in sequential extraction fractions of the filter media prestressed in the field test (D Field, S Field, V Field), sediments (S Sediment, V Sediment) and filter cake (D Filter Cake) withdrawn from the SQIDs after the field test, reported as mean contents and standard deviation (±SD) in mg kg^{-1} dry matter. Bold values indicate the largest fraction; F1–F4 were analyzed as triplicates (n = 3); recovery [%] = (sum F1–F4 / pseudo-total) × 100 (Unda-Calvo et al., 2019).

Element	Sample	F1 Acid-extractable	F2 Reducible	F3 Oxidizable	F4 Residual	Sum F1–F4 [a]	Pseudo-total [b]	Recovery [%]
Cr	D Field	0.4 ± 0.0 [c]	0.4 ± 0.0 [c]	2.4 ± 0.2	**102 ± 0**	108 ± 2	22.4	480
	D Filter Cake	0.6 ± 0.0 [c]	0.8 ± 0.4 [c]	10.8 ± 1.3	**116 ± 24**	128 ± 25	90.2	142
	S Field	0.5 ± 0.0 [c]	1.8 ± 0.3	**5.5 ± 0.1**	3.7 ± 2.0 [c]	11.5 ± 1.8	6.2 [c]	184
	S Sediment	7.9 ± 0.4	20.1 ± 0.8	35.5 ± 1.5	**97.9 ± 1.5**	161 ± 4	131	123
	V Field	0.5 ± 0.0 [c]	**4.1 ± 0.1**	3.0 ± 0.2	2.5 ± 0.0 [c]	10.2 ± 0.1	16.6	61
	V Sediment	3.5 ± 0.0	20.0 ± 0.1	35.4 ± 1.6	**121 ± 18**	180 ± 17	113	159
Cu	D Field	3.6 ± 0.2	2.2 ± 0.3	22.8 ± .5	**108 ± 9**	137 ± 8	41.1	334
	D Filter Cake	8.3 ± 0.5	20.9 ± 2.7	**119 ± 11**	113 ± 2	262 ± 10	214	123
	S Field	1.7 ± 0.4	8.9 ± 1.1	**33.2 ± 0.9**	8.6 ± 5.7 [c]	52.4 ± 6.8	32.9	159
	S Sediment	53.3 ± 2.0	**240 ± 2**	133 ± 8	36.0 ± 1.3	462 ± 9	399	116
	V Field	16.1 ± 1.1	**38.9 ± 0.4**	10.5 ± 0.4	2.5 ± 0.0 [c]	68.0 ± 1.7	64.6	105
	V Sediment	26.7 ± 1.7	**272 ± 5**	150 ± 2	48.6 ± 2.2	497 ± 8	444	112
Ni	D Field	0.4 ± 0.0 [c]	0.4 ± 0.0 [c]	0.5 ± 0.0 [c]	**38.0 ± 4.1**	39.4 ± 4.1	11.7	337
	D Filter Cake	1.3 ± 0.7 [c]	0.9 ± 0.6 [c]	3.2 ± 0.3	**40.7 ± 13.0**	46.0 ± 12.9	23.2	199
	S Field	10.1 ± 0.5	**17.8 ± 1.2**	10.5 ± 1.2	12.9 ± 2.2	51.3 ± 4.6	42.0	122
	S Sediment	11.4 ± 0.9	5.5 ± 1.9	5.6 ± 1.4	**29.1 ± 0.9**	51.6 ± 3.9	34.1	151
	V Field	0.5 ± 0.0 [c]	**1.7 ± 0.2**	0.9 ± 0.4 [c]	1.0 ± 0.0 [c]	4.1 ± 0.6	8.0	51
	V Sediment	9.0 ± 1.4	5.0 ± 1.0	5.3 ± 1.4	**32.3 ± 2.5**	51.6 ± 0.5	34.3	150
Pb	D Field	0.1 ± 0.0	0.4 ± 0.1	4.0 ± 0.7	**17.2 ± 3.0**	21.7 ± 2.3	5.0 [c]	434
	D Filter Cake	0.3 ± 0.0	2.3 ± 0.2	**13.1 ± 1.9**	6.7 ± 3.0 [c]	22.3 ± 1.5	24.7	90
	S Field	0.0 ± 0.0 [c]	0.1 ± 0.0 [c]	3.6 ± 0.3	**5.0 ± 0.0** [c]	8.7 ± 0.4	5.0 [c]	174
	S Sediment	6.6 ± 0.2	**31.6 ± 0.6**	4.7 ± 0.6	5.0 ± 0.0 [c]	47.9 ± 0.3	46.8	102
	V Field	0.1 ± 0.1	**35.3 ± 11.0**	8.3 ± 1.9	5.0 ± 0.0 [c]	48.7 ± 13.0	42.0	116
	V Sediment	3.3 ± 0.3	**31.7 ± 0.9**	7.4 ± 2.5	5.0 ± 0.0 [c]	47.4 ± 1.9	49.8	95
Zn	D Field	117 ± 1	84.5 ± 5.4	54.1 ± 7.0	**557 ± 37**	813 ± 37	333	244
	D Filter Cake	**1024 ± 46**	526 ± 54	123 ± 18	223 ± 7	1896 ± 120	1521	125
	S Field	71.7 ± 3.0	**165 ± 13**	55.8 ± 6.2	79.2 ± 10.5	372 ± 21	274	136
	S Sediment	**917 ± 15**	327 ± 4	137 ± 8	169 ± 37	1543 ± 50	1218	127
	V Field	89.1 ± 5.0	**144 ± 3**	14.0 ± 1.1	37.3 ± 2.5	285 ± 5	260	109
	V Sediment	**855 ± 16**	387 ± 4	171 ± 29	136 ± 14	1548 ± 53	1311	118

[a] Sum of means of F1, F2, F3, and F4; [b] Mean of duplicate; [c] Analysis result contains values below limit of quantification (LOQ), which were substituted by 0.5·LOQ

results are not fully comparable with ours, as they are based on a different SEP method. Furthermore, previous studies found similar heavy metal fractionations in RDS (Sutherland et al., 2012; Zhang et al., 2019b; Li et al., 2013; Pérez et al., 2008).

Potential mobility can be deduced from the distribution of heavy metals in the SEP fractions (Bacon and Davidson, 2008). The order of potential mobility of the heavy metals in the sediments, determined by the sum of F1, F2, and F3 (Kumar, 2016), Cu ≈ Zn ≈ Pb > Ni ≈ Cr. In the filter cake, the order was Zn > Pb > Cu > Ni > Cr and displayed considerably smaller potentially mobile fractions. These mobility orders are supported by the results of RDS leaching tests conducted by Zafra et al. (2017). In addition, Zn was present in large fractions in F1, which implies that it is potentially highly mobile (Bacon and Davidson, 2008). The sediments

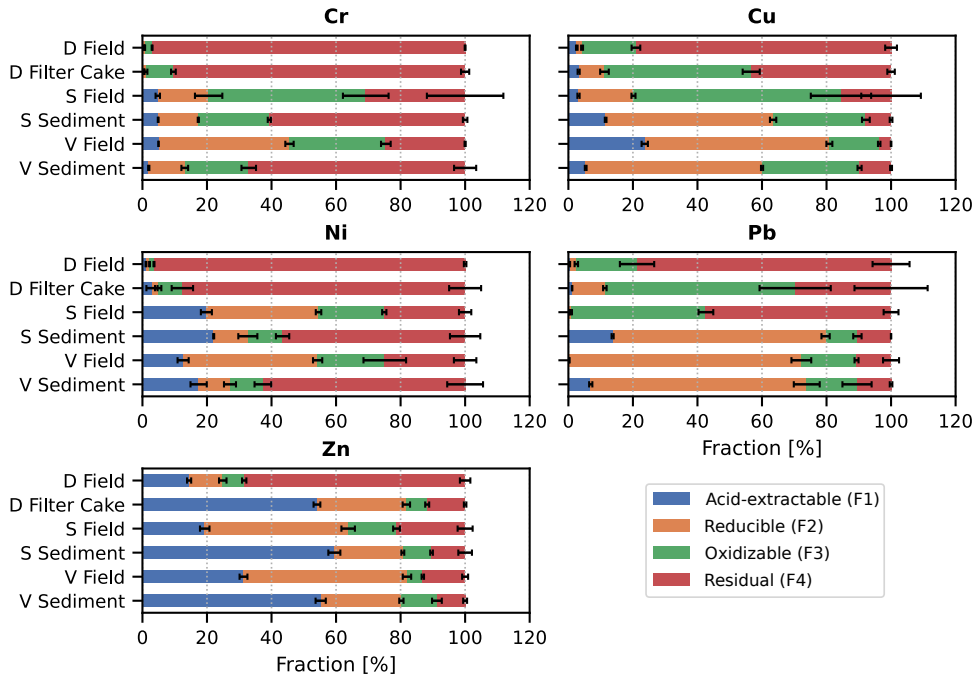

Fig. 5.3. Fractions of Cr, Cu, Ni, Pb, and Zn found in the respective sequential extraction fractions of the filter media prestressed in the field test (D Field, S Field, V Field), sediments (S Sediment, V Sediment) and filter cake (D Filter Cake) withdrawn from the SQIDs after the field test; n=3 for each sample and fraction. The bars indicate mean values and the error bars show the standard deviation.

trapped in the SQIDs showed a higher risk of remobilization in comparison to those in the filter cake. However, this interpretation is uncertain, because the potentially mobile fractions F1, F2, and F3 are associated with the operationally defined acid-extractable, reducible and oxidizable fractions, which describe conditions that are potentially only present in the SQIDs for a short length of time, if at all. However, to our best knowledge, no comprehensive data series are available on pH and redox conditions in full-scale SQIDs. Hence, future studies need to characterize these in order to enable an evaluation of the actual mobile heavy metal fractions. Datry et al. (2003) demonstrated that oxidation of organic carbon lead to almost permanent anoxic conditions in a stormwater infiltration basin. Comparable conditions can be expected in SQIDs. The fact that bacteria occurring under anoxic conditions were found more abundantly in the filter medium of SQID S than of SQID D further supports this hypothesis (Liguori et al., 2021). Nevertheless, Datry et al. (2003) only observed leaching of nutrients and DOC under anoxic conditions, not of heavy metals. Nonetheless, the sediments and filter cake deposited in the SQIDs featured different fractionation patterns, which most likely are a consequence of the anoxic conditions in the permanently submerged sediments. This assumption is further supported by dissimilarity between the sediments and the filter cake determined by the HCA (*cf.* 5.3.5).

Previous leaching experiments based on synthetic runoff, sediment from SQID V, and contact times of up to 7 d, displayed a partially contradictory mobility order: Ni > Zn > Cu $\gg$ Cr $\gg$ Pb (Rommel et al., 2020d). This highlights the influence of experimental conditions on the leaching of heavy metals. Nevertheless, the results of both studies underline the risk associated with sediments trapped in SQIDs.

5.3.3 Analysis of filter media prestressed in the field

All filter media displayed increased heavy metal content after filtering road runoff for a period of 2.75 years, with the exception of Pb in filter media D (Table 5.3, Fig. S2†). This may be due to low recovery by pseudo-total digestion (Table 5.3). The heavy metal contents were up to 26 times higher after the prestressing. Although the quality control displayed good determination quality (Supplementary Information, Appendix E†), pseudo-total digestion was generally not capable of extracting the same heavy metal content as the sum of the SEP fractions plus the residual. The samples of filter medium D point to a particularly low efficiency of pseudo-total digestion, indicating that the carbonate-rich medium is a challenging sample matrix for the selected pseudo-total digestion method. Consequently, the sum of F1–F4 was used to describe the total heavy metal content. Future studies should therefore employ a different pseudo-total digestion method to enable the heavy metal content

of filter media to be determined sufficiently. However, for this study, pseudo-total content is of minor importance. Similar deviations between the sum of F1–F4 and pseudo-total digestion have been reported by Davidson et al. (1998), who analyzed soil samples from an industrial site. Based on total heavy metal content (sum of F1–F4), the sediment samples from SQIDs S and V revealed significantly ($p < 0.05$) higher levels of Cr, Cu, and Zn than filter media after prestressing in the field. This highlights that sediments or filter cakes trapped SQIDs feature a higher contamination level than the filter media. This can be attributed to the predominantly particulate-bound fraction of heavy metals due to the pH values under real conditions. The SQID S medium showed no significant difference to the sediment in terms of Ni content due to the higher initial content (Table S1†). The Pb content of the sediment and filter medium of SQID V were not significantly different. In SQID D, only Cu and Zn levels were significantly higher in the filter cake than in the filter medium. This can be attributed to depth filtration, which leads to an increased heavy metal content in the top layers due to interception of contaminated particles.

Because particles in road runoff are predominantly present in the fine fraction ($<63\,\mu$m) (Kayhanian et al., 2012b; Selbig et al., 2016; Charters et al., 2015), the particles cannot be completely retained by sedimentation. Thus, heavy metal-containing particles are trapped in the filter media by surficial straining and depth filtration (Teng and Sansalone, 2004; Strecker et al., 2005). Since it was not possible to remove these retained particles inside the filter media, it cannot be assessed whether the contamination in the filter media originates from dissolved or particulate-bound heavy metals. However, it was possible to analyze the strength of association between heavy metals and filter media for SQIDs (with intercepted particulate matter) in full-scale application.

Disregarding filter medium S, the other two filter media featured higher organic contents after prestressing, as expressed by the LOI (Tables S1 and S4). This increase is most likely caused by the physical filtration of the particulate matter, which contained a large amount of organic matter, as observed with the sediment samples (Table S4†) and which had not been fully separated prior to media filtration (SQID S and V). In the case of SQID D, there had been no pretreatment sedimentation stage, which meant that the particulate matter was predominantly retained as filter cake by straining on the filter surface and by filtration in the filter medium. The filter cake also had a high organic content. The similarity between filter medium D and the filter cake was further demonstrated by the HCA (*cf.* 5.3.5).

The fractionations of heavy metals in the various filter media differed greatly (Figure 5.3, Table 5.3). Whereas all the analyzed heavy metals in filter medium D were predominantly associated with the residual fraction (>68%), fractionations

in the filter media S and V were more similar, and varied for each of the heavy metals. Cr was mostly bound to the oxidizable (49%) and residual fractions (31%) in filter medium S, and to the reducible (41%), oxidizable (30%), and residual fractions in filter medium V (25%). In contrast, Cu was mainly in the oxidizable fraction (64%) in filter medium S and 57% was found in the reducible fraction in filter medium V. Ni fractionations were comparable in filter media S and V with 35% and 42%, respectively, in the reducible fraction, 25% in the residual fraction of both media, and 20% and 21%, respectively, in the oxidizable fraction. Pb was present in the oxidizable (42%) and residual fractions (57%) of filter medium S, in contrast to filter medium V, where it was mostly present in the reducible fraction (72%). Finally, Zn was primarily associated with the reducible fraction in filter media S (44%) and V (51%). The largest acid-extractable fractions were observed for Zn in all filter media. The fraction differences between the heavy metals can be attributed to the varying retention processes employed by the different media. Filter medium D consists of calcium carbonate-containing sand, which can significantly increase the pH by dissolution of carbonate. As a result, heavy metals precipitate as metal oxides and carbonates (Reddy et al., 2014; Acosta et al., 2009). In addition, sorption is involved in the retention of heavy metals by calcium carbonate (Aziz et al., 2001; Haynes, 2015). Filter medium S is an iron-based filter medium with an amendment of lignite. Thus, the expected retention processes are sorption, surface complexation, and precipitation due to the calcium carbonate content (Huber et al., 2016b). Filter medium V is clinoptilolite, a zeolite mineral, which commonly exhibits rapid and reversible cation exchange and a certain degree of specific adsorption (ion sieving) (Colella, 1996; Young, 2013; Wang and Peng, 2010; Athanasiadis and Helmreich, 2005). Because filter medium S is an iron-based medium, a dominant reducible fraction was expected, since the reducible fraction is associated with iron and manganese oxides (Beckett, 1989; Davidson et al., 1998). Only Ni and Zn were present to a significant degree in the reducible fraction. However, filter medium V showed even greater reducible fractions, even though this was not expected due to the material properties. Since clinoptilolite displays ion-exchange behavior (Wang and Peng, 2010), it was assumed that the heavy metals are associated with the highly mobile, acid-extractable fraction, which is also linked to exchangeable heavy metals (Davidson et al., 1998). This was only observed to a moderate extent for Cu and Zn. Since the acid-extractable fraction also targets carbonates (Davidson et al., 1998), it was remarkable that the D filter media displayed the smallest percentages of this fraction.

Li and Davis (2008) analyzed biofilter media (sand, topsoil and mulch) and also observed Zn as the most mobile heavy metal. They found Cu distributed in all but the soluble-exchangeable fraction. Pb was mostly present in the carbonate

and residual fractions. Wang et al. (2017) analyzed biofilter media, which also consisted of zeolite with a lignin amendment, which was prestressed at lab scale. They observed Cu mostly in the oxidizable, residual, and carbonate fractions, and both Pb and Zn predominantly in the residual fraction. This is remarkable, since a high mobility of Zn (as well as Cd) has been demonstrated by previous studies (Sutherland et al., 2012; Zhang et al., 2019b; Jayarathne et al., 2017). The results of the two aforementioned studies are only partly comparable with ours, since they did not adopt the common optimized BCR method; this is therefore suggested for future studies.

Fractionation revealed that filter medium D shows the greatest immobilization of heavy metals, with potentially mobile fractions of 3%, 21%, 4%, 21%, and 32% of Cr, Cu, Ni, Pb, and Zn, respectively. The respective values for filter medium S are 69%, 84%, 75%, 43%, and 79%. Filter medium V showed the highest tendency towards remobilization, indicated by potentially mobile fractions of 75%, 96%, 75%, 89%, and 87%. This can be attributed to the aforementioned processes supplied by the medium and underlines the assumption that remobilization of previously retained heavy metals can occur. Nevertheless, strong remobilization, as indicated by Huber et al. (2016b) have not yet been demonstrated in full-scale application. This is mainly attributed to the considerably lower heavy metal content in filter media prestressed under field conditions, due to the fact that the heavy metals were mostly particulate-bound. In addition, leaching experiments with long contact times (up to 7 d), simulating submerged filter media during dry periods, did not show remobilization of previously retained heavy metals (Rommel et al., 2020d). In these experiments, the synthetic runoff more closely reflected properties of road runoff (e.g. pH, alkalinity). Consequently, future studies need to evaluate whether the potentially mobile fraction can be remobilized under full-scale application. Nevertheless, the acid-extractable fraction found in the filter media – especially that of Zn – poses a risk, since it is considered highly mobile (Bacon and Davidson, 2008). Another factor to be evaluated in additional studies is whether the good immobilization of filter medium D is due to the design of the SQID. The filter medium in D can become dry by virtue of its being located on the site surface, unlike the other SQIDs investigated, which are located underground. Kumar et al. (2013a) showed that intermittent flow conditions induce Cu retention and the release of Zn and Pb. Opposing this assumption is the fact that a previous column experiment using biofilter media (sandy loam, sand) displayed increased heavy metal retention when the filter medium was partly submerged (Blecken et al., 2009). Furthermore, bacteria occurring under anoxic conditions were found more abundantly in the filter medium of SQID S than of SQID D (Liguori et al., 2021), which indicates

that permanently submerged filter media are exposed to anoxic conditions that can facilitate remobilization of heavy metals (Bourg, 1988).

Besides the retention of dissolved heavy metal species, the physical separation of particulate-bound heavy metals by screening and filtration may be more relevant for the total heavy metal retention, since it is mostly particle-bound heavy metals that are found in road runoff (Kayhanian et al., 2012a; Zgheib et al., 2011b). Nevertheless, dissolved heavy metals are more bioavailable and therefore contribute more to the toxicity of road runoff (Karlsson et al., 2010; Paulson and Amy, 1993). Furthermore, there are also studies that report large dissolved fractions (Huber et al., 2016c). Assuming a mean grain size of 1 mm in the filter medium, particles of a diameter of 50 μm to 100 μm are primarily retained within the filter medium by depth filtration, and smaller particles by physical and chemical adsorption (Teng and Sansalone, 2004; Strecker et al., 2005). Because particle sizes below 100 μm are predominant in road runoff (Gelhardt et al., 2017), particulate matter inevitably accumulates within the filter media, even with upstream sedimentation stages. This accumulation of particulate matter in the filter medium is further suggested by the results of the HCA (*cf.* 5.3.5).

5.3.4 Comparison of filter media prestressed in the field and lab-scale

Compared with filter media prestressed in the field, the S and V media prestressed at lab scale contained significantly ($p < 0.05$) higher contents of Cu and Zn (sum of F1–F4, Table 5.4, Fig. S3†). Indeed, the Cu and Zn content after prestressing at lab scale was 7 to 32 times higher. This is even more than the ratio between lab and field loads calculated previously (*cf.* 5.3.1). It can therefore be assumed that an increased retention of dissolved heavy metals takes place in laboratory tests compared to field tests. This can mainly be attributed to the higher influent concentrations in lab-scale tests, since sorption is concentration-dependent (Blume et al., 2016b). To reduce this bias, the mass of the tested filter medium in the lab-scale tests could be reduced to achieve a comparable prestressing load with lower influent concentrations without increasing the required synthetic runoff volume. On the other hand, filter medium D contained more Cu and Zn after prestressing in the field. This can be potentially attributed to the retention of particulate-bound heavy metals within the filter medium, which is not considered when prestressing at lab scale.

All filter media in the lab-scale tests showed significantly larger acid-exchangeable fractions of Cu and Zn compared with the filter media prestressed in the field, which indicates a considerably higher mobility (Figure 5.4, Table 5.4). The filter media S

Tab. 5.4. Cu and Zn content of sequential extraction fractions from filter media prestressed either in the field or in the lab, reported as mean contents and standard deviation (± SD) in mg kg^{-1} dry matter. Bold values indicate the largest fraction; F1–F4 were analyzed as triplicates (n=3); recovery [%] = (sum F1–F4 / pseudo-total) × 100 (Unda-Calvo et al., 2019).

Element	Sample	F1 Acid-extractable	F2 Reducible	F3 Oxidizable	F4 Residual	Sum F1–F4 [a]	Pseudo-total [b]	Recovery [%]
Cu	D Field	3.6 ± 0.2	2.2 ± 0.3	22.8 ± .5	**108 ± 9**	137 ± 8	41.1	334
	D Lab	33.5 ± 2.4	0.7 ± 0.4 [c]	21.7 ± 1.3	**54.5 ± 4.5**	101 ± 8	52.9	192
	S Field	1.7 ± 0.4	8.9 ± 1.1	**33.2 ± 0.9**	8.6 ± 5.7 [c]	52.4 ± 6.8	32.9	159
	S Lab	**575 ± 5**	345+8	430 ± 22	306 ± 22	1656 ± 4	1282	129
	V Field	16.1 ± 1.1	**38.9 ± 0.4**	10.5 ± 0.4	2.5 ± 0.0 [C]	68.0 ± 1.7	64.6	105
	V Lab	**289 ± 2**	195 ± 1	6.6 ± 0.3	2.5 ± 0.0 [c]	493 ± 2	444	112
Zn	D Field	117 ± 1	84.5 ± 5.4	54.1 ± 7.0	**557 ± 37**	813 ± 37	333	244
	D Lab	**457 ± 10**	31.3 ± 2.5	11.6 ± 0.9	84.9 ± 5.8	585 ± 11	444	132
	S Field	71.7 ± 3.0	**165 ± 13**	55.8 ± 6.2	79.2 ± 10.5	372 ± 21	274	136
	S Lab	**8410 ± 65**	981 ± 47	57.9 ± 14.0	58.8 ± 33.8	9508 ± 110	8204	116
	V Field	89.1 ± 5.0	**144 ± 3**	14.0 ± 1.1	37.3 ± 2.5	285 ± 5	260	109
	V Lab	**1730 ± 40**	1693 ± 26	32.6 ± 2.8	50.5 ± 2.3	3506 ± 34	3370	104

[a] Sum of the means of F1, F2, F3, and F4; [b] Mean of duplicate; [c] Analysis result contains values below limit of quantification

and D prestressed in the field showed more similarity to the sediment and filter cake samples (also from the field) than to the same filter media prestressed in lab-scale tests (*cf.* 5.3.5). As a consequence, previous lab-scale experiments potentially overestimated the risk of heavy metal leaching due to their predominant occurrence in more mobile fractions. There are multiple possible theories for this. At lab scale, it is generally labile binding sites that are occupied, whereas heavy metals in field filter media show higher strengths of association. This would imply either that the heavy metals shift to stronger forms of association or diffuse into the filter media and are therefore less readily desorbed during extraction (Zhou and Haynes, 2010) or that the weakly bound heavy metals are remobilized in the field before sampling. Another explanation could be that the amount and distribution of filter media sorption sites change due to aging, as indicated by Kumar et al. (2013a). Also, the oxidizable fractions of Cu and Zn were larger in the field samples (with the exception of the Cu in SQID D). This implies that organic matter present in road runoff and not considered in the current lab-scale tests also needs to be considered in an assessment of heavy metal mobility. Lastly, the acidic synthetic runoff used in the lab-scale experiments can alter the filter media properties. For example, filter medium D can be dissolved under acidic conditions because it contains calcium carbonate, which would significantly increase the alkalinity of the pore water, potentially resulting in precipitation of the heavy metals. The iron-based components of filter medium S, mainly hydroxides, are known to display a pH-dependent surface charge. At pH values below 7 to 9.5, the surface is positively charged and therefore exhibits repulsive forces against heavy metal cations (Blume et al., 2016b; Young, 2013). However, adsorption of anions can reduce this effect (Blume et al., 2016b). In addition, acidic

conditions are used for the pretreatment of zeolite filter media (Wang and Peng, 2010), which would likely affect filter medium V as well. The porous concrete ring that surrounds the filter media of SQID V in the full-scale design was not considered in lab-scale prestressing. As a consequence, the pH of the V filter medium would be even higher in the field as it is in contact with concrete surfaces. These limitations demonstrate that the development of a lab-scale test protocol to assure comparability is a very challenging task due to the varying properties of (sorptive) filter media and the fact that dissolved heavy metals precipitate at higher pH values. Nevertheless, future studies should quantify the aforementioned processes to gain further insights into media filtration systems used in stormwater treatment. Moreover, the impact of alkalinity and DOM in lab-scale tests also needs to be evaluated. Barrett et al. (2014) state that heavy metal retention decreases at elevated DOM and alkalinity.

The practical implication of this study is is that current lab-scale tests have potentially a limited validity to assess heavy metal mobility in SQIDs. In many cases, current lab-scale tests focus only on the retention of dissolved heavy metals and thus neglect other important factors, which are essential for the overall treatment efficiency. Nevertheless, lab-scale tests are the only option to obtain reproducible results and to study factors influencing heavy metal retention in detail. To replicate field conditions in the laboratory, physical and physicochemical conditions still need to be further monitored in the field. However, it needs to be acknowledged that field tests are influenced by a wide range of uncontrollable local factors. The redox conditions in SQIDs are currently one of the largest gaps in knowledge, which should be studied in the field. To improve current lab-scale tests, the effect of the composition of synthetic runoffs (e.g. pH, alkalinity, particulate matter, DOM) on the heavy metal retention by sorptive filter media needs to be investigated comprehensively. SEP can be a promising tool for this task. Furthermore, the identification of surrogate materials for particulate matter and dissolved organic matter in road runoff would be useful.

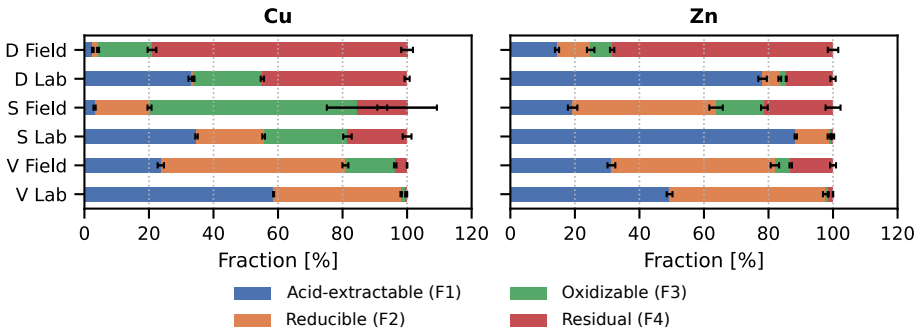

Fig. 5.4. Fractions of Cu and Zn found in the respective sequential extraction fractions of the three filter media, prestressed in lab-scale and field tests; n=3 for each sample and fraction. Bars show mean values, and error bars indicate the standard deviation.

5.3.5 Hierarchical cluster analysis

Hierarchical cluster analysis indicates that the pH values of filter media, sediments and filter cake are closely related to the acid-extractable fractions of Cu and Zn (Figure 5.5a), whereas the oxidizable fractions of Cu and Zn are clustered with the LOI. The oxidizable fractions are thus related to the organic content of the sample. The reducible fractions of Cu and Zn also formed a cluster in relation to the oxidizable fractions. This can be attributed to a dispersion between subsequent fractions. The other elements were not considered in this analysis, since the filter media in lab-scale tests were only prestressed with Cu and Zn. The dendrogram (Figure 5.5b) shows a clear separation between the samples withdrawn in the field and the filter media samples prestressed in the lab (with the exception of the V Field). This underlines the aforementioned discrepancy between prestressing at lab scale and in field tests. The samples V Field and filter media prestressed in lab-scale tests contain larger acid-extractable Cu fractions than the others, which results in sample clustering. Furthermore, these samples exhibit the highest pH values. This stresses that both the fractionation of heavy metals and the sorption process are highly pH-dependent. The clustering of D Field and D Filter Cake supports the assumption that particulate matter accumulates within the filter medium (*cf.* 5.3.3). Furthermore, the sediment samples are not directly linked to the filter cake sample. This suggests that the permanent submersion of the sediments, which is associated with anoxic conditions, results in a different fractionation in comparison to the filter cake, which dries in-between runoff events and hence is likely exposed to oxic conditions.

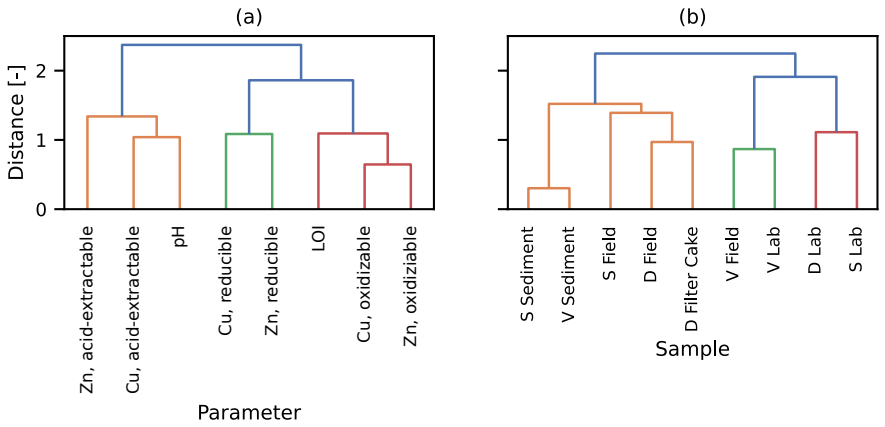

Fig. 5.5. Dendrograms obtained by hierarchical cluster analysis of the minimum-maximum transformed mean pH values, losses on ignition (LOI), Cu and Zn percentages of the potentially mobile sequential extraction fractions F1, F2, and F3 extracted from the filter media prestressed in the field test (D Field, S Field, V Field), filter media prestressed in lab-scale tests (D Lab, S Lab, V Lab), sediments (S Sediment, V Sediment) and filter cake (D Filter Cake) withdrawn from the stormwater quality improvement devices after the field test. (a) Dendrogram visualizing the clustering of analyzed parameters; (b) dendrogram visualizing clustering of samples.

5.3.6 Conclusion

The results of this study can be concluded as follows:

- Sediments and filter cake deposited in SQIDs contained significantly higher heavy metal contents than the filter media.
- Zn in the sediments and filter media displayed particularly high mobility.
- SEP was capable of characterizing the mobility of heavy metals in SQIDs. If potentially mobile fractions are actually mobile needs further investigation.
- The discrepancy between field and lab-scale conditions in terms of the runoff composition (pH, alkalinity, ionic strength, concentrations of contaminants and competing cations), redox conditions, and hydraulic retention times creates different heavy metal contents and strengths of association (mobility).
- Previous lab-scale experiments potentially overestimated the risk of heavy-metal leaching, due to their predominant occurrence in more mobile fractions.
- SEP proved to be a promising method, which can be applied in future studies to improve lab-scale experiments evaluating heavy metal mobility in SQIDs.

Funding sources

This work was supported by the Bavarian Environment Agency (AZ: 67-0270-96505/2016 and AZ: 67-0270-25598/2019).

Acknowledgments

We would like to thank Andreas Gmell and Harald Hilbig of the Centre for Building Materials, Technical University of Munich, for providing the analysis. We would also like to thank the SQID manufacturers, Fränkische Rohrwerke, Hauraton, and Mall, for allowing us to publish the data.

6

Dissolved organic matter in road runoff - Occurrence, seasonal fluctuations and its impact on speciation of heavy metals

This chapter is in preparation for publication as follows:
Rommel, S. H., G. Abbt-Braun, and B. Helmreich (2021a). "Dissolved Organic Matter in Road Runoff: Occurrence, Seasonality and Its Implication for Heavy Metal Retention". *Manuscript in preparation*

Author contributions: Rommel, S. H.: conceptualization, methodology, investigation, validation, data curation, writing - original draft, writing - review & editing, visualization, supervision; Abbt-Braun, G.: investigation, methodology, validation, data curation, writing - review & editing, visualization; Helmreich, B.: resources, writing - review & editing, supervision, project administration, funding acquisition.

† Supplementary information are available in A.4.

Abstract

Dissolved organic matter (DOM) is ubiquitous and affects the fate of contaminants, such as heavy metals, in the environment. Thus, the behaviour and interaction has been comphrensivley studied in natural waters and water treatment. However, only few studies have been published about the character of DOM in road runoff and its impact on heavy metal retention. In this study, DOM in road runoff and in effluents of strom water quality improvement devices (SQIDs) was analysed using UV-vis and fluroescence spectroscopy and size exclusion chromatography (SEC). Seasonality showed a strong effect on the quantity and quality of DOM. In summer, DOM was more prevalent and humic-like. Soil and leaf-debris are the most likley sources of DOM in road runoff. In addition, SEC was able to verify that most of the DOM

can be attributed to humic substances. The effect of the treatment in SQIDs was negligible, consquently DOM properties are assumed to be identical before and after treatment. Predictions of speciation and principal component analysis indicate that the mobility of heavy metals, especially of copper and chromium, is influenced by the presence of DOM in road runoff.

6.1 Introduction

Road runoff contains contaminants originating from traffic-activities, especially heavy metals (HMs), *e. g.* cadmium (Cd) chromium (Cr), copper (Cu), nickel (Ni) lead (Pb) and zinc (Zn) (Goonetilleke et al., 2017; Ma et al., 2017; Kayhanian et al., 2012a; Huber et al., 2016c). To mitigate the harmful impact of HMs on the environment, storm water quality improvement devices (SQIDs) are utilized as storm water control measures. These devices use sorbents to retain dissolved HMs (Transportation Research Board, 2014; Dierkes et al., 2015).

Dissolved organic matter (DOM) is ubiquitous in natural aquatic systems and is widely considered to play an important role in understanding transport, fate and bioavailability of contaminants, such as HMs and organic micropollutants, in the environment (Brezonik and Arnold, 2011; Tipping, 2002; Akkanen et al., 2004; Artifon et al., 2019; Adusei-Gyamfi et al., 2019; Zhou and Haynes, 2010; Zhang et al., 2020). While DOM in natural water systems and effluent of waste water treatment plants has been comprehensively studied (Carstea et al., 2016; Ishii and Boyer, 2012; Fellman et al., 2010), far too little attention has been paid to DOM in urban runoff, especially with respect to the increasing impact of impervious cover in urban areas (Grimm et al., 2008).

The main DOM sources are partially decomposed plant or animal residues and microbial biomass (Frimmel and Abbt-Braun, 2009; Tan, 2014). Thus, DOM is characterised either as autochthonous, originating from bacteria and algae, or allochtonous, deriving from terrestrial origin (Tuhkanen and Ignatev, 2018; Pernet-Coudrier et al., 2011; Hudson et al., 2007; Croué et al., 2003). The sources of DOM are affected by climate, season and geology (Transportation Research Board, 2014). Thus, DOM will vary from site to site. It can be expected that leaf debris and surrounding soils are the main sources of DOM in road runoff (Lee et al., 2019). The composition of DOM is described as a complex heterogenic mixture with varying chemical structure and reactivity (Brezonik and Arnold, 2011; Transportation Research Board, 2014). DOM can be divided into humic substances and non-humic substances (Frimmel and Abbt-Braun, 2009). The humic substances (HS) are further divided into humic and fulvic acids based on their solubility (Thurman

and Malcolm, 1981; Tuhkanen and Ignatev, 2018; International Humic Substances Society (IHSS), 2020). In aqueous systems, the main part of refractory DOM is attributed to fulvic acids (Tuhkanen and Ignatev, 2018). Other minor sources of DOM can be atmospheric particles (Graber and Rudich, 2006; Kristensen et al., 2015), and anthropogenic compounds like surfactants and pesticides (Brezonik and Arnold, 2011), which are not considered in this study. In the context of DOM characterization, there are numerous other terms used: autochthonous, protein-like, labile, microbial-derived organic matter can be attributed to fresh-like DOM, and allochtonous, terrestrial, soil-derived, degraded organic matter can be attributed to humic-like DOM (Hansen et al., 2016; Tuhkanen and Ignatev, 2018). Biodegradation lead to a transformation of fresh-like to humic-like material (Hansen et al., 2016).

In road runoff, only a small percentage of the HMs is dissolved (Huber et al., 2016c; Zgheib et al., 2011b; Gromaire-Mertz et al., 1999), bioavailable and consequently ecotoxic (Bartlett et al., 2012a). The mobility of these dissolved HMs can be affected by formation of complexes with DOM (Brezonik and Arnold, 2011; Adusei-Gyamfi et al., 2019), which features multiple functional groups with different strength: phenolic, carboxylic, nitrogen and sulphur groups (Croué et al., 2003; Hur and Lee, 2011). Total HM concentrations are relevant, because an alteration of the water matrix (e.g. pH, ionic strength, redox conditions) in the receiving waters can lead to a remobilization of particulate HMs (Paulson and Amy, 1993; Blume et al., 2016a). Assessing the effect of DOM on HMs mobility is very complex, because of additional influencing factors, such as pH, ionic strength, presence of other ions, composition of DOM and the oxidation state of the HMs (Transportation Research Board, 2014; Joseph et al., 2019; Kumpiene et al., 2008; Chen et al., 2013).

There are multiple potential effects of DOM affecting the heavy metal retention by sorbents: (a) competition between DOM and HMs for sorption sites, (b) DOM-HM complexes are non- or weakly adsorbing, (c) DOM-HM complexes adsorb strongly, (d) HM can adsorb to previously adsorbed DOM and (e) DOM alters electrostatic properties of the sorbent surface (Haynes, 2015). While (a) and (c) potentially decrease the treatment efficiency of SQIDs, (c) and (d) would facilitate the treatment. (e) would presumably increase treatment efficiency as well, because adsorption of DOM is known to add negative charge to mineral surfaces, which increases attraction of HM cations (Blume et al., 2016b).

It is still unknown, how DOM in road runoff affects HM retention by SQIDs under in-situ conditions. Lab experiments indicate a significant influence. Genç-Fuhrman et al. (2016) showed that HS (humic acid, Sigma-Aldrich) decrease the HM retention by sorbents in batch experiments to the half (except for Cr). Similarly, Charbonnet et al. (2019) and Barrett et al. (2014) showed that Cu and Pb retention decrease in the presence of DOM (humic acid, Sigma-Aldrich, and DOM isolated

from highway runoff, respectively). Zn and Cd removal was only slightly affected. In contrast, Ray et al. (2019) showed that DOM (isolated from Suwannee River) can increase metal retention by sorption of DOM-HM complexes on the sorbent. All aforementioned studies used different sorbents and synthetic runoffs, thus the comparability is limited.

The results of sorption tests conducted by Murakami et al. (2008) indicate that stable DOM-Cu complexes adsorb to solid surfaces of sediments present in road runoff. Thus, retention of Cu could potentially increase due to the presence of DOM. In contrast, they stated that DOM possibly enhances Zn release from soakaway sediments (Murakami et al., 2009).

To assess the metal binding capacity of DOM in road runoff, knowledge about its chemical structure (e. g. binding sites, aromaticity, molecular weight) is mandatory (Xu et al., 2019). Recent studies indicated the potential of UV-vis and fluorescence spectroscopy to infer DOM sources and predict DOM-HM complexation affinity (Xu et al., 2019; Chen et al., 2018; Chappaz and Curtis, 2013; Ahmed et al., 2014; Schamphelaere et al., 2004; Mueller et al., 2012b; Zhao et al., 2015). The studies showed that DOM in road runoff could be characterised as originating from terrestrial sources (Lee et al., 2019; Zhao et al., 2015; Chen et al., 2017). However, these studies did not consider the variability of DOM caused by seasonal effects or treatment of the road runoff with storm water control measures, such as SQIDs. Furthermore, results of recent studies, analysing freshwater and lake sediment, indicate that increasing molecular weight of DOM facilitates its affinity to form DOM-HM complexes (Chen et al., 2013; Xu et al., 2019).

Another aspect of DOM is that its quantity and quality affects ecotoxicity of dissolved HMs, since protective effects of DOM were observed (Schamphelaere et al., 2004; Luider et al., 2004; Al-Reasi et al., 2011). Consequently, DOM potentially reduces ecotoxicity of road runoff, even if HM retention of SQIDs is limited (Al-Reasi et al., 2011; Koukal et al., 2003; Lorenzo et al., 2002).

The aim of this study was to describe DOM in road runoff comprehensively before and after treatment in SQIDs to gain further insights into its seasonal variability, potential biodegradation in SQIDs, and impact on HM retention.

6.2 Material and methods

6.2.1 Study site

For this study, samples of road runoff and effluent of four different SQIDs at a heavily trafficked road in Munich, Germany, were analysed. Three shaft systems (A, B, D) and one filter substratum channel (C) were monitored. The shaft systems consisted

of two treatment stages, a sedimentation stage for the separation of particulate matter and a (sorptive) filtration stage to retain fine particulate matter and dissolved HMs. System A and B were pre-manufactured devices (SediSubstrator XL 600/12, Fränkische Rohrwerke Gebr. Kirchner, Germany and ViaPlus 500 with an upstream sedimentation shaft, Mall, Germany). Device D was constructed of commonly available pre-cast concrete parts with a substratum filter using carbonate rich media. The respective (sorptive) filter media used in device A and B were an iron-based medium with lignite amendment and zeolite. Device C treated the runoff mainly by filtration using carbonate rich media (Drainfix Clean 300, Hauraton, Germany). After treatment of the road runoff, all devices percolated the water into the groundwater. Further information to the monitored devices and a layout of the site and devices can be found in the ESI Appendix A.† All permanently impounded compartments of the SQIDs were underground and protected from sunlight, thus algae growth and photo-degradation of DOM could be neglected. The catchment areas of the systems A to D were 1,660 m², 473 m², 100/165 m² and 400 m², respectively. Two traffic lanes, one accelerating lane and one emergency lane formed the cross-sections of all catchment areas. The material of the road surface was Stone Mastic Asphalt (SMA) and the annual average daily traffic (AADT) was approximately 24,000 vehicles per day. On the road in the opposing direction, an AADT of 22,000 vehicles per day was determined. However, the lanes of the opposing direction are separated from the catchment area by an approximately 3 m wide greened median strip. Nevertheless, the contaminant load in the catchment area may be increased by wind-driven transport and splash water from the lanes of the opposing direction (Goonetilleke et al., 2017; Kluge and Wessolek, 2012). A park with lawn and trees is located next to the road, thereby an increased organic load is expected, especially in autumn. A layout and further information to the study site can be found in the electronic supplementary information (ESI),† and in Helmreich et al. (2010).

6.2.2 Sampling

The samples were withdrawn volume proportionally with automatic samplers (WaterSam WS 316, Edmund Bühler PP 84) from the influent and effluent of the SQIDs. The sampling was triggered by electro-magnetic flow meters (Krohne OPTIFLUX 2300 C, 1300 C or 1100 C, Krohne IFC 300 C, DN250 for A, DN40 for B and D, DN25 for C). The flow data were recorded with a frequency of 30 s. The sampling started, if the inflow exceeded the threshold value longer than 1 min. If the inflow was 15 min below the threshold value, sampling stopped. The threshold value was set to $0.4\,\mathrm{L\,s^{-1}\,ha^{-1}}$ discharge, based on the determined catchment areas. The samples were cooled at $4 \pm 1\,^{\circ}\mathrm{C}$. Throughout this study road runoff and influent of the SQIDs

were used as synonyms. It was not possible to sample all SQIDs at the same time, due to technical malfunction and limited labour. Samples of device D were only considered in the temporal analysis due to the low sample count. The water samples were transported to the lab within 60 h. Composite influent and effluent samples of each discharge event and SQID were prepared. Further analysis was performed after membrane filtration with 0.45 μm syringe filters (PP and PES membranes, VWR International, Germany). After filtration, the samples were stored in the dark at $4 \pm 1\,°C$.

6.2.3 Physical and aggregate properties

The electric conductivity (EC) and the pH value of the samples were determined according to the standard methods 2510 B and 4500-H+, respectively (American Public Health Association et al., 2017). Dissolved organic carbon (DOC) concentration was analysed using a varioTOC Cube analyzer (Elementar, Langenselbold, Germany) of the filtered sample according to DIN EN 1484 with a limit of quantification (LOQ) of $0.3\,mg\,L^{-1}$. Prior to storage, the DOC samples were acidified with 1%V of 32% hydrochloric acid (Merck, Germany).

Alkalinity was analysed by acidimetric titration (standard method 2320) to the pH endpoints 4.5 and 8.3 (American Public Health Association et al., 2017).

6.2.4 UV-vis and fluorescence spectroscopy

Absorbance spectra and 3D-fluorescence (EEM) were measured with an Aqualog® fluorescence spectrometer (Horiba Scientific, USA) using a 10 × 10 mm quartz glass cuvette within 24 h after sample preparation. The temperature of the sample was adjusted to 20 °C, and the pH was not adjusted. The settings were: excitation wavelength (Ex) 230–599 nm with 3 nm increments, emission wavelength (Em) 212–621 nm with 1.64 nm increments, integration time 1 s, medium CCD gain (Hellauer et al., 2019). The EEM spectra were adjusted by subtraction of a daily blank of deionized water (DI water) with an EC $<0.5\,\mu S\,cm^{-1}$. Inner filter effects were corrected with the proprietary software Aqualog® (V3.6) using an absorbance-based approach (Kothawala et al., 2013), first and second order Raman and Rayleigh scattering were removed (width 10 nm, 10 nm, 20 nm and 20 nm, respectively). The gaps were interpolated with staRdom (Pucher et al., 2019) and the EEMs were normalized by the Raman peak area (at 350 nm) of a daily blank (Raman units, R.U.).

The R package staRdom (version 1.1.3, Pucher et al. (2019)) was used to analyse the UV-vis absorbance and fluorescence data. To describe the spectro-

scopic characteristics of the DOM, following optical parameters were determined: UV absorbance at 254 nm (UVA_{254}), specific UV absorbance at 254 nm ($SUVA_{254}$) (Weishaar et al., 2003), the biological index (BIX) (Huguet et al., 2009; Hansen et al., 2016), the humification index (HIX) (Ohno, 2002), and the ratio of the fluorescence peak intensities A:T (A:T) (Ulliman et al., 2020; Hansen et al., 2016). BIX is the ratio of fluorescence intensity at Em = 380 nm divided by the intensity at Em = 430 nm at Ex = 310 nm (Huguet et al., 2009). HIX is the area under the emission spectra between 435–480 nm Em divided by the sum of the areas in the ranges of 300–345 nm and 435–480 nm Em, at 254 nm Ex (Ohno, 2002). A:T is determined as the ratio between Peak A (Ex = 260 nm, Em = 450 nm) and Peak T (Ex = 275 nm, Em = 304 nm) (Hansen et al., 2016). The aforementioned indices are commonly used to assess DOM composition, and conclude sources and degradation processes (Hansen et al., 2016). By using fluorescence indices, bias by inorganic light absorbing constituents, such as iron or nitrate, was reduced (Gabor et al., 2014).

6.2.5 PARAFAC

The parallel factor analysis (PARAFAC) analysis was carried out using the R package staRdom (version 1.1.3, Pucher et al. (2019)). To account for the high noise in low Ex and Em wavelengths, the region with Ex < 230 nm and Em < 230 nm were removed. Sample data were normalized due to highly correlated components. Non-negativity constraint was applied to build the model. One sample was removed because of very high leverage. Additionally, eight samples have been excluded because of non-random residuals. The removed samples are listed in the ESI.† Two components were isolated from the EEMs with a model fit of >99% (R^2). Split half analysis revealed good stability of the model (Figure S3†). The Tucker's Congruency Coefficients (TCC) of the splits were >0.99.

Quantitative and qualitative information on fluorescent DOM was derived based on the loadings of the PARAFAC components and the ration between these (Murphy et al., 2013). The determined components were compared to the database OpenFluor (Murphy et al., 2014).

6.2.6 Size-exclusion chromatography

The samples were filtered with 0.45 μm syringe filters (PP, VWR International, Germany; after the 6 October 2019 PES, BGB Analytik Vertrieb, Germany), and frozen at −20 °C pending the analysis. To avoid sample contamination, the filters

were previously flushed with 60 mL DI water and the first 5 mL of the filtered samples were discarded.

Characterization by size exclusion chromatography (SEC) with online DOC, UVA_{254}, and total nitrogen (TN) detection was conducted according to Huber et al. (2011) and Huber and Frimmel (1991). A more detailed description of the setup can be found in Fatoorehchi et al. (2018) and Huber et al. (2011).

The analysis was performed at the Engler-Bunte-Institut, Water Chemistry and Water Technology at the Karlsruhe Institute of Technology. A Toyopearl TSK HW 50S resin column (250 × 20 mm) was used for the chromatographic separation. The exclusion and permeation volume of the SEC column was determined with dextran blue ($2{\cdot}10^6$ g mol^{-1}, retention time: 28.8 min) and methanol (32 g mol^{-1}, retention time: 69.1 min), respectively. Due to the complex and the unknown composition of the DOC, a calibration with authentic molecules is lacking. Hence, the calibration was performed using polyethylene glycols (100,000 to 200 g mol^{-1}), diethylene glycol (106 g mol^{-1}) and ethylene glycol (62 g mol^{-1}). This result in the assignment of nominal weight fractions in the range of $2{\cdot}10^6$–62 g mol^{-1} (retention time: 29.8–65.5 min). As eluent a phosphate buffer at a flow rate of 1 mL min^{-1} was used (1.5 g L^{-1} $Na_2HPO_4 \cdot 2\,H_2O$ + 2.5 g L^{-1} KH_2PO_4). The samples were injected (1 mL) into the system directly or after dilution with DI water to achieve comparable DOC concentrations without further treatment.

For further characterization of the different size fractions, the DOC, UVA_{254}- and TN chromatograms were divided into five fractions based on the retentions time (fractions I to V). The DOC-chromatograms were dived into different fractions according to their elution behaviour. According to a classification introduced by Huber et al. (2011), the different fractions have been attributed to following fractions: I, high molecular weight substances, such as biopolymers; II, humic substances; III, building blocks, which were defined as breakdown product of humic substances; IV, the so-called salt-boundary peak which may be attributed to low molecular weight organic acids; V, low molecular-weight neutrals.

Due to adsorption and ion-exchange phenomena occurring between the resin material and the analytes, some compounds elute later than expected comparing the elution behaviour with the defined standard used for calibration (Lankes et al., 2009; Frimmel and Abbt-Braun, 2011). The different size fractions were quantified by area integration using the program ChromCalc (DOC-LABOR Dr. Huber, Germany) (Huber et al., 2011).

If specified in the y-axis label, the detection signals of the chromatograms were divided by the DOC concentration of the injected sample to assure better comparability.

Since the separation process in SEC can be influenced by the ionic strength of the sample (Brezonik and Arnold, 2011; Chon et al., 2017), the EC of the samples have to be controlled. The analysed samples showed no impact of de-icing salts, indicated by the low EC $<175\,\mu S\,cm^{-1}$. However, ECs of up to $20\,mS\,cm^{-1}$ can be found in road runoff (Hilliges et al., 2017), therefore comparability of the chromatograms can be limited.

6.2.7 Metals and anions

The concentrations of dissolved calcium (Ca_d), chromium (Cr_d), iron (Fe_d), magnesium (Mg_d), sodium (Na_d) and zinc (Zn_d) were determined by ICP-OES (DIN EN ISO 11885) with LOQs of 20, 2, 10, 1, 20 and $1\,\mu g\,L^{-1}$, respectively. Dissolved cadmium (Cd_d), copper (Cu_d), lead (Pb_d) and nickel (Ni_d) were analysed using ICP-MS (DIN EN ISO 17294-2). The LOQs were 0.5, 1.0, 1.0 and $1.0\,\mu g\,L^{-1}$, respectively.

Bromide (Br^-), chloride (Cl^-), fluoride (F^-), nitrate ($NO_3{}^-$), ortho-phosphate ($PO_4{}^{3-}$) and sulphate ($SO_4{}^{2-}$) were analysed by means of ion chromatography according to DIN EN ISO 10304-1 with a LOQ of $0.05\,mg\,L^{-1}$. The first 10 of 34 samples (until 15 March 2019) were analysed with the cuvette tests LCK311 for Cl^-, LCK153 for $SO_4{}^{2-}$, LCK339 for $NO_3{}^-$ and LCK349 for $PO_4{}^{3-}$ (Hach Lange, Germany). The LOQs were $1.0\,mg\,L^{-1}$, $40.0\,mg\,L^{-1}$, $1.0\,mg\,L^{-1}$ and $0.2\,mg\,L^{-1}$, respectively.

6.2.8 Metal speciation with Visual MINTEQ

Metal speciation in the samples was predicted using Visual MINTEQ (version 3.1, Gustafsson (2014b)). The pH was fixed to the measured values, ionic strength was calculated, temperature was set to 25 °C, the option “adjust CO3 AF to pH 4.5” was chosen because $CO_2(g)$ purging by $N_2(g)$ was not conducted for the alkalinity analysis (Gustafsson, 2014b). DOM was simulated with the NICA-Donnan model and the assumption that all DOM comprises of fulvic acid and a ratio of active DOM to DOC of 1.65 (default value) (Gustafsson, 2014b; Sjöstedt et al., 2010). This assumption is based on a large freshwater dataset (Sjöstedt et al., 2010), thus the speciation predication for road runoff needs to be treated with caution. Cd values have been neglected due to concentrations close to the LOQ. The NICA-Donnan model considers carboxylic as well as phenolic functional groups of fulvic acids Gustafsson (2014b). The abundance of DOM-HM complexes was reported as the sum of the percentages of both functional groups. Concentrations of constituents below LOQ were substituted with one-half of the LOQ. Results with a charge difference > 10% were discarded.

6.2.9 Data analysis

All concentrations below LOQ were substituted with one-half of the LOQ. The non-parametric Kruskal–Wallis H test was applied to test if data of different groups are significantly different. To test for significant differences between two data sets Mann-Whitney rank test was employed, depending on the question either one- or two-sided. A significance level of $\alpha = 0.05$ was applied, unless otherwise stated. To describe the statistical dispersion of non-normal data, the interquartile range (IQR) was reported (Altman and Bland, 1994). All statistical analysis were performed with Scipy (version 1.2.1), unless otherwise stated (Virtanen et al., 2020). Device D was not considered in the comparison between the SQIDs due to the low sample count.

Principal component analysis (PCA) was used to analyse the influence of the determined variables on the total variance of the sample data (Sleighter et al., 2010; Xue et al., 2011). The PCA was performed using statsmodels (version 0.10), a Python environment for statistical computation (Seabold and Perktold, 2010). Prior to the PCA, the data was log-transformed to account for the highly skewed data, except for the variable pH (Xue et al., 2011). Afterwards the data were standardized. The number of principal components (PCs) was chosen based on the cumulative proportion of variance explained by the number of PCs and the shape of the Scree plot (Mudge, 2015). Following parameters were considered in the PCA: pH, EC, major cations (Ca_d, Mg_d, Na_d), major anions (Cl^-, SO_4^{2-}), alkalinity, HMs (Cr_d, Cu_d, Fe_d, Ni_d, Zn_d), DOC, spectroscopic parameters (UVA_{254}, $SUVA_{254}$, A:T, BIX, HIX), and the ratio of C1:C2 of the PARAFAC components. Other parameters such as PO_4^{3-}, NO_3^-, Cd_d, and Pb_d, were not considered because of the low concentrations and consequently low influence on the speciation of the metals.

6.3 Results and discussion

6.3.1 DOC

For traffic area runoff, dissolved organic carbon (DOC) concentrations have been reported between 3.4 and 66.9 $mg\,L^{-1}$ with a mean of 18.5 $mg\,L^{-1}$ (Table 6.1). The concentrations found in traffic area runoff are comparable to the range of concentrations found in rivers ($\sim$5 $mg\,L^{-1}$), eutrophic lakes ($\sim$10 $mg\,L^{-1}$), marshes ($\sim$15 $mg\,L^{-1}$), or even as in bog lakes ($\sim$30 $mg\,L^{-1}$) in some highly polluted rain events (Thurman, 1985; Frimmel and Abbt-Braun, 2009). Thus, the DOC concentration in traffic area runoff is moderate to high. In a first approximation, the DOC corresponds to 30 to 50% of the DOM by weight (Brezonik and Arnold, 2011).

Tab. 6.1. Literature review of DOC concentrations in traffic area runoff

		DOC [mg L^{-1}]	
Source	Location	Mean	Median
Han et al. (2006)	Los Angeles, USA	66.9	28.9
Caltrans' state-wide data, state-wide[a]	California, USA	19	-
Caltrans' state-wide data, nonurban AADT<30,000[a]	California, USA	14	-
Caltrans' state-wide data, urban AADT >30,000[a]	California, USA	22.4	-
Kayhanian et al. (2007), non-urban highways AADT <30,000	California, USA	13.0	-
Kayhanian et al. (2007), urban highways 30,000 <AADT <100,000	California, USA	15.6	-
Kayhanian et al. (2007), urban highways 100,000<AADT	California, USA	23.4	-
Maniquiz et al. (2010)	Yongin City, Korea	15.9	-
Helmreich et al. (2010)	Munich, Germany	21	17
Hilliges et al. (2017)	Augsburg, Germany	6.87	5.6
Wei et al. (2010), road	Xiamen City, China	-	∼20
Wei et al. (2010), parking lot	Xiamen City, China	-	∼18
MA Highway BMP data[b]	Massachusetts, USA	9.8	9.9
Caltrans 2003[b]	California, USA	19.7	12
TX Highway runoff data (1997)[b]	Texas, USA	19.8	14
MA Highway runoff data (2010)[b]	Massachusetts, USA	4.1	3.4
Lee et al. (2019), parking lot	Daegu area, South Korea	4.51	4.51

[a] cited in Han et al. (2006). [b] withdrawn from Highway-Runoff Database (Granato and Cazenas, 2009).

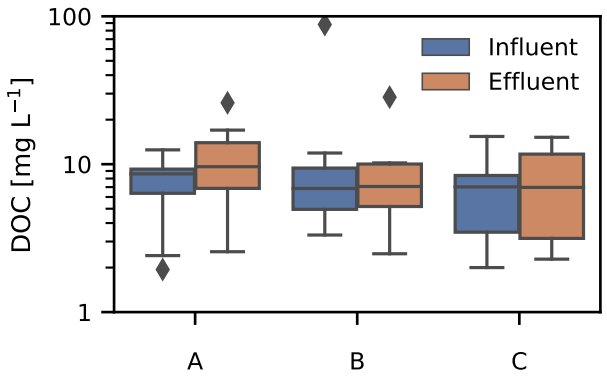

Fig. 6.1. DOC concentration in the influent and effluent of the SQIDs (A, n = 8; B, n = 7; C, n = 9); the lower and upper ends of the boxes indicate the first and third quartiles. The bands inside the boxes shows the medians, the whiskers represent 1.5 times the interquartile range (IQR), and values outside of the whiskers (rhombuses) are considered as outliers.

The median DOC observed in the influent of the SQIDs was 6.9 to 8.6 mg L^{-1} (Figure 6.1). The effluent concentration was slightly elevated with 7.1 to 9.6 mg L^{-1}, which may indicate an accumulation of particulate organic matter in the SQIDs and biodegradation of it, resulting in a release of DOC. However, the increase of DOC in the effluent was not statistically significant. Hence, sorption of DOM on the sorbents can also be neglected. No significant differences between the DOC concentrations in the effluents were observed among the investigated SQIDs.

The highest DOC concentration was 88.0 mg L^{-1} in the influent after a 10 days long dry period in the spring. No distinctive seasonal course of the influent DOC concentrations was observed (Figure S4†).

6.3.2 UVA_{254}

In contrast to the results of the DOC, the UVA_{254} data with higher temporal resolution show a distinctive seasonal pattern with a peak in spring and summer. The lowest values were observed in winter. By means of UVA_{254} it was possible to estimate the DOC of the samples (Figure 6.2 and Figure S5†). The course of the UVA_{254} was comparable to the course of monthly mean temperature (Figure S7b†), which can indicate that during the growth period of surrounding vegetation larger quantities of DOM can be found in road runoff. No relation between the precipitation pattern (Figure S7a†) and DOM quantity was observed, in contrast to natural waters, as described *e. g.* by Stedmon and Markager (2005).

No interference of the UVA_{254} measurement is expected by the inorganic constituents NO_3^- and Fe_d, due to the low concentrations, present in the samples (me-

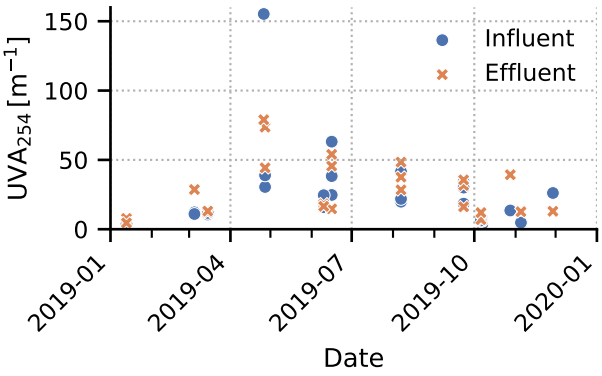

Fig. 6.2. UVA_{254} in the influent and effluent of the SQIDs (n = 28 for influent and effluent)

dian Fe_d = 71 µg L^{-1}, NO_3^- = 2.2 mg L^{-1}) (Weishaar et al., 2003). Only two samples exhibited Fe_d concentrations >0.5 mg L^{-1} (1.53 and 0.71 mg L^{-1}), which could slightly affect UVA_{254} (Weishaar et al., 2003). However, this effect showed no significant effect on the approximation of DOC using UVA_{254} (Figure S5†).

The absorbance spectra of the analysed samples showed featureless spectra (Figure S6†), which is well known for DOM in surfaces waters (Tuhkanen and Ignatev, 2018).

The concentrations of Cr_d, Cu_d, Fe_d, Mg_d, Ni_d, and Zn_d showed strong positive correlation (Spearman's rank correlation coefficient (r_s) > 0.64, $p < 0.05$) to the UVA_{254} in the influent (Table S2†). This indicates that DOM, in this case approximated by UVA_{254}, increases the mobility the mobility of metals in road runoff. Only Ca_d and Na_d exhibited no significant correlation to UVA_{254} (r_s = 0.38 and 0.12, respectively, $p > 0.05$). Because Na_d originates from de-icing salt application (Fay and Shi, 2012; Marsalek, 2003), it shows a very strong seasonality, therefore no correlation between UVA_{254} and Na_d is coherent. In the effluent of the SQIDs only moderate correlation between UVA_{254} and the analysed metals were observed ($r_s \leq 0.57$), which were not significant ($p > 0.05$). Thus, the hypothesis that DOM reduces retention of dissolved heavy metals is likely, yet other factors, like influent concentration, appear to be more crucial.

Cd_d and Pb_d were not evaluated, since only two or no sample exhibited dissolved concentrations above the LOQ.

6.3.3 UV-vis and fluorescence indices

UV-vis and fluorescence indices are widely applied to analyse DOM properties of various aquatic systems. In this study, the indices have been adopted to characterise DOM in road runoff further. Owing the fact that UV-vis and fluorescence indices were

originally developed for certain DOM sources, derived values may not be comparable without caution (Gabor et al., 2014).

The $SUVA_{254}$ values were calculated and were in the range of 1.9 to 3.0 $L\,mg^{-1}\,m^{-1}$ in median (Table 6.2). The values of the effluents A and C were higher compared to the influent, indicating that the DOM composition changed during storage in the SQIDs, whereas no changes were obvious for the SQID B. Since composite samples were analysed in this study, variations between influent and effluent samples may be reduced due to dilution of water with high residence times with fresh road runoff. For surface waters, $SUVA_{254}$ values $<2.5\,L\,mg^{-1}\,m^{-1}$ indicate the presence of fresh-like DOM leached from plants and algae according to Hansen et al. (2016). $SUVA_{254}$ values can also be used as an indicator for the aromaticity of DOM; the aromaticity of DOM is increasing with increasing $SUVA_{254}$ values (Abbt-Braun et al., 2004; Weishaar et al., 2003). Based on studies mainly analysing isolates of HS, the aromaticity in the samples was approximately 10 to 25% according to the $SUVA_{254}$ data (Abbt-Braun et al., 2004; Weishaar et al., 2003). However, this approximation is based on the assumption that DOM in the samples comprised mainly of HS. The $SUVA_{254}$ values indicate that the DOM in the effluent of the SQIDs A and C features a slightly higher aromaticity. This may be due to a preferential microbial degradation of aliphatic compounds (Hansen et al., 2016). In comparison to the other SQIDs, the effluent of device C exhibited slightly, yet significantly, higher $SUVA_{254}$ values. This can be attributed to the build-up of an approximately 3 cm thick organic-rich layer on the filter surface of device C, containing leaf debris; consequently, the DOM properties reflected more humic-like DOM features, such as a higher $SUVA_{254}$ (Hansen et al., 2016).

To further study the character of DOM and estimate the source of it in road runoff, the fluorescence peak ratio A:T was determined. The fluorescence peak A is attributed to the humic-like DOM and peak T to the protein-like, or as recently specified as fresh-like DOM (Hansen et al., 2016; Coble, 1996). The peaks were established to characterise seawater DOM, but in the meanwhile they are also applied for DOM of soil leachates or plant debris (Hansen et al., 2016; Coble, 1996). Increasing A:T ratios indicate a decreasing susceptibility to biodegradation or an increasing proportion of humic-like DOM (Hansen et al., 2016; Coble et al., 2014; Stedmon and Cory, 2014). The results of Hansen et al. (2016) suggest that A:T ratios > 4.5 in soil and plant leachates indicate a greater relative contribution of soil-derived DOM than plant- or algae-derived DOM. However, A:T ratios < 10 still show the presence of fresh-like DOM, which is labile (Hansen et al., 2016). The A:T ratio proved to be a robust surrogate to evaluate biodegradation of DOM, as well as to identify wastewater impact on rivers (Hansen et al., 2016; Ulliman et al., 2020). In the influent and effluent samples of the SQIDs A:T ratios of 4.4 (influent),

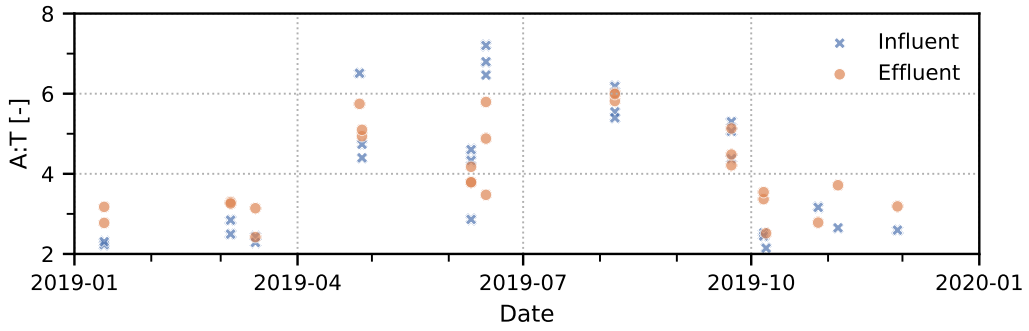

Fig. 6.3. Time-series of the A:T ratio determined in the influent and effluent of the SQIDs (n = 24 for influent and effluent), origin of the individual samples was not indicated, since no significant differences were found between each SQID

and 3.7 to 4.2 (effluents) were measured in median, and it varied between 2.1 and 7.2. A significant difference neither between the influents and effluents of the SQIDs nor between the effluents of the individual SQIDs was observed. As a result, biodegradation of DOM in SQIDs seems to be negligible, although $SUVA_{254}$ and A:T values indicate the presence of fresh-like DOM (Hansen et al., 2016). The discrepancy between A:T and $SUVA_{254}$ data can be attributed to the smaller number of samples and larger uncertainty of $SUVA_{254}$ (Ulliman et al., 2020).

According to the A:T ratio, DOM in road runoff and effluent of SQIDs shows values of soil-derived humic-like DOM with a significant contribution of labile plant-derived fresh-like DOM (Hansen et al., 2016). Furthermore, using the A:T ratio, it was possible to track seasonal variations of the DOM composition. A distinct seasonal pattern was revealed, peaking in summer (Figure 6.3). The seasonal pattern can be a result of higher temperatures in summer (Figure S7b†) facilitating biodegradation of the labile fractions of DOM. In addition, higher precipitation intensities and heights in summer can flush humic-like DOM from surrounding areas on the road surface. However, the second explanation is less likely, since the design on site reduces runoff from surrounding lawn to the road surface.

In addition to the A:T ratio, two other frequently used fluorescence indices, BIX and HIX, were calculated to enable a comparison to other studies. BIX is used as an indicator for fresh-like DOM, whereas HIX describes the humification of DOM (Hansen et al., 2016; Ohno, 2002; Huguet et al., 2009).

The BIX and $SUVA_{254}$ values in the analysed road runoff and effluents of the SQIDs were in the range of aqueous leachate samples from topsoil and plants (Lee et al., 2019). As a result, the DOM source estimated by the A:T ratio is supported. In contrast, Lee et al. (2019) observed considerably higher HIX and $SUVA_{254}$ values in road runoff, indicating a higher degree of humification. However, they analysed only one sample.

Tab. 6.2. Summary of the analysed parameters describing quantity and quality of DOM in the samples; road runoff (influent) was not grouped by the devices, since there were no significant differences ($p>0.05$); values reported as median (25th–75th percentile)

Group	Device	DOC [mg L^{-1}]	$SUVA_{254}$[a,b] [L mg^{-1} m^{-1}]	n [-]	HIX [-]	BIX [-]	A:T [-]	n [-]	C1:C2[b] [-]	n [-]
Road runoff / influent	A–C	7.2 (3.5–9.3)	1.9 (1.8–2.4)	17	0.8 (0.8–0.9)	0.6 (0.6–0.7)	4.4 (2.5–5.3)	24	0.8 (0.7–0.8)	21
Effluent	A	9.6 (6.9–14.0)	2.4 (1.9–2.8)	8 / 5	0.9 (0.8–0.9)	0.6 (0.6–0.6)	4.2 (3.3–4.9)	7	0.8 (0.8–0.8	5
	B	7.1 (5.2–10.0)	1.9 (1.8–2.8)	7 / 5	0.8 (0.8–0.8)	0.7 (0.6–0.7)	3.7 (3.1–4.8)	8	0.7 (0.7–0.7)	7
	C	7.0 (3.2–11.7)	3.0 (2.7–3.1)	9 / 7	0.8 (0.8–0.9)	0.7 (0.6–0.7)	4.2 (3.3–5.1)	9	0.8 (0.8–0.9)	9

[a] significant difference between influent and effluent samples, [b] significant difference between effluent samples of the different devices

It was expected, that a clear separation between the systems with permanent impounding (A and B) and the dry running system (C) would be discernible. This assumption was based on the higher residence times of the water in the permanently impounded systems enhancing biodegradation. However, this was not observed by the indices A:T, BIX, and HIX. Only $SUVA_{254}$ indicated slightly, yet significantly, more humic-like DOM in the effluent of device C. This was not indicated by the other indices.

This section has attempted to evaluate the source and composition of DOM in road runoff, since DOM properties affect the formation of DOM-metal complexes and thereby metal mobility. Recent studies indicate that with increasing humic-like features the amount of DOM-Cu and -Pb complexes increases (Chen et al., 2018; Chappaz and Curtis, 2013; Schamphelaere et al., 2004; Mueller et al., 2012b). Likewise, DOM-Zn complexes increase with an increasing humic-like DOM proportion, however this increase is not significant (Chen et al., 2018). Yet, there are also contradicting results for DOM-Zn complexes (Chen et al., 2018; Mueller et al., 2012a). According to this knowledge, it is unlikely that treatment of stormwater in SQIDs alters DOM significantly, and consequently does not change the amount of DOM-metal complexes.

6.3.4 PARAFAC

Using PARAFAC, two components (C1, C2) were isolated from the EEMs. C1 and C2 exhibited their maxima at 234/462 nm (Ex/Em) and 230/383 nm, respectively (Figure 6.4). Two representative EEMs for road runoff and effluent from SQIDs are shown in Figure S8†. Comparable components were identified in the OpenFluor database. C1 is related to aromatic, high molecular weight organic matter (humic-like) with terrestrial character (Gonçalves-Araujo et al., 2016; Kulkarni et al., 2018), and C2 to microbial-derived humic-like components (Derrien et al., 2019; Williams et al., 2013). Component C2 of this study is also matching with a component found in urban storm water ponds by Williams et al. (2013). Chen et al. (2017) also showed that humic- and fulvic-like components (like C1 and C2) dominate the DOM composition of road runoff. However, they also observed a minor (∼15%) protein-like component with a Ex/Em peak at 280/350 nm (similar to T peak, Coble (1996)), which was not observed in this study.

Based on the loadings of the components, fluorescent DOM of the samples comprised in median of 43% C1 and 57% C2 (IQR = 8% of C1 and C2). However, a critical interpretation is needed, since different fluorophores can have varying fluorescence signals (Murphy et al., 2013). For this study, the ratio of the components C1:C2 was used to track changes of the DOM composition. C1:C2 showed a strong positive correlation to the fluorescence peak ratio A:T ($r_s = 0.74$, $p < 0.01$). Thus, both ratios are suitable to describe the ratio between the humic-like to fresh-like DOM fraction (Ishii and Boyer, 2012). The data showed no significant difference between the influent and effluent samples. Yet, in the effluent of device B the ratio C1:C2 was significantly lower in comparison to device A and C. This indicates that DOM in the effluent of device B contained slightly more fresh-like DOM. According to Ishii and Boyer (2012), C2 should show more intense Cu complexation than C1. Same was reported for Fe and Al as well (Ishii and Boyer, 2012).

The comparison of the PARAFAC components in OpenFluor highlighted the limitations of DOM source identification by means of PARAFAC components, since ubiquitous spectra reflect DOM in most environmental samples (Rosario-Ortiz and Korak, 2017; Murphy et al., 2018). Furthermore, C1 and C2 correlated very strong ($r_s = 0.99$, $p < 0.01$), even after previous normalization of the data, suggesting that they are potentially not individual compounds.

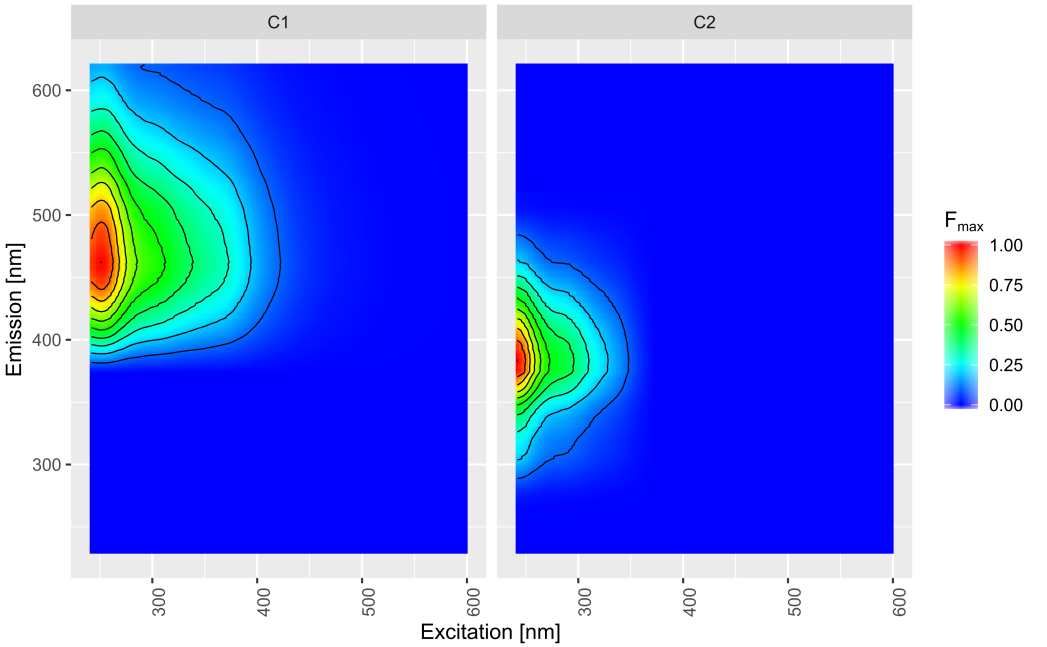

Fig. 6.4. PARAFAC components C1, humic-like with terrestrial character, and C2, microbial-derived humic-like, found in road runoff and SQID effluent. The components were normalized to their maximum fluorescence (F_{max}).

6.3.5 Size-exclusion chromatography

DOM of the influent and effluent samples was further analysed using SEC to gain information on the character with respect to molecular weight (size), UV(254 nm)-absorption and organic-N-distribution. For a detailed interpretation of chemical compounds in the different factions, a combination of SEC with high resolution mass spectrometry or Fourier transform ion cyclotron resonance (FTICR) needs to be performed (Valle et al., 2018; Patriarca, 2020; Brock et al., 2020; Valle et al., 2020).

The relative amount of the high molecular weight fraction I was quite low, in average 3.5% of the total DOC (Table 6.3, Figure 6.5). The fraction II, which is assigned to HS (Huber et al., 2011) dominated the DOC with a mean percentage of 36%. The nominal average molecular weight of fraction II was 491 g mol^{-1}. Fraction III comprised in average 14% of the DOC. Furthermore, fraction IV incorporate in average only 1% of the DOC and fraction V 22%.

The corresponding chromatograms with detection at 254 nm (UV) showed the same course for fraction II and III. This indicates that most of the DOM compounds in these fractions contain C=C and C=O double bonds, which can be conjugated. This behaviour is well known for DOM samples from bog lakes, rivers, lakes, groundwater, and soil seepage water (Frimmel and Abbt-Braun, 2009; Abbt-Braun et al., 2004;

Tab. 6.3. Percentage of the DOC assigned to the fractions of the SEC-DOC-chromatograms and nominal molecular weight (M_n) of fraction II. * calibration according to Huber et al. (2011)72 using standards of IHSS

Fraction	I	II	III	IV	V	M_n of II*
Unit	%	%	%	%	%	g mol^{-1}
Sample						
A_A_190923	1	40	10	0	21	420
A_C_190923	5	30	27	2	16	583
A_A_191007	9	27	11	1	28	481
A_C_191007	4	36	8	1	19	361
B_A_191006	2	28	14	3	31	490
B_C_191006	1	40	16	1	25	530
C_A_191006	2	40	14	1	17	520
C_C_191006	1	42	15	2	30	579
Mean±SD	4±3	36±6	14±7	1±1	22±6	491±88

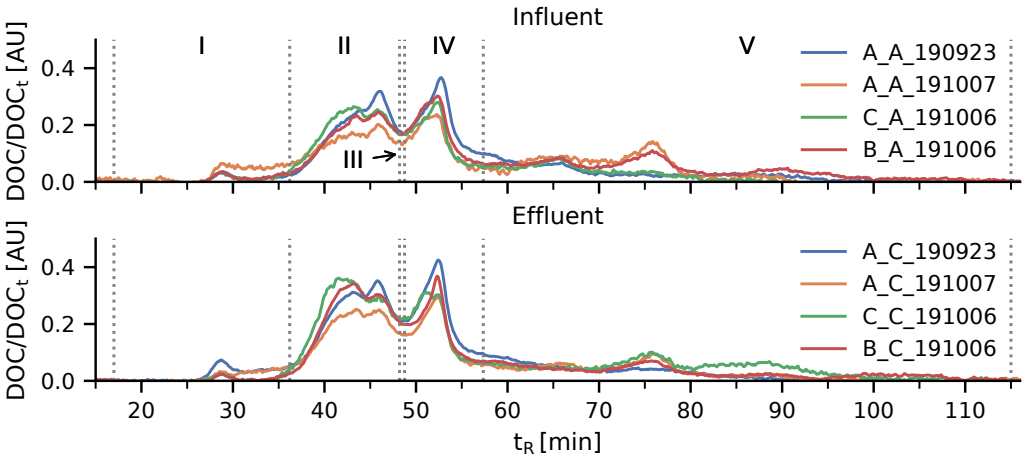

Fig. 6.5. SEC-DOC chromatograms of the influent and effluent samples, the signals were divided by the total DOC of the injected sample. The dilution prior to the SEC analysis was considered. The dotted grey lines indicate the fractions I-V based on the retentions time, however they slightly vary due to the fitting to each chromatogram according to the method of Huber et al. (2011) (n = 4 for influent and effluent respectively)

Huber et al., 2011). The substances contributing to the DOC in fraction V may be characterised by hydrophobic non-UV (254 nm) absorbing organic compounds (Figure S9†) (Her et al., 2003). Due to the high retention time (after the permeation volume at t = 69.1 min) the compounds show interactions with the resin resulting from a hydrophobic character (Huber et al., 2011). The TN-chromatograms show the inorganic compounds nitrate and ammonium (Fraction IV and V). There are only small signals in the retention times between 20 to 50 min (fractions I, II, III), indicating that the amount of organic N-containing compounds is very low (Figure S9†).

Bayarsaikhan et al. (2016) demonstrated that surrounding tree species significantly affect DOM characteristics, with the application of the SEC-DOC method proposed by Huber et al. (2011) in lab-scale experiments. For instance, only leaf fragments of some tree species released considerable amounts of Fraction I, which is attributed to biopolymers. The SEC-DOC chromatograms of degrading leaf fragments were similar to the chromatograms of DOM in the road runoff samples, although leaf fragments lead to a comparatively larger fraction II and fraction I for fresh samples (7 days contact time). This supports the assumption that leafs are a main source of DOM in road runoff. Furthermore, Bayarsaikhan et al. (2016) concluded based on the SEC results that HS released from leaf debris in aqueous solution are not biodegradable within 96 days. Whereas the high molecular weight organic matter, attributed to biopolymers (fraction I) (Huber et al., 2011), degrades. However, Hur et al. (2009) observed altering of the apparent molecular weights and spectral properties (*e. g.* $SUVA_{254}$, HIX) caused by degradation of DOM from leaf litter during microbial incubation experiments in a laboratory study. The apparent molecular weight increases with incubation time, as well as $SUVA_{254}$ and HIX, which might reflect rapid degradation of fresh-like DOM with lower molecular weight and aromaticity (Hur et al., 2009).

Chen et al. (2013) showed for DOM samples isolated from freshwater (IHSS FA, isolated from Suwannee river) that the binding affinity of Cu is increasing with increasing molecular weight. The same results were reported for the binding affinity of Zn to DOM (Hoffmann et al., 2007). Since no significant difference between molecular weight distributions of road runoff and effluent of SQIDs was observed, the treatment in SQIDs may not impact the affinity of DOM and heavy metals.

The SEC results showed that DOM of road runoff with and without further treatment in SQIDs shows comparable molecular weight distributions. Thus, the results of the spectroscopic indices are supported that no significant differences between road runoff and treated road runoff exist. Due to the small sample size, seasonal variation could not be tracked by SEC in this study.

6.3.6 Speciation with Visual MINTEQ

Knowledge about the speciation of HMs is essential to assess their mobility and retention in SQIDs, thus Visual MINTEQ was used to predict the speciation. The prediction revealed that Cr and Cu have the highest affinity to form DOM-HM complexes (median > 99%, Figure 6.6, Table S3†). The high affinity of Cu in road runoff to form DOM-HM complexes has been previously reported (Nason et al., 2012). Ni showed a moderate tendency to form complexes with DOM, with 40 to 43% DOM-Ni in the influent and effluent. In contrast, Zn was mostly found in ionic form or in compounds or complexes with inorganic compounds (median of DOM-Zn < 1%). No significant differences between the percentages of DOM-metal complexes of Cr, Cu, Ni, and Zn, were observed between influent and effluent of the SQIDs ($p > 0.05$).

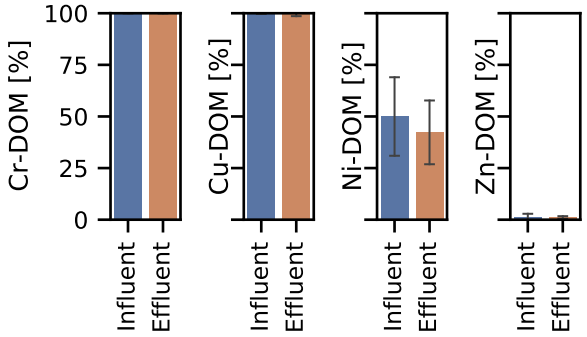

Fig. 6.6. Predicted proportion of metal-DOM complexes by Visual MINTEQ in the influent and effluent samples of the SQIDs, whiskers indicate the standard deviation (influent n = 5, effluent n = 11)

Due to the limited number of samples with a sufficient ionic balance, a differentiation between the studied SQIDs was not possible. The results of the speciation prediction indicate that especially the mobility of Cr and Cu is significantly affected by the presence of DOM, thus their retention by adsorption in SQIDs could be limited by formation of DOM-metal complexes. For Ni the same effect can be assumed to a lesser extent. The predicted order of complexation affinity to DOM was Cu $\sim$ Cr > Ni > Zn, which is supported by a review of DOM-metal complexation in surface waters (Mueller et al., 2012b). Even though, Cr showed a high affinity to form DOM-metal complexes, it is less relevant due to lower dissolved concentrations with respect to the toxic effect level (Table 6.4) (Huber et al., 2016c; Karlsson et al., 2010; Bartlett et al., 2012a). Cd and Pb were not considered due to very low dissolved concentrations, mostly below the LOQ. The DOM-Cu complexation is of special interest, since the concentrations can be comparably high in road runoff and can surpass toxic effect levels (Kayhanian et al., 2012a; Huber et al., 2016c;

Bartlett et al., 2012a; Kayhanian et al., 2008b). Murakami et al. (2008) found also a predominant proportion of DOM-Cu complexes in experiments reflecting conditions in infiltration devices for road runoff. Yet, in contrast to our results, they found a significant proportion of Cu in form of carbonates (7–49%). They found Zn as well present in the form of free ions and carbonate complexes. These results were derived from speciation modelling as well as anion and chelating resin measurements. A strong correlation between DOM and Cu in road runoff was also reported by Wüst et al. (1994).

Tab. 6.4. pH and dissolved metal concentrations used for the predication of the metal speciation, data resulting in insufficient prediction quality (ionic balance error > 10%) were removed. Values are reported as median (25th–75th percentile).

		pH [-]	c [$\mu g\,L^{-1}$]					
Position	n		Cd_d	Cr_d	Cu_d	Ni_d	Pb_d	Zn_d
Influent	5	8.1 (7.6–8.1)	<0.5	1.0 (1.0–1.2)	6.6 (6.4–12.3)	1.0 (1.0–5.9)	<1.0	64.0 (22.1–115.7)
Effluent	11	7.9 (7.6–8.0)	<0.5	1.0 (1.0–9.7)	9.3 (6.7–19.8)	2.3 (1.2–4.7)	<1.0	28.1 (21.4–62.3)

6.3.7 Data analysis

Using PCA, 72% of the variability of the sample data could be explained by two principal components PC1 and PC2, which explain 48%, and 24% of the variance, respectively. PC1 can be interpreted as vector characterizing the pollution level of the samples; it decreases with increasing dissolved metal concentrations (Figure 6.7a). PC2 reflects effects of seasonality. The cluster, which is attributed to the impact of de-icing salt (NaCl), showed the highest loading. However, PC2 also describe the previously shown seasonality of DOM in road runoff (*e. g.* Figure 6.2 and Figure 6.3). Besides the de-icing cluster two other cluster were revealed by the PCA. The first cluster comprises the dissolved metal concentrations, except for Na_d, which originates from de-icing salt (Marsalek, 2003). This covariation evidences that the metals share similar sources. The second cluster contains the DOM parameters together with Cu_d and Cr_d. This supports the hypothesis that the mobility of Cr and Cu is significantly affected by the presence of DOM. In addition, this is in good agreement with the Visual MINTEQ speciation, which predicted the strong affinity of Cr and Cu to form complexes with DOM. The covariation of A:T, C1:C2, and HIX shows that all three parameters are capable of describing the proportion of humic-like DOM to fresh-like DOM. BIX was not found in this cluster, because it

showed an inverse seasonal course to the other DOM parameters. Furthermore, PCA supports the results of the speciation prediction that the mobility of Cr and Cu is significantly affected by the presence of DOM. In addition, the clustering with A:T, C1:C2, and HIX indicates that humic-like DOM shows a higher affinity to form complexes with Cr and Cu. Another explanation for the covariation of Cr_d and Cu_d can be that both metals share the same source: brake lining wear (Ball et al., 1998). The pH showed no strong effect on the dissolved metal concentrations because of its low variability.

No clustering of influent and effluent samples was observed (Figure 6.7b), thus no significant impact of treatment by the SQIDs was observed again. The clustering of the samples was based on seasonality.

SEC results could not be included in the data analysis, because it would have significantly reduced the extent of data and its variability due to the low sample count and absence of samples with de-icing salt impact. He et al. (2016a) were able to prove a relationship between molecular weight and the optical indices HIX, $SUVA_{254}$ and BIX for riverine sediment organic matter. Their results demonstrate that molecular weight of humic substances (HS) correlates positively with HIX and $SUVA_{254}$, whereas it correlates negatively with BIX. Furthermore, they were able to investigate relationships between SEC-DOC fractions and optical indices. In contrast to our results, He et al. (2016b) found weak and negative correlations between HMs and the parameters $SUVA_{254}$ and HIX for extracted sediment organic matter. This highlights the limitations of comparability between DOM of different sources.

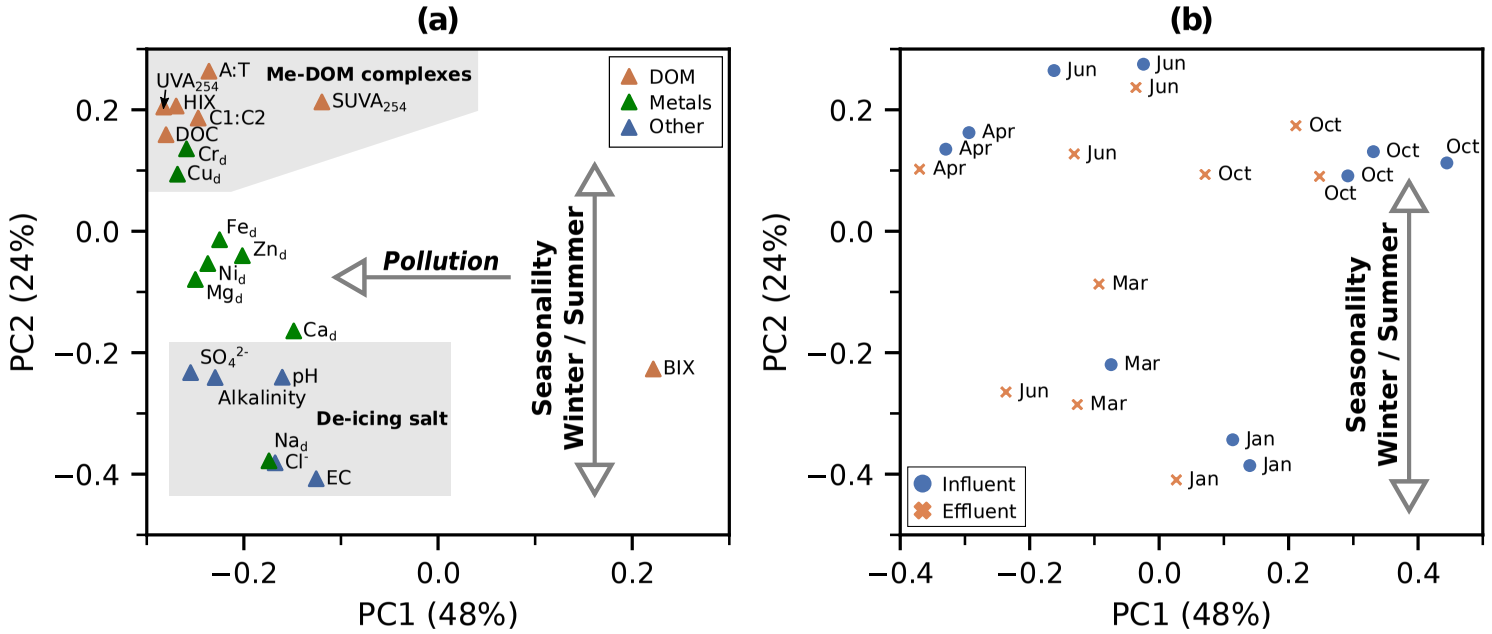

Fig. 6.7. Scatter plots of (a) the loadings and (b) scores of the principal component analysis. PC2 can be interpreted as a pollution vector and PC2 as a seasonality vector; the labels next to the data points in (b) reflect the month of the sampling date; the grey shaded areas illustrate different clusters discriminated by the PCA and causal relations between the analysed parameters. The percentages in axis labels indicate the percentage variance explained by each principal component; variables n=20, samples n = 20

6.4 Conclusion

In this study, insights in the occurrence and variability of DOM in road runoff and effluent of SQIDs were gained using UV-vis and fluorescence spectroscopy in combination with SEC.

DOM occurs in moderate to high concentrations in road runoff in comparison to other freshwater systems. The most likely source of DOM in road runoff is soil and leaf-debris. A strong seasonal variability with respect to DOM quantity and quality was observed, which followed the ambient temperature. In summer, DOM was more prevalent and humic-like. No distinct effect of the treatment in the SQIDs on DOM quantity and quality was observed. Consequently, DOM properties of road runoff before and after treatment can be assumed equal. SEC verified that most of the DOM could be attributed to humic substances. Finally, speciation prediction and PCA of the monitoring data indicated that DOM in road runoff exhibits an effect on HM mobility and thereby its retention in storm water treatment. Especially Cr and Cu showed a high affinity to form complexes with DOM.

Since HMs in road runoff are predominately found in the particulate fraction, the focus of storm water treatment should be on the separation of particulate matter. Nevertheless, consideration of the influence of DOM is important to achieve excellent HM retention by SQIDs, especially of Cu. Future studies are necessary to quantify the effect of DOM, as well as particulate organic matter, on the retention of dissolved HMs in SQIDs to reduce detrimental effect of traffic on the environment.

Acknowledgments

This research was supported by the Bavarian Environment Agency (AZ 67-0270-96505/2016 and AZ 67-0270-25598/2019). The authors thank Luca Noceti and Philipp Stinshoff for their support in the lab and at the monitoring site. We would also like to thank Matthias Weber of the Engler-Bunte-Institut, Chair of Water Chemistry and Water Technology, Karlsruhe Institute of Technology, for the SEC analysis.

7

Influence of temperature and de-icing salt on the sedimentation of particulate matter in traffic area runoff

This chapter has been previously published as follows:
Rommel, S. H. and B. Helmreich (2018c). "Influence of Temperature and De-Icing Salt on the Sedimentation of Particulate Matter in Traffic Area Runoff". *Water* 10.12, p. 1738. DOI: 10.3390/w10121738.

Author contributions: Rommel, S. H.: conceptualization, methodology, investigation, validation, data curation, writing - original draft, writing - review & editing, project administration; Helmreich, B.: conceptualization, investigation, resources, writing - review & editing, supervision, project administration, funding acquisition.

† Supplementary information are available in A.5.

Abstract

Stormwater quality improvement devices use sedimentation as a pre-treatment step to separate contaminant laden particulate matter (PM) from traffic area runoff. Since heavy metals are mostly particulate bound, they can be separated by means of sedimentation. Multiple studies describe worse settling behavior during the cold season. This paper is written in response to a decreased PM retention that was observed in the cold season during a 20-month monitoring of a sedimentation tank. However, the data was insufficient to assess the two factors that influence sedimentation during the cold season — temperature and de-icing salt application. Therefore, simplified discrete particle settling models were used to determine the influence of temperature and de-icing salt. These influences were compared to other factors, like overflow rate, particle density, and particle size distribution. To calculate the effect of temperature and de-icing salt on density and viscosity, two empirical models were applied for the first time in this field. The calculations

showed that de-icing salt (NaCl) had a negligible influence on the retention of PM. However, reducing the temperature from 20 °C to 5 °C was shown to decrease the total suspended solid removal efficiency by up to 8%. The order of influencing factors was found to be particle size distribution $\gg$ overflow rate $>$ particle density $>$ temperature.

7.1 Introduction

Traffic area runoff is contaminated by, amongst others, wear of pavement and vehicles, leakage, and atmospheric deposition (Ball et al., 1998; Legret and Pagotto, 1999; McKenzie et al., 2009; Wik and Dave, 2009; Huber et al., 2016c; Kayhanian et al., 2012a). Most of the contaminants, e.g., heavy metals, are present in particulate form (Kayhanian et al., 2012a).

In the winter season, abrasives and de-icing salts are applied on roads to ensure traffic safety (Huber et al., 2015b; Fay and Shi, 2012). This application directly causes a higher load of particulate matter (PM) to be present on the road surface (Fay and Shi, 2012). This PM is associated with higher concentrations of contaminants in traffic area runoff due to higher wear and tear of pavement and vehicles, as well as an increased corrosion, enhanced by de-icing salts (Murray and Ernst, 1976; Helmreich et al., 2010; Shi et al., 2009). Because most contaminants are particulate bound, an effective removal of PM from traffic area runoff needs to be considered before it is discharged into groundwater or surface water.

The use of decentralized sustainable urban drainage systems (SUDS) for the treatment of stormwater runoff is becoming increasingly prevalent for the treatment of stormwater runoff at the source (Dierkes et al., 2015). Sustainable urban drainage systems are particularly suitable in dense urban areas as they can provide viable alternatives to more common centralized treatment solutions, such as large end-of-line sedimentation tanks and retention-type soil filters. Among these are technical SUDS or stormwater quality improvement devices (SQIDs), including sedimentation and filtration devices. Stormwater quality improvement devices utilize, in addition to sedimentation different treatment processes based on physical adsorption, precipitation and chemical processes (Dierkes et al., 2015; Huber et al., 2015a). However, their pollution removal efficiencies can be quite different (Dierkes et al., 2015). In the most cases, sedimentation is the pre-treatment step of a multi-step treatment to avoid clogging of sorption filters. Nevertheless, sedimentation is sometimes the sole treatment step.

During a monitoring campaign of a SQID treating the runoff of a highly trafficked road, we observed considerably worse effluent quality of a sedimentation

tank during winter (Rommel and Helmreich, 2018b). Figure 7.1a gives an impression of road runoff (left) and effluent of the sedimentation tank (right) of a snowmelt event under de-icing salt influence. This finding is supported by Semadeni–Davies (Semadeni-Davies, 2006), who reported a decreased performance of an urban stormwater pond during winter and spring. Figure 7.1b highlights multiple possible influencing factors for worse effluent quality of SQIDs during the cold season adapted from Semadeni-Davies (2006).

Stratification of the water column in the sedimentation tank caused by temperature differences between the influent and the water volume in the tank can lead to disadvantageous flow patterns and shorter residence times in the system (Hendi et al., 2018; Adamsson and Bergdahl, 2006). Additionally, densimetric stratification induced by de-icing salt application is increasing this effect (Marsalek et al., 2003). Tchobanoglous et al. (2014) mention that as low as a 1 °C temperature differential between incoming wastewater and the water in the sedimentation tank will lead to a density current. Additionally, lower temperature and higher de-icing salt concentration increase density and viscosity of the water in the sedimentation basin. This reduces the settling velocity of particles, and therefore, lowers the removal efficiency of PM in the system. Winkler et al. (Winkler et al., 2012) show that in wastewater treatment, the settling velocity of granular sludge decreases with lower temperature and higher salt (NaCl) concentrations. Similar findings can be expected for particles in urban runoff. However, the properties of granular sludge in wastewater treatment are considerably different to road runoff particles. Furthermore, studies showed that the flocculation of PM is affected by the temperature (Krishnappan et al., 1999; Krishnappan and Marsalek, 2002; Lau, 1994). However due to a decreasing floc density with an increasing floc size, it is not clear if flocculation is definitely improving the settling behavior. Thus, this study is describing discrete particle settling.

Adamsson and Bergdahl (2006) indicated that temperature and salinity need to be considered to evaluate the performance of detention tanks. Spelman and Sansalone (2018) reported that temperature has a minor impact on the treatment efficiency of hydrodynamic separators and clarifiers. However, in this study a minimum temperature of 10 °C was used, which is not representative for the temperate climate zone. Yet, no study covered the influence of temperature and de-icing salt concentration on the settling behavior of PM in traffic area runoff. Because of the relatively low concentration of PM, measured as total suspended solids (TSS), an experimental approach would be affected by huge uncertainties. Reliable statements for a better understanding of the processes, and thus estimation of maintenance intervals is necessary to aid in increasing the acceptance of SQIDs in the future.

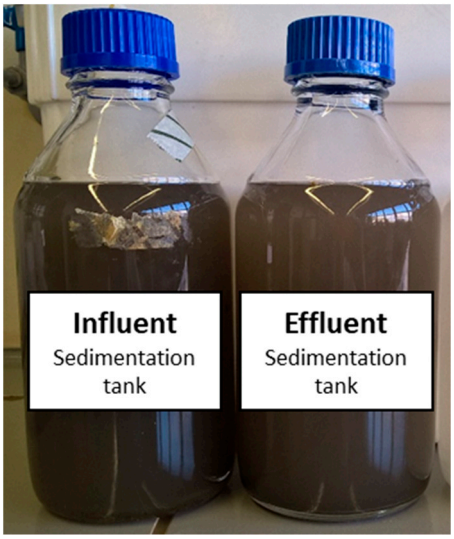

(a)

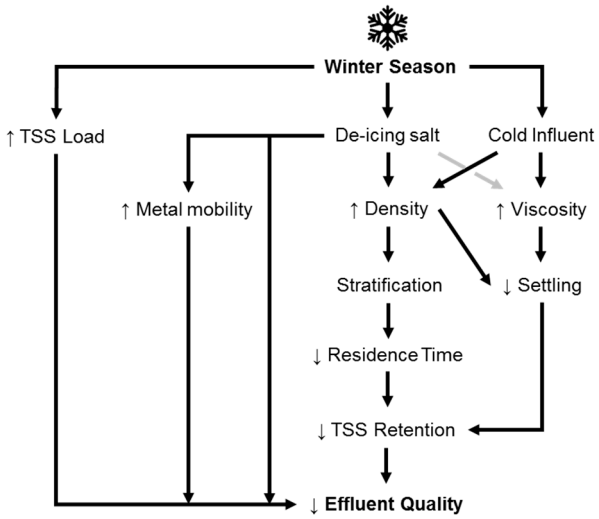

(b)

Fig. 7.1. (**a**) Influent (**left**) and effluent (**right**) samples of a sedimentation tank for road runoff treatment withdrawn during the cold season. Minor difference can be seen in turbidity between the two samples. (**b**) Diagram showing which influencing factors cause worse effluent quality and total suspended solids (TSS) retention of sedimentation tanks for treatment of road runoff during winter season; grey arrow indicates weaker influence (adapted from Semadeni-Davies (2006)).

The aim of this study was to evaluate the ranking of influencing factors causing decreased performance during the cold season of sedimentation tanks as part of SQIDs used for treatment of traffic area runoff. After analyzing data from a 20-month monitoring of a full-scale sedimentation tank, the influencing processes based on physical settling models were evaluated to substantiate the results.

To calculate densities and viscosities of various de-icing salt solutions the models of Laliberté and Cooper (2004) and Laliberté (2007) were applied for the first time in this field. Future numerical models could be performed based on those models to consider temperature as well as de-icing salt effects in SQIDs.

7.2 Materials and methods

7.2.1 Monitoring of full-scale sedimentation tank

To investigate PM removal efficiency of SQIDs for road runoff a full-scale sedimentation tank was monitored. The monitored sedimentation tank is the primary stage of a two-step SQID for road runoff located in Munich, Germany. It is operated as a continuous flow sedimentation tank. The tank consists of a round concrete shaft with a diameter of 2 m, an impounding depth of 2.4 m and a storage volume of 7.5 m^3. Runoff from 400 m^2 of a heavily trafficked road form the influent to the

treatment plant. The annual average daily traffic (AADT) is approximately 24,000 vehicles per day on the attached road surface (46,000 vehicles per day including the separated opposing traffic). The cross-section of the road consists of two traffic lanes, one accelerating lane and one emergency lane with an asphalt surface.

Samples of the influent and effluent of the sedimentation tank were withdrawn time-proportionally (5 min intervals, 250 mL each) during rain events by automatic samplers (WaterSam WS 316 and Edmund Bühler PP 84). The sampling took place from May 2016 to January 2018. The sampling started after the inflow exceeded 1 L min^{-1} for longer than 1 min. Flow was measured by an electro-magnetic flow meter (Krohne Optiflux 1100 C, DN40, error of measurement <1.6% for q > 2.6 L s^{-1} ha^{-1}). At the end of the discharge events the sampling stopped. To prevent alteration of samples, they were kept in coolers at 4 $\pm$ 1 °C until transport to the lab. Analyses were performed within 72 h.

The discrete samples withdrawn during one discharge event were combined to create one composite sample. Electric conductivity (EC) and pH values were analyzed according to SM 2510 B (detection limit: 1 μS cm^{-1}) and SM 4500-H^+, respectively (Baird et al., 2017). Electric conductivity was used to verify the de-icing salt application, here sodium chloride (NaCl). Particulate matter was analyzed as total suspended solids (TSS), coarse suspended solids with a diameter greater than 63 μm (SS > 63 μm), and suspended solids between 0.45 μm and 63 μm (SS63). To determine the PM, one liter of sample was sieved by a 1000 μm sieve in the first step, followed by a 63 μm sieve as the second step. In the third step the sieved sample was filtrated under a vacuum over a 0.45 μm membrane filter (cellulose nitrate). Large constituents ($\gg$ 1 mm; e.g., leaves, cigarette stubs), which are not representative for the sample, were manually removed. All sieves and filters were dried at 105 °C $\pm$ 2 °C until constant mass was achieved. The fine suspended solids (SS63) are the fraction between 0.45 μm and 63 μm, found as residue on the membrane filter. The coarse suspended solids (SS > 63) are the fraction between 1000 μm and 63 μm, found on the 63 μm sieve. Total suspended solids was calculated by the sum of the residues on the 1000 μm and 63 μm sieves, and the 0.45 μm membrane filter after drying. The procedure was a modified method of Dierschke and Welker (2015).

Climate data of the measurement station 3379 of The German Weather Service (DWD) was used. The meteorological station is located approximately 5 km from the study site. The annual precipitation height was 955 mm in 2016 and 931 mm in 2017. In 2016, there were 64 days of frost (minimum air temperature < 0 °C) and 71 days in 2017. The temperature of the water in the sedimentation tank was assumed to be equal to the soil temperature at 50 cm depth.

7.2.2 Calculations

Density Densities of water ρ_{w} (kg m^{-3}) were calculated with equation 7.1 (Laliberté and Cooper, 2004),

$$\rho_{\mathrm{w}} = \frac{(((((-2.8054253\times10^{-10}t+1.0556302\times10^{-7})t-4.6170461\times10^{-5})t-0.0079870401)t+16.945176)t+999.83952)}{1+0.01687985t} \tag{7.1}$$

where t is the temperature (°C). The densities of solutions ρ_{m}, in this case sodium chloride (NaCl) solutions, were calculated using the model of Laliberté and Cooper (2004). The model considers temperature and concentration of the solute. ρ_{m} (kg m^{-3}) was determined with the following Equations 7.2 and 7.3:

$$\rho_{\mathrm{m}} = \frac{1}{\frac{\mathrm{w_{H_2O}}}{\rho_{\mathrm{H_2O}}} + \mathrm{w_{NaCl}}\ \overline{v}_{app,NaCl}} \tag{7.2}$$

$$\overline{v}_{app,NaCl} = \frac{\mathrm{w_{NaCl}} + 1.01660 + 0.014624\ t}{(-0.00433\ \mathrm{w_{NaCl}} + 0.06471)\ e^{(0.000001(t+3315.6)^2)}} \tag{7.3}$$

where $\mathrm{w_{H_2O}}$ = mass fraction of water in the solution (-), $\mathrm{w_{NaCl}}$ = mass fraction of the NaCl in the solution (-) and $\overline{v}_{app,NaCl}$ = NaCl specific volume (m^3 kg^{-1}). Equation 7.3 is valid for $\mathrm{w_{NaCl}} > 0.00006$ (Laliberté and Cooper, 2004), therefore densities of pure water (without NaCl) were calculated with Equation 7.1.

This study examines the de-icing salt NaCl concerning the by far greatest application rate (Huber et al., 2015b; Sansalone and Glenn, 2002). Concentrations of up to 15 g L^{-1} NaCl could be present in traffic area runoff (Huber et al., 2015b; Sansalone and Glenn, 2002; Hilliges et al., 2017). Because of the thermal expansivity, this study used the mass fraction of solute NaCl ($\mathrm{w_{NaCl}}$) to describe the concentration of the solution. A $\mathrm{w_{NaCl}}$ of 0.01 corresponds to 10 g L^{-1} at 20 °C. To cover extrema, the calculations were conducted up to $\mathrm{w_{NaCl}} = 0.02$, unless otherwise stated.

Viscosity Dynamic viscosities of the solutions were calculated as a function of temperature and concentration of the solute by means of the model of Laliberté (2007), following Equation 7.4. In the first step the dynamic viscosity of water η_{w} (kg m^{-1} s^{-1}) was calculated at temperature t (°C). Equation 7.4 is valid for t from 0 °C to 100 °C (Laliberté, 2007).

$$\eta_{\mathrm{w}} = \frac{(\mathrm{t}+246)\times10^{-3}}{(0.05594\mathrm{t}+5.2842)\,\mathrm{t}\ +\ 137.37} \tag{7.4}$$

In the second step the viscosity of the various NaCl solutions η_m (kg m^{-1} s^{-1}) were calculated with Equation 7.5, based on the model of Laliberté (2007):

$$\eta_m = \eta_w^{w_{H_2O}} \left(\exp\left(\frac{16.222\,(1 - w_{H_2O})^{1.3229} + 1.4849}{(0.0074691t + 1)\left(30.78\,(1 - w_{H_2O})^{2.0583} + 1\right)} \right) \times 10^{-3} \right)^{w_{NaCl}} \tag{7.5}$$

where η_m = dynamic viscosity of the NaCl solution (kg m^{-1} s^{-1}), η_w = dynamic viscosity of water (kg m^{-1} s^{-1}), w_{H_2O} = mass fraction of water in the solution (−), w_{NaCl} = mass fraction of NaCl in the solution (−) and t = temperature (°C). This formula is valid for t ranging from 5 °C to 154 °C and w_{NaCl} up to 0.264 (Laliberté, 2007).

Settling velocity Stokes' Law was used to determine the terminal settling velocity v_t (m s^{-1}) of the particles (Sansalone et al., 2009),

$$v_t = \frac{g\,(\rho_s - \rho_m)\,d^2}{18\eta_m} \tag{7.6}$$

where g = gravitational acceleration (9.81 m s^{-2}), η_m = dynamic viscosity of the solution (kg m^{-1} s^{-1}), ρ_m = density of the solution (kg m^{-3}), ρ_s = density of particles (kg m^{-3}), and d = particle diameter (m).

Because Equation 7.6 is only applicable for laminar flow (Reynold's number Re < 1) (Tchobanoglous et al., 2014), Re was calculated afterwards with Equation 7.7,

$$Re = \frac{v_t d}{\nu_m} \tag{7.7}$$

where ν_m = kinematic viscosity of the solution (m^2 s^{-1}). Reported settling velocities fulfilled this condition, meaning laminar flow conditions were present.

The mostly non-spherical shape of road runoff particles (Sansalone et al., 1998; Kayhanian et al., 2012b) was neglected due to a lack of data about sphericity factors. To investigate the influence of particle density, a low ρ_s (1.35 g cm^{-3}) (Li et al., 2008) and a high ρ_s (2.25 g cm^{-3}) (Kayhanian et al., 2012b) were used. Because fine SS63 are prevalent in traffic area runoff (Hilliges et al., 2017; Li et al., 2006; Gunawardana et al., 2014; Charters et al., 2015) and showed a significant worse settling behavior, this study focused on those particles <63 μm.

Retention of suspended solids To determine the retention of suspended solids a stationary idealized discrete settling approach was selected. Inflow Q_{In} and outflow Q_{Eff} were assumed to be equal and constant over time as well as inflow TSS. Scouring of retained particles was neglected. In this model particles with a terminal settling

velocity equal to or greater than the critical terminal settling velocity v_{crit} were removed (Tchobanoglous et al., 2014). The v_{crit} (m s^{-1}) was equal to the overflow rate determined with Equation (8),

$$v_{crit} = \frac{Q}{A} = overflow\ rate \tag{7.8}$$

where Q (m^3 s^{-1}) = flow rate and A (m^2) = surface of the sedimentation basin.

By means of v_{crit} the critical particle diameter d_{crit} (μm) was calculated for given conditions like solution temperature, viscosity, density, and particle density. The calculation was conducted with Excel Solver and the solving method GRG nonlinear. Because de-icing salt (NaCl) showed a neglectable effect on the settling velocity (cf. 7.3.2), in this step w_{NaCl} was not considered (set to 0). The water temperature was altered in the range from 5 °C to 25 °C. Additionally, the effect of particle density was studied.

The model system corresponded to the monitored system (cf. 7.2.1). The discharge coefficient ψ was set to 1.0, to represent a fully impervious surface and ensure comparability to the test protocol of the Deutsches Insitut für Bautechnik (DIBt) (DIBt, 2017). Rain intensities of 2.5 L s^{-1} ha^{-1} and 15 L s^{-1} ha^{-1} were investigated. The upper value was chosen based on the knowledge that more intense design rain intensities lead to a minor increase in treatment efficiency (*DWA-A 102 (Entwurf)* 2016).

In real traffic area runoff, particles are not uniform in particle size, and therefore, the particle size distribution (PSD) was characterized by a parametric cumulative distribution function (CDF). Selbig and Fienen (2012) proposed the usage of the Rosin–Rammler distribution, which is equivalent to the Weibull distribution. This approach was continued by Lee et al. (2014). Based on this knowledge, this method was used to generate a synthetic PSD. The formula of the Rosin–Rammler CDF is

$$W(d, \lambda, \kappa) = 1 - e^{\left(-\frac{d}{\lambda}\right)^{\kappa}} \tag{7.9}$$

where $W(d, \lambda, \kappa)$ = mass fraction less than d (−); d = particle diameter (μm); λ = shape parameter (−); κ = scale parameter (−) (Selbig and Fienen, 2012). For our simulation we used λ = {9.3, 60, 116}, equal to a d_{50} from 6 to 75 μm, and κ was fixed to 0.84 (Lee et al., 2014).

The TSS removal efficiency (−) was calculated with Equation (10) based on the critical particle diameter d_{crit}, which is derived from v_{crit} following Equation (8). Preassigned λ and κ values were used.

$$TSS\ removal\ efficiency = 1 - W(d_{crit}, \lambda, \kappa) \tag{7.10}$$

7.3 Results and discussion

7.3.1 Monitoring of the full-scale sedimentation tank

The monitoring of the full-scale sedimentation tank was executed over a period of 20 months. To cover all seasonal influences, 23 rain events were taken and analyzed. Table 7.1 presents the statistics of all measured values from the influent and effluent of the sedimentation tank as well as the calculated retention of TSS, SS > 63, and SS63. Due to the flushing of PM of former events, a few negative removal rates were determined. Remarkable was that the PM occurred almost completely as SS63 (98% of mean TSS). Thereby the focus on the fine fraction of this study was supported.

Tab. 7.1. Statistics of full-scale sedimentation tank monitoring: q = mean inflow; t = water temperature in sedimentation tank; TSS Inf. = influent TSS; SS63 Inf. = influent SS63; EC Eff. = electric conductivity in effluent.

Parameter	Unit	*n*	Min	25%	Median	Mean	75%	Max	SD
q	$L\ s^{-1}\ ha^{-1}$	23	1.6	3.4	5.7	8.1	7.2	26.1	7.5
t	°C	23	3.0	8.8	17.5	17.5	21.7	24.6	7.3
TSS Inf.	$mg\ L^{-1}$	23	7	32	82	123	166	433	129
SS > 63 Inf.	$mg\ L^{-1}$	15	3	18	26	35	46	122	30
SS63 Inf.	$mg\ L^{-1}$	15	8	18	73.3	121	140	394	130
EC Eff.	$\mu S\ cm^{-1}$	22	59	95	119	119	867	4790	1225
TSS retention	%	21	−365	22	44	18	68	95	105
SS > 63 retention	%	15	−4	65	83	71	93	100	31
SS63 retention	%	15	−49	−1	37	25	57	80	40

Figure 7.2 shows the annual course of TSS influent and effluent of the sedimentation tank, as well as TSS retention. Due to strong seasonal courses (Helmreich et al., 2010), data points of different years are plotted together in one figure. At the start of the sampling campaign two events showed strong scouring of sediments (−185% and −365% TSS retention) from previous rain events or maybe even residues of the construction work. Therefore, those two events were removed. In the annual course of TSS the strong increase in the cold seasons was recognizable. Likewise, a decrease of TSS retention during the cold season is shown. Furthermore, in summer three events showed conspicuous low TSS retentions (1%, 2%, and 28%). The event with the lowest TSS retention was the event with the highest inflow. Thus, the high inflow resulted in the low TSS retention. Although the data was not adequate to explain the reason for the low TSS retentions of the other two events. Due to less frequent and less intensive rain events in the cold season, only a few events could be sampled. Therefore, monitoring will be continued to gain more statistical significance.

To evaluate the influence of temperature on the PSD, Figure 7.3 shows the ratio SS63/TSS in the influent and effluent of the sedimentation tank. During the cold season, the particles were smaller than during summer. Thus, a decreased settling velocity was expected during the cold season. Because SS63/TSS was higher in the effluent than in the influent, the worse removal efficiency of SS63 was visible. The increasing particle size with increasing temperature can be explained by enhanced flocculation (Krishnappan et al., 1999; Krishnappan and Marsalek, 2002). Since SS63 is describing a range of particle sizes, the ration SS63/TSS can only be an indicator for the PSD.

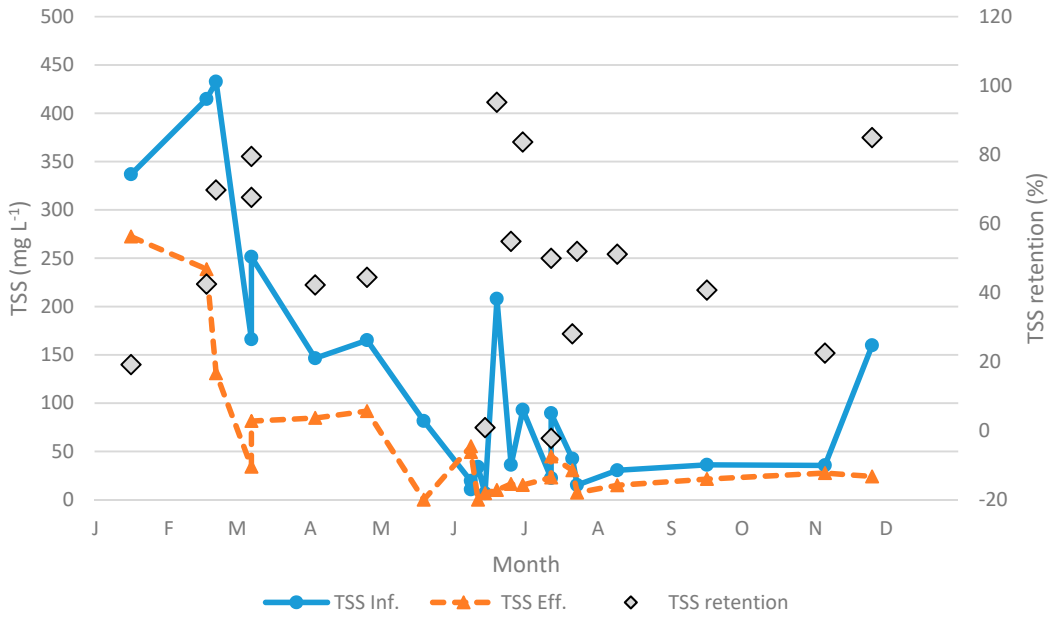

Fig. 7.2. Annual course of TSS influent and effluent of the sedimentation tank and TSS retention; two successive data points of TSS retention were removed due to strong scouring of sediments of previous events (−185% and −365% TSS retention).

The following correlation matrix (Figure 7.4) shows multiple effects influencing the settling of PM. During cold temperatures, a higher EC, due to the application of de-icing salt, and influent TSS was present ($r_s < -0.68$). Between SS63 removal and mean inflow q a weak correlation was observable($r_s = -0.34$), which induces that even longer residence times in the studied sedimentation tank do not improve the SS63 retention. In contrast, the retention of SS > 63 correlates considerably with q ($r_s = -0.71$). Overall, this means that the used settling tank is only partially suitable for the retention of fine particulate matter. Only in recent years the SS63 parameter has become popular, and therefore settling tanks were mainly designed to separate the sand fraction (>63 μm). To achieve better settling, the geometry needs to be changed to achieve lower surface loadings, and thus, increased settling times.

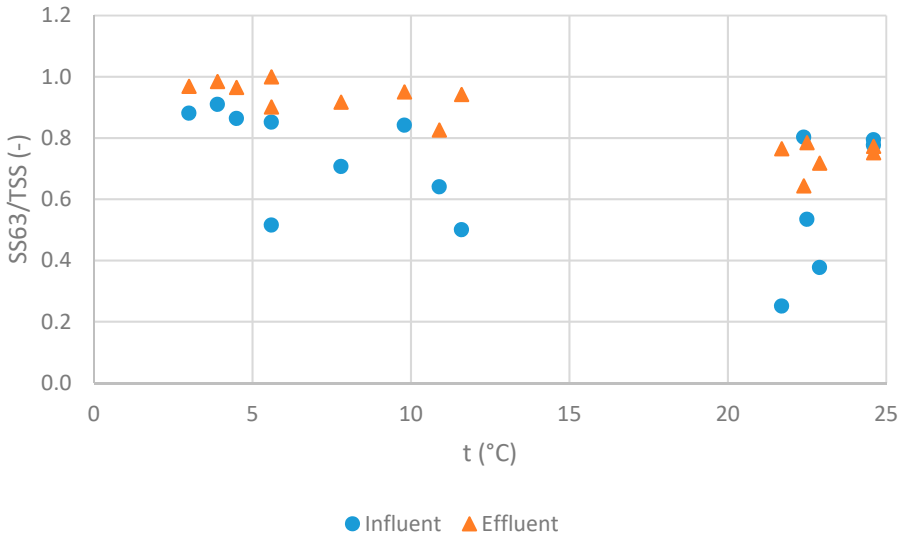

Fig. 7.3. Fraction of fine particulate matter (PM) (SS63) in the TSS in the influent and effluent of the sedimentation tank as a function of temperature.

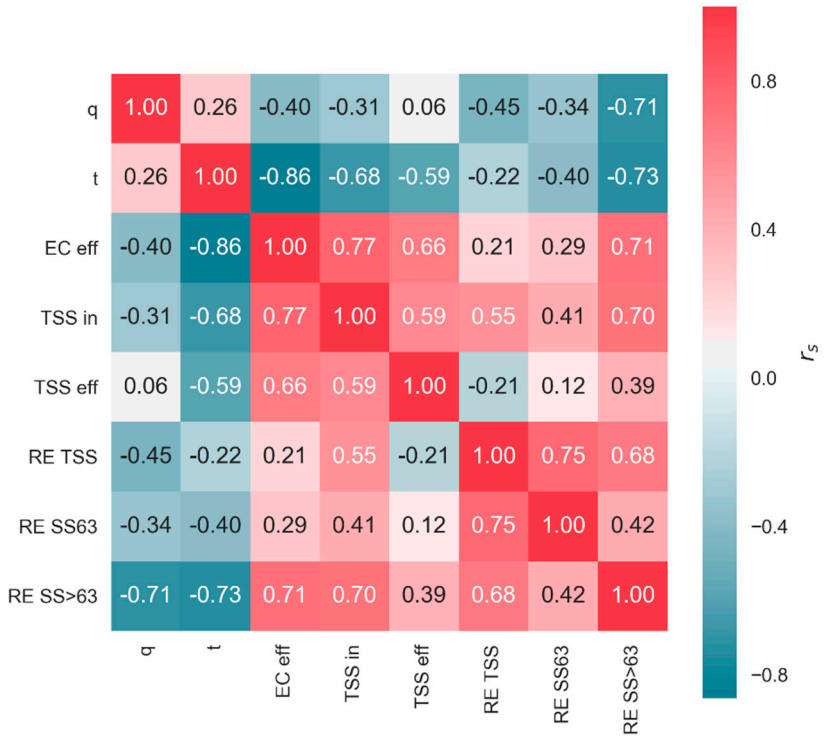

Fig. 7.4. Correlation matrix of Spearman's rank correlation coefficients r_s of full-scale sedimentation tank monitoring; q = mean inflow (L s^{-1} ha^{-1}), t = water temperature in tank (°C), EC eff. = effluent electrical conductivity (µS cm^{-1}), TSS in = influent TSS (mg L^{-1}), TSS eff = effluent TSS (mg L^{-1}), RE TSS = removal efficiency of TSS (%), RE SS63 = removal efficiency of SS63 (%), RE SS63 = removal efficiency of SS > 63 (%), n = 15 for SS63 and n = 23 for all other parameters.

Although it was expected that TSS, SS63, and SS > 63 retentions would increase with increasing temperature, following sedimentation theory (cf. 7.2.2), this was not observable in the data. However, an inverse effect is shown in Figure 7.4, which conflicts with the physical basics of settling. Due to the complex nature of the system, it looks like there is a spurious correlation between temperature and the PM retention. The same unexpected correlation is visible between EC and PM retention. Though TSS and SS63 retention correlate moderately to weakly with t and EC ($|r_s| \leq 0.40$). Because q is increasing with t and decreasing with EC, it can be assumed that this is masking the expected effects. In addition, PSD was not constant (cf. Figure 7.3), and therefore removal efficiency of the PM was varying. The monitoring will proceed and with increasing data the trend may alter.

Given that our findings are based on a limited number of sampled events and the uncertainty of sampling, the results of that monitoring should be treated with caution. Bardin et al. (2001) demonstrated with a comparable system that established methods of performance measurement are accompanied with a wide margin of uncertainty. Assuming an ideal sampling and preservation of the samples, the removal efficiency of TSS is already within a range of 39% to 59% due to the error of TSS analysis ($\pm$10%). This approximation is based on the mean TSS concentrations in the influent and the effluent of the sedimentation tank. Furthermore, there are uncertainties related to the sampling conditions, the sampling cycle performance and the preparation of the composite samples (Bardin et al., 2001).

To further evaluate the ranking of influencing factors on PM retention, the following calculations, based on simplified approaches, were made to substantiate the results.

7.3.2 Calculations

Density The densities of various NaCl solutions were calculated with the model of Laliberté and Cooper (2004). Figure 7.5a shows the calculated densities of solutions ρ_m with different w_{NaCl} at various temperatures. The solution with $w_{NaCl} = 0.00$ equates to pure water. Density declines with increasing temperature and increases with increasing w_{NaCl}. The density anomaly of water affected the NaCl solutions as well. While the highest density of pure water was found at 3.98 °C, in accordance with Kell (1975), the density of the NaCl solutions peaked at lower temperatures: 1.58 °C with $w_{NaCl} = 0.02$ and up to 3.38 °C with $w_{NaCl} = 0.005$. Thereby a trend of shifting the maximum density point towards lower temperatures with increasing w_{NaCl} was derivable. In Figure 7.5b, density is plotted as a function of w_{NaCl}. A linear correlation between ρ_m and w_{NaCl} is observable. Density affects settling velocity linearly following Equation 7.6 (7.2.2), causing colder temperatures and higher

w_{NaCl} to lead to a decrease of settling velocity and consequently worse PM retention. Assuming the particle density of $\rho_s = 1.35$ g cm^{-1}, the settling velocity at 5 °C and $w_{NaCl} = 0.02$ is 5% less than at 20 °C and $w_{NaCl} = 0.00$. Though, w_{NaCl} is an extreme value in this example. Under more likely winter conditions ($w_{NaCl} = 0.01$), the effect of density variation on settling velocity is <1%. Consequently, this effect is negligible and probably not measurable in full scale. Please refer the Supplementary Materials (S1) for the densities of NaCl solutions at various temperatures.

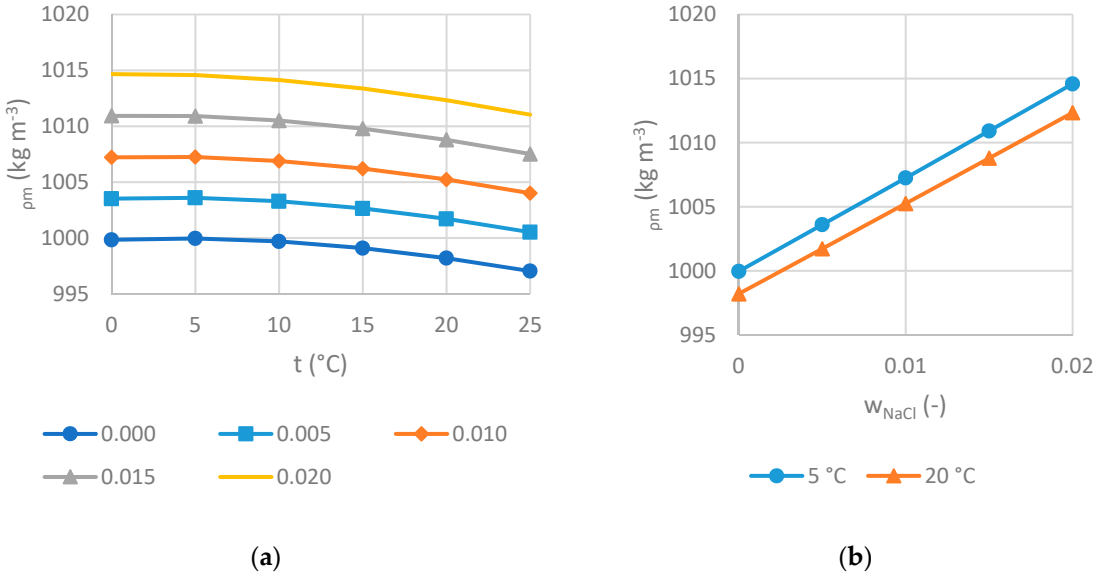

(**a**) (**b**)

Fig. 7.5. (**a**) Density of aqueous NaCl solutions as a function of temperature for various w_{NaCl}; (**b**) density of aqueous NaCl solutions as a function of w_{NaCl} for t = 5 °C and t = 20 °C.

Viscosity Based on the model of Laliberté (2007), the viscosity of various NaCl solutions were calculated at 20 °C. Figure 7.6a shows the viscosity as a function of the mass fraction of NaCl in the solution w_{NaCl}. NaCl showed a kosmotropic effect, meaning it acts as a structure maker and increases the viscosity of the solution compared to pure water (Corridoni et al., 2011). The viscosity of pure water is depicted by the solution with $w_{NaCl} = 0.00$.

In traffic area runoff values of $w_{NaCl} < 0.015$ (15 g L^{-1} at 5 to 25 °C) occur (Huber et al., 2015b; Hilliges et al., 2017). Consequently, the viscosity alteration by NaCl does not occur in the full magnitude, which Figure 7.6a indicates. To investigate the influence of the temperature, the viscosity calculation was carried out with solution temperatures t from 5 to 25 °C with increments of 5 °C following the method of Laliberté (2007). The minimal temperature covered by the model is 5 °C, thus the density peak (cf. 7.3.2) cannot be included in the viscosity calculation. Figure 7.6b

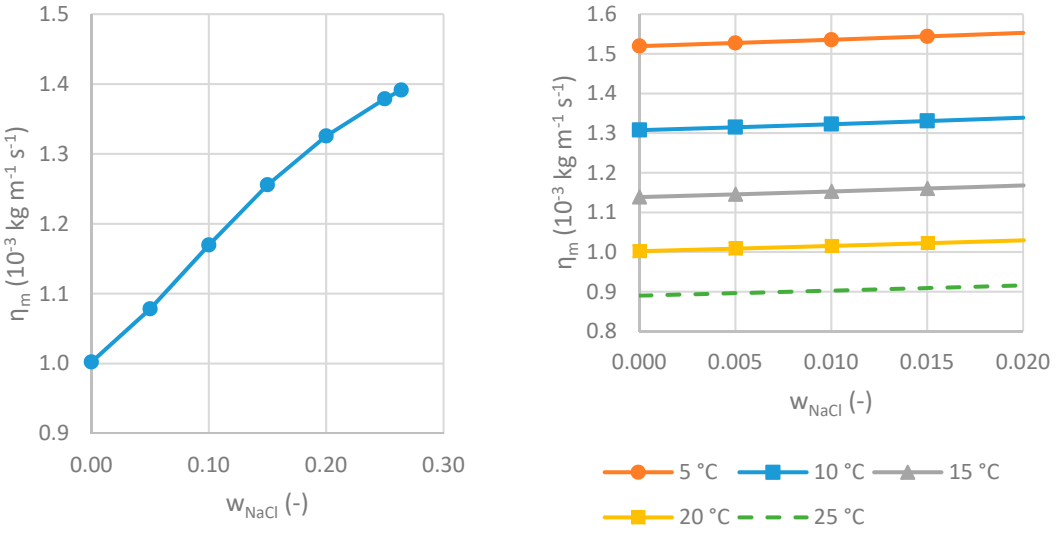

(**a**) (**b**)

Fig. 7.6. (**a**) Viscosity of various aqueous NaCl solutions at 20 °C; (**b**) viscosity of aqueous NaCl solutions at various temperatures.

shows the viscosity of solutions η_m as a function of w_{NaCl} at various temperatures. In the considered mass fraction range, a slightly positive linear relation between w_{NaCl} and η_m is observable. However, the influence of the solution temperature was significantly stronger. Thereby the solutions revealed a higher viscosity at lower temperatures. The settling velocity in a solution with w_{NaCl} = 0.02 at 5 °C is 35% less than in a solution with w_{NaCl} = 0.00 at 20 °C. Accordingly, viscosity is the main influencing factor on the settling velocity if particle density and size are constant. The viscosity variation was mainly caused by temperature alteration, not by de-icing salt (NaCl). Please refer the Supplementary Materials (S1) for the viscosities of NaCl solutions at various temperatures.

Settling velocity To assess the influence of temperature and de-icing salt on the settling velocity two scenarios were assumed: Winter conditions with t = 5 °C and w_{NaCl} = 0.02 and summer conditions with t = 20 °C and w_{NaCl} = 0.00. Figure 7.7 illustrates settling velocity v_t as a function of particle diameter d. There was a severe difference observable between both scenarios. In winter, 38% lower settling velocities were determined.

To analyze the influence of de-icing salt (NaCl) another scenario was modeled at 5 °C solution temperature with w_{NaCl} = 0.00. In this case, a 34% lower settling velocity was calculated for winter conditions without NaCl influence. This resulted

in the temperature influencing the settling velocity at a bigger magnitude than the de-icing salt.

Based on that knowledge, it is recommended to design sedimentation tanks with a larger surface area, and thus, lower overflow rates to cope with challenging winter conditions.

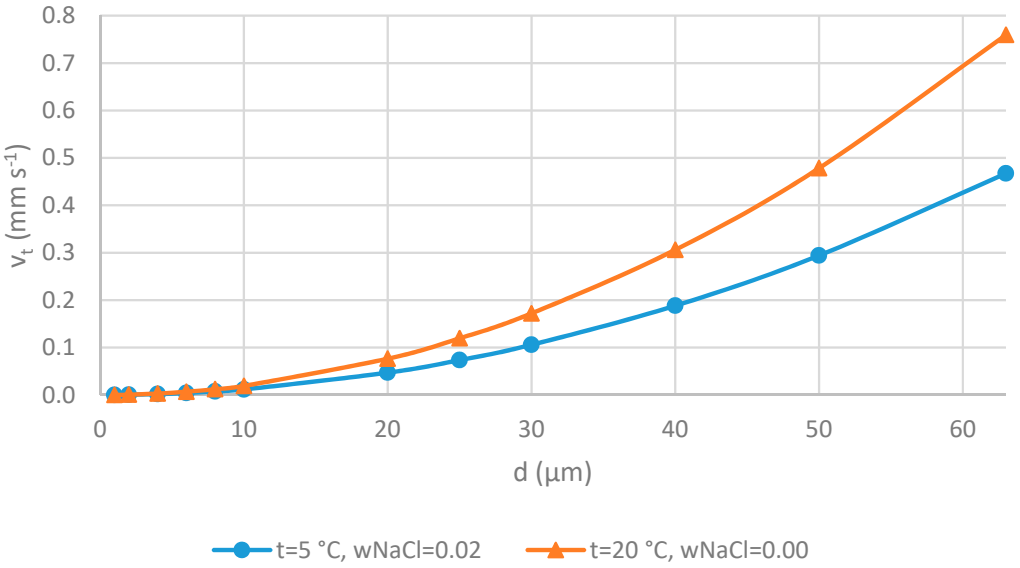

Fig. 7.7. Settling velocity as a function of particle diameter in two aqueous solutions at various temperatures and w_{NaCl} simulating winter and summer conditions (extrema); both ρ_s = 1.35 g $cm^{-1.}$

Retention of suspended solids Based on the monitored sedimentation tank (cf. 7.2.1) critical particle diameters d_{crit} under varying boundary conditions (temperature, flow q, particle density) were determined. The critical particle diameter characterizes the lower limit of particle size, which can be separated in the sedimentation tank.

Figure 7.8 shows that the influence of the temperature on the particle retention is more severe with increasing flow. Furthermore, the influence of the particle density on the separation increases with flow. To assess the TSS removal efficiency PSD was considered. Hereby the information of Figure 7.8 was relativized. A reduced temperature from 25 to 5 °C lead to differences of ≤8% TSS removal efficiency (Figure 7.9a).

A decisive influence of de-icing salt on the TSS removal efficiency was not observable (Figure 7.9b). Increasing w_{NaCl} from 0.00 to 0.02 was shown to decrease the TSS removal efficiency by less than 0.7%. Therefore, de-icing salt was classified as a negligible factor, which was not considered in the following ranking of the influencing factors.

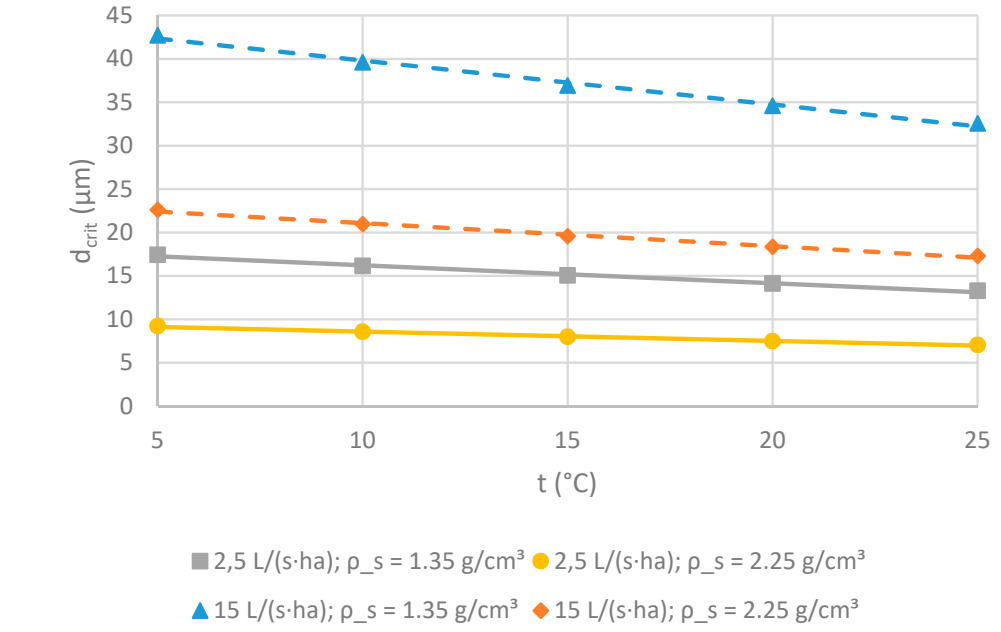

Fig. 7.8. Critical particle diameter d_{crit} for settling, various water temperatures and particle densities.

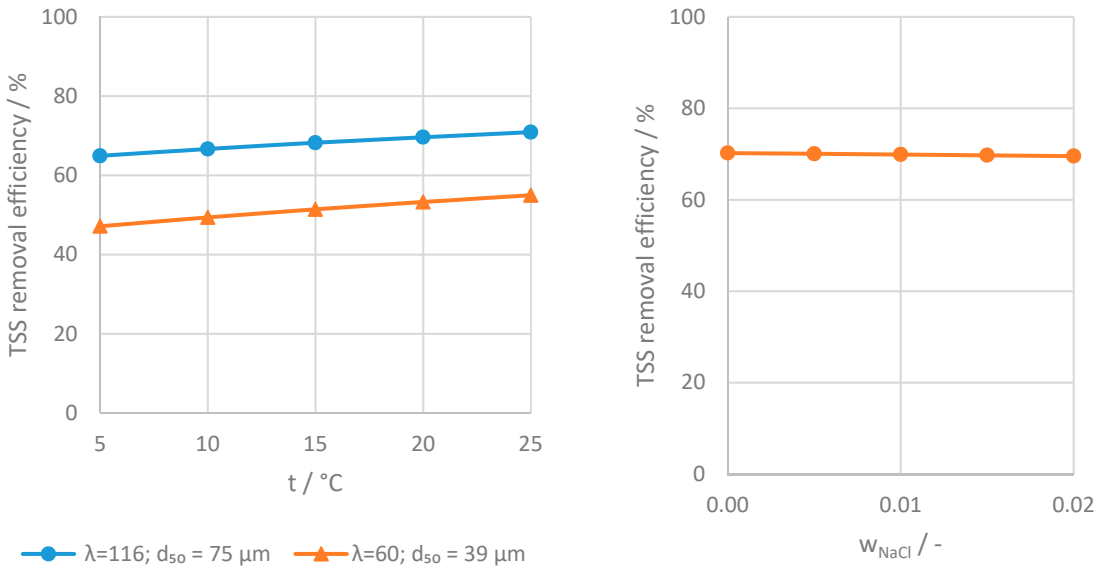

(**a**) (**b**)

Fig. 7.9. (**a**) TSS removal efficiency as a function of temperature; (**b**) TSS removal efficiency as a function of w_{NaCl}, $\lambda = 60$, $d_{50} = 39$ µm; (**a**,**b**): $\rho_s = 1.35$ g cm^{-1}; q = 15 L s^{-1} ha^{-1}.

The Pearson correlation coefficients were calculated based on various scenarios (t, ρ_s, λ or d_{50} and q) (Table 7.2). This allowed the influencing factors on the TSS removal efficiency to be ranked. The PSD, specified by d_{50} or λ, showed the most

distinct influence, followed by q and ρ_s. t was classified as the least influencing factor. However, physical characteristics of particles (ρ_s and d_{50}/PSD) are regarded site-specific (Faram et al., 2007; Gunawardana et al., 2012; Gunawardena et al., 2018; Ferreira and Stenstrom, 2013; Selbig and Bannerman, 2011). Thus, temperature needs to be considered in future SQID designs to improve treatment efficiency during the cold season. Because the applied model cannot represent effects of occurring density currents caused by temperature and de-icing salt, the effect could occur at bigger magnitudes.

Tab. 7.2. Pearson correlation coefficients between TSS removal efficiency, temperature t, particle density ρ_s, median particle diameter d_{50} and discharge rate q.

	t	**ρ_s**	**d_{50}**	**q**
TSS removal efficiency	0.07	0.22	0.85	−0.32

The ranking of the influencing factors PSD > ρ_s > t of this study was affirmed by Spelman and Sansalone (2018). Additionally, they identified influent hydrograph unsteadiness as the most powerful influencing factor. The hydrograph unsteadiness describes the shape of the hydrograph. A highly unsteady hydrograph rises fast and drops fast after a short time. In comparison to this, a highly steady hydrograph rises slow and drops slow after a long time. Due to the stationary method used in this study, this factor was not assessed. Spelman and Sansalone (2018) altered the flow rate q together with the unsteadiness of the influent hydrograph, and therefore, it is not determinable if q or the unsteadiness was the dominant factor. Furthermore, the minimum temperature was 10 °C (Spelman and Sansalone, 2018), which is not adequate for the use in the temperate climate zone.

To approximate realistic conditions coming from lab-scale experiments, a variety of effects were neglected in this present study. Kayhanian et al. (2012b) showed that particles are neither smooth nor spherical, and therefore, models need to be established considering this influence. The current knowledge is that particles in road runoff are not spherical; however, there is no sufficient data describing the shape of runoff particles. Therefore, a representation in simulations is currently not possible. Furthermore, particles were assumed to be non-cohesive. Kayhanian et al. (2012b) derived from zeta-potential analysis that runoff particles have a relatively low tendency to aggregate. However, experience of handling runoff samples in the lab showed us that aggregation of particles does occur. Li et al. (2005) proved this assumption with PSD analysis. Furthermore, the influence of temperature on the flocculation of PM (Krishnappan et al., 1999; Krishnappan and Marsalek, 2002; Lau, 1994) is not considered, yet. In addition, the influence of de-icing salt on

the flocculation of runoff particles is still open. Faltermaier et al. (2017) showed an increased settling velocity under de-icing influence. Studies about settling of marine clay-size sediments reported a positive correlation between salinity and settling velocity (Portela et al., 2013; Sutherland et al., 2015). Since the mineralogy of the particles does have an influence on flocculation, those findings may have limited adaptability to road runoff particles, which contain clay minerals in minor quantities (Gunawardana et al., 2012; Duzgoren-Aydin et al., 2006). Slight variation in particle density can affect the removal efficiency of PM in sedimentation tanks. Therefore, the common method of particle density determination needs to be verified. Wet particle density (Li et al., 2008) could reflect more realistic conditions. It can be expected that the above-mentioned uncertainties affect smaller particles more intensely than bigger size fractions (Li et al., 2006; Bäckström, 2002). In addition, future studies should be conducted under non-stationary conditions to consider the unsteadiness of the influent hydrograph, like that proposed by Spelman and Sansalone (2018).

Further works should improve knowledge about the aforementioned aspects to improve particle separation, and therefore, achieve better effluent quality of SQIDs.

7.4 Conclusions

A sedimentation tank treating road runoff was monitored for 20 months. During the cold season, reduced PM removal efficiency was observed. However, the data was not sufficient to distinctively assess the influence of temperature and de-icing salt. Therefore, simplified settling models were applied to determine which of the influencing factors had the greatest effect on PM removal. The determined order was PSD $\gg$ q > ρ_s > t. The influence of de-icing salt (NaCl) on the sedimentation of PM was negligible. Since PSD and ρ_s are assumed to be site-specific, low temperatures need to be considered to improve effluent quality of SQIDs in the cold season. Low temperatures (5 °C) revealed a decrease of up to 8% TSS removal efficiency compared to higher temperatures (20 °C). The simplified models can be extended in future studies by considering de-icing salt induced particle coagulation, stratification, alternated flow patterns, and non-spherical shape of particles.

Two empirical models were applied the first time in this field to calculate density and viscosity of various solutions as a function of temperature and the solute concentration of de-icing salt. These seem promising and can improve future numerical models by considering non-steady water matrices.

Based on the knowledge gained about the sedimentation of PM from road runoff under cold season conditions, we recommend considering low temperatures

when designing the sedimentation stages of SQIDs. Effluent quality can be thereby improved. By minimizing the PM load in the effluent of the sedimentation stage, clogging of optional downstream filtration elements can be retarded. Consequently, the intervals between maintenance events could be prolonged.

Acknowledgments

This work was supported by the German Research Foundation (DFG) and the Technical University of Munich (TUM) in the framework of the Open Access Publishing Program. We thank Philipp Stinshoff of the Chair of Urban Water Systems Engineering, Technical University of Munich, for the assistance in operating the study site. We especially thank Claire Sembera for editing the draft.

8

Settling of road-deposited sediment: Influence of particle density, shape, low temperatures, and de-icing salt

This chapter has been previously published as follows:
Rommel, S. H., L. Gelhardt, A. Welker, and B. Helmreich (2020a). "Settling of Road-Deposited Sediment: Influence of Particle Density, Shape, Low Temperatures, and Deicing Salt". *Water* 12.11 (11), p. 3126. DOI: 10.3390/w12113126.

Author contributions: Rommel, S. H.: conceptualization, methodology, software, validation, investigation, data curation, writing - original draft, writing - review & editing, visualization; Gelhardt, L.: conceptualization, methodology, investigation, data curation, writing - review & editing; Welker, A.: conceptualization, resources, writing - review & editing, supervision, project administration, funding acquisition; Helmreich, B.: resources, writing - review & editing, supervision, project administration, funding acquisition.

† Supplementary information are available in A.6.

Abstract

Separation of particulate matter (PM) is the most important process to achieve a reduction of contaminants present in road runoff. To further improve knowledge about influencing factors on the settling of road-deposited sediment (RDS), samples from three sites were collected. Since particle size distribution (PSD) has the strongest effect on settling, the samples were sieved to achieve comparable PSDs so that the effects of particle density, shape, fluid temperature, and deicing salt concentration on settling could be assessed using settling experiments. Based on the experimental data, a previously proposed model that describes the settling of

PM was further developed and validated. In addition, RDS samples were compared to a standard mineral material, which is currently in use to evaluate treatment efficiency of stormwater quality improvement devices. The main finding was that besides PSD, particle density is the most important influencing factor. Particle shape was thoroughly described but showed no significant improvement of the prediction of the settled mass. Temperature showed an effect on PM settling; deicing salts were negligible. The proposed models can sufficiently predict the settling of RDS in settling column experiments under varying boundary conditions and are easily applicable.

8.1 Introduction

Road-deposited sediment (RDS) is an important source of contamination in urban environments (Stone and Marsalek, 1996; Sutherland and Tolosa, 2000; Sutherland et al., 2012). RDS contains inorganic and organic pollutants such as heavy metals (e.g., Cu, Zn, Pb, Cd, Cr, Ni) and polycyclic aromatic hydrocarbons (PAH) (Loganathan et al., 2013; Murakami et al., 2005; Zgheib et al., 2011b). To mitigate the effect caused by RDS on the environment, stormwater control measures (SCMs) such as stormwater quality improvement devices (SQIDs) and detention basins are designed to retain RDS from stormwater runoff by sedimentation or filtration (Dierkes et al., 2015; Goonetilleke and Lampard, 2019). However, previous studies have shown that SCMs exhibit reduced retention efficiency under winter conditions caused by low temperature and deicing salts (Rommel and Helmreich, 2018c; Roseen et al., 2009; Semadeni-Davies, 2006). To design the sedimentation stages of SQIDs, knowledge about particle characteristics and settling velocity distributions of RDSs is crucial (Torres and Bertrand-Krajewski, 2008; Kang et al., 2007), especially to separate fine particles and particles with low density, which show an increased contaminant load (Murakami et al., 2005; Gunawardana et al., 2014; Kayhanian et al., 2012b; McKenzie et al., 2008; Gelhardt et al., 2017). In addition, the influence on settling by particle size distribution (PSD), particle density, and runoff event-specific properties, such as first flush and runoff volume and intensity, has been comprehensively studied (Li et al., 2005; Li et al., 2006; Kayhanian et al., 2008a; Li et al., 2008; Spelman and Sansalone, 2018; Lin et al., 2009). Other factors such as temperature, deicing salt, and particle shape have not been sufficiently investigated yet.

The first predictions of Rommel and Helmreich (2018c) indicated that the presence of deicing salt (sodium chloride) had a negligible influence on the retention of particles. However, reducing the temperature from 20 to 5 °C was shown to

decrease the removal efficiency of RDS in a sedimentation shaft by up to 8%. To calculate densities and viscosities of various deicing salt solutions, the equations of Laliberté and Cooper (2004) and Laliberté (2007) were adapted. The order of influencing factors for the sedimentation was found to be particle size distribution >> overflow rate > particle density > temperature. Even though the results of a 20-month monitoring of full-scale sedimentation indicated worse particulate matter (PM) separation in the cold season, the data were not sufficient to quantify the influencing factors. Thus, lab-scale experiments, with a comparable setup, would be necessary to exclude other environmental influences on the sedimentation, which are always present under real conditions (i.e., varying discharge rates and PM properties, stratification and mixing of water with different temperature and deicing salt concentrations), and validate the modeling predictions.

There are various protocols to determine settling velocity distribution (Torres and Bertrand-Krajewski, 2008; Gelhardt et al., 2017; Hettler et al., 2011; Aiguier et al., 1996; Michelbach and Wöhrle, 1993); however, they have not been utilized yet to quantify the influence of temperature and deicing salts on the settling velocity of RDSs. Commonly, artificial test materials are used to reduce variations of PM properties (Gelhardt et al., 2017). Gelhardt et al. (2017) developed a laboratory method to measure and compare the settling behavior of artificial and real particle collectives with a reproducible PSD. Real RDSs were used in the study, yet the focus was on method development and not on the influence of boundary conditions on the settling behavior of RDS. Ying and Sansalone (2011) were, to our best knowledge, the first authors who adapted settling experiments to study the effect of temperature and concentration of deicing salts on the settling of PM from urban runoff. They concluded—based on a computational fluid dynamics (CFD) model of a hydrodynamic separator—that temperature and deicing salt is negligible to describe the discrete settling of PM.

As these results partly differ from the results of Rommel and Helmreich (2018c) and the investigation was done with the model of a hydrodynamic separator and not a basic sedimentation unit, the settling column experiments proposed by Gelhardt et al. (2017) were adapted to further evaluate the effects of particle density, shape, temperature, and deicing salt (sodium chloride, NaCl) concentration. Based on these results, the model proposed by Rommel and Helmreich (2018c) was further developed to be able to model settling experiments and was consecutively validated.

Hence, RDSs were thoroughly characterized, and the effects of the influencing factors studied in settling column experiments. Furthermore, the nonspherical shape of RDS was evaluated using dynamic image analysis and considered in an additional model. Since the determination of particle sphericity is still difficult

to measure for engineering purposes (Blott and Pye, 2008; Breakey et al., 2018), sphericity was approximated by 2D projections of the particles captured using dynamic image analysis.

There exist recent studies that have determined the drag or settling velocity of irregular particles based on more complex descriptions of particle shapes (Connolly et al., 2020; Wang et al., 2018; Bagheri and Bonadonna, 2016). However, our approach was to simplify the particle description and model so that it is more accessible for the engineering purposes of stormwater treatment. In addition, the standard mineral material, which is in use for the technical approval of SQIDs in Germany (DIBt, 2017; Dierkes et al., 2013), was compared to RDSs.

8.2 Materials and methods

8.2.1 Materials—study site and characterization

Three RDS samples were collected using a vacuum cleaner (DCV 582, Dewalt, Deutschland, Idstein, Germany) at three locations in Frankfurt, Germany, with varying annual average daily traffic (AADT) and land usage, which affects RDS properties (Table 8.1). Solids on the road surface were loosened by means of a paintbrush. In addition to the RDS, the standard mineral material MiW4 (Millisil W4, Quarzwerke, Haltern, Germany) was used for comparison to the RDSs. MiW4 is a milled quartz material, which is in use in the German technical approval procedure of SQIDs to assess PM separation efficiency. It reflects the PSD of road runoff (Gelhardt et al., 2017; DIBt, 2017). Prior to sieving, the samples were dried at 105 °C until constant weight was achieved. Fractions > 2 mm were removed using a stainless steel sieve.

To achieve a comparable PSD of all studied RDS, the samples were sieved using a sieve stack with the mesh sizes 1000, 500, 250, 200, 160, 125, 100, 63, and 40 μm, respectively. Subsequently, the obtained fractions were again dried at 105 °C and merged with the percentages summarized in Table 8.2. The sieving process is described in detail in Gelhardt et al. (2017).

The sieve fractions were characterized by measuring particle density ρ_s and the loss on ignition (LOI). The ρ_s was determined using a gas pycnometer (Quantachrome Microultrapyk 1200 eT, Anton Paar QuantaTec, Boynton Beach, USA) with helium (5.0, Air Liquide, Düsseldorf, Germany, Purity $\geq$ 99.999%), according to DIN 66137-2. To determine the LOI, the dried materials were ignited in a muffle furnace at 550 °C for 2 h (DIN EN 15169). LOI is an indicator to assess the organic fraction of the RDS. The characteristics of the studied materials are summarized in Table 8.1.

Tab. 8.1. Characteristics of sampling site and studied materials (< 250 μm), LOI (loss on ignition), and ρ_s (particle density) were calculated after fractionation and recomposition, as described below.

Sample	Location	Coordinate	Sampling Date	AADT (Vehicles/d)	LOI (%)	ρ_s ($g\,cm^{-3}$)
MiW4 [a]	–	–	–	–	<0.1	2.65
ECL	Eckenheimer Landstraße	50°07'57.2" N 8°41'03.5" E	2017-07-18	8500	7.6	2.60
GBS [b]	Glauburg–straße	50°07'38.6" N 8°41'28.0" E	2017-04-06 [b] 2017-04-12 [b] 2017-04-21 [b]	9600	17.5	2.32
FRS	Frauenstein–straße	50°07'51.1" N 8°40'47.7" E	2017-10-17	150	22.2	2.25

[a] Standard mineral material; [b] The sample GBS was a composite sample of three samples due to low quantity.

Tab. 8.2. Particle size distribution of the road-deposited sediments used within this study.

Size Fraction (μm)	Weight (%)	Cumulative Weight (%)
200–250	4	100
160–200	6	96
125–160	12	90
100–125	8	78
63–100	21	70
40–63	15	49
<40	34	34

Particle size and shape were determined by dynamic image analysis according to ISO 13322-2 (2006) using the system QICPIC+LIXELL+LIQXI (Sympatec, Clausthal-Zellerfeld, Germany). The module M5 was used, with a measuring range between 1.8 and 3755 μm. Prior to the analysis, the samples were dispersed in deionized water using ultrasonic homogenization at 50% amplitude for 60 s (Sonopuls HD 2200.2, Bandelin, Berlin, Germany). Approximately 0.25 g of the sample was applied to 200 mL of deionized water to achieve an optimum concentration of < 2% during the measurement. Settings of the device were 800 U min^{-1} stirring rate, 125 U min^{-1} recirculation rate, 30 Hz frame rate, and 60 s acquisition time. These settings were optimized for the reproducibility of the PSD of MiW4. Data were analyzed using the proprietary software PAQXOS (Sympatec, Clausthal-Zellerfeld, Germany).

Based on suggestions by the manufacturer of the device, particles <5.4 μm were discarded for size analysis and particles <16 μm were discarded for the shape analysis to assure sufficient image resolution. One million particles were analyzed for each sample due to the aforementioned thresholds; particle counts decreased. The following size and shape parameters were determined: the area equivalent circle diameter (d_{eq}); the Riley circularity $\varphi_{Riley} = \sqrt{D_i/D_c}$ (Riley, 1941), where D_i is the diameter of the largest inscribed circle and D_c is the smallest circumscribed circle; the aspect ratio $AR = x_{Fmin}/x_{Fmax}$, where x_{Fmin} is the minimal Feret diameter and x_{Fmax} is the maximal Feret diameter (ISO 9276-6:2008). Values of $\varphi_{Riley} > 1$ were substituted by 1, since the value 1 would be the value of a circle and values >1 were caused by measuring uncertainties. Numerous other definitions of circularity exist; we selected φ_{Riley} because it was suggested by Bagheri et al. (2015) as a predictor for particle sphericity. As the experiments were focused on the settled mass, size and shape distributions were weighted by the mass fractions of the particles. These were determined under the assumptions of constant density for each sample and a spherical particle shape with the diameter d_{eq}.

8.2.2 Settling experiments

The settling experiment utilized in this study is based on the method proposed by Gelhardt et al. (2017), which was adapted from the method, developed by the company UFT (Michelbach and Wöhrle, 1993). A comprehensive description can be found in Gelhardt et al. (2017).

In the experiments, glass columns with a length of 780 mm and an inner diameter of 50 mm were used. The settling height was 760 mm. This method is a floating layer method (Aiguier et al., 1996). Since this study did not intend to determine settling velocity distributions, only the settled fraction after 4 min was evaluated. This fraction exhibits a settling velocity of $\geq$ 11.4 m h^{-1}, which approximately reflects the fraction $\geq$ 63 μm of mineral material with a density of 2.65 g cm^{-3}.

Prior to each experiment, the columns filled with deionized water (DI water) were adjusted to either 21.0 $\pm$ 0.1 or 10.0 $\pm$ 0.1 °C in a climate chamber (Thermo-TEC, Rochlitz, Germany), depending on the experiment. Additional experiments with 20 g L^{-1} NaCl (VWR, p.A., CAS: 7647-14-5; w_{NaCl} = 0.02) were performed to assess the influence of deicing salt at 10 °C. This NaCl concentration can be considered an extreme value for deicing salt concentration in road runoff (Huber et al., 2015b; Hilliges et al., 2017). The names of the experiments used in the remaining text consist of the following information: material, temperature and NaCl concentration (e.g., MiW4, 21 °C, 0 g/L).

Temperature and electrical conductivity (EC) were measured according to standard method 2510 B (American Public Health Association et al., 2017). A suspension containing 0.5 g RDS or MiW4 was applied in the experiments. The suspension was prepared prior to the experiment in 15 mL glass vials by adding 10 mL of the same solution in the columns to the RDS or MiW4. The suspension was homogenized by 1 min of manual shaking. The settling experiments were conducted without delay after the preparation of the suspension. Thus, no alteration of the samples can be expected (Li et al., 2005). The sample of the settled fraction was withdrawn after 4 min. The mass of the settled fraction was determined after the evaporation of the withdrawn sample according to standard method 2540 B (American Public Health Association et al., 2017). Since dissolved NaCl would severely bias the results, the samples of experiments with $w_{NaCl} > 0$ were analyzed using membrane filtration with 0.45 μm membrane filters (cellulose nitrate, Sartorius, Type 113, 47 mm diameter) in accordance with standard method 2540 D (American Public Health Association et al., 2017). Both methods for the determination of the settled fraction, either evaporation or filtration, were in good agreement with each other (cf. Figure S1†). To determine the nonsettled fraction, the water remaining in the column after the experiment was filtered and the total suspended solids (TSS) were determined according to standard method 2510 B (American Public Health Association et al., 2017). The lost particulate mass was calculated by the initial particulate mass subtracted by the sum of the settled and nonsettled particulate mass. In the experiments, 3.3% ± 1.9% of the particulate mass was lost; this was not considered in the determination of the settled mass fractions. Each experiment was conducted in triplicate.

8.2.3 Modeling of settling experiments

The entire model was implemented in Python with the packages Pandas, Matplotlib, SciPy, and Seaborn (Virtanen et al., 2020; The pandas development team, 2020; Hunter, 2007; Waskom et al., 2020). It is accessible in Supplementary Material A.

The PSD of the preprocessed RDSs were modeled using a Weibull cumulative probability density function (Rommel and Helmreich, 2018c; Lee et al., 2014; Selbig and Fienen, 2012), following Equation 8.1

$$W\left(d, \lambda, \kappa\right) = 1 - e^{\left(-\frac{d}{\lambda}\right)^{\kappa}} \tag{8.1}$$

where W(d, λ, κ) = mass fraction less than d (-); d = particle diameter (μm); λ = shape parameter (-); κ = scale parameter (-) (Rommel and Helmreich, 2018c; Lee et al., 2014; Selbig and Fienen, 2012). The determined λ and κ were 85.09 and

1.247 for the used PSD. These parameters were determined by the curve fitting in Matlab R2019a (MathWorks, Natick, USA) using the upper particle diameters of the fractions and nonlinear least squares method with the Trust-Region algorithm (R^2 = 0.998, RMSE = 0.016). The λ and κ are within the range of previously reported values for PSD in urban stormwater or RDS (Rommel and Helmreich, 2018c; Selbig and Fienen, 2012). The PSD was described in the range of 0–250 μm, with 1-μm increments (Figure S2†).

Density (ρ_f), dynamic viscosity (η_f), and kinematic viscosity (ν_f) of the evaluated fluids at varying fluid temperatures (t) and NaCl mass fractions (w_{NaCl}) were determined using the equations established by Laliberté and Cooper (2004) and Laliberté (2007), as described in Rommel and Helmreich (2018c).

The terminal settling velocity (w) was determined by means of different approaches, with further consideration of influencing factors for each particle diameter (d), ρ_s, t, w_{NaCl}, and sphericity (ϕ) for Model C. In addition, d was approximated by the Weibull fit of the PSD since the diameter of isotropic-shaped particles can be approximated by the screen size (Haider and Levenspiel, 1989).

- Model A: Spherical particles
- Model B: Spherical particles with consideration of the withdrawn sample volume
- Model C: Nonspherical particles

The different models are explained in following subsections. All models used the simplification of constant ρ_s (and ϕ for Model C) with respect to particle size. The models used the respective ρ_s and ϕ of the samples used in the experiments. Furthermore, they solely considered discrete settling without the interaction of the particles and no wall effect. Since the PSD was previously defined, a continuous settling velocity distribution was derived for each experiment.

To determine the mass of the settled fraction, the mass fraction at the critical settling velocity (w_{crit}) was calculated by linear interpolation. All settled particles exhibit a settling velocity greater or equal than w_{crit}. The settled mass fraction was determined by the difference of 1 and the mass fraction at w_{crit}.

Model A: Spherical particles

Model A determined w (m s^{-1}) using the explicit formulas (Equations 8.2–8.6) proposed by Cheng (2009) for spherical particles in the subcritical region ($Re < 2 \cdot 10^5$)

$$\Delta = (\rho_s - \rho_f) / \rho_f \tag{8.2}$$

$$d_* = \left(\Delta g/{\nu_f}^2\right)^{1/3} d \tag{8.3}$$

$$C_D = \frac{432}{d_*^3}\left(1 + 0.022 d_*^3\right)^{0.54} + 0.47\left[1 - \exp\left(-0.15 d_*^{0.45}\right)\right] \tag{8.4}$$

$$w_* = \sqrt{4 d_* / 3 C_D} \tag{8.5}$$

$$w = w_* \left(\Delta g \nu_f\right)^{1/3} \tag{8.6}$$

where d_* is the dimensionless grain diameter, g is the gravitational acceleration (m s^{-2}), C_D is the drag coefficient (-), and w_* is the dimensionless settling velocity (Cheng, 2009). Even if Re remains in the low region (< 10), this method avoids the necessity of checking Re during the calculation since it is valid for Re $< 2 \cdot 10^5$.

Model B: Spherical particles with consideration of the withdrawn sample volume

Model B is based on Model A and additionally considers the withdrawn sample volume. Since additional water will be withdrawn with the sediment, not-yet-settled particles will be withdrawn as well. Thus, w_{crit} needs to be reduced with respect to the withdrawn sample volume. This was considered by reducing w_{crit} by the height of the truncated cone (h_{cone}) with the same shape as the utilized glass columns and the volume of the withdrawn sample; h_{cone} of each experiment was determined following Equation 8.7.

$$h_{cone} = 5^{2/3} \sqrt[3]{\frac{12 V_{sample}}{\pi} + 5} - 5 \text{ for } 0 < V_{sample} \leq 162.32 \text{ mL} \tag{8.7}$$

where V_{sample} is the measured withdrawn sample volume of each experiment in mL and h_{cone} is the height of the truncated cone in cm. The determined h_{cone} was used to adjust w_{crit} to simulate the results of the experiments following Equation 8.8

$$w_{crit} = \frac{76 - h_{cone}}{0.417} \tag{8.8}$$

where w_{crit} is the critical settling velocity in m s^{-1}, which is the minimal settling velocity of the particles-withdrawn sample after 4 min, and h_{cone} the height of the truncated cone with the same shape as the utilized glass columns and the volume of the withdrawn sample in mL.

Model C: Nonspherical particles

To consider the influence of a nonspherical particle shape, Model C included the average sphericity of each RDS determined by dynamic image analysis. Since dynamic image analysis only delivers 2D projections of the particles, the sphericity of the particles (ϕ) was approximated by the circularity of the 2D projections of the particles, as proposed by Bagheri et al. (2015). Settling velocity of the nonspherical particles was predicted using the formulas proposed by Haider and Levenspiel (1989) (Equations 8.9–8.11) since it is an explicit and simple solution. Furthermore, it shows an acceptable average error (Chhabra et al., 1999).

$$d_* = d\left[\frac{g\rho_f\left(\rho_s - \rho_f\right)}{{\eta_f}^2}\right]^{1/3} \tag{8.9}$$

$$w_* = \left[\frac{18}{d_*^2} + \frac{2.3348 - 1.7439\phi}{d_*^{0.5}}\right]^{-1} \text{ for } 0.5 \leq \phi \leq 1 \tag{8.10}$$

$$w = w_*\left[\frac{\rho_f^2}{g\eta_f\left(\rho_s - \rho_f\right)}\right]^{-1/3} \tag{8.11}$$

where ϕ was approximated by the circularity of the 2D projections of the particles (Blott and Pye, 2008; Bagheri et al., 2015). Bagheri et al. (2015) suggested the use of φ_{Riley} for particles with a nonvesicular surface. Based on dynamic image analysis, the particles of the analyzed RDSs showed a nonvesicular surface; thus, the mass fraction weighted median of φ_{Riley} was used to approximate ϕ.

8.2.4 Statistics

All statistical methods were implemented using Python with the packages Pandas 1.0.5 (The pandas development team, 2020), Scipy 1.5.0 (Virtanen et al., 2020), Scikit-learn 0.23.1 (Pedregosa et al., 2011), and Statsmodel 0.11.1 (Seabold and Perktold, 2010). Data was visualized using the packages Matplotlib 3.2.2 (Hunter, 2007) and Seaborn 0.11.0 (Waskom et al., 2020). Hypothesis testing was conducted using a two-sided *t*-test with a significance level of 5%. The error of the predicted settled fraction was assessed using the mean absolute error and the maximum residual error.

8.3 Results and discussion

8.3.1 Particle size and shape

By using dynamic image analysis, it was possible to obtain PSDs of the analyzed samples (Figure 8.1a). The mass fraction weighted medians of d_{eq} for ECL, FRS, GBS, and MiW4 were 72, 85, 74, and 73 µm, respectively. A minor difference between MiW4 and the nonartificial RDSs was revealed. In the fraction below approximately 50 µm, MiW4 showed a greater mass fraction of smaller particles compared to all RDSs. For $d_{eq} > 50$ µm, all materials showed good agreement with the Weibull PSD, which is based on the target PSD of the sieving process (c.f. Section 8.2.1) and will be used for the consecutive modeling of settling. Thus, discrepancies between experimental and modeled results for the RDSs can be attributed to the deviation of the present PSDs and the Weibull PSD. As the smallest mesh size was 40 µm, the deviation in the small particle size fraction was anticipated. Consequently, this is one potential source of deviation between predicted and measured settled mass fractions. In order to analyze this fine fraction, future experiments should adopt an addition nylon sieve with a 20-µm mesh size (Kayhanian and Givens, 2011).

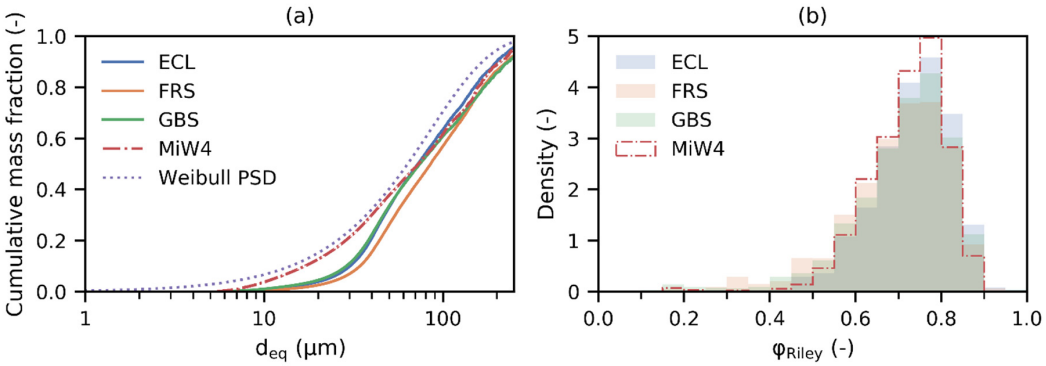

Fig. 8.1. (**a**) Particle size distribution (PSD) of the analyzed samples and the fitted Weibull PSD used for the subsequent modeling, particle count: Eckenheimer Landstraße (ECL) $n = 515{,}545$; Frauensteinstraße (FRS) $n = 593{,}302$; Glauburgstraße (GBS) $n = 540{,}036$; MiW4 $n = 501{,}254$. (**b**) Mass fraction weighted histogram of φ_{Riley} of the analyzed samples, particle count: ECL $n = 130{,}986$; FRS $n = 211{,}209$; GBS $n = 134{,}392$; MiW4 $n = 57{,}973$.

As shown in Figure 8.2, the RDSs exhibit nonspherical shapes. The mass fraction weighted median φ_{Riley} of the analyzed samples were 0.744 for ECL, 0.717 for FRS, 0.732 for GBS, and 0.733 for MiW4, respectively (Figure 8.1b). According to Blott and Pye (2008), the particles of the samples exhibit low to high circularity; thus, a low to high sphericity can be estimated. This finding is supported by the results of Kayhanian et al. (2012b). No distinct differences between the samples were

observed. φ_{Riley} was almost constant with respect to d_{eq}; however, with decreasing particle size, the range of φ_{Riley} was wider (Figure S3†). In addition, MiW4 showed a narrower distribution of φ_{Riley} with respect to d_{eq}.

The RDS particles were moderately to slightly elongated, with a mass fraction weighted median aspect ratio of 0.62–0.63 (Blott and Pye, 2008). This finding is supported by Gunawardana et al. (2014), who reported that RDSs feature particles with an irregular surface and contain a high proportion of elongated particles. Furthermore, the size and shape of the analyzed samples are comparable to tire wear particles (Kreider et al., 2010).

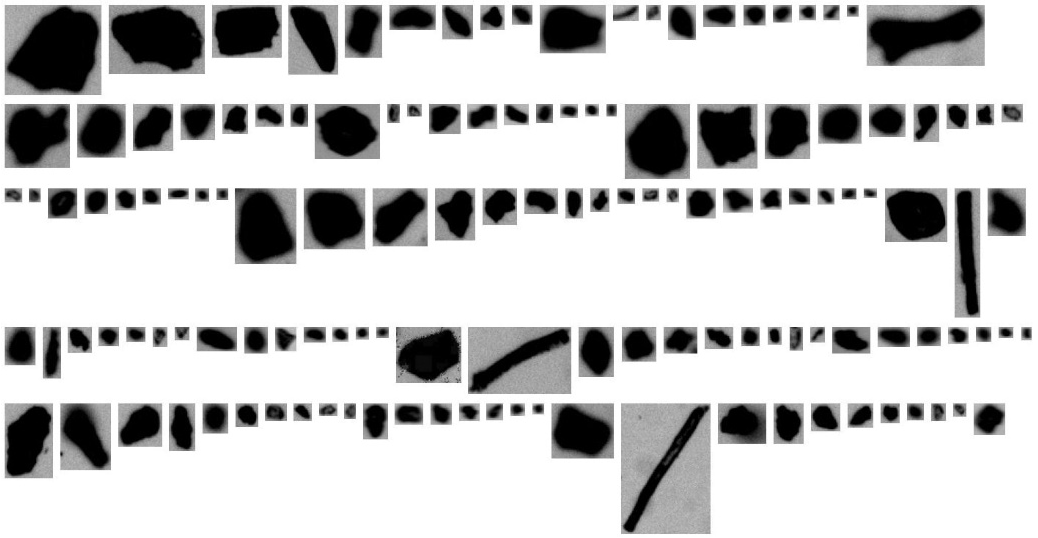

Fig. 8.2. Microscopic images of some road-deposited sediment (RDS) particles of the sample ECL, captured using dynamic image analysis. The particle shape of the other samples was comparable. The images are not scaled.

Based on the observed aspect ratios, the majority of the particles were isometric, with aspect ratios >0.2 (Figure S4†), which is a requirement for the approximation of particle sphericity based on 2D projections because particle orientation can bias the determination of the circularity of highly nonisometric particles (Breakey et al., 2018).

8.3.2 Particle density with respect to particle size

The particle density of the total preprocessed samples is given in Table 8.1. In order to evaluate the particle density with respect to particle size, ρ_s of the individual fractions was determined. No distinct trend of decreasing or increasing ρ_s with particle size was observable (Table 8.3). The density of MiW4 was constant with respect to particle size since it is a milled quartz material. Based on these results,

the simplification of constant ρ_s in the modeling is applicable. However, previous studies have shown that smaller particles feature larger organic fractions, resulting in lower ρ_s (Kayhanian et al., 2012b; Kayhanian et al., 2008a).

Tab. 8.3. Particle density (ρ_s) of the fractionated samples ECL, FRS, and GBS.

Size Fraction (µm)	ρ_s (g cm^{-3})		
	ECL	**FRS**	**GBS**
200–250	2.56	2.25	2.41
160–200	2.54	2.17	2.37
125–160	2.57	2.14	2.31
100–125	2.55	2.18	2.32
63–100	2.61	2.20	2.30
40–63	2.65	2.31	2.31
<40	2.61	2.34	2.32

8.3.3 Settling experiments

Using the proposed method, it was possible to quantify the influence of ρ_s, t, and w_{NaCl}. Within 4 min, 30% to 60% of the particles settled.

As predicted by the calculations of Rommel and Helmreich (2018c), ρ_s showed the greatest impact on the settling at constant PSD (Figure 8.3). Thus, MiW4 showed the biggest settled fraction overall, followed by ECL, GBS, and FRS in the order of their ρ_s. Furthermore, settling decreased with decreasing temperature for all materials. The addition of deicing salt showed a very minor effect of reducing the settled fraction. However, the experiments with deicing salt were associated with higher uncertainty due to the necessary filtration step to quantify the settled fraction. Thus, an increased w_{NaCl} does not significantly ($p > 0.05$) influence settling, even at very high concentrations. This is in accordance with the results of Rommel and Helmreich (2018c) and Ying and Sansalone (2011). However, these experiments were not able to study the potential stratification present in SQIDs. In the experiments conducted at 10 °C, a significantly ($p < 0.05$) lower settled mass fraction was observed in contrast to the experiments at 21 °C, except for GBS. The settled mass fraction was 3% to 7% smaller at 10 °C in comparison to the experiments conducted at 21 °C.

As shown in Figure 8.4, the settled mass fraction increased with ρ_s and t. With increasing LOI, the settled mass fraction decreased. Thus, ρ_s can be considered as a function of LOI. This is in accordance with previous studies (Kayhanian et al.,

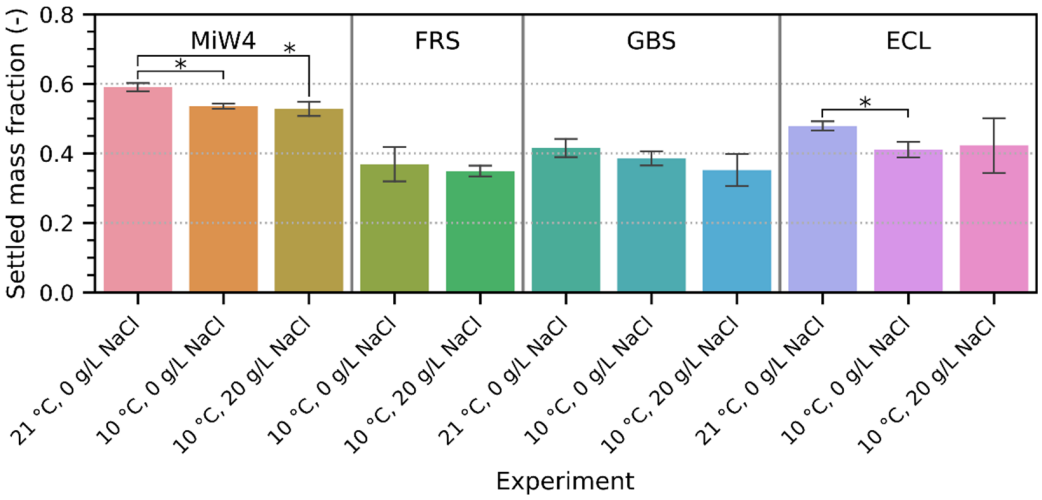

Fig. 8.3. Settled mass fraction in the settling experiments with varying temperatures (21 and 10 °C) and NaCl concentrations (0 and 20 g/L); $n = 3$ for each experiment. The error bars indicate the standard deviation; the asterisks (*) indicate statistically significant differences between two experiments ($p < 0.05$). Experiment FRS 21 °C 0 g/L NaCl was not conducted due to low sample quantity.

2012b; Kayhanian et al., 2008a). The settled mass fraction with respect to w_{NaCl} was not shown in this figure because only 10 °C experiments with $w_{NaCl} > 0$ were conducted; thereby, this figure could be easily misinterpreted.

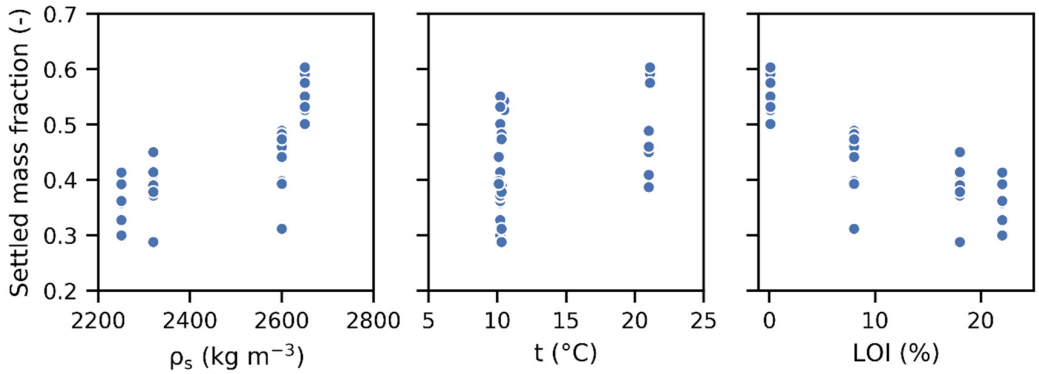

Fig. 8.4. Settled mass fraction in the settling experiments with respect to ρ_s, t, and LOI; $n = 33$.

The utilized settling experiment method is simple to handle, but the results were very user-dependent (Figure S5†); therefore, only the results of one executor should be compared. Nevertheless, the results of each setup and executor were consistent and able to show the effects of ρ_s, t, and w_{NaCl}. In addition, manual sampling can lead to a significant error. If the sampling were to be performed 30 s later, the settled mass fraction would increase by 0.03.

The VICAS protocol can be used to determine the settling velocity distributions of PM (Torres and Bertrand-Krajewski, 2008; Chebbo and Gromaire, 2009); it has been comprehensively studied and increases the comparability of settling velocity distributions. However, the determination of the settling velocity was not the focus of this study. Furthermore, the UFT columns enabled an analysis of particle properties, such as contaminant content, with respect to settling velocity. Another promising method for the determination of settling velocity distributions and fractionation of particles with respect to settling velocity is the elutriation device proposed by Hettler et al. (2011).

8.3.4 Validation of settling model

By means of using the results of the settling experiments, it was possible to validate the settling model for RDS, which is based on the PSD and ρ_s of the RSD, as well as t and w_{NaCl} of the fluid.

All settling models predicted the settled mass fraction with respect to t and w_{NaCl} very well (Figure 8.5 and Figure S6†). Model A was already able to predict the settled fraction, with a mean absolute error of 0.054 and a maximum residual error of 0.143. Thus, this simple model, with input variables PSD, ρ_s, t, and w_{NaCl}, was sufficient to predict the outcome of the settling experiments. Model B considered additionally the withdrawn sample volume, which can extract nonsettled particles. However, it was not able to improve the prediction quality (mean absolute error of 0.059 and a maximum residual error of 0.161). Thus, the withdrawn sample volume seemed to be negligible. However, to meet quality assurance principles, the sample volume should be recorded. With consideration of the average particle shape of each RDS, Model C achieved a slight reduction of the mean absolute error to 0.050. The maximum residual error was 0.123. According to these results, the consideration of the nonsphericity of the particles does not considerably improve the prediction of RDS settling. If MiW4 is not considered, the mean absolute error of Models A and C are reduced to 0.050 and 0.037, respectively. The mean absolute error of Model B is increased to 0.064. The order of the predicted settled mass fractions by the models is Model C < Model A < Model B.

One unanticipated finding was that all models slightly underestimated the settled mass fraction of MiW4, while the settled mass of the nonartificial RDS was overestimated to a minor extent. As dynamic image analysis revealed that the PSDs of all samples, except for MiW4, differ from the Weibull PSD in the fine fraction, the deviation can be partly explained by the PSD. However, within the experiment duration of 4 min, it is mainly particles $d_{eq} > 60$ μm that settle. Another possible explanation can be that even though all samples showed comparable mass fraction

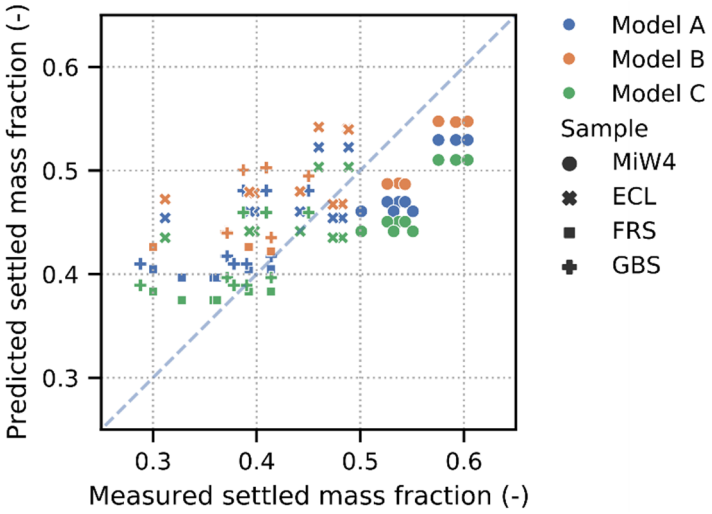

Fig. 8.5. Comparison between measured and predicted settled mass fraction by Models A, B, and C of all samples (MiW4, ECL, FRS, and GBS); $n = 33$.

weighted median φ_{Riley}, MiW4 showed a narrower φ_{Riley} distribution with respect to d_{eq} (Figure 8.1b and Figure S3†). Consequently, MiW4 settles faster due to the smaller fraction of irregular-shaped particles, which exhibit lower settling velocities (Figure S7†). Another source of bias was that the loss of particulate mass was considerably lower in the MiW4 experiments (1.8%) in contrast to the experiments with the real RDSs (3.6%). Thus, the overestimation of the settled fraction of the real RDSs can be partly explained by a mass loss during the experiments. Furthermore, the results are biased by the assumption of constant density with respect to particle size. The settled fractions of samples ECL and FRS, which mainly consisted of particles with d_{eq} >60 µm, showed lower ρ_s than the average ρ_s of the whole sample. Hence, the mass of the settled fraction was overestimated, although this is not valid for GBS. With respect to these uncertainties in the experiments and modeling, the used models showed an acceptable error. Nevertheless, it must be emphasized that the proposed models are designed to evaluate influencing factors in settling column experiments under varying boundary conditions (PSD, ρ_s, t, w_{NaCl}, ϕ). Other approaches to model settling in full-scale SQIDs under dynamic conditions exist (Li et al., 2008; Spelman and Sansalone, 2018; Abrishamchi et al., 2010).

8.4 Conclusions

This study used preprocessed RDSs to reduce the effect of varying PSDs in order to assess effects caused by particle density, particle shape, temperature, and deicing salt concentration of the fluid.

Based on the experimental results, it was possible to validate and further develop the proposed method of Rommel and Helmreich (2018c), which is capable of modeling settling experiments with varying boundary conditions (PSD, ρ_s, t, w_{NaCl}, ϕ). All analyzed RDSs featured comparable particle shapes, independent from their origin. Consideration of the particle shape did not significantly improve the modeling results. Based on these findings, particle shape was negligible to describe the settling of RDS. Future studies are needed to verify this based on more samples of various sites. Furthermore, very fine particles, significantly smaller than 60 μm, need to be studied as they potentially stay in suspensions for a long time and can be elutriated from SQIDs. This is of special importance due to the well-described high contaminant load in the fine particulate fraction.

The main limitation of the utilized settling experiments is that potentially occurring stratification in SQIDs cannot be reproduced. Thus, direct conclusions for SQIDs cannot be drawn. Future studies should assess the effect of stratification caused by temperature and salinity deviations using pilot or full-scale SQIDs and CFD modeling. Furthermore, road runoff underlies varying PM and hydraulic properties of intra- and inter-rain events. As RDS properties are site-specific, further investigations are necessary to predict site-specific PM properties.

Nevertheless, the gained knowledge on RDS properties can be used to evaluate future artificial RDSs for the assessment of SQIDs. In addition, the proposed model was able to deliver further insights into the relative contribution of the fluid and particle properties on the settling of RDS.

Acknowledgments

We thank Matthias Schwibinger of the Institute of Urban Water Management and Hydromechanics, Frankfurt University of Applied Science, and Sebastian Schott of the Chair of Urban Water Systems Engineering, Technical University of Munich, for their assistance in the experiments. This research received no external funding.

9 Research outcome and overall discussion

Stormwater quality improvement devices are one promising example of decentralized stormwater treatment options, especially for space-constrained urban settings, to mitigate the negative impact of traffic on the environment. However, their treatment efficiency underlies various influencing factors, which had not been sufficiently evaluated. In this dissertation four SQIDs were monitored for more than two years (Chapter 3). The suitability of three SQIDs with technical approval by the DIBt was assessed for the first time in full-scale application under comparable conditions. Furthermore, a SQID design using commonly available precast parts was evaluated, which can be a promising alternative to proprietary SQIDs for municipalities. Based on the acquired knowledge during the monitoring, four research hypotheses were derived and investigated through further experimental approaches. In this chapter, the main research results of this dissertation are summarized, previously stated research hypothesis are tested, and the results are discussed overall.

The first part of the thesis addressed the question whether leaching of heavy metals bound to sorptive filter media in SQIDs occurs during dry periods (Chapter 4). To answer this question, which had not been studied before, a new experimental procedure was developed using quiescent batch leaching tests, to replicate *in situ* conditions more closely than previous leaching studies (Degaffe and Turner, 2011; Huber et al., 2016b) and evaluate the effect of different synthetic runoff compositions. In contrast to Huber et al. (2016b), who studied leaching during runoff events, no leaching from sorptive media was observed – even in the presence of de-icing salt or DOM. Consequently, the research hypothesis that leaching occurs during dry periods, if the filter media are permanently submerged, was rejected. The tested filter media are therefore capable of retaining heavy metals during dry periods. The strong leaching observed by Huber et al. (2016b) even at short contact times in the presence of de-icing salts was attributed to the considerably higher prestressing loads close to the capacity limit. Thus, the risk of heavy metal leaching was potentially overestimated. Nevertheless, the same experiments demonstrated that sediments trapped in SQIDs exhibit strong leaching of heavy metals. Hence, the service life of downstream media filter stages can be shortened or effluent quality may deteriorate. These findings suggest that removal of sediment trapped in SQIDs

is crucial for the longevity and overall treatment efficiency. This demonstrates that inspection and maintenance is essential for SQIDs.

The second research topic considered the geochemical fractionation of heavy metals in sorptive media after prestressing at lab scale or in field tests (Chapter 5). Based on the results, it was revealed that the current lab-scale test used to approve SQIDs in Germany leads to significantly larger potentially mobile and especially highly mobile fractions of Cu and Zn. The research hypothesis that the geochemical fractionation of heavy metals retained on (sorptive) filter media of SQIDs is significantly different, if the filter media are prestressed in lab-scale experiments or full-scale operation, was therefore accepted. Furthermore, sequential extraction proved to be a suitable method to evaluate heavy metal mobility in sorptive filter media used in SQIDs. It can be therefore applied to test the influence of synthetic road runoff compositions to improve tests assessing heavy metal retention by sorptive filter media. As a consequence, the discrepancy between lab-scale and field tests can be reduced in future studies. Furthermore, the observed significantly higher heavy metal content in sediments trapped in SQIDs highlighted the major contribution of particulate-bound heavy metals to the contamination of road runoff. These results imply that designs for treatment of road runoff should focus predominantly on particle separation.

The third research topic covered dissolved organic matter in road runoff and effluent of SQIDs, which had not been comprehensively described before (Chapter 6). The results of this study showed that DOM in road runoff and effluent of SQIDs shows a strong seasonality with respect to quantity and quality. In summer, DOM was present in higher concentrations and showed more humic-like properties. Consequently, the first part of the research hypothesis that the occurrence of DOM shows a strong seasonality was accepted. The treatment in SQIDs did not alter DOM quantity and properties. In addition, it was verified that most of the DOM found in road runoff and effluent of SQIDs can be attributed to humic substances. The influence of DOM on heavy metal speciation in road runoff was subsequently evaluated using the geochemical model Visual MINTEQ and principal component analysis. The obtained results indicate that DOM affects the speciation of dissolved heavy metals. In order to verify this and thereby provide direct evidence for the second part of the research hypothesis, further experiments are necessary to quantify the effect of DOM on the speciation of heavy metals and consequently on the treatment efficiency of SQIDs. The findings of this research provide the fundamental basis for further evaluation of the effect of DOM on heavy metal retention in SQIDs.

The last research topic considered the influence of temperature and de-icing salt on sedimentation of RDS (Chapter 7 and 8). The results of modeling and lab-scale

experiments demonstrated that temperature shows an influence on sedimentation, whereas de-icing salt is negligible even at high concentrations. Consequently, the research hypothesis that de-icing salt is the main influencing factor reducing sedimentation of particulate matter in SQIDs under winter conditions was rejected. Based on the results, only low temperatures lead to low treatment efficiency under winter conditions. It is unlikely that variations in particle size and density cause this effect, since Gelhardt (2020) demonstrated that PSD is not affected by season and particle density tends to increase in winter, which would result in better settleability. Furthermore, knowledge was gained on how to characterize RDS sufficiently to estimate settling. In this context, it was shown that particle shapes of RDSs can be neglected for the determination of sedimentation. Based on the obtained knowledge worst case scenarios can be derived to improve future designs of sedimentation stages for SQIDs. In order to ensure the retention of particulate-bound contaminants even under harsh winter conditions, additional treatment stages like filtration are recommended to avoid contamination of sensitive receiving waters such as groundwater.

10 Outlook and future research needs

This dissertation contributes to the current knowledge about stormwater treatment by describing and evaluating currently insufficiently studied factors influencing treatment efficiency of SQIDs and other stormwater treatment methods. Nevertheless, there are still gaps of knowledge, which need to be closed by future studies.

In Chapter 4, the hydraulic retention time in a SQID was estimated using a SWMM model. To gain further insight into the HRT in SQIDs, which influences treatment and leaching processes, future studies should conduct tracer experiments in order to draw certain conclusions. In addition, the experiments could be repeated using filter media prestressed in full-scale application to prove the results of this study.

As a consequence of the discrepancy between the field and lab-scale conditions expressed by the geochemical fractionation of heavy metals in the filter media of SQIDs (Chapter 5), future studies should evaluate the effects of different synthetic runoff compositions on the geochemical fractionation; thereby full-scale conditions can be reproduced more realistically. However, the higher heavy metal contents in retained sediments compared to the filter media highlighted that particle separation needs to be the main treatment objective of SQIDs.

The monitoring of DOM occurrence and properties (Chapter 6) was a necessary step to understand the effect of DOM on heavy metal retention in SQIDs. Though, DOM properties are site-specific (Transportation Research Board, 2014). Additional studies at different sites are therefore necessary to gain knowledge about the variability of DOM in road runoff and effluent of SQIDs. Furthermore, the influence of DOM on heavy metal retention was only indicated by the used methods. Additional studies, should therefore quantify the effect of DOM on heavy metal retention. If these results indicate a considerable influence on the treatment efficiency, surrogates for road runoff DOM should be identified for lab-scale experiments or extraction of road runoff DOM should be applied as suggested by Barrett et al. (2014). Particulate organic matter was also not considered in this study, which can affect heavy metal mobility in SQIDs as indicated in Chapter 5 and previous studies (*e. g.*, Kumar et al. (2013a)).

The last research objective (Chapter 7 and 8) demonstrated that temperature needs to be considered to assess the treatment efficiency of SQIDs. The presence of de-icing salt exhibited a negligible impact. Yet, the conducted lab-scale experiments can not reproduce potentially occurring stratification caused by thermal and salinity differentials. Future studies should therefore study if stratification in SQIDs occurs and quantify its impact on the overall treatment efficiency.

Finally, it must be emphasized that the extensive application of SQIDs can pose a challenge for their operators. To study feasibility of SQID application, comprehensive knowledge about cost, operation and maintenance needs to be gathered. An extensive summary of knowledge gaps also with respect to maintenance can be found in Transportation Research Board and National Academies of Sciences, Engineering, and Medicine, 2004. This background would enable a well-founded assessment and selection of appropriate stromwater control measures.

Bibliography

Abbt-Braun, G., U. Lankes, and F. H. Frimmel (2004). "Structural Characterization of Aquatic Humic Substances – The Need for a Multiple Method Approach". *Aquatic Sciences* 66.2, pp. 151–170. DOI: 10.1007/s00027-004-0711-z.

Abrishamchi, A., A. Massoudieh, and M. Kayhanian (2010). "Probabilistic Modeling of Detention Basins for Highway Stormwater Runoff Pollutant Removal Efficiency". *Urban Water Journal* 7.6, pp. 357–366. DOI: 10.1080/1573062X.2010.528434.

AbwV (2020). *Abwasserverordnung in der Fassung der Bekanntmachung vom 17. Juni 2004 (BGBl. I S. 1108, 2625), die zuletzt durch Artikel 1 der Verordnung vom 16. Juni 2020 (BGBl. I S. 1287) geändert worden ist*.

Acosta, J. A., A. F. Cano, J. M. Arocena, F. Debela, and S. Martínez-Martínez (2009). "Distribution of Metals in Soil Particle Size Fractions and Its Implication to Risk Assessment of Playgrounds in Murcia City (Spain)". *Geoderma* 149.1, pp. 101–109. DOI: 10.1016/j.geoderma.2008.11.034.

Acosta, J. A., B. Jansen, K. Kalbitz, A. Faz, and S. Martínez-Martínez (2011). "Salinity Increases Mobility of Heavy Metals in Soils". *Chemosphere* 85.8, pp. 1318–1324. DOI: 10.1016/j.chemosphere.2011.07.046.

Adamsson, s. and L. Bergdahl (2006). "Simulation of Temperature Influence on Flow Pattern and Residence Time in a Detention Tank". *Hydrology Research* 37.1, pp. 53–68. DOI: 10.2166/nh.2006.0005.

Adusei-Gyamfi, J., B. Ouddane, L. Rietveld, J.-P. Cornard, and J. Criquet (2019). "Natural Organic Matter-Cations Complexation and Its Impact on Water Treatment: A Critical Review". *Water Research* 160, pp. 130–147. DOI: 10.1016/j.watres.2019.05.064.

Ahmed, I. A. M., J. Hamilton–Taylor, M. Bieroza, H. Zhang, and W. Davison (2014). "Improving and Testing Geochemical Speciation Predictions of Metal Ions in Natural Waters". *Water Research* 67, pp. 276–291. DOI: 10.1016/j.watres.2014.09.004.

Aiguier, E., G. Chebbo, J.-L. Bertrand-Krajewski, P. Hedgest, and N. Tyack (1996). "Methods for Determining the Settling Velocity Profiles of Solids in Storm Sewage". *Water Science and Technology*. Solids in Sewers 33.9, pp. 117–125. DOI: 10.1016/0273-1223(96)00377-0.

Akkanen, J., R. D. Vogt, and J. V. K. Kukkonen (2004). "Essential Characteristics of Natural Dissolved Organic Matter Affecting the Sorption of Hydrophobic Organic Contaminants". *Aquatic Sciences* 66.2, pp. 171–177. DOI: 10.1007/s00027-004-0705-x.

Al-Ameri, M., B. Hatt, S. Le Coustumer, et al. (2018). "Accumulation of Heavy Metals in Stormwater Bioretention Media: A Field Study of Temporal and Spatial Variation". *Journal of Hydrology* 567, pp. 721–731. DOI: 10.1016/j.jhydrol.2018.03.027.

Al-Reasi, H. A., C. M. Wood, and D. S. Smith (2011). "Physicochemical and Spectroscopic Properties of Natural Organic Matter (NOM) from Various Sources and Implications for Ameliorative Effects on Metal Toxicity to Aquatic Biota". *Aquatic Toxicology* 103.3, pp. 179–190. DOI: 10.1016/j.aquatox.2011.02.015.

Alloway, B. J. (2013). "Introduction". *Heavy Metals in Soils: Trace Metals and Metalloids in Soils and Their Bioavailability*. Ed. by B. J. Alloway. Dordrecht: Springer Netherlands, pp. 3–9. DOI: 10.1007/978-94-007-4470-7.

Almakki, A., E. Jumas-Bilak, H. Marchandin, and P. Licznar-Fajardo (2019). "Antibiotic Resistance in Urban Runoff". *Science of The Total Environment* 667, pp. 64–76. DOI: 10.1016/j.scitotenv.2019.02.183.

Altman, D. G. and J. M. Bland (1994). "Statistics Notes: Quartiles, Quintiles, Centiles, and Other Quantiles". *BMJ* 309.6960, pp. 996–996. DOI: 10.1136/bmj.309.6960.996.

American Public Health Association, American Water Works Association, and Water Environment Federation, eds. (2017). *Standard Methods for the Examination of Water and Wastewater*. Washington, DC, USA.

Artifon, V., E. Zanardi-Lamardo, and G. Fillmann (2019). "Aquatic Organic Matter: Classification and Interaction with Organic Microcontaminants". *Science of The Total Environment* 649, pp. 1620–1635. DOI: 10.1016/j.scitotenv.2018.08.385.

ASTRA (2013). *Methodik zur Prüfung der Verhältnismässigkeit von Strassenabwasserbehandlungsanlagen*. 88003. Bern, Switzerland: Bundesamt für Strassen ASTRA.

Athanasiadis, K. and B. Helmreich (2005). "Influence of Chemical Conditioning on the Ion Exchange Capacity and on Kinetic of Zinc Uptake by Clinoptilolite". *Water Research* 39.8, pp. 1527–1532. DOI: 10.1016/j.watres.2005.01.024.

Aziz, H. A., N. Othman, M. S. Yusuff, et al. (2001). "Removal of Copper from Water Using Limestone Filtration Technique: Determination of Mechanism of Removal". *Environment International* 26.5–6, pp. 395–399. DOI: 10.1016/S0160-4120(01)00018-6.

Bacon, J. R. and C. M. Davidson (2008). "Is There a Future for Sequential Chemical Extraction?" *Analyst* 133.1, pp. 25–46. DOI: 10.1039/B711896A.

Bagheri, G. H., C. Bonadonna, I. Manzella, and P. Vonlanthen (2015). "On the Characterization of Size and Shape of Irregular Particles". *Powder Technology* 270, pp. 141–153. DOI: 10.1016/j.powtec.2014.10.015.

Bagheri, G. and C. Bonadonna (2016). "On the Drag of Freely Falling Non-Spherical Particles". *Powder Technology* 301, pp. 526–544. DOI: 10.1016/j.powtec.2016.06.015.

Baird, R., A. D. Eaton, E. W. Rice, et al. (2017). *Standard Methods for the Examination of Water and Wastewater*.

Baker-Austin, C., M. S. Wright, R. Stepanauskas, and J. V. McArthur (2006). "Co-Selection of Antibiotic and Metal Resistance". *Trends in Microbiology* 14.4, pp. 176–182. DOI: 10.1016/j.tim.2006.02.006.

Ball, J. E., R. Jenks, and D. Aubourg (1998). “An Assessment of the Availability of Pollutant Constituents on Road Surfaces”. *Science of The Total Environment* 209.2–3, pp. 243–254. DOI: 10.1016/S0048-9697(98)80115-0.

Bannerman, R. T., D. W. Owens, R. B. Dodds, and N. J. Hornewer (1993). “Sources of Pollutants in Wisconsin Stormwater”. *Water Science and Technology* 28.3 - 5, pp. 241–259.

Bardin, J. P., S. Barraud, and B. Chocat (2001). “Uncertainty in Measuring the Event Pollutant Removal Performance of Online Detention Tanks with Permanent Outflow”. *Urban Water* 3.1, pp. 91–106. DOI: 10.1016/S1462-0758(01)00031-0.

Barjenbruch, M., B. Heinzmann, P. Kober, et al. (2016). *Dezentrale Reinigung von Straßenabflüssen - Projekt im Berliner Umweltentlastungsprogramm UEPII/2, Abschlussbericht*.

Barrett, M., L. Katz, and S. Taylor (2014). “Removal of Dissolved Heavy Metals in Highway Runoff”. *Transportation Research Record* 2436.1, pp. 131–138. DOI: 10.3141/2436-13.

Bartlett, A. J., Q. Rochfort, L. R. Brown, and J. Marsalek (2012a). “Causes of Toxicity to Hyalella Azteca in a Stormwater Management Facility Receiving Highway Runoff and Snowmelt. Part I: Polycyclic Aromatic Hydrocarbons and Metals”. *Science of The Total Environment* 414, pp. 227–237. DOI: 10.1016/j.scitotenv.2011.11.041.

Bartlett, A. J., Q. Rochfort, L. R. Brown, and J. Marsalek (2012b). “Causes of Toxicity to Hyalella Azteca in a Stormwater Management Facility Receiving Highway Runoff and Snowmelt. Part II: Salts, Nutrients, and Water Quality”. *Science of The Total Environment* 414, pp. 238–247. DOI: 10.1016/j.scitotenv.2011.11.036.

Bayarsaikhan, U., A. S. Ruhl, and M. Jekel (2016). “Characterization and Quantification of Dissolved Organic Carbon Releases from Suspended and Sedimented Leaf Fragments and of Residual Particulate Organic Matter”. *Science of The Total Environment* 571, pp. 269–274. DOI: 10.1016/j.scitotenv.2016.07.148.

BBodSchV (2020). *Bundes-Bodenschutz- und Altlastenverordnung vom 12. Juli 1999 (BGBl. I S. 1554), die zuletzt durch Artikel 126 der Verordnung vom 19. Juni 2020 (BGBl. I S. 1328) geändert worden ist*.

Bäckström, M. (2002). “Sediment Transport in Grassed Swales during Simulated Runoff Events”. *Water Science and Technology* 45.7, pp. 41–49. DOI: 10.2166/wst.2002.0115.

Bäckström, M., S. Karlsson, and B. Allard (2004a). “Metal Leachability and Anthropogenic Signal in Roadside Soils Estimated from Sequential Extraction and Stable Lead Isotopes”. *Environmental Monitoring and Assessment* 90.1-3, pp. 135–160. DOI: 10.1023/B:EMAS.0000003572.40515.31.

Bäckström, M., S. Karlsson, L. Bäckman, L. Folkeson, and B. Lind (2004b). “Mobilisation of Heavy Metals by Deicing Salts in a Roadside Environment”. *Water Research* 38.3, pp. 720–732. DOI: 10.1016/j.watres.2003.11.006.

Beckett, P. H. T. (1989). “The Use of Extractants in Studies on Trace Metals in Soils, Sewage Sludges, and Sludge-Treated Soils”. *Advances in Soil Science: Volume 9*. Ed. by B. A. Stewart. New York, NY: Springer US, pp. 143–176.

Blecken, G.-T., Y. Zinger, A. Deletić, T. D. Fletcher, and M. Viklander (2009). "Influence of Intermittent Wetting and Drying Conditions on Heavy Metal Removal by Stormwater Biofilters". *Water Research* 43.18, pp. 4590–4598. DOI: 10.1016/j.watres.2009.07.008.

Blecken, G.-T., W. F. H. III, A. M. Al-Rubaei, M. Viklander, and W. G. Lord (2017). "Stormwater Control Measure (SCM) Maintenance Considerations to Ensure Designed Functionality". *Urban Water Journal* 14.3, pp. 278–290. DOI: 10.1080/1573062X.2015.1111913.

Blott, S. J. and K. Pye (2008). "Particle Shape: A Review and New Methods of Characterization and Classification". *Sedimentology* 55.1, pp. 31–63. DOI: 10.1111/j.1365-3091.2007.00892.x.

Blume, H.-P., G. W. Brümmer, H. Fleige, et al. (2016a). "Threats to the Soil Functions". *Scheffer/Schachtschabel Soil Science*. Berlin, Heidelberg: Springer Berlin Heidelberg, pp. 485–559. DOI: 10.1007/978-3-642-30942-7.

Blume, H.-P., G. W. Brümmer, H. Fleige, et al. (2016b). "Chemical Properties and Processes". *Scheffer/Schachtschabel Soil Science*. Berlin, Heidelberg: Springer Berlin Heidelberg, pp. 123–174. DOI: 10.1007/978-3-642-30942-7.

Boller, M. (2004). "Towards Sustainable Urban Stormwater Management". *Water Supply* 4.1, pp. 55–65. DOI: 10.2166/ws.2004.0007.

Bordas, F. and A. Bourg (2001). "Effect of Solid/Liquid Ratio on the Remobilization of Cu, Pb, Cd and Zn from Polluted River Sediment". *Water, Air, and Soil Pollution* 128.3, pp. 391–400. DOI: 10.1023/A:1010319004844.

Bourg, A. C. M. (1988). "Metals in Aquatic and Terrestrial Systems: Sorption, Speciation, and Mobilization". *Chemistry and Biology of Solid Waste: Dredged Material and Mine Tailings*. Ed. by W. Salomons and U. Förstner. Berlin, Heidelberg: Springer, pp. 3–32. DOI: 10.1007/978-3-642-72924-9_1.

Bourg, A. C. M. and J. P. G. Loch (1995). "Mobilization of Heavy Metals as Affected by pH and Redox Conditions". *Biogeodynamics of Pollutants in Soils and Sediments: Risk Assessment of Delayed and Non-Linear Responses*. Ed. by W. Salomons and W. M. Stigliani. Berlin, Heidelberg: Springer Berlin Heidelberg, pp. 87–102. DOI: 10.1007/978-3-642-79418-6âĆD̃.

Breakey, D. E. S., F. Vaezi G., J. H. Masliyah, and R. S. Sanders (2018). "Side-View-Only Determination of Drag Coefficient and Settling Velocity for Non-Spherical Particles". *Powder Technology* 339, pp. 182–191. DOI: 10.1016/j.powtec.2018.07.056.

Brezonik, P. and W. Arnold (2011). *Water Chemistry: An Introduction to the Chemistry of Natural and Engineered Aquatic Systems*. Oxford University Press, USA. 809 pp.

British Water (n.d.). *Code of Practice: Assessment of Manufactured Treatment Devices Designed to Treat Surface Water Runoff*. n.p.: British Water, pp. 1–15.

Brock, O., R. Helmus, K. Kalbitz, and B. Jansen (2020). "Non-Target Screening of Leaf Litter-Derived Dissolved Organic Matter Using Liquid Chromatography Coupled to High-Resolution Mass Spectrometry (LC-QTOF-MS)". *European Journal of Soil Science* 71.3, pp. 420–432. DOI: 10.1111/ejss.12894.

Broich, K., S. Rommel, P. Wasmeier, B. Helmreich, and M. Disse (2018). “Ein Modell mit doppeltem Nutzen: Die Messung von Verkehrsflächenabflüssen am Münchner Mittleren Ring”. *Tag der Hydrologie 2018*. Dresden, Germany.

Burant, A., W. Selbig, E. T. Furlong, and C. P. Higgins (2018). “Trace Organic Contaminants in Urban Runoff: Associations with Urban Land-Use”. *Environmental Pollution* 242, pp. 2068–2077. DOI: 10.1016/j.envpol.2018.06.066.

Burkart, K., I. Nehls, T. Win, and W. Endlicher (2013). “The Carcinogenic Risk and Variability of Particulate-Bound Polycyclic Aromatic Hydrocarbons with Consideration of Meteorological Conditions”. *Air Quality, Atmosphere & Health* 6.1, pp. 27–38. DOI: 10.1007/s11869-011-0135-6.

Camponelli, K. M., S. M. Lev, J. W. Snodgrass, E. R. Landa, and R. E. Casey (2010). “Chemical Fractionation of Cu and Zn in Stormwater, Roadway Dust and Stormwater Pond Sediments”. *Environmental Pollution*. Advances of Air Pollution Science: From Forest Decline to Multiple-Stress Effects on Forest Ecosystem Services 158.6, pp. 2143–2149. DOI: 10.1016/j.envpol.2010.02.024.

Carstea, E. M., J. Bridgeman, A. Baker, and D. M. Reynolds (2016). “Fluorescence Spectroscopy for Wastewater Monitoring: A Review”. *Water Research* 95, pp. 205–219. DOI: 10.1016/j.watres.2016.03.021.

Chappaz, A. and P. J. Curtis (2013). “Integrating Empirically Dissolved Organic Matter Quality for WHAM VI Using the DOM Optical Properties: A Case Study of Cu–Al–DOM Interactions”. *Environmental Science & Technology* 47.4, pp. 2001–2007. DOI: 10.1021/es3022045.

Charbonnet, J. A., Y. Duan, and D. L. Sedlak (2019). “The Use of Manganese Oxide-Coated Sand for the Removal of Trace Metal Ions from Stormwater”. *Environmental Science: Water Research & Technology*. DOI: 10.1039/C9EW00781D.

Charters, F. J., T. A. Cochrane, and A. D. O’Sullivan (2015). “Particle Size Distribution Variance in Untreated Urban Runoff and Its Implication on Treatment Selection”. *Water Research* 85 (Supplement C), pp. 337–345. DOI: 10.1016/j.watres.2015.08.029.

Chebbo, G. and M. C. Gromaire (2009). “VICAS - An Operating Protocol to Measure the Distributions of Suspended Solid Settling Velocities within Urban Drainage Samples”. *Journal of Environmental Engineering* 135.9, pp. 768–775. DOI: 10.1061/(ASCE)0733-9372(2009)135:9(768).

Chen, H., Z.-l. Liao, X.-y. Gu, et al. (2017). “Anthropogenic Influences of Paved Runoff and Sanitary Sewage on the Dissolved Organic Matter Quality of Wet Weather Overflows: An Excitation–Emission Matrix Parallel Factor Analysis Assessment”. *Environmental Science & Technology* 51.3, pp. 1157–1167. DOI: 10.1021/acs.est.6b03727.

Chen, S.-C. and C.-M. Liao (2006). “Health Risk Assessment on Human Exposed to Environmental Polycyclic Aromatic Hydrocarbons Pollution Sources”. *Science of The Total Environment* 366.1, pp. 112–123. DOI: 10.1016/j.scitotenv.2005.08.047.

Chen, W. B., D. S. Smith, and C. Guéguen (2013). "Influence of Water Chemistry and Dissolved Organic Matter (DOM) Molecular Size on Copper and Mercury Binding Determined by Multiresponse Fluorescence Quenching". *Chemosphere* 92.4, pp. 351–359. DOI: 10.1016/j.chemosphere.2012.12.075.

Chen, W., C. Guéguen, D. S. Smith, et al. (2018). "Metal (Pb, Cd, and Zn) Binding to Diverse Organic Matter Samples and Implications for Speciation Modeling". *Environmental Science & Technology* 52.7, pp. 4163–4172. DOI: 10.1021/acs.est.7b05302.

Chen, X., M. Guo, J. Feng, et al. (2019). "Characterization and Risk Assessment of Heavy Metals in Road Dust from a Developing City with Good Air Quality and from Shanghai, China". *Environmental Science and Pollution Research* 26.11, pp. 11387–11398. DOI: 10.1007/s11356-019-04550-2.

Cheng, N.-S. (2009). "Comparison of Formulas for Drag Coefficient and Settling Velocity of Spherical Particles". *Powder Technology* 189.3, pp. 395–398. DOI: 10.1016/j.powtec.2008.07.006.

Chhabra, R. P., L. Agarwal, and N. K. Sinha (1999). "Drag on Non-Spherical Particles: An Evaluation of Available Methods". *Powder Technology* 101.3, pp. 288–295. DOI: 10.1016/S0032-5910(98)00178-8.

Chon, K., K. Chon, and J. Cho (2017). "Characterization of Size Fractionated Dissolved Organic Matter from River Water and Wastewater Effluent Using Preparative High Performance Size Exclusion Chromatography". *Organic Geochemistry* 103, pp. 105–112. DOI: 10.1016/j.orggeochem.2016.11.003.

Clark, S and R Pitt (1999). *Stormwater Treatment at Critical Areas: Evaluation of Filtration Media for Stormwater Treatment*. US Environmental Protection Agency: Cincinnati, Ohio.

Coble, P. G. (1996). "Characterization of Marine and Terrestrial DOM in Seawater Using Excitation-Emission Matrix Spectroscopy". *Marine Chemistry* 51.4, pp. 325–346. DOI: 10.1016/0304-4203(95)00062-3.

Coble, P. G., R. G. M. Spencer, A. Baker, and D. M. Reynolds (2014). "Aquatic Organic Matter Fluorescence". *Aquatic Organic Matter Fluorescence*. Ed. by P. G. Coble, J. Lead, A. Baker, D. M. Reynolds, and R. G. M. Spencer. Cambridge Environmental Chemistry Series. Cambridge: Cambridge University Press, pp. 75–122. DOI: 10.1017/CBO9781139045452.006.

Colella, C. (1996). "Ion Exchange Equilibria in Zeolite Minerals". *Mineralium Deposita* 31.6, pp. 554–562. DOI: 10.1007/BF00196136.

Connolly, B. J., E. Loth, and C. F. Smith (2020). "Shape and Drag of Irregular Angular Particles and Test Dust". *Powder Technology* 363, pp. 275–285. DOI: 10.1016/j.powtec.2019.12.045.

Corridoni, T., R. Mancinelli, M. A. Ricci, and F. Bruni (2011). "Viscosity of Aqueous Solutions and Local Microscopic Structure". *The Journal of Physical Chemistry B* 115.48, pp. 14008–14013. DOI: 10.1021/jp202755u.

Councell, T. B., K. U. Duckenfield, E. R. Landa, and E. Callender (2004). "Tire-Wear Particles as a Source of Zinc to the Environment". *Environmental Science & Technology* 38.15, pp. 4206–4214. DOI: 10.1021/es034631f.

Crabtree, B., P. Dempsey, F. Moy, C. Brown, and M. Song (2008). *Improved Determination of Pollutants in Highway Runoff Phase 2: Final Report*. WRc, pp. 1–102.

Criscenti, L. J. and D. A. Sverjensky (1999). "The Role of Electrolyte Anions (ClO4- , NO3- , and Cl-) in Divalent Metal (M2+) Adsorption on Oxide and Hydroxide Surfaces in Salt Solutions". *American Journal of Science* 299.10, pp. 828–899. DOI: 10.2475/ajs.299.10.828.

Croué, J.-P., M. F. Benedetti, D. Violleau, and J. A. Leenheer (2003). "Characterization and Copper Binding of Humic and Nonhumic Organic Matter Isolated from the South Platte River: Evidence for the Presence of Nitrogenous Binding Site". *Environmental Science & Technology* 37.2, pp. 328–336. DOI: 10.1021/es020676p.

D'Amore, J. J., S. R. Al-Abed, K. G. Scheckel, and J. A. Ryan (2005). "Methods for Speciation of Metals in Soils". *Journal of Environment Quality* 34.5 (5), pp. 1707–1745. DOI: 10.2134/jeq2004.0014.

Datry, T, F Malard, L Vitry, F Hervant, and J Gibert (2003). "Solute Dynamics in the Bed Sediments of a Stormwater Infiltration Basin". *Journal of Hydrology* 273.1, pp. 217–233. DOI: 10.1016/S0022-1694(02)00388-8.

Davidson, C. M., A. L. Duncan, D. Littlejohn, A. M. Ure, and L. M. Garden (1998). "A Critical Evaluation of the Three-Stage BCR Sequential Extraction Procedure to Assess the Potential Mobility and Toxicity of Heavy Metals in Industrially-Contaminated Land". *Analytica Chimica Acta* 363.1, pp. 45–55. DOI: 10.1016/S0003-2670(98)00057-9.

Degaffe, F. S. and A. Turner (2011). "Leaching of Zinc from Tire Wear Particles under Simulated Estuarine Conditions". *Chemosphere* 85.5, pp. 738–743. DOI: 10.1016/j.chemosphere.2011.06.047.

Derrien, M., K.-H. Shin, and J. Hur (2019). "Biodegradation-Induced Signatures in Sediment Pore Water Dissolved Organic Matter: Implications from Artificial Sediments Composed of Two Contrasting Sources". *Science of The Total Environment* 694, p. 133714. DOI: 10.1016/j.scitotenv.2019.133714.

DIBt (2017). *Teil 1: Anlagen zur dezentralen Behandlung des Abwassers von Kfz-Verkehrsflächen zur anschließenden Versickerung in Boden und Grundwasser*. Berlin, Germany: Deutsches Institut für Bautechnik, pp. 1–26.

DIBt (2020). *Verzeichnis der allgemeinen bauaufsichtlichen Zulassungen, Zulassungsbereich: Bauprodukte und Bauarten zur Behandlung und Versickerung mineralölhaltiger Niederschlagsabflüsse*.

Dierkes, C., T. Lucke, and B. Helmreich (2015). "General Technical Approvals for Decentralised Sustainable Urban Drainage Systems (SUDS)—The Current Situation in Germany". *Sustainability* 7.3, pp. 3031–3051. DOI: 10.3390/su7033031.

Dierkes, C., A. Welker, and M. Dierschke (2013). “Development of Testing Procedures for the Certification of Decentralized Stormwater Treatment Facilities – Results of Laboratory Tests”. Novatech. Lyon, France, pp. 1–10.

Dierschke, M. and A. Welker (2015). “Bestimmung von Feststoffen in Niederschlagsabflüssen”. *gwf Wasser/Abwasser* 156.4, pp. 440–446.

Dijkstra, J. J., J. C. L. Meeussen, and R. N. J. Comans (2004). “Leaching of Heavy Metals from Contaminated Soils: An Experimental and Modeling Study”. *Environmental Science & Technology* 38.16, pp. 4390–4395. DOI: 10.1021/es049885v.

Duffus, J. H. (2002). “"Heavy Metals" a Meaningless Term?” *Pure and Applied Chemistry* 74.5, pp. 793–807. DOI: 10.1351/pac200274050793.

Duzgoren-Aydin, N. S., C. S. C. Wong, Z. G. Song, et al. (2006). “Fate of Heavy Metal Contaminants in Road Dusts and Gully Sediments in Guangzhou, SE China: A Chemical and Mineralogical Assessment”. *Human and Ecological Risk Assessment: An International Journal* 12.2, pp. 374–389. DOI: 10.1080/10807030500538005.

DWA-A 102-1/BWK-A 3-1 (2020). *DWA-A 102-1/BWK-A 3-1: Grundsätze zur Bewirtschaftung und Behandlung von Regenwetterabflüssen zur Einleitung in Oberflächengewässer – Teil 1: Allgemeines*. Hennef, Germany: Deutsche Vereinigung für Wasserwirtschaft, Abwasser und Abfall; Bund der Ingenieure für Wasserwirtschaft, Abfallwirtschaft und Kulturbau.

DWA-A 102-2/BWK-A 3-2 (2020). *DWA-A 102-2/BWK-A 3-2: Grundsätze zur Bewirtschaftung und Behandlung von Regenwetterabflüssen zur Einleitung in Oberflächengewässer – Teil 2: Emissionsbezogene Bewer- tungen und Regelungen*. Hennef, Germany: Deutsche Vereinigung für Wasserwirtschaft, Abwasser und Abfall; Bund der Ingenieure für Wasserwirtschaft, Abfallwirtschaft und Kulturbau.

DWA-A 102 (Entwurf) (2016). *DWA-A 102 (Entwurf): Grundsätze zur Bewirtschaftung und Behandlung von Regenwetterabflüssen zur Einleitung in Oberflächengewässer*. Hennef, Germany: Deutsche Vereinigung für Wasserwirtschaft, Abwasser und Abfall.

DWA-A 138-1 (Entwurf) (2020). *DWA-A 138-1: Anlagen zur Versickerung von Niederschlagswasser - Teil 1: Planung, Bau, Betrieb*. Hennef, Germany: Deutsche Vereinigung für Wasserwirtschaft, Abwasser und Abfall.

DWA-M 153 (2007). *DWA-M 153: Handlungsempfehlungen zum Umgang mit Regenwasser*. Hennef, Germany: Deutsche Vereinigung für Wasserwirtschaft, Abwasser und Abfall.

Eriksson, E., A. Baun, L. Scholes, et al. (2007). “Selected Stormwater Priority Pollutants — a European Perspective”. *Science of The Total Environment* 383.1–3, pp. 41–51. DOI: 10.1016/j.scitotenv.2007.05.028.

Essel, R., L. Engel, M. Carus, and R. H. Ahrens (2015). *Quellen für Mikroplastik mit Relevanz für den Meeresschutz in Deutschland*.

Ettinger, F., D. Grotehusmann, B. Helmreich, and U. Kasting (2018). “Auswirkungen der Grundwasserverordnung auf die Überarbeitung der Regelwerke des DWA-Hauptausschusses Entwässerungssysteme”. *Korrespondenz Abwasser, Abfall* 65.5, pp. 378–379.

Fairbairn, D. J., S. M. Elliott, R. L. Kiesling, et al. (2018). "Contaminants of Emerging Concern in Urban Stormwater: Spatiotemporal Patterns and Removal by Iron-Enhanced Sand Filters (IESFs)". *Water Research* 145, pp. 332–345. DOI: 10.1016/j.watres.2018.08.020.

Faltermaier, S., S. Krause, and F. W. Günther (2017). "Einfluss von Streusalz auf die Flockung partikulärer Stoffe in Regenbecken an Autobahnen". Aqua Urbanica 2017. Ed. by D. Muschalla and G. Gruber. Vol. 75. Schriftenreihe zur Wasserwirtschaft. TU Graz, Institut für Siedlungswasserwirtschaft und Landschaftswasserbau.

Faram, M. G., K. O. Iwugo, and R. Y. G. Andoh (2007). "Characteristics of Urban Runoff Derived Sediments Captured by Proprietary Flow-through Stormwater Interceptors". *Water Science and Technology* 56.12, pp. 21–27. DOI: 10.2166/wst.2007.747.

Fatoorehchi, E., S. West, G. Abbt-Braun, and H. Horn (2018). "The Molecular Weight Distribution of Dissolved Organic Carbon after Application off Different Sludge Disintegration Techniques". *Separation and Purification Technology* 194, pp. 338–345. DOI: 10.1016/j.seppur.2017.11.047.

Fay, L. and X. Shi (2012). "Environmental Impacts of Chemicals for Snow and Ice Control: State of the Knowledge". *Water, Air, & Soil Pollution* 223.5, pp. 2751–2770. DOI: 10.1007/s11270-011-1064-6.

Fellman, J. B., E. Hood, and R. G. M. Spencer (2010). "Fluorescence Spectroscopy Opens New Windows into Dissolved Organic Matter Dynamics in Freshwater Ecosystems: A Review". *Limnology and Oceanography* 55.6, pp. 2452–2462. DOI: 10.4319/lo.2010.55.6.2452.

Ferreira, M. and M. K. Stenstrom (2013). "The Importance of Particle Characterization in Stormwater Runoff". *Water Environment Research* 85.9, pp. 833–842. DOI: 10.2175/106143013X13736496909103.

Field, R., E. J. Struzeski, H. E. Masters, and A. N. Tafuri (1973). *Water Pollution and Associated Effects from Street Salting*. National environmental research center, Environmental protection agency.

Fletcher, T. D., W. Shuster, W. F. Hunt, et al. (2015). "SUDS, LID, BMPs, WSUD and More – The Evolution and Application of Terminology Surrounding Urban Drainage". *Urban Water Journal* 12.7, pp. 525–542. DOI: 10.1080/1573062X.2014.916314.

Folkeson, L., T. Bækken, M. Brenčič, et al. (2009). "Sources and Fate of Water Contaminants in Roads". *Water in Road Structures: Movement, Drainage and Effects*. Ed. by A. Dawson. Dordrecht: Springer Netherlands, pp. 107–146.

Frimmel, F. H. and G. Abbt-Braun (2011). "Sum Parameters: Potential and Limitations". *Treatise on Water Science*. Ed. by P. Wilderer. Oxford: Elsevier, pp. 3–29. DOI: 10.1016/B978-0-444-53199-5.00048-8.

Frimmel, F. H. and G. Abbt-Braun (2009). "Dissolved Organic Matter (DOM) in Natural Environments". *Biophysico-Chemical Processes Involving Natural Nonliving Organic Matter in Environmental Systems*. John Wiley & Sons, Ltd, pp. 367–406. DOI: 10.1002/9780470494950.ch10.

Fu, F. and Q. Wang (2011). “Removal of Heavy Metal Ions from Wastewaters: A Review”. *Journal of Environmental Management* 92.3, pp. 407–418. DOI: 10.1016/j.jenvman.2010.11.011.

Gabor, R. S., A. Baker, D. M. McKnight, and M. P. Miller (2014). “Fluorescence Indices and Their Interpretation”. *Aquatic Organic Matter Fluorescence*. Ed. by P. G. Coble, J. Lead, A. Baker, D. M. Reynolds, and R. G. M. Spencer. Cambridge Environmental Chemistry Series. Cambridge: Cambridge University Press, pp. 303–338. DOI: 10.1017/CBO9781139045452.015.

Gasperi, J., C. Sebastian, V. Ruban, et al. (2014). “Micropollutants in Urban Stormwater: Occurrence, Concentrations, and Atmospheric Contributions for a Wide Range of Contaminants in Three French Catchments”. *Environmental Science and Pollution Research* 21.8, pp. 5267–5281. DOI: 10.1007/s11356-013-2396-0.

Gautam, R. K., S. K. Sharma, S. Mahiya, and M. C. Chattopadhyaya (2014). “Contamination of Heavy Metals in Aquatic Media: Transport, Toxicity and Technologies for Remediation”. *Heavy Metals In Water*, pp. 1–24. DOI: 10.1039/9781782620174-00001.

Gelhardt, L., M. Huber, and A. Welker (2017). “Development of a Laboratory Method for the Comparison of Settling Processes of Road-Deposited Sediments with Artificial Test Material”. *Water, Air, & Soil Pollution* 228.12, p. 467. DOI: 10.1007/s11270-017-3650-8.

Gelhardt, L. (2020). “Charakterisierung von Feststoffen auf urbanen Verkehrsflächen als potenzielle Schadstoffträger im Niederschlagsabfluss”. doctoralthesis. Technische Universität Kaiserslautern, pp. XI, 321.

Genç-Fuhrman, H., P. S. Mikkelsen, and A. Ledin (2007). “Simultaneous Removal of As, Cd, Cr, Cu, Ni and Zn from Stormwater: Experimental Comparison of 11 Different Sorbents”. *Water Research* 41.3, pp. 591–602. DOI: 10.1016/j.watres.2006.10.024.

Genç-Fuhrman, H., P. S. Mikkelsen, and A. Ledin (2016). “Simultaneous Removal of As, Cd, Cr, Cu, Ni and Zn from Stormwater Using High-Efficiency Industrial Sorbents: Effect of pH, Contact Time and Humic Acid”. *Science of The Total Environment* 566-567, pp. 76–85. DOI: 10.1016/j.scitotenv.2016.04.210.

Giacomino, A., O. Abollino, M. Malandrino, and E. Mentasti (2011). “The Role of Chemometrics in Single and Sequential Extraction Assays: A Review. Part II. Cluster Analysis, Multiple Linear Regression, Mixture Resolution, Experimental Design and Other Techniques”. *Analytica Chimica Acta* 688.2, pp. 122–139. DOI: 10.1016/j.aca.2010.12.028.

Gonçalves-Araujo, R., M. A. Granskog, A. Bracher, et al. (2016). “Using Fluorescent Dissolved Organic Matter to Trace and Distinguish the Origin of Arctic Surface Waters”. *Scientific Reports* 6.1 (1), pp. 1–12. DOI: 10.1038/srep33978.

Goonetilleke, A. and J.-L. Lampard (2019). “Chapter 3 - Stormwater Quality, Pollutant Sources, Processes, and Treatment Options”. *Approaches to Water Sensitive Urban Design*. Ed. by A. K. Sharma, T. Gardner, and D. Begbie. Woodhead Publishing, pp. 49–74. DOI: 10.1016/B978-0-12-812843-5.00003-4.

Goonetilleke, A., B. Wijesiri, and E. R. Bandala (2017). “Water and Soil Pollution Implications of Road Traffic”. *Environmental Impacts of Road Vehicles*, pp. 86–106. DOI: 10.1039/9781788010221-00086.

Graber, E. R. and Y. Rudich (2006). "Atmospheric HULIS: How Humic-like Are They? A Comprehensive and Critical Review". *Atmospheric Chemistry and Physics* 6.3, pp. 729–753.

Granato, G. and P. Cazenas (2009). *Highway-Runoff Database (HRDB Version 1.0)—A Data Warehouse and Preprocessor for the Stochastic Empirical Loading and Dilution Model*.

Grimm, N. B., S. H. Faeth, N. E. Golubiewski, et al. (2008). "Global Change and the Ecology of Cities". *Science* 319.5864, pp. 756–760. DOI: 10.1126/science.1150195.

Gromaire-Mertz, M. C., S. Garnaud, G. Gonzalez, and G. Chebbo (1999). "Characterisation of Urban Runoff Pollution in Paris". *Water Science and Technology* 39.2, pp. 1–8.

Grotehusmann, D., B. Lambert, S. Fuchs, and J. Graf (2014). *Schlussbericht zum BASt Forschungsvorhaben FE-Nr. 05.152/2008/GRB „Konzentrationen und Frachten organischer Schadstoffe im Straßenabfluss"*. Bundesanstalt für Straßenwesen, Bergisch Gladbach: Ingenieurgesellschaft für Stadthydrologie mbH, Hannover, pp. 1–89.

GrwV (2017). *Grundwasserverordnung vom 9. November 2010 (BGBl. I S. 1513), die zuletzt durch Artikel 1 der Verordnung vom 4. Mai 2017 (BGBl. I S. 1044) geändert worden ist*.

Gunawardana, C., P. Egodawatta, and A. Goonetilleke (2014). "Role of Particle Size and Composition in Metal Adsorption by Solids Deposited on Urban Road Surfaces". *Environmental Pollution* 184, pp. 44–53. DOI: 10.1016/j.envpol.2013.08.010.

Gunawardana, C., P. Egodawatta, and A. Goonetilleke (2015). "Adsorption and Mobility of Metals in Build-up on Road Surfaces". *Chemosphere* 119, pp. 1391–1398. DOI: 10.1016/j.chemosphere.2014.02.048.

Gunawardana, C., A. Goonetilleke, P. Egodawatta, L. Dawes, and S. Kokot (2012). "Source Characterisation of Road Dust Based on Chemical and Mineralogical Composition". *Chemosphere* 87.2, pp. 163–170. DOI: 10.1016/j.chemosphere.2011.12.012.

Gunawardena, J. M. A., A. Liu, P. Egodawatta, G. A. Ayoko, and A. Goonetilleke (2018). "Influence of Traffic and Land Use on Pollutant Transport Pathways". *Influence of Traffic and Land Use on Urban Stormwater Quality: Implications for Urban Stormwater Treatment Design*. Singapore: Springer Singapore, pp. 27–54.

Guo, Q. (2017). *Stormwater Manufactured Treatment Devices: Certification Guidelines*.

Gustafsson, J. P. (2014a). *Visual MINTEQ 3.1 User Guide*. Stockholm, Sweden: KTH, Department of Land and Water Recources.

Gustafsson, J. P. (2014b). "Visual MINTEQ 3.1 User Guide". *KTH, Department of Land and Water Recources, Stockholm, Sweden*.

Haider, A. and O. Levenspiel (1989). "Drag Coefficient and Terminal Velocity of Spherical and Nonspherical Particles". *Powder Technology* 58.1, pp. 63–70. DOI: 10.1016/0032-5910(89)80008-7.

Haile, T. M. and M. Fürhacker (2017). "Filtermaterialprüfung: Anwendung der ÖNORM B 2506 Teil 3 für das hochrangige Straßennetz". *Österreichische Wasser- und Abfallwirtschaft* 69.11, pp. 495–502. DOI: 10.1007/s00506-017-0427-7.

Hamilton, R. S., D. M. Revitt, and R. S. Warren (1984). "Levels and Physico-Chemical Associations of Cd, Cu, Pb and Zn in Road Sediments". *Science of The Total Environment*. Highway Pollution 33.1, pp. 59–74. DOI: 10.1016/0048-9697(84)90381-4.

Han, Y., S.-L. Lau, M. Kayhanian, and M. K. Stenstrom (2006). "Characteristics of Highway Stormwater Runoff". *Water Environment Research* 78.12, pp. 2377–2388. DOI: 10.2175/106143006X95447.

Hansen, A. M., T. E. C. Kraus, B. A. Pellerin, et al. (2016). "Optical Properties of Dissolved Organic Matter (DOM): Effects of Biological and Photolytic Degradation". *Limnology and Oceanography* 61.3, pp. 1015–1032. DOI: 10.1002/lno.10270.

Hass, A. and P. Fine (2010). "Sequential Selective Extraction Procedures for the Study of Heavy Metals in Soils, Sediments, and Waste Materials—a Critical Review". *Critical Reviews in Environmental Science and Technology* 40.5, pp. 365–399. DOI: 10.1080/10643380802377992.

Hatt, B., T. Fletcher, and A. Deletic (2007). "Hydraulic and Pollutant Removal Performance of Stormwater Filters under Variable Wetting and Drying Regimes". *Water Science and Technology* 56.12, pp. 11–19. DOI: 10.2166/wst.2007.751.

Hatt, B. E., T. D. Fletcher, and A. Deletic (2008). "Hydraulic and Pollutant Removal Performance of Fine Media Stormwater Filtration Systems". *Environmental Science & Technology* 42.7, pp. 2535–2541. DOI: 10.1021/es071264p.

Haynes, R. J. (2015). "Use of Industrial Wastes as Media in Constructed Wetlands and Filter Beds—Prospects for Removal of Phosphate and Metals from Wastewater Streams". *Critical Reviews in Environmental Science and Technology* 45.10, pp. 1041–1103. DOI: 10.1080/10643389.2014.924183.

He, W., M. Chen, J.-E. Park, and J. Hur (2016a). "Molecular Diversity of Riverine Alkaline-Extractable Sediment Organic Matter and Its Linkages with Spectral Indicators and Molecular Size Distributions". *Water Research* 100, pp. 222–231. DOI: 10.1016/j.watres.2016.05.023.

He, W., J.-H. Lee, and J. Hur (2016b). "Anthropogenic Signature of Sediment Organic Matter Probed by UV–Visible and Fluorescence Spectroscopy and the Association with Heavy Metal Enrichment". *Chemosphere* 150, pp. 184–193. DOI: 10.1016/j.chemosphere.2016.01.116.

Hellauer, K., S. Martínez Mayerlen, J. E. Drewes, and U. Hübner (2019). "Biotransformation of Trace Organic Chemicals in the Presence of Highly Refractory Dissolved Organic Carbon". *Chemosphere* 215, pp. 33–39. DOI: 10.1016/j.chemosphere.2018.09.166.

Helmreich, B., R. Hilliges, A. Schriewer, and H. Horn (2010). "Runoff Pollutants of a Highly Trafficked Urban Road – Correlation Analysis and Seasonal Influences". *Chemosphere* 80.9, pp. 991–997. DOI: 10.1016/j.chemosphere.2010.05.037.

Helmreich, B. and S. H. Rommel (2019). "Dezentrale Behandlung von Straßenabflüssen im urbanen Raum – wohin geht die Reise?" *Kolloquium kommunales Verkehrswesen*. Kassel, Germany.

Helmreich, B., V. Ebert, and S. H. Rommel (2019). “Performance of Vegetated Infiltration Swales for Treatment of Zinc Roof Runoff”. *Novatech 2019*. Lyon, France.

Helmreich, B. and S. Rommel (2020). “Dezentrale Behandlung von Straßenabflüssen im urbanen Raum – wohin geht die Reise?” *Straßenverkehrstechnik* 03/2020, pp. 154–158.

Hendi, E., A. Y. Shamseldin, B. W. Melville, and S. E. Norris (2018). “Experimental Investigation of the Effect of Temperature Differentials on Hydraulic Performance and Flow Pattern of a Sediment Retention Pond”. *Water Science and Technology*. DOI: 10.2166/wst.2018.286.

Her, N., G. Amy, D. McKnight, J. Sohn, and Y. Yoon (2003). “Characterization of DOM as a Function of MW by Fluorescence EEM and HPLC-SEC Using UVA, DOC, and Fluorescence Detection”. *Water Research* 37.17, pp. 4295–4303. DOI: 10.1016/S0043-1354(03)00317-8.

Hettler, E. N., J. S. Gulliver, and M. Kayhanian (2011). “An Elutriation Device to Measure Particle Settling Velocity in Urban Runoff”. *Science of The Total Environment* 409.24, pp. 5444–5453. DOI: 10.1016/j.scitotenv.2011.08.045.

Hilliges, R., M. Endres, A. Tiffert, E. Brenner, and T. Marks (2017). “Characterization of Road Runoff with Regard to Seasonal Variations, Particle Size Distribution and the Correlation of Fine Particles and Pollutants”. *Water Science and Technology* 75.5, pp. 1169–1176. DOI: 10.2166/wst.2016.576.

Hoban, A. (2019). “Chapter 2 - Water Sensitive Urban Design Approaches and Their Description”. *Approaches to Water Sensitive Urban Design*. Ed. by A. K. Sharma, T. Gardner, and D. Begbie. Woodhead Publishing, pp. 25–47. DOI: 10.1016/B978-0-12-812843-5.00002-2.

Hoffmann, S. R., M. M. Shafer, and D. E. Armstrong (2007). “Strong Colloidal and Dissolved Organic Ligands Binding Copper and Zinc in Rivers”. *Environmental Science & Technology* 41.20, pp. 6996–7002. DOI: 10.1021/es070958v.

Hong, N., Y. Guan, B. Yang, et al. (2020). “Quantitative Source Tracking of Heavy Metals Contained in Urban Road Deposited Sediments”. *Journal of Hazardous Materials* 393, p. 122362. DOI: 10.1016/j.jhazmat.2020.122362.

Hong, N., P. Zhu, and A. Liu (2017). “Modelling Heavy Metals Build-up on Urban Road Surfaces for Effective Stormwater Reuse Strategy Implementation”. *Environmental Pollution* 231, pp. 821–828. DOI: 10.1016/j.envpol.2017.08.056.

Horstmeyer, N., M. Huber, J. E. Drewes, and B. Helmreich (2016). “Evaluation of Site-Specific Factors Influencing Heavy Metal Contents in the Topsoil of Vegetated Infiltration Swales”. *Science of The Total Environment* 560–561, pp. 19–28. DOI: 10.1016/j.scitotenv.2016.04.051.

Hou, S., N. Zheng, L. Tang, et al. (2019). “Pollution Characteristics, Sources, and Health Risk Assessment of Human Exposure to Cu, Zn, Cd and Pb Pollution in Urban Street Dust across China between 2009 and 2018”. *Environment International* 128, pp. 430–437. DOI: 10.1016/j.envint.2019.04.046.

Huber, M., B. Helmreich, and A. Welker (2015a). *Einführung in die dezentrale Niederschlagswasserbehandlung für Verkehrsflächen-und Metalldachabflüsse: Schacht-/Kompaktsysteme, Rinnensysteme, Straßeneinläufe und Flächenbeläge*. Vol. 213. Berichte aus der Siedlungswasserwirtschaft. Technische Universität München Garching. 96 pp.

Huber, M., A. Welker, J. E. Drewes, and B. Helmreich (2015b). "Auftausalze im Straßenwinterdienst - Aufkommen und Bedeutung für dezentrale Behandlungsanlagen von Verkehrsflächenabflüssen zur Versickerung". *gwf Wasser/Abwasser* 156, pp. 1138–1152.

Huber, M., S. Badenberg, M. Wulff, J. Drewes, and B. Helmreich (2016a). "Evaluation of Factors Influencing Lab-Scale Studies to Determine Heavy Metal Removal by Six Sorbents for Stormwater Treatment". *Water* 8.2, p. 62.

Huber, M. and B. Helmreich (2016). "Stormwater Management: Calculation of Traffic Area Runoff Loads and Traffic Related Emissions". *Water* 8.7, p. 294.

Huber, M., H. Hilbig, S. C. Badenberg, et al. (2016b). "Heavy Metal Removal Mechanisms of Sorptive Filter Materials for Road Runoff Treatment and Remobilization under De-Icing Salt Applications". *Water Research* 102, pp. 453–463. DOI: 10.1016/j.watres.2016.06.063.

Huber, M., A. Welker, and B. Helmreich (2016c). "Critical Review of Heavy Metal Pollution of Traffic Area Runoff: Occurrence, Influencing Factors, and Partitioning". *Science of The Total Environment* 541, pp. 895–919. DOI: 10.1016/j.scitotenv.2015.09.033.

Huber, M., A. Welker, M. Dierschke, J. E. Drewes, and B. Helmreich (2016d). "A Novel Test Method to Determine the Filter Material Service Life of Decentralized Systems Treating Runoff from Traffic Areas". *Journal of Environmental Management* 179, pp. 66–75. DOI: 10.1016/j.jenvman.2016.05.003.

Huber, M. J. (2016). "Development and Evaluation of an Assessment Method for Decentralized Stormwater Treatment Systems for Runoff from Traffic Areas". Technische Universität München.

Huber, S. A., A. Balz, M. Abert, and W. Pronk (2011). "Characterisation of Aquatic Humic and Non-Humic Matter with Size-Exclusion Chromatography – Organic Carbon Detection – Organic Nitrogen Detection (LC-OCD-OND)". *Water Research* 45.2, pp. 879–885. DOI: 10.1016/j.watres.2010.09.023.

Huber, S. A. and F. H. Frimmel (1991). "Flow Injection Analysis for Organic and Inorganic Carbon in the Low-Ppb Range". *Analytical Chemistry* 63.19, pp. 2122–2130. DOI: 10.1021/ac00019a011.

Hudson, N., A. Baker, and D. Reynolds (2007). "Fluorescence Analysis of Dissolved Organic Matter in Natural, Waste and Polluted Waters—a Review". *River Research and Applications* 23.6, pp. 631–649. DOI: 10.1002/rra.1005.

Huguet, A., L. Vacher, S. Relexans, et al. (2009). "Properties of Fluorescent Dissolved Organic Matter in the Gironde Estuary". *Organic Geochemistry* 40.6, pp. 706–719. DOI: 10.1016/j.orggeochem.2009.03.002.

Hunter, J. D. (2007). "Matplotlib: A 2D Graphics Environment". *Computing in Science & Engineering* 9.3, pp. 90–95. DOI: 10.1109/MCSE.2007.55.

Hur, J. and B.-M. Lee (2011). "Characterization of Binding Site Heterogeneity for Copper within Dissolved Organic Matter Fractions Using Two-Dimensional Correlation Fluorescence Spectroscopy". *Chemosphere* 83.11, pp. 1603–1611. DOI: 10.1016/j.chemosphere.2011.01.004.

Hur, J., M.-H. Park, and M. A. Schlautman (2009). "Microbial Transformation of Dissolved Leaf Litter Organic Matter and Its Effects on Selected Organic Matter Operational Descriptors". *Environmental Science & Technology* 43.7, pp. 2315–2321. DOI: 10.1021/es802773b.

International Humic Substances Society (IHSS) (2020). *What Are Humic Substances*. URL: http://humic-substances.org/what-are-humic-substances-2/ (visited on Oct. 4, 2020).

International Stormwater BMP Database, ed. (2007). *Frequently Asked Questions: Why Does the International Stormwater BMP Database Project Omit Percent Removal as a Measure of BMP Performance?*

Ishii, S. K. L. and T. H. Boyer (2012). "Behavior of Reoccurring PARAFAC Components in Fluorescent Dissolved Organic Matter in Natural and Engineered Systems: A Critical Review". *Environmental Science & Technology* 46.4, pp. 2006–2017. DOI: 10.1021/es2043504.

Jayarathne, A., P. Egodawatta, G. A. Ayoko, and A. Goonetilleke (2017). "Geochemical Phase and Particle Size Relationships of Metals in Urban Road Dust". *Environmental Pollution* 230, pp. 218–226. DOI: 10.1016/j.envpol.2017.06.059.

Jayarathne, A., P. Egodawatta, G. A. Ayoko, and A. Goonetilleke (2018). "Assessment of Ecological and Human Health Risks of Metals in Urban Road Dust Based on Geochemical Fractionation and Potential Bioavailability". *Science of The Total Environment* 635, pp. 1609–1619. DOI: 10.1016/j.scitotenv.2018.04.098.

Joseph, L., B.-M. Jun, J. R. V. Flora, C. M. Park, and Y. Yoon (2019). "Removal of Heavy Metals from Water Sources in the Developing World Using Low-Cost Materials: A Review". *Chemosphere* 229, pp. 142–159. DOI: 10.1016/j.chemosphere.2019.04.198.

Järlskog, I., A.-M. Strömvall, K. Magnusson, et al. (2020). "Occurrence of Tire and Bitumen Wear Microplastics on Urban Streets and in Sweepsand and Washwater". *Science of The Total Environment* 729, p. 138950. DOI: 10.1016/j.scitotenv.2020.138950.

Järup, L. (2003). "Hazards of Heavy Metal Contamination". *British Medical Bulletin* 68.1, pp. 167–182. DOI: 10.1093/bmb/ldg032.

Kang, J., Y. Li, S. Lau, M. Kayhanian, and M. Stenstrom (2007). "Particle Destabilization in Highway Runoff to Optimize Pollutant Removal". *Journal of Environmental Engineering* 133.4, pp. 426–434. DOI: 10.1061/(ASCE)0733-9372(2007)133:4(426).

Karlsson, K., M. Viklander, L. Scholes, and M. Revitt (2010). "Heavy Metal Concentrations and Toxicity in Water and Sediment from Stormwater Ponds and Sedimentation Tanks". *Journal of Hazardous Materials* 178.1, pp. 612–618. DOI: 10.1016/j.jhazmat.2010.01.129.

Kayhanian, M., B. D. Fruchtman, J. S. Gulliver, et al. (2012a). "Review of Highway Runoff Characteristics: Comparative Analysis and Universal Implications". *Water Research* 46.20, pp. 6609–6624. DOI: 10.1016/j.watres.2012.07.026.

Kayhanian, M., E. R. McKenzie, J. E. Leatherbarrow, and T. M. Young (2012b). "Characteristics of Road Sediment Fractionated Particles Captured from Paved Surfaces, Surface Run-off and Detention Basins". *Science of The Total Environment* 439, pp. 172–186. DOI: 10.1016/j.scitotenv.2012.08.077.

Kayhanian, M., E. Rasa, A. Vichare, and J. Leatherbarrow (2008a). "Utility of Suspended Solid Measurements for Storm-Water Runoff Treatment". *Journal of Environmental Engineering* 134.9, pp. 712–721. DOI: 10.1061/(ASCE)0733-9372(2008)134:9(712).

Kayhanian, M., C. Stransky, S. Bay, S. L. Lau, and M. K. Stenstrom (2008b). "Toxicity of Urban Highway Runoff with Respect to Storm Duration". *Science of The Total Environment* 389.2–3, pp. 386–406. DOI: 10.1016/j.scitotenv.2007.08.052.

Kayhanian, M., C. Suverkropp, A. Ruby, and K. Tsay (2007). "Characterization and Prediction of Highway Runoff Constituent Event Mean Concentration". *Journal of Environmental Management* 85.2, pp. 279–295. DOI: 10.1016/j.jenvman.2006.09.024.

Kayhanian, M. and B. Givens (2011). "Processing and Analysis of Roadway Runoff Micro (< 20 μm) Particles". *Journal of Environmental Monitoring* 13.10, pp. 2720–2727. DOI: 10.1039/C1EM10375J.

Kell, G. S. (1975). "Density, Thermal Expansivity, and Compressibility of Liquid Water from 0° to 150°C: Correlations and Tables for Atmospheric Pressure and Saturation Reviewed and Expressed on 1968 Temperature Scale". *Journal of Chemical & Engineering Data* 20.1, pp. 97–105. DOI: 10.1021/je60064a005.

Kesraoui-Ouki, S., C. R. Cheeseman, and R. Perry (1994). "Natural Zeolite Utilisation in Pollution Control: A Review of Applications to Metals' Effluents". *Journal of Chemical Technology & Biotechnology* 59.2, pp. 121–126. DOI: 10.1002/jctb.280590202.

Kim, G. and S. Lee (2018). "Characteristics of Tire Wear Particles Generated by a Tire Simulator under Various Driving Conditions". *Environmental Science & Technology*. DOI: 10.1021/acs.est.8b03459.

Kluge, B. and G. Wessolek (2012). "Heavy Metal Pattern and Solute Concentration in Soils along the Oldest Highway of the World – the AVUS Autobahn". *Environmental Monitoring and Assessment* 184.11, pp. 6469–6481. DOI: 10.1007/s10661-011-2433-8.

Kothawala, D. N., K. R. Murphy, C. A. Stedmon, G. A. Weyhenmeyer, and L. J. Tranvik (2013). "Inner Filter Correction of Dissolved Organic Matter Fluorescence". *Limnology and Oceanography: Methods* 11.12, pp. 616–630. DOI: 10.4319/lom.2013.11.616.

Koukal, B., C. Guéguen, M. Pardos, and J. Dominik (2003). "Influence of Humic Substances on the Toxic Effects of Cadmium and Zinc to the Green Alga Pseudokirchneriella Subcapitata". *Chemosphere* 53.8, pp. 953–961. DOI: 10.1016/S0045-6535(03)00720-3.

Kreider, M. L., J. M. Panko, B. L. McAtee, L. I. Sweet, and B. L. Finley (2010). "Physical and Chemical Characterization of Tire-Related Particles: Comparison of Particles Generated Using Different Methodologies". *Science of The Total Environment* 408.3, pp. 652–659. DOI: 10.1016/j.scitotenv.2009.10.016.

Krishnappan, B. G., J. Marsalek, W. E. Watt, and B. C. Anderson (1999). "Seasonal Size Distributions of Suspended Solids in a Stormwater Management Pond". *Water Science and Technology* 39.2, pp. 127–134. DOI: 10.1016/S0273-1223(99)00016-5.

Krishnappan, B. G. and J. Marsalek (2002). "Modelling of Flocculation and Transport of Cohesive Sediment from an On-Stream Stormwater Detention Pond". *Water Research* 36.15, pp. 3849–3859. DOI: 10.1016/S0043-1354(02)00087-8.

Kristensen, T. B., L. Du, Q. T. Nguyen, et al. (2015). "Chemical Properties of HULIS from Three Different Environments". *Journal of Atmospheric Chemistry* 72.1, pp. 65–80. DOI: 10.1007/s10874-015-9302-8.

Kulkarni, H. V., N. Mladenov, S. Datta, and D. Chatterjee (2018). "Influence of Monsoonal Recharge on Arsenic and Dissolved Organic Matter in the Holocene and Pleistocene Aquifers of the Bengal Basin". *Science of The Total Environment* 637-638, pp. 588–599. DOI: 10.1016/j.scitotenv.2018.05.009.

Kumar, M. (2016). "Understanding the Remobilization of Copper, Zinc, Cadmium and Lead Due to Ageing through Sequential Extraction and Isotopic Exchangeability". *Environmental Monitoring and Assessment* 188.6, p. 381. DOI: 10.1007/s10661-016-5379-z.

Kumar, M., H. Furumai, F. Kurisu, and I. Kasuga (2013a). "Potential Mobility of Heavy Metals through Coupled Application of Sequential Extraction and Isotopic Exchange: Comparison of Leaching Tests Applied to Soil and Soakaway Sediment". *Chemosphere* 90.2, pp. 796–804. DOI: 10.1016/j.chemosphere.2012.09.082.

Kumar, M., H. Furumai, F. Kurisu, and I. Kasuga (2013b). "Tracing Source and Distribution of Heavy Metals in Road Dust, Soil and Soakaway Sediment through Speciation and Isotopic Fingerprinting". *Geoderma* 211-212, pp. 8–17. DOI: 10.1016/j.geoderma.2013.07.004.

Kumpiene, J., A. Lagerkvist, and C. Maurice (2008). "Stabilization of As, Cr, Cu, Pb and Zn in Soil Using Amendments – A Review". *Waste Management* 28.1, pp. 215–225. DOI: 10.1016/j.wasman.2006.12.012.

Laliberté, M. (2007). "Model for Calculating the Viscosity of Aqueous Solutions". *Journal of Chemical & Engineering Data* 52.2, pp. 321–335. DOI: 10.1021/je0604075.

Laliberté, M. and W. E. Cooper (2004). "Model for Calculating the Density of Aqueous Electrolyte Solutions". *Journal of Chemical & Engineering Data* 49.5, pp. 1141–1151. DOI: 10.1021/je0498659.

Lankes, U., M. B. Müller, M. Weber, and F. H. Frimmel (2009). "Reconsidering the Quantitative Analysis of Organic Carbon Concentrations in Size Exclusion Chromatography". *Water Research* 43.4, pp. 915–924. DOI: 10.1016/j.watres.2008.11.025.

LANUV (2012). *Nachweis der Vergleichbarkeit von dezentralen Behandlungsanlagen Zusammenfassende Darstellung der Prüfungsvorgaben*.

LANUV (2020). *Dezentrale Niederschlagswasserbehandlung*. URL: https://www.lanuv.nrw.de/umwelt/wasser/abwasser/niederschlagswasser/dezentrale-systeme/ (visited on Oct. 8, 2020).

Lassen, C., S. F. Hansen, K. Magnusson, et al. (2015). *Microplastics - Occurrence, Effects and Sources of Releases to the Environment in Denmark*.

Lau, Y. L. (1994). "Temperature Effect on Settling Velocity and Deposition of Cohesive Sediments". *Journal of Hydraulic Research* 32.1, pp. 41–51. DOI: 10.1080/00221689409498788.

LAWA (2016). *Ableitung von Geringfügigkeitsschwellenwerten für das Grundwasser - Aktualisierte und überarbeitete Fassung*.

Lee, D. H., K. S. Min, and J.-H. Kang (2014). "Performance Evaluation and a Sizing Method for Hydrodynamic Separators Treating Urban Stormwater Runoff". *Water Science and Technology* 69.10, pp. 2122–2131. DOI: 10.2166/wst.2014.125.

Lee, M.-H., Y. K. Lee, M. Derrien, et al. (2019). "Evaluating the Contributions of Different Organic Matter Sources to Urban River Water during a Storm Event via Optical Indices and Molecular Composition". *Water Research* 165, p. 115006. DOI: 10.1016/j.watres.2019.115006.

Legret, M. and C. Pagotto (1999). "Evaluation of Pollutant Loadings in the Runoff Waters from a Major Rural Highway". *Science of The Total Environment* 235.1–3, pp. 143–150. DOI: 10.1016/S0048-9697(99)00207-7.

Leisenring, M., J. Clary, and M. Quigley (2012). *Manufactured Devices Performance Summary*. International Stormwater Best Management Practices (BMP) Database, pp. 1–22.

Li, H. and A. P. Davis (2008). "Heavy Metal Capture and Accumulation in Bioretention Media". *Environmental Science & Technology* 42.14, pp. 5247–5253. DOI: 10.1021/es702681j.

Li, H., X. Qian, W. Hu, Y. Wang, and H. Gao (2013). "Chemical Speciation and Human Health Risk of Trace Metals in Urban Street Dusts from a Metropolitan City, Nanjing, SE China". *Science of The Total Environment* 456-457, pp. 212–221. DOI: 10.1016/j.scitotenv.2013.03.094.

Li, Y., S. Lau, M. Kayhanian, and M. Stenstrom (2006). "Dynamic Characteristics of Particle Size Distribution in Highway Runoff: Implications for Settling Tank Design". *Journal of Environmental Engineering* 132.8, pp. 852–861. DOI: 10.1061/(ASCE)0733-9372(2006)132:8(852).

Li, Y., J.-H. Kang, S.-L. Lau, M. Kayhanian, and M. K. Stenstrom (2008). "Optimization of Settling Tank Design to Remove Particles and Metals". *Journal of Environmental Engineering* 134.11, pp. 885–894. DOI: 10.1061/(ASCE)0733-9372(2008)134:11(885).

Li, Y., S.-L. Lau, M. Kayhanian, and M. K. Stenstrom (2005). "Particle Size Distribution in Highway Runoff". *Journal of Environmental Engineering* 131.9, pp. 1267–1276. DOI: 10.1061/(ASCE)0733-9372(2005)131:9(1267).

Liguori, R., S. H. Rommel, J. Bengtsson-Palme, B. Helmreich, and C. Wurzbacher (2021). "Microbial Retention and Resistances in Stormwater Quality Improvement Devices Treating Road Runoff". *bioRxiv*, p. 2021.01.12.426166. DOI: 10.1101/2021.01.12.426166.

Lin, H., G. Ying, and J. Sansalone (2009). "Granulometry of Non-Colloidal Particulate Matter Transported by Urban Runoff". *Water, Air, and Soil Pollution* 198.1, pp. 269–284. DOI: 10.1007/s11270-008-9844-3.

Liu, C., J. Lu, J. Liu, T. Mehmood, and W. Chen (2020). “Effects of Lead (Pb) in Stormwater Runoff on the Microbial Characteristics and Organics Removal in Bioretention Systems”. *Chemosphere* 253, p. 126721. DOI: 10.1016/j.chemosphere.2020.126721.

Liu, D., J. J. Sansalone, and F. K. Cartledge (2005). “Comparison of Sorptive Filter Media for Treatment of Metals in Runoff”. *Journal of Environmental Engineering* 131.8, pp. 1178–1186. DOI: 10.1061/(ASCE)0733-9372(2005)131:8(1178).

Liu, F., K. B. Olesen, A. R. Borregaard, and J. Vollertsen (2019). “Microplastics in Urban and Highway Stormwater Retention Ponds”. *Science of The Total Environment* 671, pp. 992–1000. DOI: 10.1016/j.scitotenv.2019.03.416.

Liu, L., A. Liu, Y. Li, et al. (2016). “Polycyclic Aromatic Hydrocarbons Associated with Road Deposited Solid and Their Ecological Risk: Implications for Road Stormwater Reuse”. *Science of The Total Environment* 563-564, pp. 190–198. DOI: 10.1016/j.scitotenv.2016.04.114.

Loganathan, P., S. Vigneswaran, and J. Kandasamy (2013). “Road-Deposited Sediment Pollutants: A Critical Review of Their Characteristics, Source Apportionment, and Management”. *Critical Reviews in Environmental Science and Technology* 43.13, pp. 1315–1348. DOI: 10.1080/10643389.2011.644222.

Lorenzo, J. I, O Nieto, and R Beiras (2002). “Effect of Humic Acids on Speciation and Toxicity of Copper to Paracentrotus Lividus Larvae in Seawater”. *Aquatic Toxicology* 58.1, pp. 27–41. DOI: 10.1016/S0166-445X(01)00219-3.

Lucke, T., D. Drapper, and A. Hornbuckle (2018). “Urban Stormwater Characterisation and Nitrogen Composition from Lot-Scale Catchments — New Management Implications”. *Science of The Total Environment* 619-620, pp. 65–71. DOI: 10.1016/j.scitotenv.2017.11.105.

Lucke, T., P. Nichols, E. Shaver, et al. (2017). “Pathways for the Evaluation of Stormwater Quality Improvement Devices - the Experience of Six Countries”. *CLEAN – Soil, Air, Water* 45.8, 1600596–n/a. DOI: 10.1002/clen.201600596.

Luider, C. D., J. Crusius, R. C. Playle, and P. J. Curtis (2004). “Influence of Natural Organic Matter Source on Copper Speciation As Demonstrated by Cu Binding to Fish Gills, by Ion Selective Electrode, and by DGT Gel Sampler”. *Environmental Science & Technology* 38.10, pp. 2865–2872. DOI: 10.1021/es030566y.

Ma, Y., P. Egodawatta, J. McGree, A. Liu, and A. Goonetilleke (2016). “Human Health Risk Assessment of Heavy Metals in Urban Stormwater”. *Science of The Total Environment* 557-558, pp. 764–772. DOI: 10.1016/j.scitotenv.2016.03.067.

Ma, Y., A. Liu, P. Egodawatta, J. McGree, and A. Goonetilleke (2017). “Assessment and Management of Human Health Risk from Toxic Metals and Polycyclic Aromatic Hydrocarbons in Urban Stormwater Arising from Anthropogenic Activities and Traffic Congestion”. *Science of The Total Environment* 579, pp. 202–211. DOI: 10.1016/j.scitotenv.2016.11.015.

Maniquiz, M. C., S. Lee, and L.-H. Kim (2010). "Multiple Linear Regression Models of Urban Runoff Pollutant Load and Event Mean Concentration Considering Rainfall Variables". *Journal of Environmental Sciences* 22.6, pp. 946–952. DOI: 10.1016/S1001-0742(09)60203-5.

Marsalek, J. (2003). "Road Salts in Urban Stormwater: An Emerging Issue in Stormwater Management in Cold Climates". *Water Science and Technology* 48.9, pp. 61–70.

Marsalek, J., G. Oberts, K. Exall, and M. Viklander (2003). "Review of Operation of Urban Drainage Systems in Cold Weather: Water Quality Considerations". *Water Science and Technology* 48.9, pp. 11–20. DOI: 10.2166/wst.2003.0481.

Martin, J. M, P Nirel, and A. J Thomas (1987). "Sequential Extraction Techniques: Promises and Problems". *Marine Chemistry*. IX International Symposium on the Chemistry of the Mediterranean 22.2, pp. 313–341. DOI: 10.1016/0304-4203(87)90017-X.

Masoner, J. R., D. W. Kolpin, I. M. Cozzarelli, et al. (2019). "Urban Stormwater: An Overlooked Pathway of Extensive Mixed Contaminants to Surface and Groundwaters in the United States". *Environmental Science & Technology* 53.17, pp. 10070–10081. DOI: 10.1021/acs.est.9b02867.

McBride, B (2000). "Chemisorption and Precipitation Reactions". *Handbook of Soil Science*. Boca Raton, Fla: CRC Press.

McKenzie, E., C. Wong, P. Green, M. Kayhanian, and T. Young (2008). "Size Dependent Elemental Composition of Road-Associated Particles". *Science of The Total Environment* 398.1–3, pp. 145–153. DOI: 10.1016/j.scitotenv.2008.02.052.

McKenzie, E. R., J. E. Money, P. G. Green, and T. M. Young (2009). "Metals Associated with Stormwater-Relevant Brake and Tire Samples". *Science of The Total Environment* 407.22, pp. 5855–5860. DOI: 10.1016/j.scitotenv.2009.07.018.

Merian, E. (1984). *Metalle in der Umwelt: Verteilung, Analytik und biologische Relevanz*. Verlag Chemie.

Michelbach, S. and C. Wöhrle (1993). "Settleable Solids in a Combined Sewer System, Settling Characteristics, Heavy Metals, Efficiency of Storm Water Tanks". *Water Science and Technology* 27.5-6, pp. 153–164. DOI: 10.2166/wst.1993.0495.

Müller, A., H. Österlund, J. Marsalek, and M. Viklander (2020). "The Pollution Conveyed by Urban Runoff: A Review of Sources". *Science of The Total Environment* 709, p. 136125. DOI: 10.1016/j.scitotenv.2019.136125.

Moll, B. and A. Quadflieg (2014). "Aktualisierung der Ableitung von Geringfügigkeitsschwellenwerten für das Grundwasser". *Wasser und Abfall* 3, pp. 10–14.

Monrabal-Martinez, C., A. Ilyas, and T. M. Muthanna (2017). "Pilot Scale Testing of Adsorbent Amended Filters under High Hydraulic Loads for Highway Runoff in Cold Climates". *Water* 9.3 (3), p. 230. DOI: 10.3390/w9030230.

Moreda-Piñeiro, A., A. Marcos, A. Fisher, and S. J. Hill (2001). "Evaluation of the Effect of Data Pre-Treatment Procedures on Classical Pattern Recognition and Principal Components Analysis: A Case Study for the Geographical Classification of Tea". *Journal of Environmental Monitoring* 3.4, pp. 352–360.

Mudge, S. M. (2015). “Chapter 19 - Multivariate Statistical Methods and Source Identification in Environmental Forensics”. *Introduction to Environmental Forensics (Third Edition)*. Ed. by B. L. Murphy and R. D. Morrison. San Diego: Academic Press, pp. 655–675. DOI: 10.1016/B978-0-12-404696-2.00019-9.

Mueller, K. K., C. Fortin, and P. G. C. Campbell (2012a). “Spatial Variation in the Optical Properties of Dissolved Organic Matter (DOM) in Lakes on the Canadian Precambrian Shield and Links to Watershed Characteristics”. *Aquatic Geochemistry* 18.1, pp. 21–44. DOI: 10.1007/s10498-011-9147-y.

Mueller, K. K., S. Lofts, C. Fortin, and P. G. C. Campbell (2012b). “Trace Metal Speciation Predictions in Natural Aquatic Systems: Incorporation of Dissolved Organic Matter (DOM) Spectroscopic Quality”. *Environmental Chemistry* 9.4, pp. 356–368. DOI: 10.1071/EN11156.

Murakami, M., M. Fujita, H. Furumai, I. Kasuga, and F. Kurisu (2009). “Sorption Behavior of Heavy Metal Species by Soakaway Sediment Receiving Urban Road Runoff from Residential and Heavily Trafficked Areas”. *Journal of Hazardous Materials* 164.2–3, pp. 707–712. DOI: 10.1016/j.jhazmat.2008.08.052.

Murakami, M., F. Nakajima, and H. Furumai (2005). “Size- and Density-Distributions and Sources of Polycyclic Aromatic Hydrocarbons in Urban Road Dust”. *Chemosphere* 61.6, pp. 783–791. DOI: 10.1016/j.chemosphere.2005.04.003.

Murakami, M., F. Nakajima, and H. Furumai (2008). “The Sorption of Heavy Metal Species by Sediments in Soakaways Receiving Urban Road Runoff”. *Chemosphere* 70.11, pp. 2099–2109. DOI: 10.1016/j.chemosphere.2007.08.073.

Murphy, K., S. Timko, M. Gonsior, et al. (2018). “Photochemistry Illuminates Ubiquitous Organic Matter Fluorescence Spectra”. *Environmental Science & Technology* 52. DOI: 10.1021/acs.est.8b02648.

Murphy, K. R., C. A. Stedmon, D. Graeber, and R. Bro (2013). “Fluorescence Spectroscopy and Multi-Way Techniques. PARAFAC”. *Analytical Methods* 5.23, pp. 6557–6566. DOI: 10.1039/C3AY41160E.

Murphy, K. R., C. A. Stedmon, P. Wenig, and R. Bro (2014). “OpenFluor–an Online Spectral Library of Auto-Fluorescence by Organic Compounds in the Environment”. *Analytical Methods* 6.3, pp. 658–661.

Murray, D. C. and U. F. W. Ernst (1976). *An Economic Analysis of the Environmental Impact of Highway Deicing*. USEPA 600/2-76-033. Washington, DC: U.S. EPA.

Muthanna, T. M., M. Viklander, G.-T. Blecken, and S. T. Thorolfsson (2007). “Snowmelt Pollutant Removal in Bioretention Areas”. *Water Research* 41.18, pp. 4061–4072. DOI: 10.1016/j.watres.2007.05.040.

Nason, J. A., M. S. Sprick, and D. J. Bloomquist (2012). “Determination of Copper Speciation in Highway Stormwater Runoff Using Competitive Ligand Exchange – Adsorptive Cathodic Stripping Voltammetry”. *Water Research* 46.17, pp. 5788–5798. DOI: 10.1016/j.watres.2012.08.008.

National Research Council (2003). *Bioavailability of Contaminants in Soils and Sediments: Processes, Tools, and Applications*. Washington, DC: The National Academies Press. DOI: 10.17226/10523.

Nelson, S., D. Yonge, and M. Barber (2009). "Effects of Road Salts on Heavy Metal Mobility in Two Eastern Washington Soils". *Journal of Environmental Engineering* 135.7, pp. 505–510. DOI: 10.1061/(ASCE)0733-9372(2009)135:7(505).

NJCAT (2013). *Procedure for Obtaining Verification of a Stormwater Manufactured Treatment Device from New Jersey Corporation for Advanced Technology*.

NJDEP (2020a). *Expired Stormwater Manufactured Treatment Devices*. URL: https://www.nj.gov/dep/stormwater/mtd_expired.htm (visited on Oct. 8, 2020).

NJDEP (2020b). *Stormwater Manufactured Treatment Devices*. URL: https://www.nj.gov/dep/stormwater/treatment.html (visited on Oct. 8, 2020).

ÖNORM B 2506-3 (2018). *ÖNORM B 2506-3, Regenwasser-Sickeranlagen für Abläufe von Dachflächen und befestigten Flächen - Teil 3, Filtermaterialien Anforderungen und Prüfmethoden*. Vienna, Austria: Komitee 120 Abwassertechnik, Austrian Standards International, pp. 1–26.

Norrström, A. C. (2005). "Metal Mobility by De-Icing Salt from an Infiltration Trench for Highway Runoff". *Applied Geochemistry* 20.10, pp. 1907–1919. DOI: 10.1016/j.apgeochem.2005.06.002.

Novotny, V., D. Muehring, D. H. Zitomer, D. W. Smith, and R. Facey (1998). "Cyanide and Metal Pollution by Urban Snowmelt: Impact of Deicing Compounds". *Water Science and Technology* 38.10, pp. 223–230. DOI: 10.1016/S0273-1223(98)00753-7.

OGewV (2016). *Oberflächengewässerverordnung vom 20. Juni 2016 (BGBl. I S. 1373)*.

Ohno, T. (2002). "Fluorescence Inner-Filtering Correction for Determining the Humification Index of Dissolved Organic Matter". *Environmental Science & Technology* 36.4, pp. 742–746. DOI: 10.1021/es0155276.

Okaikue-Woodi, F. E. K., K. Cherukumilli, and J. R. Ray (2020). "A Critical Review of Contaminant Removal by Conventional and Emerging Media for Urban Stormwater Treatment in the United States". *Water Research* 187, p. 116434. DOI: 10.1016/j.watres.2020.116434.

Opher, T. and E. Friedler (2010). "Factors Affecting Highway Runoff Quality". *Urban Water Journal* 7.3, pp. 155–172. DOI: 10.1080/15730621003782339.

Padoan, E., C. Romè, and F. Ajmone-Marsan (2017). "Bioaccessibility and Size Distribution of Metals in Road Dust and Roadside Soils along a Peri-Urban Transect". *Science of The Total Environment* 601-602, pp. 89–98. DOI: 10.1016/j.scitotenv.2017.05.180.

Pant, P. and R. M. Harrison (2013). "Estimation of the Contribution of Road Traffic Emissions to Particulate Matter Concentrations from Field Measurements: A Review". *Atmospheric Environment* 77, pp. 78–97. DOI: 10.1016/j.atmosenv.2013.04.028.

Parkhurst, D. and C. Appelo (2013). "Description of Input and Examples for PHREEQC Version 3—A Computer Program for Speciation, Batch-Reaction, One-Dimensional Transport, and Inverse Geochemical Calculation". *U.S. Geological Survey Techniques and Method*. Vol. 6, p. 497.

Paschka, M. G., R. S. Ghosh, and D. A. Dzombak (1999). "Potential Water-Quality Effects from Iron Cyanide Anticaking Agents in Road Salt". *Water Environment Research* 71.6, pp. 1235–1239.

Patriarca, C. (2020). "Characterisation of Natural Dissolved Organic Matter with Liquid Chromatography and High Resolution Mass Spectrometry". PhD Thesis. Uppsala University, Analytical Chemistry. 67 pp.

Paul, M. J. and J. L. Meyer (2001). "Streams in the Urban Landscape". *Annual Review of Ecology and Systematics* 32.1, pp. 333–365. DOI: 10.1146/annurev.ecolsys.32.081501.114040.

Paulson, C. and G. Amy (1993). "Regulating Metal Toxicity in Stormwater". *Water Environment & Technology*, pp. 44–49.

Pedregosa, F., G. Varoquaux, A. Gramfort, et al. (2011). "Scikit-Learn: Machine Learning in Python". *Journal of Machine Learning Research* 12, pp. 2825–2830.

Pengchai, P., F. Nakajima, and H. Furumai (2005). "Estimation of Origins of Polycyclic Aromatic Hydrocarbons in Size-Fractionated Road Dust in Tokyo with Multivariate Analysis". *Water Science and Technology* 51.3-4, pp. 169–175. DOI: 10.2166/wst.2005.0588.

Pernet-Coudrier, B., G. Varrault, M. Saad, et al. (2011). "Characterisation of Dissolved Organic Matter in Parisian Urban Aquatic Systems: Predominance of Hydrophilic and Proteinaceous Structures". *Biogeochemistry* 106.1, pp. 89–106. DOI: 10.1007/s10533-010-9480-z.

Pick, V. and J. Fettig (2009). *Vergleich Zweier Dezentraler Behandlungssysteme Für Niederschlagswasser von Verkehrsflächen. AQUAFOEL - CENTRIFOEL*. Hochschule Ostwestfalen-Lippe.

Portela, L. I., S. Ramos, and A. T. Teixeira (2013). "Effect of Salinity on the Settling Velocity of Fine Sediments of a Harbour Basin". *Journal of Coastal Research* 65 (sp2), pp. 1188–1193. DOI: 10.2112/SI65-201.1.

Pérez, G., M. López-Mesas, and M. Valiente (2008). "Assessment of Heavy Metals Remobilization by Fractionation: Comparison of Leaching Tests Applied to Roadside Sediments". *Environmental Science & Technology* 42.7, pp. 2309–2315. DOI: 10.1021/es0712975.

Pucher, M., U. Wünsch, G. Weigelhofer, et al. (2019). "staRdom: Versatile Software for Analyzing Spectroscopic Data of Dissolved Organic Matter in R". *Water* 11.11, p. 2366. DOI: 10.3390/w11112366.

Pueyo, M., J. Mateu, A. Rigol, et al. (2008). "Use of the Modified BCR Three-Step Sequential Extraction Procedure for the Study of Trace Element Dynamics in Contaminated Soils". *Environmental Pollution* 152.2, pp. 330–341. DOI: 10.1016/j.envpol.2007.06.020.

Radcliffe, J. C. (2019). “Chapter 1 - History of Water Sensitive Urban Design/Low Impact Development Adoption in Australia and Internationally”. *Approaches to Water Sensitive Urban Design*. Ed. by A. K. Sharma, T. Gardner, and D. Begbie. Woodhead Publishing, pp. 1–24. DOI: 10.1016/B978-0-12-812843-5.00001-0.

Rauret, G., J. F. López-Sánchez, D. Lück, et al. (2001). “The Certification of the Extractable Contents (Mass Fractions) of Cd, Cr, Cu, Ni, Pb and Zn in Freshwater Sediment Following a Sequential Extraction Procedure, BCR-701”. Ed. by E. E. European Commission, p. 88.

Rauret, G., J. F. López-Sánchez, A. Sahuquillo, et al. (1999). “Improvement of the BCR Three Step Sequential Extraction Procedure Prior to the Certification of New Sediment and Soil Reference Materials”. *Journal of Environmental Monitoring* 1.1, pp. 57–61. DOI: 10.1039/A807854H.

Ray, J. R., I. A. Shabtai, M. Teixidó, Y. G. Mishael, and D. L. Sedlak (2019). “Polymer-Clay Composite Geomedia for Sorptive Removal of Trace Organic Compounds and Metals in Urban Stormwater”. *Water Research* 157, pp. 454–462. DOI: 10.1016/j.watres.2019.03.097.

Reddy, K. R., T. Xie, and S. Dastgheibi (2014). “Removal of Heavy Metals from Urban Stormwater Runoff Using Different Filter Materials”. *Journal of Environmental Chemical Engineering* 2.1, pp. 282–292. DOI: 10.1016/j.jece.2013.12.020.

Revitt, D. M. and G. M. Morrison (1987). “Metal Speciation Variations within Separate Stormwater Systems”. *Environmental Technology Letters* 8.1-12, pp. 373–380. DOI: 10.1080/09593338709384496.

Rhodes, E. P., Z. Ren, and D. C. Mays (2012). “Zinc Leaching from Tire Crumb Rubber”. *Environmental Science & Technology* 46.23, pp. 12856–12863. DOI: 10.1021/es3024379.

RAS-Ew (2005). *Richtlinie für die Anlage von Straßen - Teil: Entwässerung*. 539. Köln, Germany: Forschungsgesellschaft für Straßen- und Verkehrswesen.

RiStWag (2016). *Richtlinien Für Bautechnische Maßnahmen an Straßen in Wasserschutzgebieten*. 514. Köln, Germany: Forschungsgesellschaft für Straßen- und Verkehrswesen, de.

Riley, N. A. (1941). “Projection Sphericity”. *Journal of Sedimentary Research* 11.2, pp. 94–95. DOI: 10.1306/D426910C-2B26-11D7-8648000102C1865D.

RÖMPP-Redaktion and W. Blaß (2016). *Schwermetalle*. Ed. by F. Böckler, B. Dill, U. Dingerdissen, et al.

Robertson, D. J, K. G Taylor, and S. R Hoon (2003). “Geochemical and Mineral Magnetic Characterisation of Urban Sediment Particulates, Manchester, UK”. *Applied Geochemistry* 18.2, pp. 269–282. DOI: 10.1016/S0883-2927(02)00125-7.

Rommel, S. H., G. Abbt-Braun, and B. Helmreich (2021a). “Dissolved Organic Matter in Road Runoff: Occurrence, Seasonality and Its Implication for Heavy Metal Retention”. *Manuscript in preparation*.

Rommel, S. and B. Helmreich (2019a). “Drei dezentrale Behandlungsanlagen für Verkehrsflächenabflüsse im Feldversuch – sind die Einzugsgebiete an der gleichen Straße vergleichbar?” *Aqua urbanica 2019*. Verband Schweizer Abwasser- und Gewässerschutzfachleute. Rigi-Kaltbad, Switzerland.

Rommel, S. and B. Helmreich (2020). *Endbericht zum Projekt: Wissenschaftliche Untersuchung der Effizienz der Kombination Absetzschacht und Versickerungsschacht zur Reduzierung der stofflichen Belastung von Verkehrsflächenabflüssen*. Garching, Germany: Landeshauptstadt München, Baureferat, pp. 1–46.

Rommel, S. H., V. Ebert, M. Huber, J. E. Drewes, and B. Helmreich (2019). “Spatial Distribution of Zinc in the Topsoil of Four Vegetated Infiltration Swales Treating Zinc Roof Runoff”. *Science of The Total Environment* 672, pp. 806–814. DOI: 10.1016/j.scitotenv.2019.04.016.

Rommel, S. H., L. Gelhardt, A. Welker, and B. Helmreich (2020a). “Settling of Road-Deposited Sediment: Influence of Particle Density, Shape, Low Temperatures, and Deicing Salt”. *Water* 12.11 (11), p. 3126. DOI: 10.3390/w12113126.

Rommel, S. H. and B. Helmreich (2018a). “Practical Experience in Handling Decentralized Stormwater Quality Treatment Devices for Traffic Area Runoff”. Doctoral Candidates Day 2018. Munich, Germany: Department of Civil, Geo and Environmental Engineering, Technical University of Munich.

Rommel, S. H. and B. Helmreich (2018b). “Feinpartikuläre Stoffe (AFS63) in Verkehrsflächenabflüssen–Vorkommen und Relevanz für dezentrale Behandlungsanlagen”. *Aqua urbanica trifft RegenwasserTage 2018*. Aqua urbanica trifft RegenwasserTage 2018. Landau (Pfalz), Germany.

Rommel, S. H. and B. Helmreich (2018c). “Influence of Temperature and De-Icing Salt on the Sedimentation of Particulate Matter in Traffic Area Runoff”. *Water* 10.12, p. 1738. DOI: 10.3390/w10121738.

Rommel, S. H. and B. Helmreich (2019b). “Are Different Catchment Areas at One Heavily Trafficked Road Comparable as Monitoring Sites for Stormwater Quality Improvement Devices?” *Novatech 2019*. Lyon, France.

Rommel, S. H., S. Krüger, and B. Helmreich (2020b). *Schlussbericht zum Einzelvorhaben (AZ: 67-0270-96505/2016 und AZ: 67-0270-25598/2019): Praxiserfahrungen zum Umgang mit dezentralen Behandlungsanlagen für Verkehrsflächenabflüsse*. Garching, Germany: Bayerisches Landesamt für Umwelt, pp. 1–87.

Rommel, S. H., L. Noceti, P. Stinshoff, and B. Helmreich (2020c). “Data: Leaching Potential of Heavy Metals from Road-Deposited Sediment and Sorptive Media during Dry Periods in Storm Water Quality Improvement Devices”. *Mendeley Data* V2. DOI: 10.17632/vzn73d448s.2.

Rommel, S. H., L. Noceti, P. Stinshoff, and B. Helmreich (2020d). “Leaching Potential of Heavy Metals from Road-Deposited Sediment and Sorptive Media during Dry Periods in Storm Water Quality Improvement Devices”. *Environmental Science: Water Research & Technology* 6.7, pp. 1890–1901. DOI: 10.1039/D0EW00351D.

Rommel, S. H., P. Stinshoff, and B. Helmreich (2021b). "Sequential Extraction of Heavy Metals from Sorptive Filter Media and Sediments Trapped in Stormwater Quality Improvement Devices for Road Runoff". *Science of The Total Environment* 782, p. 146875. DOI: 10.1016/j.scitotenv.2021.146875.

Rosario-Ortiz, F. L. and J. A. Korak (2017). "Oversimplification of Dissolved Organic Matter Fluorescence Analysis: Potential Pitfalls of Current Methods". *Environmental Science & Technology* 51.2, pp. 759–761. DOI: 10.1021/acs.est.6b06133.

Roseen, R. M., T. P. Ballestero, J. J. Houle, et al. (2009). "Seasonal Performance Variations for Storm-Water Management Systems in Cold Climate Conditions". *Journal of Environmental Engineering* 135.3, pp. 128–137. DOI: 10.1061/(ASCE)0733-9372(2009)135:3(128).

Rossman, L. A. and W. C. Huber (2016). *Storm Water Management Model Reference Manual: Volume III – Water Quality*. U.S. Environmental Protection Agency.

Rösel, L., C. Hildmann, M. Walko, and T. Heinkele (2020). *Anwendungsgrundsätze für Geringfügigkeitsschwellen zum Schutz des Grundwassers (GFS-Werte) am Beispiel der Niederschlagswasserversickerung*. 151/2020.

Sample, D. J., T. J. Grizzard, J. Sansalone, et al. (2012). "Assessing Performance of Manufactured Treatment Devices for the Removal of Phosphorus from Urban Stormwater". *Journal of Environmental Management* 113, pp. 279–291. DOI: 10.1016/j.jenvman.2012.08.039.

Sansalone, J., H. Lin, and G. Ying (2009). "Experimental and Field Studies of Type I Settling for Particulate Matter Transported by Urban Runoff". *Journal of Environmental Engineering* 135.10, pp. 953–963. DOI: 10.1061/(ASCE)EE.1943-7870.0000078.

Sansalone, J. J. and S. G. Buchberger (1997). "Partitioning and First Flush of Metals in Urban Roadway Storm Water". *Journal of Environmental Engineering* 123.2, pp. 134–143. DOI: 10.1061/(ASCE)0733-9372(1997)123:2(134).

Sansalone, J. J. and D. W. Glenn (2002). "Accretion of Pollutants in Snow Exposed to Urban Traffic and Winter Storm Maintenance Activities. I". *Journal of Environmental Engineering* 128.2, pp. 151–166. DOI: 10.1061/(ASCE)0733-9372(2002)128:2(151).

Sansalone, J. J., J. M. Koran, J. A. Smithson, and S. G. Buchberger (1998). "Physical Characteristics of Urban Roadway Solids Transported during Rain Events". *Journal of Environmental Engineering* 124.5, pp. 427–440. DOI: 10.1061/(ASCE)0733-9372(1998)124:5(427).

Schamphelaere, K. A. C. D., F. M. Vasconcelos, F. M. G. Tack, H. E. Allen, and C. R. Janssen (2004). "Effect of Dissolved Organic Matter Source on Acute Copper Toxicity to Daphnia Magna". *Environmental Toxicology and Chemistry* 23.5, pp. 1248–1255. DOI: 10.1897/03-184.

Schiff, K., S. Bay, and C. Stransky (2002). "Characterization of Stormwater Toxicants from an Urban Watershed to Freshwater and Marine Organisms". *Urban Water* 4.3, pp. 215–227. DOI: 10.1016/S1462-0758(02)00007-9.

Schuler, M. S. and R. A. Relyea (2018). "A Review of the Combined Threats of Road Salts and Heavy Metals to Freshwater Systems". *BioScience*, biy018–biy018. DOI: 10.1093/biosci/biy018.

Seabold, S. and J. Perktold (2010). “Statsmodels: Econometric and Statistical Modeling with Python”. *9th Python in Science Conference*.

Selbig, W. R. and M. N. Fienen (2012). “Regression Modeling of Particle Size Distributions in Urban Storm Water: Advancements through Improved Sample Collection Methods”. *Journal of Environmental Engineering* 138.12, pp. 1186–1193. DOI: 10.1061/(ASCE)EE.1943-7870.0000612.

Selbig, W. R., M. N. Fienen, J. A. Horwatich, and R. T. Bannerman (2016). “The Effect of Particle Size Distribution on the Design of Urban Stormwater Control Measures”. *Water* 8.1, p. 17. DOI: 10.3390/w8010017.

Selbig, W. R. and R. T. Bannerman (2011). *Characterizing the Size Distribution of Particles in Urban Stormwater by Use of Fixed-Point Sample-Collection Methods*. 2331-1258. US Geological Survey.

Semadeni-Davies, A. (2006). “Winter Performance of an Urban Stormwater Pond in Southern Sweden”. *Hydrological Processes* 20.1, pp. 165–182. DOI: 10.1002/hyp.5909.

Sheldon, F., C. Leigh, W. Neilan, et al. (2019). “Chapter 11 - Urbanization: Hydrology, Water Quality, and Influences on Ecosystem Health”. *Approaches to Water Sensitive Urban Design*. Ed. by A. K. Sharma, T. Gardner, and D. Begbie. Woodhead Publishing, pp. 229–248. DOI: 10.1016/B978-0-12-812843-5.00011-3.

Shi, X., M. Akin, T. Pan, et al. (2009). “Deicer Impacts on Pavement Materials: Introduction and Recent Developments”. *The Open Civil Engineering Journal* 3.1, pp. 16–27. DOI: 10.2174/1874149500903010016.

Shinya, M., T. Tsuchinaga, M. Kitano, Y. Yamada, and M. Ishikawa (2000). “Characterization of Heavy Metals and Polycyclic Aromatic Hydrocarbons in Urban Highway Runoff”. *Water Science and Technology* 42.7-8, pp. 201–208.

Sjöstedt, C. S., J. P. Gustafsson, and S. J. Köhler (2010). “Chemical Equilibrium Modeling of Organic Acids, pH, Aluminum, and Iron in Swedish Surface Waters”. *Environmental Science & Technology* 44.22, pp. 8587–8593. DOI: 10.1021/es102415r.

Sleighter, R. L., Z. Liu, J. Xue, and P. G. Hatcher (2010). “Multivariate Statistical Approaches for the Characterization of Dissolved Organic Matter Analyzed by Ultrahigh Resolution Mass Spectrometry”. *Environmental Science & Technology* 44.19, pp. 7576–7582. DOI: 10.1021/es1002204.

Sonnenberg, R., M. Beier, P. Kober, and Y. Lund-Weiß (2019). *Abschlussbericht zum Forschungsprojekt „Ertüchtigung von vorhandenen Dezentralen Regenwasserbehandlungssystemen am Beispiel des Nassschlammfangs Modell Hannover unter besonderer Berücksichtigung des Einflusses von Organik“*.

Spahr, S., M. Teixidó, D. L. Sedlak, and R. G. Luthy (2020). “Hydrophilic Trace Organic Contaminants in Urban Stormwater: Occurrence, Toxicological Relevance, and the Need to Enhance Green Stormwater Infrastructure”. *Environmental Science: Water Research & Technology*. DOI: 10.1039/C9EW00674E.

Spelman, D. and J. J. Sansalone (2018). “Is the Treatment Response of Manufactured BMPs to Urban Drainage PM Loads Portable?” *Journal of Environmental Engineering* 144.4. DOI: 10.1061/(ASCE)EE.1943-7870.0001326.

Stedmon, C. A. and R. M. Cory (2014). “Biological Origins and Fate of Fluorescent Dissolved Organic Matter in Aquatic Environments”. *Aquatic Organic Matter Fluorescence*. Ed. by P. G. Coble, J. Lead, A. Baker, D. M. Reynolds, and R. G. M. Spencer. Cambridge Environmental Chemistry Series. Cambridge: Cambridge University Press, pp. 278–300. DOI: 10.1017/CBO9781139045452.013.

Stedmon, C. A. and S. Markager (2005). “Resolving the Variability in Dissolved Organic Matter Fluorescence in a Temperate Estuary and Its Catchment Using PARAFAC Analysis”. *Limnology and Oceanography* 50.2, pp. 686–697. DOI: 10.4319/lo.2005.50.2.0686.

Steiner, M., P. Goosse, F. Rutz, R. Brodmann, and A. Pazeller (2010). *Strassenabwasserbehandlungsverfahren–Stand Der Technik*. 88 002. Bundesamt für Straßen ASTRA. Bundesamt für Umwelt BAFU, pp. 1–131.

Stone, M. and J. Marsalek (1996). “Trace Metal Composition and Speciation in Street Sediment: Sault Ste. Marie, Canada”. *Water, Air, and Soil Pollution* 87.1, pp. 149–169. DOI: 10.1007/BF00696834.

Stormwater Australia (2018). *Stormwater Quality Improvement Device Evaluation Protocol, Version 1.2 December 2018*.

Strecker, E., W. Huber, J. Heaney, et al. (2005). *Critical Assessment of Stormwater Treatment and Control Selection Issues*. DOI: 10.13140/RG.2.1.2231.7921.

Sun, W. and H. M. Selim (2019). “A General Stirred-Flow Model for Time-Dependent Adsorption and Desorption of Heavy Metal in Soils”. *Geoderma* 347, pp. 25–31. DOI: 10.1016/j.geoderma.2019.03.034.

Sutherland, B. R., K. J. Barrett, and M. K. Gingras (2015). “Clay Settling in Fresh and Salt Water”. *Environmental Fluid Mechanics* 15.1, pp. 147–160. DOI: 10.1007/s10652-014-9365-0.

Sutherland, R. A., F. M. G. Tack, C. A. Tolosa, and M. G. Verloo (2000). “Operationally Defined Metal Fractions in Road Deposited Sediment, Honolulu, Hawaii”. *Journal of Environmental Quality* 29.5, pp. 1431–1439. DOI: 10.2134/jeq2000.00472425002900050009x.

Sutherland, R. A and C. A Tolosa (2000). “Multi-Element Analysis of Road-Deposited Sediment in an Urban Drainage Basin, Honolulu, Hawaii”. *Environmental Pollution* 110.3, pp. 483–495. DOI: 10.1016/S0269-7491(99)00311-5.

Sutherland, R. A. (2002). “Comparison between Non-Residual Al, Co, Cu, Fe, Mn, Ni, Pb and Zn Released by a Three-Step Sequential Extraction Procedure and a Dilute Hydrochloric Acid Leach for Soil and Road Deposited Sediment”. en. *Applied Geochemistry* 17.4, pp. 353–365. DOI: 10.1016/S0883-2927(01)00095-6.

Sutherland, R. A. (2010). “BCR®-701: A Review of 10-Years of Sequential Extraction Analyses”. *Analytica Chimica Acta* 680.1, pp. 10–20. DOI: 10.1016/j.aca.2010.09.016.

Sutherland, R. A., F. M. G. Tack, and A. D. Ziegler (2012). "Road-Deposited Sediments in an Urban Environment: A First Look at Sequentially Extracted Element Loads in Grain Size Fractions". *Journal of Hazardous Materials* 225-226, pp. 54–62. DOI: 10.1016/j.jhazmat.2012.04.066.

Sutherland, R. A. and F. M. Tack (2000). "Metal Phase Associations in Soils from an Urban Watershed, Honolulu, Hawaii". *Science of The Total Environment* 256.2-3 (2-3), pp. 103–113. DOI: 10.1016/S0048-9697(00)00458-7.

Tan, K. H. (2014). *Humic Matter in Soil and the Environment: Principles and Controversies*. Boca Raton: CRC press. 495 pp.

Taylor, K. G. and D. J. Robertson (2009). "Electron Microbeam Analysis of Urban Road-Deposited Sediment, Manchester, UK: Improved Source Discrimination and Metal Speciation Assessment". *Applied Geochemistry* 24.7, pp. 1261–1269. DOI: 10.1016/j.apgeochem.2009.03.011.

Tchobanoglous, G., F. L. Burton, and H. D. Stensel (2014). *Wastewater Engineering: Treatment and Resource Recovery*. Bd. 1. Berkshire, UK: McGraw-Hill Education.

Tedoldi, D., G. Chebbo, D. Pierlot, Y. Kovacs, and M.-C. Gromaire (2016). "Impact of Runoff Infiltration on Contaminant Accumulation and Transport in the Soil/Filter Media of Sustainable Urban Drainage Systems: A Literature Review". *Science of The Total Environment* 569-570, pp. 904–926. DOI: 10.1016/j.scitotenv.2016.04.215.

Tedoldi, D., K. Flanagan, J. Le Roux, et al. (2019). "Evaluation of Contaminant Retention in the Soil of Sustainable Drainage Systems: Methodological Reflections on the Determination of Sorption Isotherms". *Blue-Green Systems* 1.1, pp. 1–17. DOI: 10.2166/bgs.2019.196.

Teng, Z. and J. Sansalone (2004). "In Situ Partial Exfiltration of Rainfall Runoff. II: Particle Separation". *Journal of Environmental Engineering* 130.9, pp. 1008–1020. DOI: 10.1061/(ASCE)0733-9372(2004)130:9(1008).

The pandas development team (2020). *Pandas-Dev/Pandas: Pandas*. Version latest. Zenodo. DOI: 10.5281/zenodo.3509134.

Thurman, E. M. and R. L. Malcolm (1981). "Preparative Isolation of Aquatic Humic Substances". *Environmental Science & Technology* 15.4, pp. 463–466. DOI: 10.1021/es00086a012.

Thurman, E. (1985). "Amount of Organic Carbon in Natural Waters". *Organic Geochemistry of Natural Waters*. Springer, pp. 7–65.

Tipping, E. (2002). *Cation Binding by Humic Substances*. Cambridge University Press. 446 pp.

Torres, A. and J.-L. Bertrand-Krajewski (2008). "Evaluation of Uncertainties in Settling Velocities of Particles in Urban Stormwater Runoff". *Water Science and Technology* 57.9, pp. 1389–1396. DOI: 10.2166/wst.2008.307.

Transportation Research Board (2014). *Measuring and Removing Dissolved Metals from Stormwater in Highly Urbanized Areas*. Ed. by National Academies of Sciences, Engineering, and Medicine, M. Barrett, L. Katz, et al. National Cooperative Highway Research Program. Washington, DC: The National Academies Press.

Transportation Research Board and National Academies of Sciences, Engineering, and Medicine (2004). *Identification of Research Needs Related to Highway Runoff Management*. Washington, DC: The National Academies Press. DOI: 10.17226/13791.

Transportation Research Board and National Academies of Sciences, Engineering, and Medicine (2012). *Guidelines for Evaluating and Selecting Modifications to Existing Roadway Drainage Infrastructure to Improve Water Quality in Ultra-Urban Areas*. Ed. by G. Consultants, O. S. University, V. Consulting, L. I. D. Center, and W. W. Engineers. Washington, DC: The National Academies Press. DOI: 10.17226/22031.

Tromp, K., A. T. Lima, A. Barendregt, and J. T. A. Verhoeven (2012). "Retention of Heavy Metals and Poly-Aromatic Hydrocarbons from Road Water in a Constructed Wetland and the Effect of de-Icing". *Journal of Hazardous Materials* 203–204, pp. 290–298. DOI: 10.1016/j.jhazmat.2011.12.024.

Tuhkanen, T. and A. Ignatev (2018). "Humic and Fulvic Compounds". *Reference Module in Chemistry, Molecular Sciences and Chemical Engineering*. Elsevier.

Ulliman, S. L., J. A. Korak, K. G. Linden, and F. L. Rosario-Ortiz (2020). "Methodology for Selection of Optical Parameters as Wastewater Effluent Organic Matter Surrogates". *Water Research* 170, p. 115321. DOI: 10.1016/j.watres.2019.115321.

Unda-Calvo, J., E. Ruiz-Romera, S. Fdez-Ortiz de Vallejuelo, M. Martínez-Santos, and A. Gredilla (2019). "Evaluating the Role of Particle Size on Urban Environmental Geochemistry of Metals in Surface Sediments". *Science of The Total Environment* 646, pp. 121–133. DOI: 10.1016/j.scitotenv.2018.07.172.

Ure, A. M., P. Quevauviller, H. Muntau, and B. Griepink (1993). "Speciation of Heavy Metals in Soils and Sediments. An Account of the Improvement and Harmonization of Extraction Techniques Undertaken Under the Auspices of the BCR of the Commission of the European Communities". *International Journal of Environmental Analytical Chemistry* 51.1-4, pp. 135–151. DOI: 10.1080/03067319308027619.

Valle, J., M. Gonsior, M. Harir, et al. (2018). "Extensive Processing of Sediment Pore Water Dissolved Organic Matter during Anoxic Incubation as Observed by High-Field Mass Spectrometry (FTICR-MS)". *Water Research* 129, pp. 252–263. DOI: 10.1016/j.watres.2017.11.015.

Valle, J., M. Harir, M. Gonsior, et al. (2020). "Molecular Differences between Water Column and Sediment Pore Water SPE-DOM in Ten Swedish Boreal Lakes". *Water Research* 170, p. 115320. DOI: 10.1016/j.watres.2019.115320.

Van Wezel, A., L. Puijker, C. Vink, A. Versteegh, and P. De Voogt (2009). "Odour and Flavour Thresholds of Gasoline Additives (MTBE, ETBE and TAME) and Their Occurrence in Dutch Drinking Water Collection Areas". *Chemosphere* 76.5, pp. 672–676. DOI: 10.1016/j.chemosphere.2009.03.073.

Vega-Garcia, P., R. Schwerd, C. Scherer, et al. (2020). "Influence of Façade Orientation on the Leaching of Biocides from Building Façades Covered with Mortars and Plasters". *Science of The Total Environment* 734, p. 139465. DOI: 10.1016/j.scitotenv.2020.139465.

Vesting, A. (2018). “Entwicklung und Evaluation eines dezentralen Behandlungssystems zum Rückhalt von organischen Spurenstoffen und Schwermetallen aus Verkehrsflächenabflüssen”.

Virtanen, P., R. Gommers, T. E. Oliphant, et al. (2020). “SciPy 1.0: Fundamental Algorithms for Scientific Computing in Python”. *Nature Methods*. DOI: 10.1038/s41592-019-0686-2.

Vogelsang, C., A. L. Lusher, M. E. Dadkhah, et al. (2019). *Microplastics in Road Dust – Characteristics, Pathways and Measures*.

VSA (2019). *VSA-Leistungsprüfung für Behandlungsanlagen: Merkblatt «Leistungsprüfung für Adsorbermaterialien und dezentrale technische Anlagen zur Behandlung von Niederschlagswasser»*. Verband Schweizer Abwasser- und Gewässerschutzfachleute, pp. 1–28. DOI: 10.13140/RG.2.2.35087.84641.

Wagner, S., T. Hüffer, P. Klöckner, et al. (2018). “Tire Wear Particles in the Aquatic Environment - A Review on Generation, Analysis, Occurrence, Fate and Effects”. *Water Research* 139, pp. 83–100. DOI: 10.1016/j.watres.2018.03.051.

Walsh, C. J., A. H. Roy, J. W. Feminella, et al. (2005). “The Urban Stream Syndrome: Current Knowledge and the Search for a Cure”. *Journal of the North American Benthological Society* 24.3, pp. 706–723. DOI: 10.1899/04-028.1.

Wang, J., Y. Zhao, L. Yang, et al. (2017). “Removal of Heavy Metals from Urban Stormwater Runoff Using Bioretention Media Mix”. *Water* 9.11 (11), p. 854. DOI: 10.3390/w9110854.

Wang, J., S. Yuan, L. Tang, et al. (2020). “Contribution of Heavy Metal in Driving Microbial Distribution in a Eutrophic River”. *Science of The Total Environment* 712, p. 136295. DOI: 10.1016/j.scitotenv.2019.136295.

Wang, S. and Y. Peng (2010). “Natural Zeolites as Effective Adsorbents in Water and Wastewater Treatment”. *Chemical Engineering Journal* 156.1, pp. 11–24. DOI: 10.1016/j.cej.2009.10.029.

Wang, Y., L. Zhou, Y. Wu, and Q. Yang (2018). “New Simple Correlation Formula for the Drag Coefficient of Calcareous Sand Particles of Highly Irregular Shape”. *Powder Technology* 326, pp. 379–392. DOI: 10.1016/j.powtec.2017.12.004.

Washington State Department of Ecology (2011). *Technical Guidance Manual for Evaluating Emerging Stormwater Treatment Technologies: Technology Assessment Protocol – Ecology (TAPE)*. 11-10-061.

Waskom, M., O. Botvinnik, J. Ostblom, et al. (2020). *Mwaskom/Seaborn: V0.10.1 (April 2020)*. Version v0.10.1. Zenodo. DOI: 10.5281/zenodo.3767070.

Water Environment Federation (2014). *Investigation into the Feasibility of a National Testing and Evaluation Program for Stormwater Products and Practices*. n.p., pp. 1–40.

Wei, Q., G. Zhu, P. Wu, et al. (2010). “Distributions of Typical Contaminant Species in Urban Short-Term Storm Runoff and Their Fates during Rain Events: A Case of Xiamen City”. *J Environ Sci (China)* 22.4, pp. 533–539. DOI: 10.1016/S1001-0742(09)60138-8.

Weishaar, J. L., G. R. Aiken, B. A. Bergamaschi, et al. (2003). "Evaluation of Specific Ultraviolet Absorbance as an Indicator of the Chemical Composition and Reactivity of Dissolved Organic Carbon". *Environmental Science & Technology* 37.20, pp. 4702–4708. DOI: 10.1021/es030360x.

Werker, H., J Twardon, S Schmitz, et al. (2011). *Dezentrale Niederschlagswasserbehandlung in Trennsystemen – Umsetzung Des Trennerlasses*. Stadtentwässerungsbetriebe Köln, Stadtbetrieb Königswinter, Stadtentwässerung Schwerte GmbH.

WHG (2020). *Wasserhaushaltsgesetz vom 31. Juli 2009 (BGBl. I S. 2585), das zuletzt durch Artikel 1 des Gesetzes vom 19. Juni 2020 (BGBl. I S. 1408) geändert worden ist*.

Wijesiri, B., P. Egodawatta, J. McGree, and A. Goonetilleke (2016). "Influence of Uncertainty Inherent to Heavy Metal Build-up and Wash-off on Stormwater Quality". *Water Research* 91, pp. 264–276. DOI: 10.1016/j.watres.2016.01.028.

Wik, A. and G. Dave (2009). "Occurrence and Effects of Tire Wear Particles in the Environment – A Critical Review and an Initial Risk Assessment". *Environmental Pollution* 157.1, pp. 1–11. DOI: 10.1016/j.envpol.2008.09.028.

Wik, A., J. Lycken, and G. Dave (2008). "Sediment Quality Assessment of Road Runoff Detention Systems in Sweden and the Potential Contribution of Tire Wear". *Water, Air, and Soil Pollution* 194.1, pp. 301–314. DOI: 10.1007/s11270-008-9718-8.

Williams, C. J., P. C. Frost, and M. A. Xenopoulos (2013). "Beyond Best Management Practices: Pelagic Biogeochemical Dynamics in Urban Stormwater Ponds". *Ecological Applications* 23.6, pp. 1384–1395. DOI: 10.1890/12-0825.1.

Winkler, M. K. H., J. P. Bassin, R. Kleerebezem, R. G. J. M. van der Lans, and M. C. M. van Loosdrecht (2012). "Temperature and Salt Effects on Settling Velocity in Granular Sludge Technology". *Water Research* 46.16, pp. 5445–5451. DOI: 10.1016/j.watres.2012.07.022.

Worch, E. (2012a). "Adsorbents and Adsorbent Characterization". *Adsorption Technology in Water Treatment*. De Gruyter, pp. 11–40.

Worch, E. (2012b). "Introduction". *Adsorption Technology in Water Treatment*. De Gruyter, pp. 1–10.

Wright Water Engineers, Geosyntec Consultants, Water Research Foundation (WRF), et al. (2020). *International Stormwater BMP Database*. URL: https://www.bmpdatabase.org (visited on Oct. 23, 2020).

Wüst, W., U. Kern, and R. Herrmann (1994). "Street Wash-off Behaviour of Heavy Metals, Polyaromatic Hydrocarbons and Nitrophenols". *Science of The Total Environment* 146–147, pp. 457–463. DOI: 10.1016/0048-9697(94)90269-0.

Xu, H., L. Zou, D. Guan, W. Li, and H. Jiang (2019). "Molecular Weight-Dependent Spectral and Metal Binding Properties of Sediment Dissolved Organic Matter from Different Origins". *Science of The Total Environment* 665, pp. 828–835. DOI: 10.1016/j.scitotenv.2019.02.186.

Xue, J., C. Lee, S. G. Wakeham, and R. A. Armstrong (2011). "Using Principal Components Analysis (PCA) with Cluster Analysis to Study the Organic Geochemistry of Sinking Particles in the Ocean". *Organic Geochemistry* 42.4, pp. 356–367. DOI: 10.1016/j.orggeochem.2011.01.012.

Yin, Y., C. A. Impellitteri, S.-J. You, and H. E. Allen (2002). "The Importance of Organic Matter Distribution and Extract Soil:Solution Ratio on the Desorption of Heavy Metals from Soils". *Science of The Total Environment* 287.1, pp. 107–119. DOI: 10.1016/S0048-9697(01)01000-2.

Ying, G. and J. Sansalone (2011). "Gravitational Settling Velocity Regimes for Heterodisperse Urban Drainage Particulate Matter". *Journal of Environmental Engineering* 137.1, pp. 15–27. DOI: 10.1061/(ASCE)EE.1943-7870.0000298.

Young, S. D. (2013). "Chemistry of Heavy Metals and Metalloids in Soils". *Heavy Metals in Soils: Trace Metals and Metalloids in Soils and Their Bioavailability*. Ed. by B. J. Alloway. Dordrecht: Springer Netherlands, pp. 51–95.

Zafra, C., J. Temprano, and J. Suárez (2017). "A Simplified Method for Determining Potential Heavy Metal Loads Washed-off by Stormwater Runoff from Road-Deposited Sediments". *Science of The Total Environment* 601-602, pp. 260–270. DOI: 10.1016/j.scitotenv.2017.05.178.

Zahraeifard, V. and Z. Deng (2011). "Hydraulic Residence Time Computation for Constructed Wetland Design". *Ecological Engineering* 37.12, pp. 2087–2091. DOI: 10.1016/j.ecoleng.2011.08.011.

Zawilski, M. and G Sakson (2008). "Modelling of Detention-Sedimentation Basins for Stormwater Treatment Using SWMM Software". 11th International Conference on Urban Drainage. Edinburgh, UK.

Zgheib, S., R. Moilleron, and G. Chebbo (2011a). "Priority Pollutants in Urban Stormwater: Part 1 – Case of Separate Storm Sewers". *Water Research* 46.20, pp. 6683–6692. DOI: 10.1016/j.watres.2011.12.012.

Zgheib, S., R. Moilleron, M. Saad, and G. Chebbo (2011b). "Partition of Pollution between Dissolved and Particulate Phases: What about Emerging Substances in Urban Stormwater Catchments?" *Water Research* 45.2, pp. 913–925. DOI: 10.1016/j.watres.2010.09.032.

Zhang, J., P. Hua, and P. Krebs (2016). "The Influences of Dissolved Organic Matter and Surfactant on the Desorption of Cu and Zn from Road-Deposited Sediment". *Chemosphere* 150, pp. 63–70. DOI: 10.1016/j.chemosphere.2016.02.015.

Zhang, J., R. Li, X. Zhang, et al. (2019a). "Vehicular Contribution of PAHs in Size Dependent Road Dust: A Source Apportionment by PCA-MLR, PMF, and Unmix Receptor Models". *Science of The Total Environment* 649, pp. 1314–1322. DOI: 10.1016/j.scitotenv.2018.08.410.

Zhang, J., X. Wang, Y. Zhu, et al. (2019b). "The Influence of Heavy Metals in Road Dust on the Surface Runoff Quality: Kinetic, Isotherm, and Sequential Extraction Investigations". *Ecotoxicology and Environmental Safety* 176, pp. 270–278. DOI: 10.1016/j.ecoenv.2019.03.106.

Zhang, Z., J. J. Wang, A. Ali, and R. D. DeLaune (2018). "Physico-Chemical Forms of Copper in Water and Sediments of Lake Pontchartrain Basin, USA". *Chemosphere* 195, pp. 448–454. DOI: 10.1016/j.chemosphere.2017.12.115.

Zhang, Z., W. Shi, H. Ma, et al. (2020). "Binding Mechanism Between Fulvic Acid and Heavy Metals: Integrated Interpretation of Binding Experiments, Fraction Characterizations, and Models". *Water, Air, & Soil Pollution* 231.4, p. 184. DOI: 10.1007/s11270-020-04558-2.

Zhao, C., C.-C. Wang, J.-Q. Li, et al. (2015). "Dissolved Organic Matter in Urban Stormwater Runoff at Three Typical Regions in Beijing: Chemical Composition, Structural Characterization and Source Identification". *RSC Advances* 5.90, pp. 73490–73500. DOI: 10.1039/C5RA14993B.

Zhao, Z. and P. Hazelton (2016). "Evaluation of Accumulation and Concentration of Heavy Metals in Different Urban Roadside Soil Types in Miranda Park, Sydney". *Journal of Soils and Sediments* 16.11, pp. 2548–2556. DOI: 10.1007/s11368-016-1460-z.

Zhou, Y.-F. and R. J. Haynes (2010). "Sorption of Heavy Metals by Inorganic and Organic Components of Solid Wastes: Significance to Use of Wastes as Low-Cost Adsorbents and Immobilizing Agents". *Critical Reviews in Environmental Science and Technology* 40.11, pp. 909–977. DOI: 10.1080/10643380802586857.

Appendix A

A.1 List of publications

Research articles (peer-reviewed)

1. Rommel, S. H. and B. Helmreich (2018c). "Influence of Temperature and De-Icing Salt on the Sedimentation of Particulate Matter in Traffic Area Runoff". *Water* 10.12, p. 1738. DOI: 10.3390/w10121738

   This publication is included in Chapter 7.

   Author contributions: Rommel, S. H.: conceptualization, methodology, investigation, validation, data curation, writing - original draft, writing - review & editing, project administration; Helmreich, B.: conceptualization, investigation, resources, writing - review & editing, supervision, project administration, funding acquisition.

2. Rommel, S. H., L. Noceti, P. Stinshoff, and B. Helmreich (2020d). "Leaching Potential of Heavy Metals from Road-Deposited Sediment and Sorptive Media during Dry Periods in Storm Water Quality Improvement Devices". *Environmental Science: Water Research & Technology* 6.7, pp. 1890–1901. DOI: 10.1039/D0EW00351D

   This publication is included in Chapter 4.

   Author contributions: Rommel, S. H.: conceptualization, methodology, validation, data curation, writing - original draft, writing - review & editing, visualization, supervision; Noceti, L.: investigation, data curation, visualization; Stinshoff, P.: methodology, investigation; Helmreich, B.: resources, writing - review & editing, supervision, project administration, funding acquisition.

3. Rommel, S. H., L. Gelhardt, A. Welker, and B. Helmreich (2020a). "Settling of Road-Deposited Sediment: Influence of Particle Density, Shape, Low Temperatures, and Deicing Salt". *Water* 12.11 (11), p. 3126. DOI: 10.3390/w12113126

   This publication is included in Chapter 8.

   Author contributions: Rommel, S. H.: conceptualization, methodology, software, validation, investigation, data curation, writing - original draft, writing - review & editing, visualization; Gelhardt, L.: conceptualization, methodology, investigation, data curation, writing - review & editing; Welker, A.: conceptualization, resources, writing - review & editing, supervision, project administration, funding acquisition; Helmreich, B.: resources, writing - review & editing, supervision, project administration, funding acquisition.

4. Rommel, S. H., P. Stinshoff, and B. Helmreich (2021b). "Sequential Extraction of Heavy Metals from Sorptive Filter Media and Sediments Trapped in Stormwater Quality Improvement Devices for Road Runoff". *Science of The Total Environment* 782, p. 146875. DOI: 10.1016/j.scitotenv.2021.146875

   This publication is included in Chapter 5.

   Author contributions: Rommel‡, S. H.: conceptualization, methodology, validation, data curation, writing - original draft, writing - review & editing, visualization, supervision; Stinshoff,‡ P.: investigation, methodology, data curation, writing - original draft, writing - review & editing; Helmreich, B.: resources, writing - review & editing, supervision, project administration, funding acquisition; ‡ these authors contributed equally.

Research articles (in preparation for peer-reviewed publication)

1. Rommel, S. H., G. Abbt-Braun, and B. Helmreich (2021a). "Dissolved Organic Matter in Road Runoff: Occurrence, Seasonality and Its Implication for Heavy Metal Retention". *Manuscript in preparation*

   This publication is included in Chapter 6.

   Author contributions: Rommel, S. H.: conceptualization, methodology, validation, data curation, writing - original draft, writing - review & editing, visualization, supervision; Abbt-Braun, G.: investigation, methodology, validation, data curation, writing - review & editing, visualization; Helmreich, B.: resources, writing - review & editing, supervision, project administration, funding acquisition.

Research articles (non-peer-reviewed)

1. Helmreich, B. and S. Rommel (2020). "Dezentrale Behandlung von Straßenabflüssen im urbanen Raum – wohin geht die Reise?" *Straßenverkehrstechnik* 03/2020, pp. 154–158

Additional research articles (peer-reviewed or submitted for peer-reviewed publication) in other research areas

1. Rommel, S. H., V. Ebert, M. Huber, J. E. Drewes, and B. Helmreich (2019). "Spatial Distribution of Zinc in the Topsoil of Four Vegetated Infiltration Swales Treating Zinc Roof Runoff". *Science of The Total Environment* 672, pp. 806–814. DOI: 10.1016/j.scitotenv.2019.04.016

2. Vega-Garcia, P., R. Schwerd, C. Scherer, C. Schwitalla, S. Johann, S. H. Rommel, and B. Helmreich (2020). "Influence of Façade Orientation on the Leaching of Biocides from Building Façades Covered with Mortars and Plasters".

Science of The Total Environment 734, p. 139465. DOI: 10.1016/j.scitotenv.2020.139465

3. Liguori, R., S. H. Rommel, J. Bengtsson-Palme, B. Helmreich, and C. Wurzbacher (2021). "Microbial Retention and Resistances in Stormwater Quality Improvement Devices Treating Road Runoff". *bioRxiv*, p. 2021.01.12.426166. DOI: 10.1101/2021.01.12.426166

Conference talks

1. Rommel, S. H. and B. Helmreich (2018b). "Feinpartikuläre Stoffe (AFS63) in Verkehrsflächenabflüssen–Vorkommen und Relevanz für dezentrale Behandlungsanlagen". *Aqua urbanica trifft RegenwasserTage 2018*. Aqua urbanica trifft RegenwasserTage 2018. Landau (Pfalz), Germany

2. Rommel, S. H. and B. Helmreich (2019b). "Are Different Catchment Areas at One Heavily Trafficked Road Comparable as Monitoring Sites for Stormwater Quality Improvement Devices?" *Novatech 2019*. Lyon, France

3. Helmreich, B., V. Ebert, and S. H. Rommel (2019). "Performance of Vegetated Infiltration Swales for Treatment of Zinc Roof Runoff". *Novatech 2019*. Lyon, France

4. Rommel, S. and B. Helmreich (2019a). "Drei dezentrale Behandlungsanlagen für Verkehrsflächenabflüsse im Feldversuch – sind die Einzugsgebiete an der gleichen Straße vergleichbar?" *Aqua urbanica 2019*. Verband Schweizer Abwasser- und Gewässerschutzfachleute. Rigi-Kaltbad, Switzerland

5. Helmreich, B. and S. H. Rommel (2019). "Dezentrale Behandlung von Straßenabflüssen im urbanen Raum – wohin geht die Reise?" *Kolloquium kommunales Verkehrswesen*. Kassel, Germany

Conference posters

1. Rommel, S. H. and B. Helmreich (2018a). "Practical Experience in Handling Decentralized Stormwater Quality Treatment Devices for Traffic Area Runoff". Doctoral Candidates Day 2018. Munich, Germany: Department of Civil, Geo and Environmental Engineering, Technical University of Munich

2. Broich, K., S. Rommel, P. Wasmeier, B. Helmreich, and M. Disse (2018). "Ein Modell mit doppeltem Nutzen: Die Messung von Verkehrsflächenabflüssen am Münchner Mittleren Ring". *Tag der Hydrologie 2018*. Dresden, Germany

Research reports

1. Rommel, S. H., S. Krüger, and B. Helmreich (2020b). *Schlussbericht zum Einzelvorhaben (AZ: 67-0270-96505/2016 und AZ: 67-0270-25598/2019): Praxiserfahrungen zum Umgang mit dezentralen Behandlungsanlagen für Verkehrsflächenabflüsse*. Garching, Germany: Bayerisches Landesamt für Umwelt, pp. 1–87

2. Rommel, S. and B. Helmreich (2020). *Endbericht zum Projekt: Wissenschaftliche Untersuchung der Effizienz der Kombination Absetzschacht und Versickerungsschacht zur Reduzierung der stofflichen Belastung von Verkehrsflächenabflüssen*. Garching, Germany: Landeshauptstadt München, Baureferat, pp. 1–46

A.2 Supplementary information for Chapter 4

Table S1 Physical characteristics of all materials before pre-stressing based on dry matter.

Parameter	d_{10}	d_{30}	d_{60}	Bulk density	Loss on ignition (550 °C)	Surface area (BET)	Total pore volume	CEC
Unit	mm	mm	mm	g L^{-1}	%	m^2 g-1	cm^3 g^{-1}	$cmol^+$ kg^{-1}
GAL	1.1	1.4	1.8	499	7.5	264.3	0.17	8.3
GFH	1.1	1.3	1.6	599	10.9	206.5	0.37	43.2
SED	0.004	0.012	0.055	781	16.3	2.4	-[a]	16.6
ZEO	0.7	1.1	1.6	915	6.2	31.2	0.07	23.0

[a] Determination of the total pore volume of SED was not possible due to the small particle size

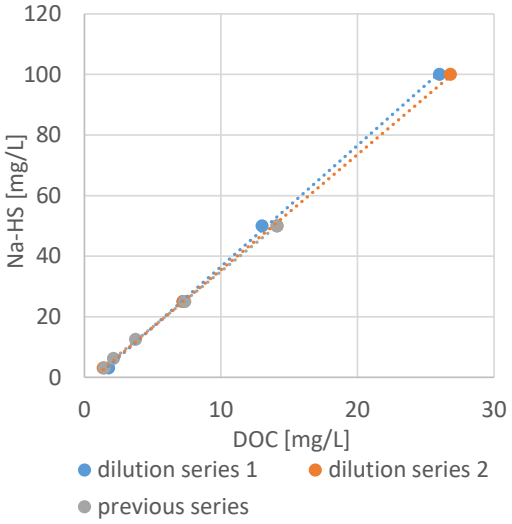

Fig. S1 Dilution-series of the used humic acid sodium salt (CAS-No. 68131-04-4; Carl Roth, Germany) in ultrapure water, linear regression of the data.

Pre-stressing of sorptive media

The target mass contents of Cu and Zn in the sorptive media after pre-stressing were determined following equation S1 and S2,

$$w_{m,Cu} = 5\ CEC_m M_{Cu} \cdot 0.106\ x_{CEC} \quad \text{(S1)}$$

$$w_{m,Zn} = 5\ CEC_m M_{Zn} \cdot 0.894\ x_{CEC} \quad \text{(S2)}$$

where $w_{m,i}$ is the mass content of the metal i (Cu or Zn) in media m (mg kg^{-1}), CEC_m is the cationic exchange capacity of media m ($cmol^+$ kg^{-1}), M_i is the molar mass of metal i (g mol^{-1}) and x_{CEC} is the target pre-stressing level defined as fraction of CEC_m. The target contents of Cu and Zn after pre-stressing are summarized in table S2.

Table S2 Target Cu and Zn content for the pre-stressing of the sorptive media

Experiment	Sorptive filter media					
	ZEO		GFH		GAL	
	Cu [g kg^{-1}]	Zn [g kg^{-1}]	Cu [g kg^{-1}]	Zn [g kg^{-1}]	Cu [g kg^{-1}]	Zn [g kg^{-1}]
10% CEC	0.075	0.675	0.141	1.268	0.027	0.244
40% CEC	0.301	2.699	-*	-*	-*	-*
60% CEC	0.452	4.048	-*	-*	-*	-*
80% CEC	0.602	5.398	-*	-*	-*	-*

* Experiments with 40, 60 and 80% CEC were only conducted with the media ZEO

Cleaning procedure of glass ware

1. Clean with DI water and a brush
2. Flush with DI water
3. Flush with acetone
4. Flush with DI water
5. Fill container with 0.1 M HNO_3 and let it rest for 24 h, dispose solution afterwards
6. Flush with DI water

Microwave-assisted hydrofluoric acid digestion method

1. Approximately 200 mg of sample was digested using 8 mL 65% nitric acid, 2 mL 40% hydrofluoric acid (s.p.) and 1 mL 30% hydrogen peroxide (s.p.) in a microwave digestion system (Mars 6, CEM, USA) at 200 °C.
2. Temperature was increased to 200 °C within 15 min. The temperature remained at 200 °C for 20 min. Afterwards it was cooled down for 20 min.
3. Subsequently, 1 mL hydrofluoric acid and 10 mL 4% boric acid were added and a second digestion at 180 °C was conducted. Excessive hydrofluoric acid was masked.
4. The digested solution was transferred quantitatively in a 250 mL volumetric flask and filled up with ultrapure water.
5. Afterwards, a 10 times diluted sample was analyzed using ICP-OES or ICP-MS.

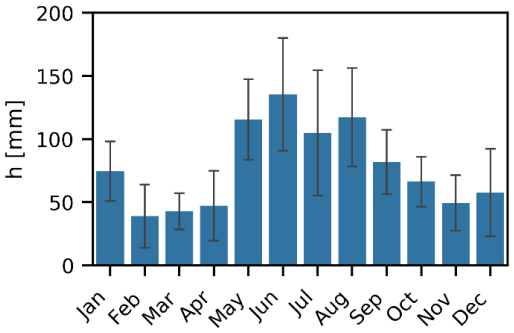

Fig. S2 Monthly precipitation height observed in Munich, Germany, at weather station 3379 of the Deutscher Wetterdienst. Data of the years 2010–2018 is shown, bar heights indicate mean values, the error bars denotes the SD.

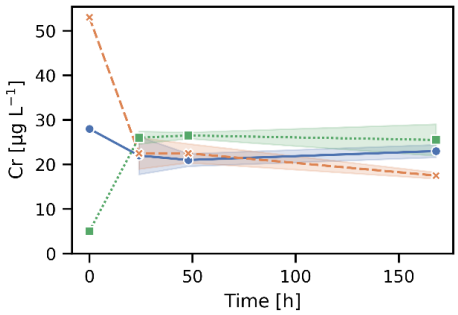

Fig. S3 Time-series of dissolved Cr in the leachates of SED the different media and SRRs. Shown is the mean of two replicates. The shaded area denotes the SD.

Modeling of leaching behavior

Degaffe and Turner (2011) modeled the leaching behavior of Zn from tire wear particles with a diffusion-controlled leaching model following equation S3,

$$[\mathrm{Me}] = \mathrm{kt}^{1/2} \quad \text{(S3)}$$

where [Me] represents dissolved metal concentrations at time t. The parameter k (µg L^{-1} $h^{-0.5}$) is the rate constant of the diffusion-controlled leaching process (Degaffe and Turner, 2011).

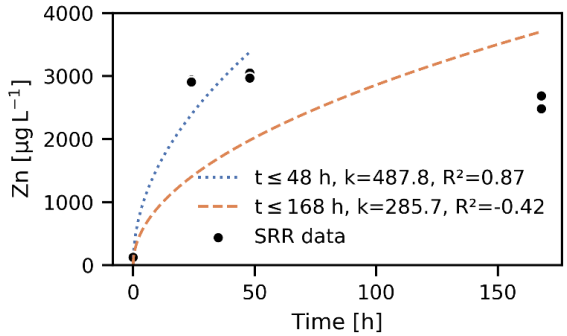

Fig. S4 Time-series of dissolved Zn in the SRR leachates of SED. Dotted and dashed line showed the diffusion-controlled fitted for t≤48 h data and all data, respectively.

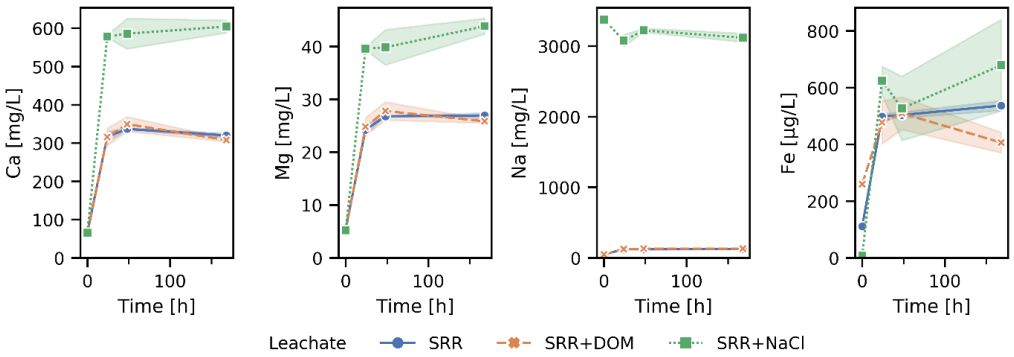

Fig. S5 Time-series of dissolved Ca, Mg, Na and Fe in the leachates of SED the different media and SRRs. Shown is the mean of two replicates. The shaded area denotes the SD.

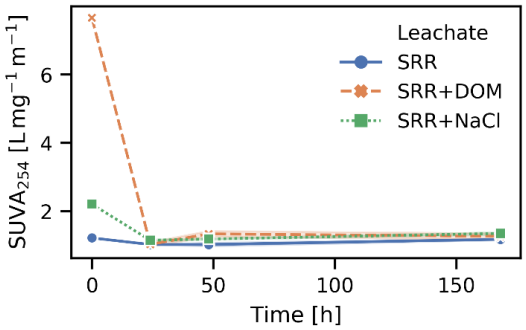

Fig. S6 Time-series of $SUVA_{254}$ in the leachates of SED. Shown is the mean of two replicates. The shaded area denotes the SD.

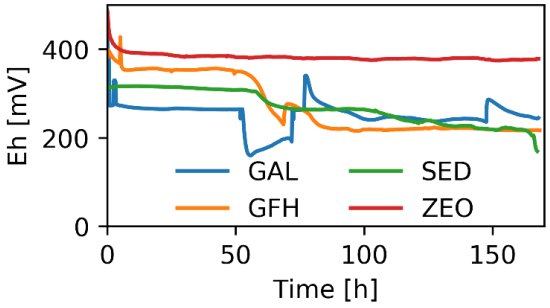

Fig. S7 Time-series of the ORP relative to the standard hydrogen electrode (Eh)in the SRR+DOM leachates of GAL, GFH, ZEO (all 10% pre-stressed) and SED

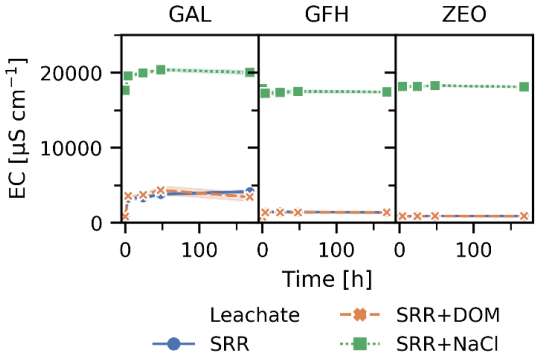

Fig. S8 Time-series of EC in the leachates of the different media and SRRs. Shown is the mean of two replicates. The shaded area denotes the SD.

Table S3 Speciation of SRRs predicted by Visual MINTEQ, species with fractions <1% were removed.

SRR		SRR+NaCl		SRR+DOM	
77.7	$CuCO_3$ (aq)	68.1	$CuCO_3$ (aq)	96.0	HA2-Cu(6)(aq)
13.0	$CuOH^+$	13.5	Cu^{2+}	4.0	HA1-Cu(6)(aq)
5.9	Cu^{2+}	13.5	$CuOH^+$		
2.0	$Cu(OH)_2$ (aq)	1.6	$Cu(CO_3)_2^{2-}$		
1.0	$Cu(CO_3)_2^{2-}$	1.5	$CuCl^+$		
		1.3	$Cu(OH)_2$ (aq)		
75.6	Zn^{2+}	77.5	Zn^{2+}	50.2	HA2-Zn(6)(aq)
9.8	$ZnCO_3$ (aq)	12.0	$ZnCl^+$	23.3	Zn^{2+}
5.7	$Zn(OH)_2$ (aq)	3.8	$ZnCO_3$ (aq)	18.0	HA1-Zn(6)(aq)
5.3	$ZnOH^+$	2.5	$ZnOH^+$	3.1	$ZnCO_3$ (aq)
1.4	$ZnSO_4$ (aq)	1.7	$Zn(OH)_2$ (aq)	2.0	$Zn(OH)_2$ (aq)
1.4	$ZnHCO_3^+$	1.1	$ZnCl_2$ (aq)	1.8	$ZnOH^+$

References

Degaffe, F.S., Turner, A., 2011. Leaching of zinc from tire wear particles under simulated estuarine conditions. Chemosphere 85, 738–743. https://doi.org/10.1016/j.chemosphere.2011.06.047

A.3 Supplementary information for Chapter 5

Appendix A. Study site

The runoff samples were withdrawn volume proportionally with automatic samplers (WS 316, WaterSam, Balingen, Germany; PP 84, Edmund Bühler, Bodelshausen, Germany) in the period from November 2017 to October 2019. Because of the design of SQID D, an additional drainage channel needed to be installed (D in, Figure 1; Faserfix Super 300 Typ 01H, Hauraton, Rastatt, Germany) next to the filter substratum channel to sample the influent (i.e. road runoff) which as well enters SQID D (D eff in Figure 1). The layout of the stormwater quality improvement devices (SQIDs) are illustrated in Figure S1. The sampling was triggered by electro-magnetic flow meters (Krohne Optiflux 2300 C or 1300 C, Krohne IFC 300 C, DN250 for S, DN40 for V, DN25 for D). The flow data were recorded with a frequency of 30 s. The sampling started, if the inflow exceeded the threshold value longer than 1 min. If the inflow was 15 min below the threshold value, sampling stopped. The threshold value was set to 0.4 L s^{-1} ha^{-1} discharge, based on the determined catchment areas. It was attempted to sample all three SQIDs at the same time, however this was not possible at each event due to failure. The effluent samples of the SQIDs are not considered in this study. The samples were kept in coolers at 4±1 °C and transported to the lab within 60 h.

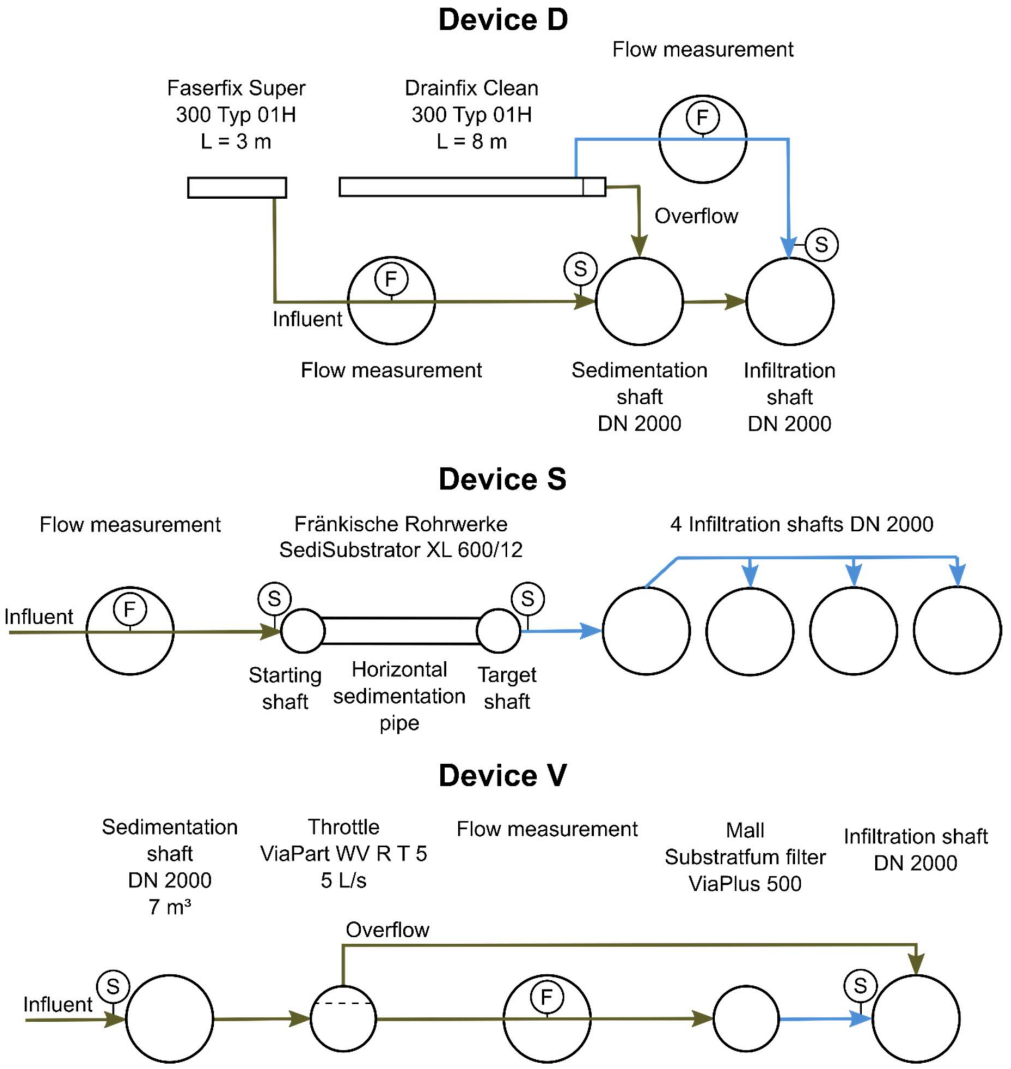

Figure S1. Layout of the monitored storm water quality improvement devices, brown arrows indicate untreated road runoff, blue arrows indicate treated road runoff, points labeled with F show flow measurement, points labeled with S show sampling positions

Appendix B. Analysis of road runoff

One composite sample for each discharge event and SQID was prepared using the discrete samples of each automatic sampler. Analyses of pH, electric conductivity (EC) and suspended solids (TSS) and fine suspended solids (SS63) were performed within 60 h. The samples for the analyses of heavy metals were acidified to pH < 2 with nitric acid (65%). The analysis of TSS and SS63 followed the method, described in Rommel and Helmreich[1]. Total concentrations of cadmium (Cd), chromium (Cr), copper (Cu), nickel (Ni), lead (Pb) and zinc (Zn) were

determined after *aqua regia* digestion according to EN ISO 15587-1:2002. The analyses of Cr and Zn were conducted using ICP-OES (DIN EN ISO 11885, Ultima II, Horiba Jobin Yvon, Kyoto, Japan), Cd, Cu, Ni, Pb were analyzed using ICP-MS (NexION 300D, Perkin Elmer, Waltham, USA). The limits of quantification (LOQs) were 0.1 µg L^{-1} Cd, 1 µg L^{-1} Cr, 0.1 µg L^{-1} Cu, 0.4 µg L^{-1} Ni, 0.1 µg L^{-1} Pb and 2 µg L^{-1} Zn. Dissolved concentrations of Cd, Cr, Cu, Ni, Pb, and Zn were analyzed after filtration using syringe filter (0.45 µm, PES, VWR International, Darmstadt, Germany). The aforementioned instruments were applied and the LOQs were 0.5 µg L^{-1} Cd, 2.0 µg L^{-1} Cr, 1.0 µg L^{-1} for Cu, Ni, Pb, and Zn. The dissolved organic carbon (DOC) concentration was determined after filtration (0.45 µm) using a varioTOC Cube analyzer (Elementar, Langenselbold, Germany) according to DIN EN 1484 with a LOQ of 0.25 mg L^{-1}. Alkalinity was analyzed by acidimetric titration (standard method 2320) to the pH endpoints 4.5 and 8.3.

Appendix C. Heavy metal contents and physical properties of the blank filter media prior to prestressing

Table S1. Heavy metal contents and physical properties of the blank filter media, metal contents and loss on ignition (LOI) refer to dry matter; d_{50} is the median particle size; sampling of S Field was not possible without altering the filter cartridge

Parameter	**Cr**	**Cu**	**Ni**	**Pb**	**Zn**	**pH**	**LOI**	**d_{50}**
Unit	mg kg^{-1}	mg kg^{-1}	mg kg^{-1}	mg kg^{-1}	mg kg^{-1}	-	%	mm
D Field Blank	2.5 [a]	2.5 [a]	1.0 [a]	5.0 [a]	43.3	8.4	0.5	0.7
D Lab Blank	13.7	2.5 [a]	10.0	5.0 [a]	13.7	8.3	0.4	0.7
S Lab Blank	2.5 [a]	2.5 [a]	36.4	5.0 [a]	53.6	8.8	56.3	1.5
V Field Blank	12.2	2.5 [a]	5.2	5.0 [a]	17.5	9.5	5.9	1.5
V Lab Blank	2.5 [a]	2.5 [a]	3.9	45.5	34.9	8.7	5.7	1.5

[a] value was below the limit of quantification (LOQ) and was substituted by 0.5·LOQ

Appendix D. Prestressing of the filter media at lab scale

Table S2. Analysis of the synthetic runoff for the prestressing of the filter media at lab scale

Parameter	pH	EC	TSS	Cd	Cr	Cu	Ni	Pb	Zn
Unit	-	µS cm^{-1}	mg L^{-1}	µg L^{-1}	µg L^{-1}	µg L^{-1}	µg L^{-1}	µg L^{-1}	µg L^{-1}
D	5.1	115	–[a]	–[a]	–[a]	3,670	–[a]	–[a]	32,010
S, 1st run	5.0	115	–[a]	–[a]	–[a]	3,670	–[a]	–[a]	32,010
S, 2nd run	5.0	207	–[a]	–[a]	–[a]	487	–[a]	–[a]	>6,000[b]
S, 3rd run	5.0	248	–[a]	–[a]	–[a]	<100	–[a]	–[a]	3,870
V	5.1	116	–[a]	–[a]	–[a]	3,670	–[a]	–[a]	32,010

[a] was not analyzed because the element was not added to the synthetic runoff, the content in the filter media were analyzed (Table 5), [b] was not again analyzed with higher dilution, because the end criterion was not reached

Appendix E. Quality control of the sequential extraction procedure

The reference material BCR-701 was analyzed threefold together with other samples. Each analysis of the BCR-701 was analyzed in one separate sample batch together with the other samples as quality control. Only BCR-701 of the same subsample (container) was analyzed throughout the entire sequential extraction procedure (SEP) analyses. The quality of the SEP analysis was determined by precision and pseudo-accuracy, defined as follows:[2]

$$\text{Precision} = \frac{\sigma}{\bar{x}} \times 100$$

$$\text{Pseudo–accuracy} = \frac{1}{n}\sum \frac{measured\ value\ -\ certified\ value}{certified\ value} \times 100$$

where $\bar{x}$ is the mean, σ is the standard deviation of the measured values, n is the number of analyses, and the certified values are the values reported by Rauret et al.[3].

In total, good precision and pseudo-accuracy were achieved (Table S3). However, the results for the residuals (F4) showed an increased overestimation in comparison to the other extractions steps. Poor pseudo-accuracy for Cr in the residual fraction (F4) was achieved. Mean recoveries of 106, 98, 101, 108, and 101% were achieved for the pseudo-total analysis of Cr, Cu, Ni, Pb, and Zn in BCR-701. Thus, good agreement between the indicative and determined values was achieved. In addition, the reagents and the acid cleaned centrifuge tubes were analyzed to assess potential contamination. All samples, except minor traces of Zn in one sample of reagent B, showed concentrations below the limits of quantification for Cr, Cu, Ni, Pb, and Zn. The minor traces of Zn in one sample of reagent B was not further considered, because the error would be ≤ 3% for the respective samples, the reducible fraction and the element Zn.

Table S3. Mean fraction-specific precision and pseudo-accuracy in percent for the optimized BCR SEP for Cr, Cu, Ni, Pb, and Zn of BCR-701, n=3

Element/ parameter	Acid-extractable (F1)	Reducible (F2)	Oxidizable (F3)	Residual (F4)	Pseudo-total
Cr					
Precision	9.4	5.4	12.3	5.5	1.5
pseudo-accuracy	7.9	9.1	2.8	78.5	5.7
Cu					
Precision	3.5	3.9	12.2	14.1	5.3
pseudo-accuracy	11.7	8.4	12.5	35.0	-1.7
Ni					
Precision	6.1	6.2	9.9	8.4	1.6
pseudo-accuracy	10.0	22.1	10.1	26.4	0.5
Pb					
Precision	1.7	2.5	23.0	36.3	4.5
pseudo-accuracy	-4.1	6.3	17.1	23.7	8.4
Zn					
Precision	5.6	6.0	15.0	9.6	1.6
pseudo-accuracy	2.5	5.5	-3.6	33.0	0.6

Appendix F. Sequential Extraction

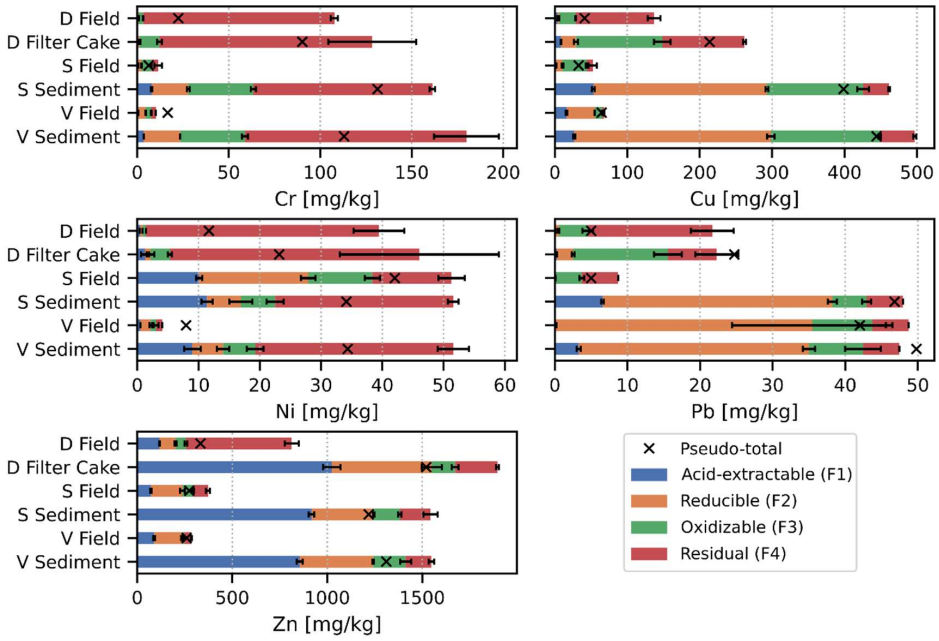

Figure S2. Cr, Cu, Ni, Pb, and Zn contents found in the respective sequential extraction fractions of the filter media prestressed in the field test (D Field, S Field, V Field), sediments (S Sediment, V Sediment) and filter cake (D Filter Cake) withdrawn from the SQIDs after the field test, n=3 for each sample and fraction except for the pseudo-total fraction; pseudo-total fraction n=2, mean value is illustrated. Bars show mean values and error bars indicate the standard deviation.

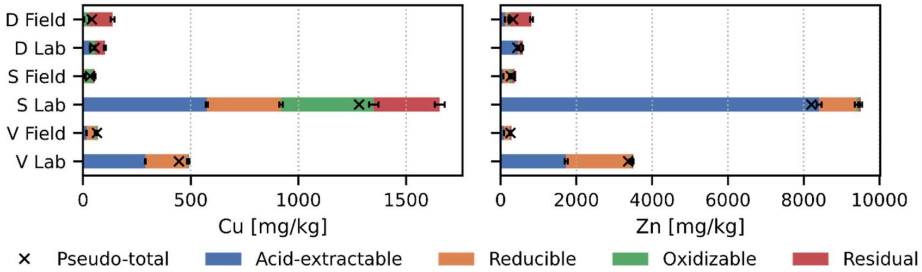

Figure S3. Cr, Cu, Ni, Pb, and Zn contents found in the respective sequential extraction fractions of the filter media prestressed in the lab-scale and field tests, n=3 for each sample and fraction except for the pseudo-total fraction; pseudo-total fraction n=2, mean value is illustrated. Bars show mean values and error bars indicate the standard deviation.

Appendix G. pH values and losses on ignition of the filter-media, sediments, and filter cake

Table S4. pH values and losses on ignition (LOI) of the filter-media prestressed in the lab and field tests, sediments, and filter cake

Parameter **Unit**	**pH** -	**LOI** %
D Field	7.7	2.8
D Filter Cake	6.8	10.0
D Lab	8.3	0.6
S Field	7.6	28.2
S Lab	7.9	35.3
S Sediment	6.9	17.8
V Field	7.9	8.2
V Lab	8.4	4.5
V Sediment	6.6	20.5

References

(1) Rommel, S. H.; Helmreich, B. Influence of Temperature and De-Icing Salt on the Sedimentation of Particulate Matter in Traffic Area Runoff. *Water* **2018**, *10* (12), 1738. https://doi.org/10.3390/w10121738.

(2) Sutherland, R. A.; Tack, F. M. G.; Ziegler, A. D. Road-Deposited Sediments in an Urban Environment: A First Look at Sequentially Extracted Element Loads in Grain Size Fractions. *Journal of Hazardous Materials* **2012**, *225–226*, 54–62. https://doi.org/10.1016/j.jhazmat.2012.04.066.

(3) Rauret, G.; López-Sánchez, J. F.; Lück, D.; Yli-Halla, M.; Muntau, H.; Quevauviller, P. The Certification of the Extractable Contents (Mass Fractions) of Cd, Cr, Cu, Ni, Pb and Zn in Freshwater Sediment Following a Sequential Extraction Procedure, BCR-701. **2001**, 88.

A.4 Supplementary information for Chapter 6

Appendix A. Study site

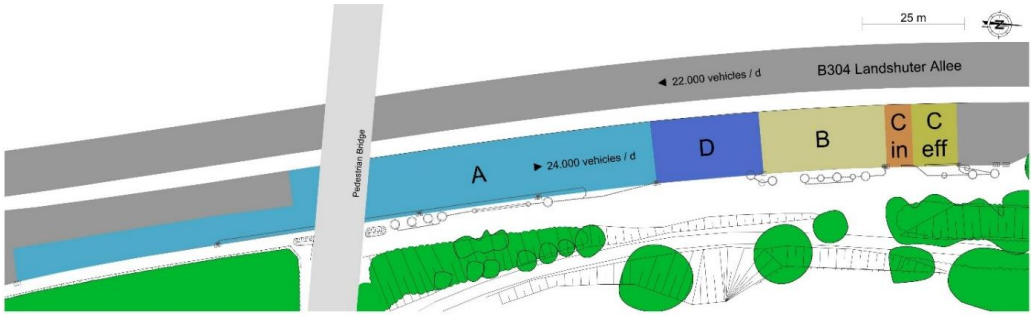

Fig. S1 Layout of the monitoring site, the different colors (except for green) indicate the catchment areas

Table S1 Characteristics of the monitored SQIDs and their catchment areas, settings of the automatic samplers

		A	B	C influent [a]	C effluent	D
Device name	Unit	SediSubstrator XL 600/12	ViaPlus 500	- [a]	Drainfix Clean 300	LHM
Manufacturer	-	Fränkische Rohrwerke Gebr. Kirchner GmbH & Co. KG, Germany	Mall, Germany	Hauraton GmbH & Co. KG, Germany		None
Device type		Shaft system	Shaft system	- [a]	Filter substratum channel	Shaft system
Catchment area	m²	1660	473	100	165	400
Filter media	-	Iron-based medium with lignite amendment	Zeolite	-	Carbonate-rich sand	Carbonate-rich sand
Diameter flow meter	mm	250	40	25	25	40
Volumetric sampling intervals	L	270	78	18	27	67
Minimal discharge rate for sampling	L $s^{-1} \cdot ha^{-1}$	0.4	0.4	0.4	0.4	0.4
Maximum discharge rate [c]	L $s^{-1} \cdot ha^{-1}$	30	30	30	30	31

[a] influent samples were withdrawn in a separate drainage channel without filter medium, [c] values higher than the maximum discharge rate are substituted by the value of the maximum discharge rate

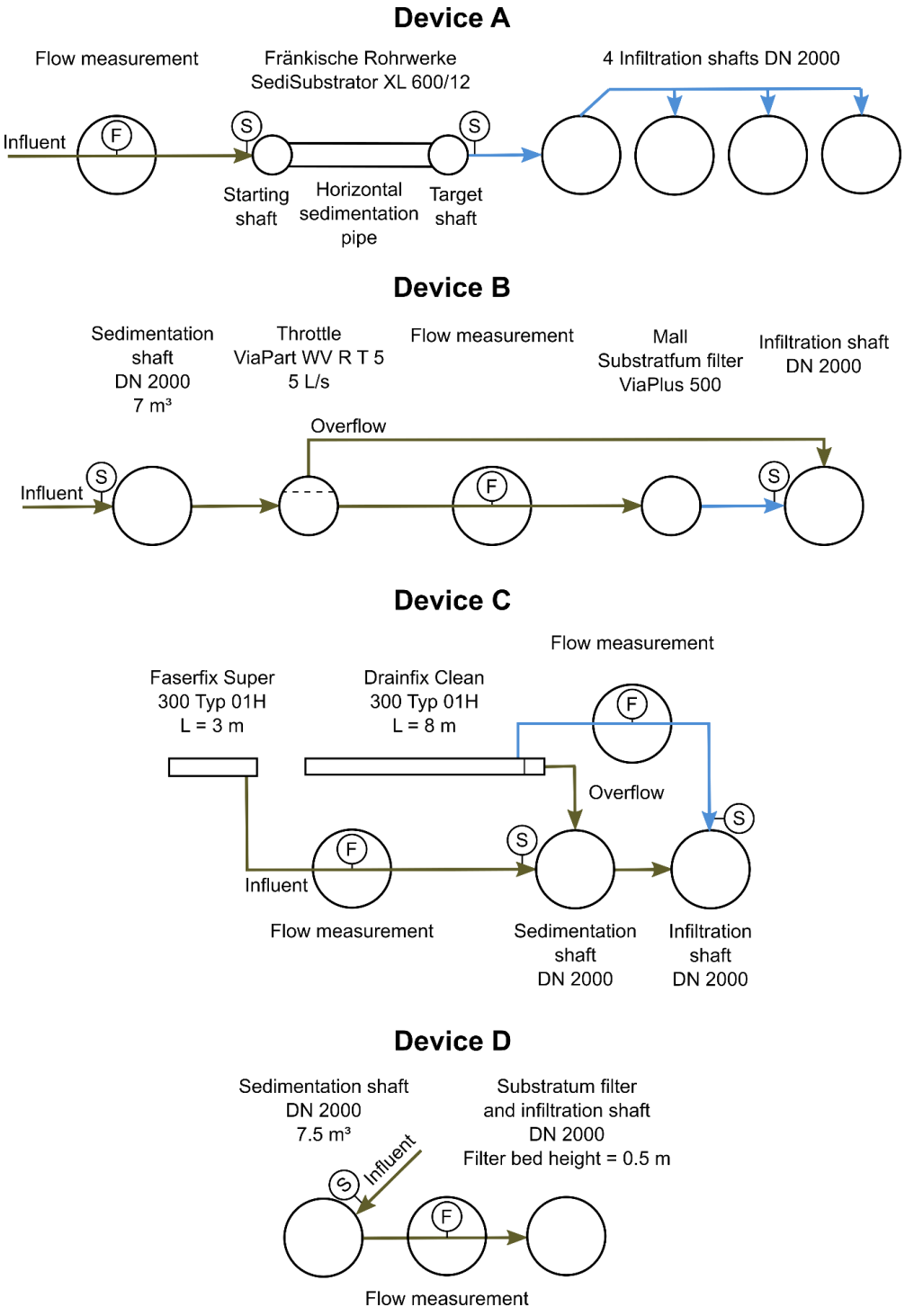

Fig. S2 Layout of the monitored devices, brown arrows indicate untreated road runoff, blue arrows indicate treated road runoff, points labeled with F show flow measurement, points labeled with S show sampling positions

Appendix B. PARAFAC

The sample C_C_190113 was excluded due to very high leverage in the model. Furthermore the samples B_C_190426, B_A_190426, C_A_190616, A_C_191028, C_A_190315, A_B_190427, A_C_190427 and A_A_190610_2 needed to be excluded because of non-random residuals.

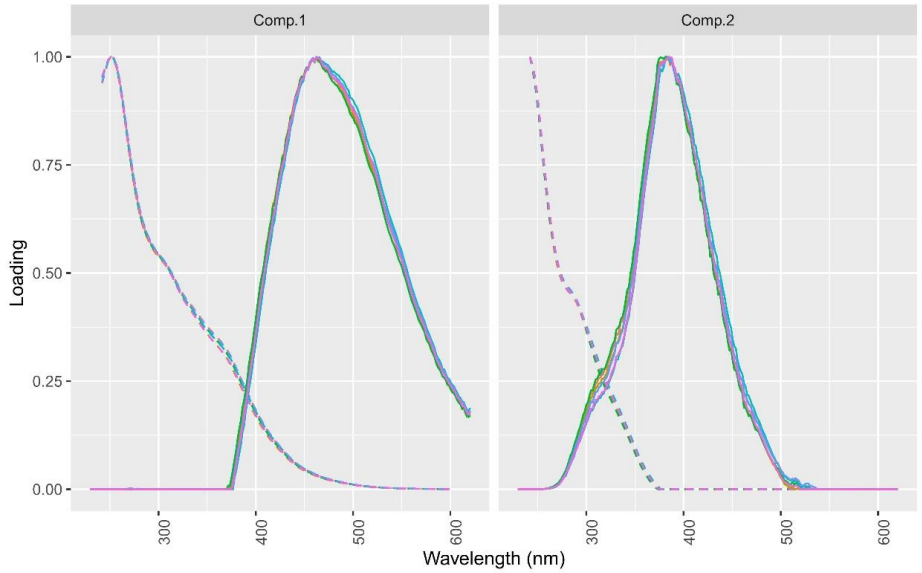

Fig. S3 Excitation and emission spectra of PARAFAC components C1 and C2 in the split-half analysis

Appendix C. DOC, UVA_{254}, UV-vis and fluorescence indices

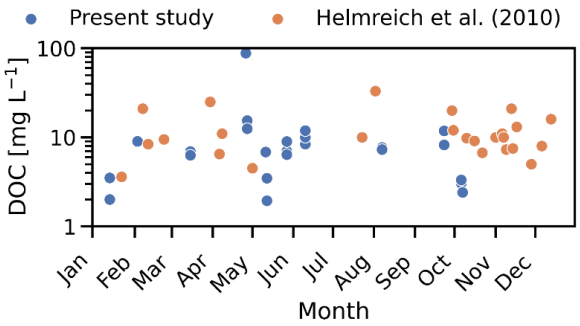

Fig. S4 Seasonal course of DOC in road runoff (influent, n = 24), sampling of Helmreich *et al.* (2010)[1] was conducted at the same site (n = 25)

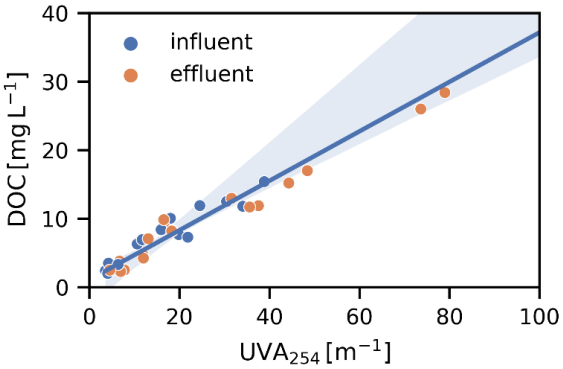

Fig. S5 Scatterplot with robust linear regression of UVA_{254} and DOC of the influent and effluent samples, the shaded region reflects the 95% confidence interval (n = 34)

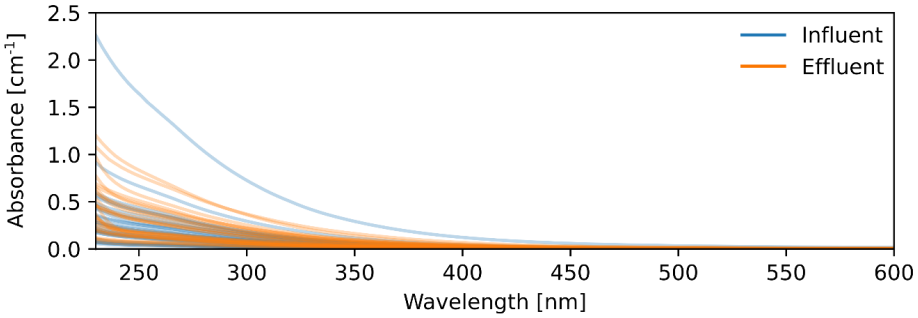

Fig. S6 Absorbance spectra of the influent and effluent samples (respectively n = 28)

Table S2. Spearman's rank correlation coefficient of UVA_{254} and the analysed dissolved metal concentrations (n = 11 for influent and effluent, respectively)

	Position	Ca_d	Cr_d	Cu_d	Fe_d	Mg_d	Na_d	Ni_d	Zn_d
UVA_{254}	Influent	0.38	0.79**	0.91**	0.74**	0.77**	0.12	0.73*	0.64*
	Effluent	0.31	0.54	0.57	0.49	0.44	-0.02	0.44	0.57

* Statistically significant ($p < 0.05$), ** $p < 0.01$

Appendix D. Weather data

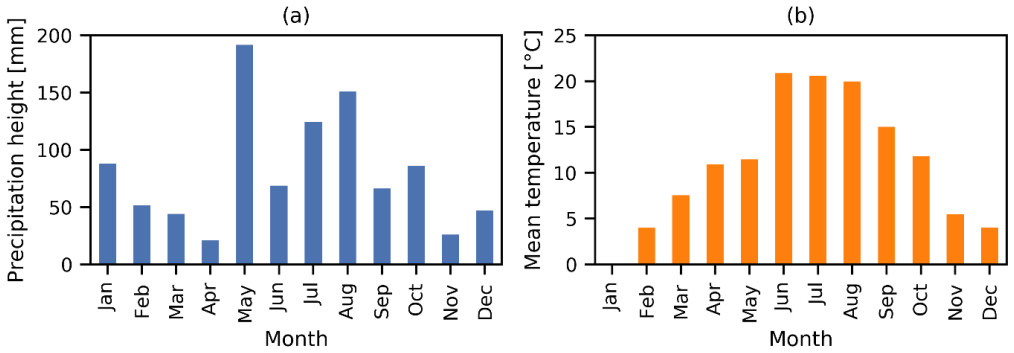

Fig. S7 Monthly (a) precipitation height and (b) mean temperature in 2019, data of the Deutscher Wetterdienst, station 3379 (Munich City, Germany); mean temperature in January was 0.0, thus it is not visible

Appendix E. Fluorescence Excitation-Emission Matrices

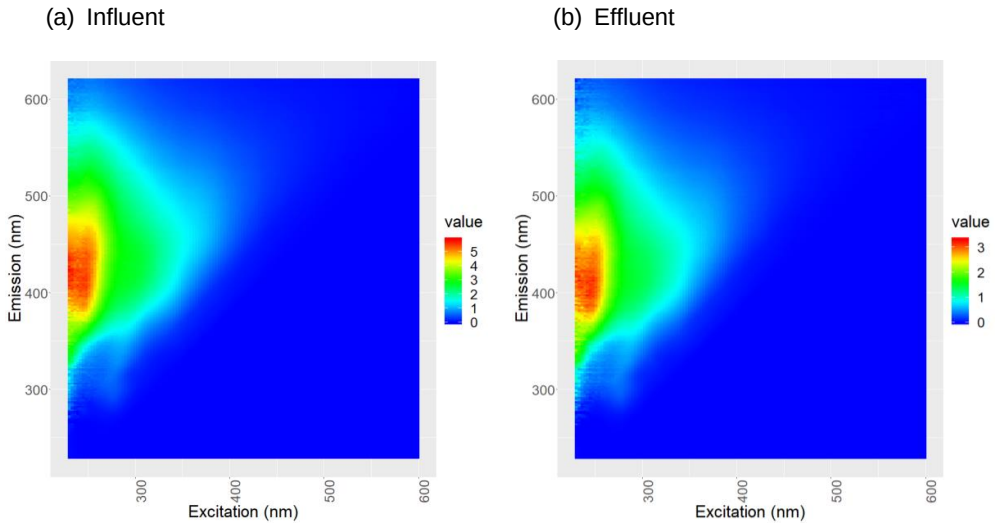

Fig. S8 Fluorescence excitation-emission matrices of a representative influent (a) and an effluent sample (b), values in Raman units. Scattering was removed and the values of the areas were interpolated. Samples were withdrawn from device B at 23 September 2019.

Appendix F. Size-exclusion chromatography

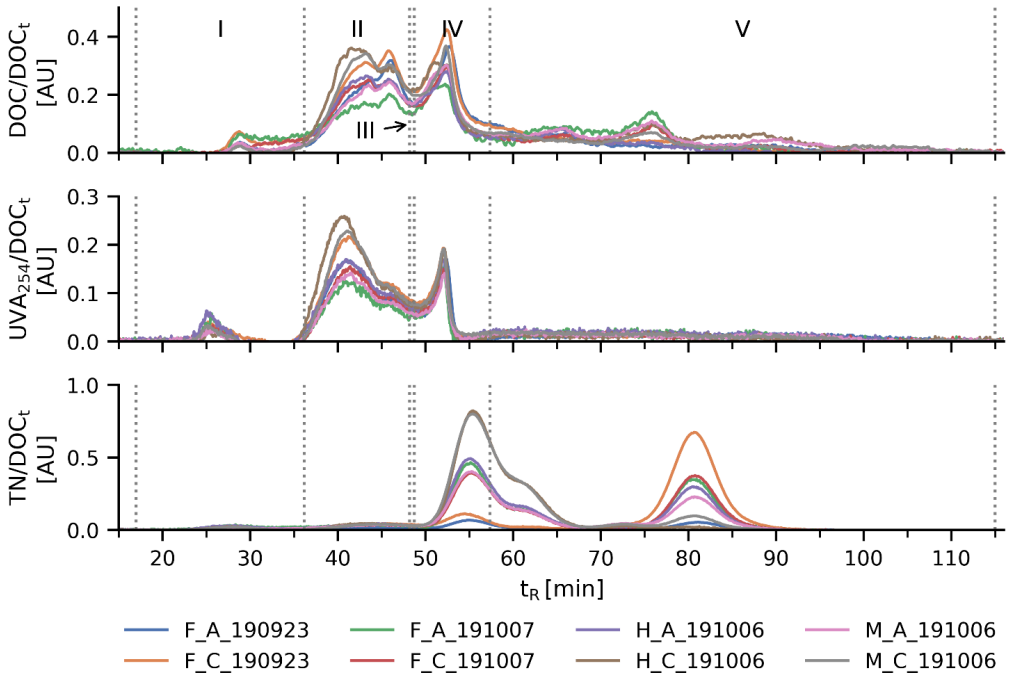

Fig. S9 SEC chromatograms of DOC, UVA_{254}, and TN detection of all samples divided by the total DOC of the injected sample (DOC_t). The dilution ratio for the SEC analysis was considered. The dotted grey lines indicate the fractions I-V related to the retention times, however they slightly vary due to the fitting to each chromatogram according to the method of Huber *et al.* [2] (n = 8).

Appendix G. Visual MINTEQ

Table S3. Results of species prediction by Visual MINTEQ showing the charge difference and fractions of the DOM-metal complexes

Device	Position	Date	Charge difference [%]	Cr-DOM [%]	Cu-DOM [%]	Ni-DOM [%]	Pb-DOM [%]	Zn-DOM [%]	Ca-DOM [%]	Fe-DOM [%]	Mg-DOM [%]	Na-DOM [%]
B	Influent	13.01.2019	6.2	100.0	99.9	52.6	99.6	0.9	0.6	100.0	2.0	0.0
B	Effluent	13.01.2019	5.7	100.0	99.8	39.9	99.3	0.7	0.4	100.0	1.4	0.0
C	Influent	13.01.2019	2.2	100.0	99.5	34.5	100.0	0.4	0.4	100.0	1.2	0.0
A	Influent	03.02.2019	1.9	100.0	100.0	42.5	100.0	0.7	0.5	100.0	1.1	0.0
A	Effluent	03.02.2019	6.0	100.0	100.0	54.8	100.0	0.9	0.6	100.0	1.4	0.0
B	Effluent	15.03.2019	4.6	100.0	99.7	50.5	100.0	1.2	1.4	100.0	3.7	0.0
A	Effluent	27.04.2019	1.3	100.0	98.5	39.7	94.3	1.2	1.2	99.9	3.2	0.0
B	Influent	26.04.2019	8.4	100.0	100.0	85.6	100.0	4.3	4.4	100.0	10.9	0.0
B	Effluent	26.04.2019	2.8	100.0	99.9	68.5	100.0	2.7	2.5	100.0	5.9	0.0
B	Effluent	11.05.2019	0.5	100.0	99.9	63.2	100.0	1.7	1.1	100.0	2.8	0.0
A	Effluent	12.05.2019	5.6	100.0	98.3	23.8	100.0	0.5	0.3	100.0	1.0	0.0
C	Effluent	12.05.2019	7.4	100.0	99.6	30.0	100.0	0.6	0.3	100.0	0.8	0.0
B	Effluent	10.06.2019	0.5	100.0	100.0	48.5	99.9	1.3	0.7	100.0	1.9	0.0
B	Influent	06.10.2019	9.7	100.0	99.9	34.6	100.0	0.6	0.3	100.0	1.1	0.0
B	Effluent	06.10.2019	8.8	100.0	97.7	22.9	98.0	0.6	0.3	100.0	1.1	0.0
C	Effluent	06.10.2019	10.0	100.0	99.5	23.5	100.0	0.6	0.2	100.0	0.6	0.0

References

1 B. Helmreich, R. Hilliges, A. Schriewer and H. Horn, *Chemosphere*, 2010, **80**, 991–997.
2 S. A. Huber, A. Balz, M. Abert and W. Pronk, *Water Research*, 2011, **45**, 879–885.

A.5 Supplementary information for Chapter 7

Table S1. Density and viscosity of NaCl solutions at various temperatures

	w_{NaCl} = 0.000			w_{NaCl} = 0.005		
t / °C	ρ_m / kg m^{-3}	η_m / kg m^{-1} s^{-1}	**ν** / m² s^{-1}	ρ_m / kg m^{-3}	η_m / kg m^{-1} s^{-1}	**ν** / m² s^{-1}
5	999.964	1.52E-03	1.52E-06	1003.601	1.53E-03	1.52E-06
10	999.700	1.31E-03	1.31E-06	1003.291	1.31E-03	1.31E-06
15	999.100	1.14E-03	1.14E-06	1002.650	1.15E-03	1.14E-06
20	998.204	1.00E-03	1.00E-06	1001.718	1.01E-03	1.01E-06
25	997.045	8.90E-04	8.93E-07	1000.525	8.96E-04	8.96E-07
	w_{NaCl} = 0.010			w_{NaCl} = 0.015		
t / °C	ρ_m / kg m^{-3}	η_m / kg m^{-1} s^{-1}	**ν** / m² s^{-1}	ρ_m / kg m^{-3}	η_m / kg m^{-1} s^{-1}	**ν** / m² s^{-1}
5	1007.250	1.54E-03	1.52E-06	1010.912	1.54E-03	1.53E-06
10	1006.896	1.32E-03	1.31E-06	1010.513	1.33E-03	1.32E-06
15	1006.214	1.15E-03	1.15E-06	1009.789	1.16E-03	1.15E-06
20	1005.243	1.02E-03	1.01E-06	1008.781	1.02E-03	1.01E-06
25	1004.017	9.03E-04	8.99E-07	1007.521	9.09E-04	9.03E-07
	w_{NaCl} = 0.020					
t / °C	ρ_m / kg m^{-3}	η_m / kg m^{-1} s^{-1}	**ν** / m² s^{-1}			
5	1014.588	1.55E-03	1.53E-06			
10	1014.143	1.34E-03	1.32E-06			
15	1013.377	1.17E-03	1.15E-06			
20	1012.332	1.03E-03	1.02E-06			
25	1011.037	9.16E-04	9.06E-07			

A.6 Supplementary information for Chapter 8

Materials and Methods

To assess the comparability of filtration and evaporation to determine the settled mass fraction, 100 mg of MiW4 were added to 10 mL DI water and analyzed.

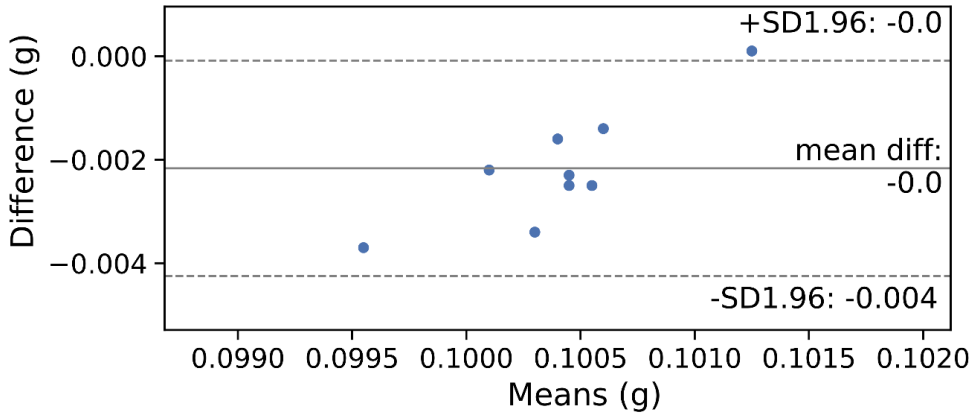

Figure S1. Bland–Altman plot for comparison of the two methods for the determination of the settled fraction (evaporation and filtration), the area between the dashed lines indicates the 95% confidence interval, n=9, one outlier was removed.

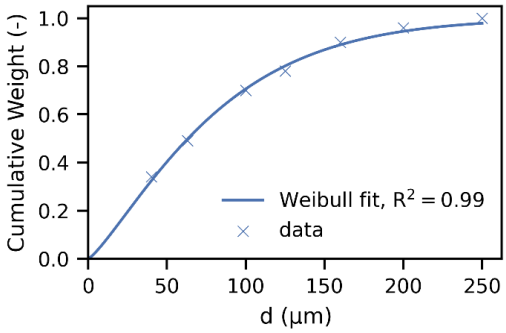

Figure S2. Particle size distribution of the pre-processed road-deposited sediments, fitted Weibull distribution for subsequent modeling of the sedimentation processes.

Results

Particle size and shape

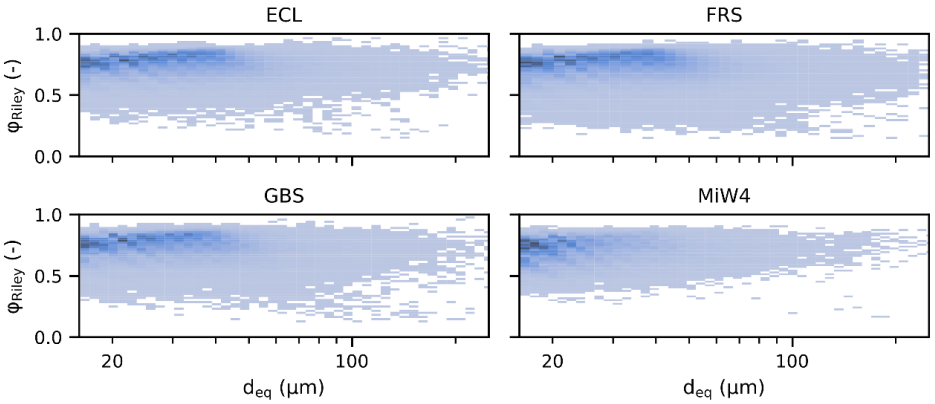

Figure S3. 2D histogram of φ_{Riley} with respect to d_{eq} of all analyzed samples, color opacity indicates the density of counts, ECL n=130,986, FRS n=211,209, GBS n=134,392, MiW4 n=57,973.

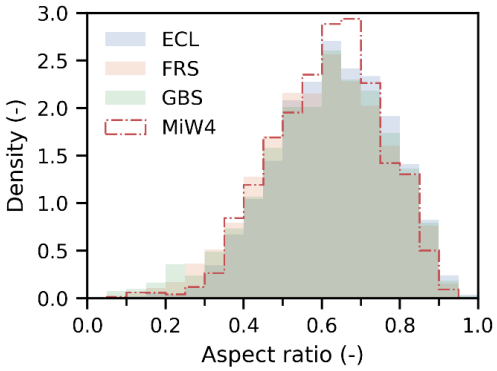

Figure S4. Mass fraction weighted histogram of the aspect ratios of the analyzed samples, ECL n=130,986, FRS n=211,209, GBS n=134,392, MiW4 n=57,973.

Settling experiments

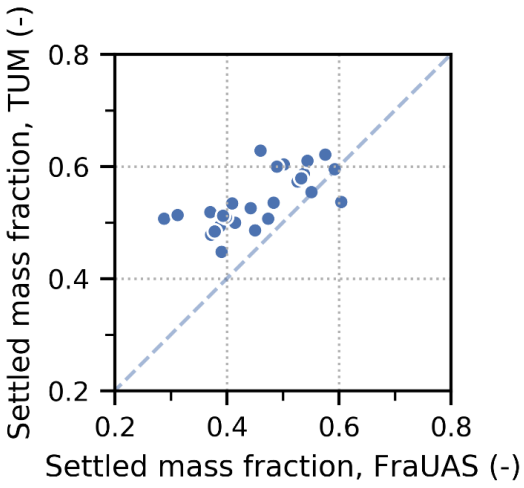

Figure S5. Comparison of the experimental results of settling experiments using the method described in this paper conducted by two different executers, n=27.

Validation of settling model

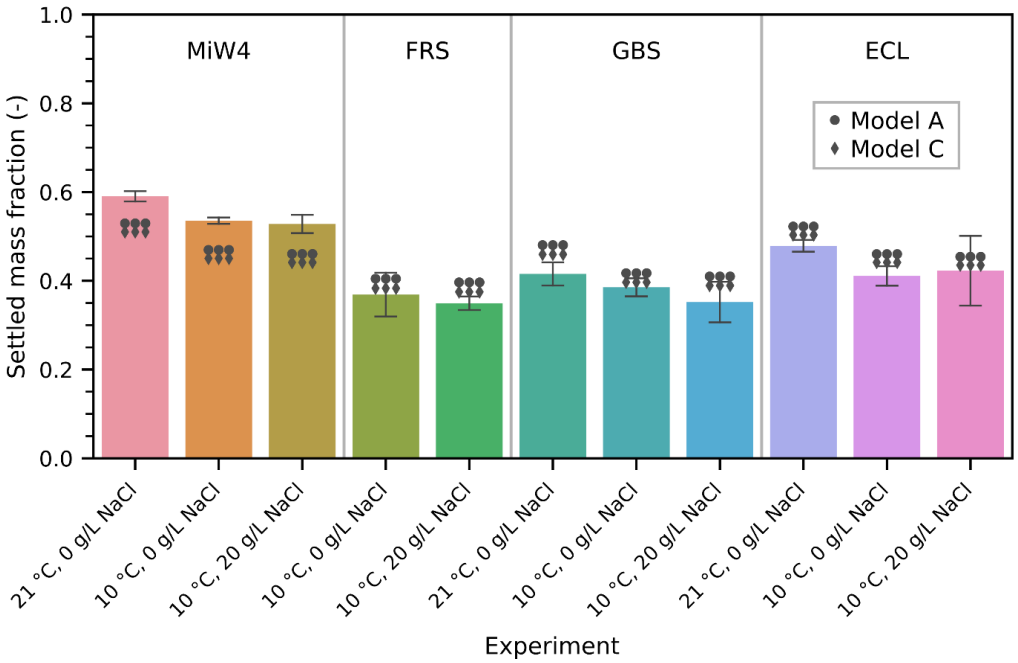

Figure S6. Settled mass fraction in the settling experiments with varying temperature (21 and 10 °C) and NaCl concentration (0 and 20 g/L), n=3 for each experiment. The error bars indicate the standard deviation. Experiment FRS, 21 °C, 0g/L was not conducted due to low sample quantity. Marker show the predicted settled mass fraction determined by Model A and C.

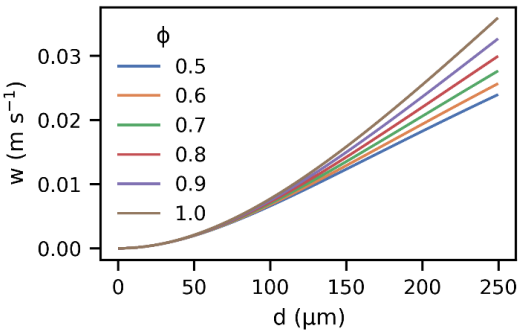

Figure S7. Settling velocity determined with the equations proposed by Haider and Levenspiel (model C) with respect to particle diameter and sphericity at 20 °C, ϱ_s of MiW4, and w_{NaCl}=0.